Energy Research and Development Division
FINAL PROJECT REPORT

EFFICIENT HEAT AND POWER SYSTEMS FOR CHP APPLICATIONS

Prepared for: California Energy Commission
Prepared by: CMCE, Inc. (dba CMC-Engineering)

MARCH 2012
CEC-500-2014-002

CMC-Engineering

PREPARED BY:

Primary Author(s):
Carlo Castaldini

CMCE, Inc.
d.b.a CMC-Engineering
2900 Gordon Avenue, Suite 100
Santa Clara, CA 95051

Contract Number: PIR-07-003

Prepared for:

California Energy Commission

Mike Kane
Contract Manager

Linda Spiegel
Office Manager
Energy Generation Research Office

Laurie ten Hope
Deputy Director
ENERGY RESEARCH AND DEVELOPMENT DIVISION

Robert P. Oglesby
Executive Director

DISCLAIMER

This report was prepared as the result of work sponsored by the California Energy Commission. It does not necessarily represent the views of the Energy Commission, its employees or the State of California. The Energy Commission, the State of California, its employees, contractors and subcontractors make no warranty, express or implied, and assume no legal liability for the information in this report; nor does any party represent that the uses of this information will not infringe upon privately owned rights. This report has not been approved or disapproved by the California Energy Commission nor has the California Energy Commission passed upon the accuracy or adequacy of the information in this report.

ACKNOWLEDGEMENTS

The authors are grateful to the California Energy Commission for its support of this project, to the members of Altex Technologies Corporation for their support in the development of the EHPS technology and to Mr. Robert Feldeisen, ex field service engineer of Elliott Energy Systems (Calnetix) for assistance in the TA-100 component operational readiness and evaluation of proposed system upgrades. We also acknowledge the financial contribution made by the Southern California Gas Company (SCG) and to the leadership of Mr. Cherif Youssef and Mr. Henry Mak at SCG.

PREFACE

The California Energy Commission Energy Research and Development Division supports public interest energy research and development that will help improve the quality of life in California by bringing environmentally safe, affordable, and reliable energy services and products to the marketplace.

The Energy Research and Development Division conducts public interest research, development, and demonstration (RD&D) projects to benefit California.

The Energy Research and Development Division strives to conduct the most promising public interest energy research by partnering with RD&D entities, including individuals, businesses, utilities, and public or private research institutions.

Energy Research and Development Division funding efforts are focused on the following RD&D program areas:

- Buildings End-Use Energy Efficiency
- Energy Innovations Small Grants
- Energy-Related Environmental Research
- Energy Systems Integration
- Environmentally Preferred Advanced Generation
- Industrial/Agricultural/Water End-Use Energy Efficiency
- Renewable Energy Technologies
- Transportation

Efficient Heat and Power Energy System for CHP Applications is the final report for the Efficient Heat and Power Energy System project (contract number PIR-07-003) conducted by CMC Engineering. The information from this project contributes to Energy Research and Development Division's Industrial/Agricultural/Water End-Use Energy Efficiency Program.

For more information about the Energy Research and Development Division, please visit the Energy Commission's website at www.energy.ca.gov/research/ or contact the Energy Commission at 916-327-1551.

ABSTRACT

This research developed and partially demonstrated a 2007 California Air Resources Board-compliant combined heat and power system suited for distributed generation applications at commercial or industrial sites with high power-to-heat requirements. Researchers combined detailed engineering and computational modeling with laboratory- and bench-scale testing to develop components for a microturbine-based combined heat and power system that used steam injection to improve the microturbine's power conversion efficiency to 38 percent and employed latent heat recapture to improve overall combined heat and power efficiency to as high as 87 percent. Key technical achievements included development of an emissions-compliant steam injected silo combustor fitted to a modified 100-kilowatt turbine housing and scroll assembly, and integration of three advanced heat exchangers for the production of steam for injection and for recovery of condensed steam from the microturbine exhaust to form a closed-loop water recycling system. The components were assembled into a complete combined heat and power system in a laboratory facility and component performance tests were initiated.

Keywords: Public Interest Energy Research (PIER) Program, power generation, boilers, microturbines, generators, low exhaust emissions, combined heat and power (CHP), Efficient Heat and Power System (EHPS)

Please use the following citation for this report:

Castaldini, Carlo. (EMC Engineering). 2012. ***Efficient Heat and Power System for CHP Applications.*** California Energy Commission. Publication number: CEC-500-2014-002.

TABLE OF CONTENTS

Acknowledgements ..... **i**

PREFACE ..... **ii**

ABSTRACT ..... **iii**

TABLE OF CONTENTS ..... **iv**

LIST OF FIGURES ..... **vii**

LIST OF TABLES ..... **x**

EXECUTIVE SUMMARY **1**

Introduction 1

Project Purpose 1

Project Results 1

Project Benefits 2

CHAPTER 1: Introduction **4**

1.1 Background 4

1.2 Project Goals and Objectives 5

1.3 Project Approach 7

CHAPTER 2: Engineer and Model CHP System and Components **1**

2.1 Goal and Objectives 1

2.2 Approach to Engineering and Modeling 1

2.3 EHPS Process, Predicted Performance and E&M Balances 2

2.4 Microturbine Test Bed for EHPS 17

2.5 TA-100 Microturbine Compressor 20

2.6 Ultra Low NOx Combustor 21

2.7 Recuperator 28

2.8 Boiler and Condensing Heat Exchangers 28

2.9 Auxiliary Equipment 31

CHAPTER 3: Combustor Design Specifications **32**

3.1 Goal and Objectives 32

3.2 Approach to Combustor Design 32
3.3 Elliott TA-100 Combustor 37
3.4 Operating Conditions Conducive to Ultra Low NOx Combustor Emissions 41
3.5 Design, Fabrication and Modeling of Combustor Test Unit 43
3.5.1 Combustor Design and Fabrication 44
3.5.2 Modeling of Combustor 48
3.6 Assemble A Combustor Rig 51
3.7 Laboratory Testing 53
3.7.1 Test Results with Air Dilution Only 55
3.7.2 Effects of Steam Rate 57
3.8 Test Results Conclusions 60
3.9 Final Combustor Design and EHPS Interface 63
3.9.1 Full-Scale Test Rig Combustor 63
3.9.2 Fabrication of EHPS Combustor and Turbine Housing 68
3.10 Final Combustor Fabrication and Assembly 72
3.11 Combustor Operating Conditions 75
CHAPTER 4: Develop, Fabricate and Test Water-Steam Heat Exchangers 76
4.1 Goal and Objectives 76
4.2 Approach to Developing and Testing Heat Exchangers 76
4.3 Review of EHPS Design and Operating Objectives of the Steam Generation and Heat Recovery System 77
4.4 Conventional Steam Generation and Heat Recovery Systems 78
4.5 Design and Fabrication of Test Units 84
4.5.1 Innovative Heat Exchanger Design 84
4.5.2 Modeling of Heat Exchangers 86
4.6 Heat Exchanger Test Article Fabrication 88
4.7 Heat Exchanger Test Rig 91
4.8 Laboratory Testing 94
4.8.1 Non-Condensing Test Results 95

4.8.2 Condensing Test Results 97
4.8.3 Boiling Results 101
4.8.4 Demister Design and Test Results 103
4.9 Final Heat Exchanger Design and EHPS Interface 108
CHAPTER 5: EHPS Component Assembly and Checkout Tests 117
5.1 Goal and Objectives 117
5.2 Approach to Component Assembly and Checkout Tests 119
5.3 Description of Key Components 119
5.3.1 Engine Core, Power Electronics and Control 119
5.3.2 Combustor and Housing 123
5.3.4 Heat Exchangers 132
5.3.5 Condensate Collection, Storage and Pumping System 136
5.3.5 Other System Components 137
5.4 EHPS Assembly 142
5.5 System Checkout Tests 146
CHAPTER 6: EHPS CHP Performance Testing 147
6.1 Goals and Objectives 147
6.2 Approach 147
6.3 Test Plan 148
6.3.1 Baseline System Shakedown 148
6.3.2 Rationale for EHPS Component and System Tests 149
6.3.3 Measurement Instrumentation 155
6.3.4 Data Collection 156
6.4 EHPS Performance Tests 159
6.4.1 EHPS Component Tests 159
6.4.2 Heat Recovery System Tests 165
CHAPTER 7: Conclusions and Recommendations 166
GLOSSARY 167

REFERENCES **169**

LIST OF FIGURES

Figure 1: EHPS Process Diagram 2
Figure 2: TA 100 ISO and Non-standard Conditions Performance Predictions 4
Figure 3: Effect of Steam Injection on EHPS Power and Power Efficiency 4
Figure 4: Steam Injection Rate Potential 5
Figure 5: Effect of Turbine Inlet Temperature without Steam Injection on Performance 6
Figure 6: Higher TIT Gives Higher Recuperator Inlet Temperature 6
Figure 7: Recuperator Hot Front End Duty and Volume Estimates 7
Figure 8: Recuperator Thermal Efficiency Impact 8
Figure 9: EHPS Performance with Steam Injection 8
Figure 10: Best EHPS Performance Conditions 10
Figure 11: Reduced Load Baseline and EHPS Power Efficiency Comparison 11
Figure 12: Better Performance Conditions with Enhanced Engine Mass Flow 11
Figure 13: Elliott/Calnetix TA100 Microturbine 18
Figure 14: Inside View of the Engine Compartment 19
Figure 15: TA 100 Component Arrangement of Purchased Engine 19
Figure 16: Microturbine with Planned New Housing for Silo Combustor Retrofit 20
Figure 17: Standard TA100 Combustor Showing Injectors (top view) and Cooling Slots (bottom view) 23
Figure 18: Preliminary View of Steam Injector Combustor Configuration 24
Figure 19: Advanced Silo Combustor Design 24
Figure 20: Combustor Flow with Cyclone Secondary 25
Figure 21: Combustor Flow with Jet Secondary 25
Figure 22: NOx Emissions Results with Steam Injection 26
Figure 23: View of New Modified Turbine Housing for Silo Combustor Configuration 27
Figure 24: Modified Housing with Silo Combustor Developed under Project 500-03-037 27
Figure 25: TA100 Recuperator, External View (top) and Internal Fins (bottom) 28
Figure 26: TA-100 Hot Water Boiler 29
Figure 27: Photograph of Steam Condenser and Boiler 30
Figure 28: Load Bank 31
Figure 29: CMCE Calculated Energy-Mass Balance 36
Figure 30: Standard TA-100 Combustor Showing Injectors (top view) and Cooling Slots (bottom view) 38
Figure 31: TA-100 Turbine Housing Showing Fuel Injector Holes 39
Figure 32: View of Combustor in Turbine Housing 39
Figure 33: Combustor High Temperature Failure 40
Figure 34: Laboratory Measured NOx versus Flame Equivalence Ratio 42
Figure 35: Predicted NOx levels 43
Figure 36: Preliminary View of Steam Injected Combustor Configuration 44
Figure 37: EHPS Test Combustor Illustration 45
Figure 38: EHPS Cyclone Combustor Cutaway Illustration 46

Figure 39: EHPS Complete Combustor Cutaway Illustration 47
Figure 40: View of the Back of Cyclone Combustor 47
Figure 41: Front of Cyclone Combustor 48
Figure 42: Second-Stage Combustor with Heat Exchanger 48
Figure 43: Cutout of Steam-Injected Silo Combustor for Computational Modeling 49
Figure 44: Combustor Flow with Cyclone Secondary 50
Figure 45: Combustor Flow with Jet Secondary 50
Figure 46: Combustor Test Rig at Altex Test Facility 51
Figure 47: Continuous Emission Monitoring Instrumentation 52
Figure 48: NOx Emissions versus Primary Zone Stoichiometry - Air Dilution Tests 56
Figure 49: CO Emissions versus Primary Zone Stoichiometry - Air Dilution Tests 56
Figure 50: Combustor NOx Emissions versus Steam Injection - Rich-Lean Condition 57
Figure 51: Combustor CO Emissions versus Steam Injection - Rich-Lean 58
Figure 52: Combustor Hydrocarbon Emissions versus Steam Injection 58
Figure 53: NOx Results with Steam Injection in Lean-Lean Combustor Configuration 59
Figure 54: CO Emission Results with Steam Injection in Lean-Lean Combustor Configuration . 60
Figure 55: EHPS Combustor NOx Emissions versus Steam Injection 61
Figure 56: EHPS Combustor NOx Emissions versus Combustor Temperature 61
Figure 57: EHPS Combustor NOx versus CO Emissions 62
Figure 58: Full-scale 1-atm test combustor 63
Figure 59: Fabricated Full-scale Test Unit for One Atmosphere Tests 64
Figure 60: New Square Test Section 65
Figure 61: View of Interface between the Combustor and the Exhaust Tube 66
Figure 62: Combustor Emissions of Full-scale Test Cell Unit at One Atmosphere 67
Figure 63: Configuration of New Combustor and Modified Turbine Housing 68
Figure 64: Fabricated Components Prior to Welding and Assembly 69
Figure 65: Fabrication Drawing of the New Turbine Housing 71
Figure 66: Mechanical Drawing of Updated Turbine Housing 71
Figure 67: Diagram of Annular Liner 72
Figure 68: Silo Combustor and Housing Configuration 73
Figure 69: Combustor Igniter Location 74
Figure 70: Fabricated EHPS Steam Injected Combustor 74
Figure 71: Engine Start Sequence 75
Figure 72: Conventional TA-100 CHP System Components 79
Figure 73: External and Internal Photographs of the TA-100 Recuperator 80
Figure 74: Finned Cylindrical Tube Heat Exchanger 81
Figure 75: Finned Cylindrical Heat recovery Heat Exchanger Core 81
Figure 76: Clayton Heat Recovery Boiler 83
Figure 77: Condex Condensing Heat Exchanger 83
Figure 78: Innovative HASF Heat Exchanger Core Design 85
Figure 79: Comparison of HASF and Advanced HMMWV Radiator Performance 85
Figure 80: Heat and Mass Transfer at Exchanger Surface Model Process at Each Location 87
Figure 81: Flattened Copper Coolant Tubes 89

Figure 82: Photograph of Special EHPS HASF Test Article 89
Figure 83: Drawing of HASF Article Manifolds and Overall Structure 90
Figure 84: Manifold End Plates with Some Tubes Inserted 90
Figure 85: Heat Exchanger Test Facility - Heat Exchanger Test Duct Component 92
Figure 86: Heat Exchanger Test Facility - Condensing Component 93
Figure 87: Heat Exchanger Test Facility - Boiling Water Heat Exchanger Duct Component 94
Figure 88: Volumetric Based Heat Transfer Coefficient Comparison 96
Figure 89: Heat Exchanger Coefficient of Performance Comparison 96
Figure 90: Comparison of Special HASF and Conventional Heat Exchanger Heat Transfer Coefficients 97
Figure 91: Comparison of HASF and Conventional Heat Exchanger Pressure Drop 98
Figure 92: Comparison of HASF Heat Exchanger Heat Transfer Coefficients 99
Figure 93: Comparison of HASF Heat Exchanger Pressure Drop 100
Figure 94: HASF Volumetric Heat Transfer Coefficient During Boiling 102
Figure 95: HASF Pressure Drop During Boiling 102
Figure 96: Comparison of HASF Boiling and Non-Boiling Volumetric Heat Transfer Coefficient 104
Figure 97: Commercial Blade Mist Eliminator Configuration and Pressure Drop 106
Figure 98: Test Diameter Droplet Removal Efficiency Versus Face Velocity 108
Figure 99: Demister Pressure Drop versus Face Velocity 109
Figure 100: Decrease in Gas Temperature Along Boiler Length 110
Figure 101: Decrease in Gas Temperature Along the Water Preheater Length 110
Figure 102: Decrease in Gas Temperature Along the Condensed/Heat Recovery Heat Exchanger Length 111
Figure 103: CHRHE Design Side View 112
Figure 104: CHRHE Design Separate Sections - Coolant Inlet and Outlet Side 112
Figure 105: CHRHE Design Separate Sections - Coolant Section Connection Side 113
Figure 106: Heat Exchanger Effectiveness for Multiple Pass and True Counter Flow Design 114
Figure 107: Boiling Water Heat Exchanger (BWHE) Configuration 115
Figure 108: Water Preheater (WPHE) Configuration 116
Figure 109: EHPS Process Diagram 118
Figure 110: TA-100 CHP System 120
Figure 111: TA-100 Component Illustration 121
Figure 112: TA-100 Engine Core 121
Figure 113: Engine Removal Tool 122
Figure 114: TA-100 Power Electronics 123
Figure 115: EHPS CARB 2007 Compatible Steam Injected Silo Combustor and Turbine Housing 124
Figure 116: Silo Combustor Components in Pre-Assembly 125
Figure 117: Fully Assembled Steam-Injected Silo Combustor 126
Figure 118: Combustor Housing Design 127
Figure 119: EHPS New Turbine Housing 128
Figure 120: Close-up of the New Microturbine Housing 128

Figure 121: Close-up of the New Scroll Section 129
Figure 122: Performing a Fit Check by Comparing New and Old Scroll Sections 129
Figure 123: Selected Option for Needed Space 130
Figure 124: Detail of Available Space for Extending the CHP Cabinet 131
Figure 125: CHP Cabinet Rendering Showing Placement of Combustor 131
Figure 126: Section View of Three Heat Exchangers in Place 132
Figure 127: Side (left) and Top (right) Views of Heat Exchanger with the Cabinet 133
Figure 128: Fabricated Boilers Ready for Installation Assembly 134
Figure 129: Condensate Preheater Heat Exchanger 134
Figure 130: Condensing Heat Recovery Heat Exchanger 135
Figure 131: Fabricated Demister Ready for Assembly 135
Figure 132: Heat Exchanger Manifold Structure Picture 136
Figure 133: Condensate Collecting Station 137
Figure 134: Purchased Water Circulating Pump 137
Figure 135: Recuperator to Heat Recovery Heat Exchanger Transition Duct 138
Figure 136: Complete Assembly of Transition, HEX Section, Bypass, and Stack 139
Figure 137: Redesigned Combustor Fuel Control Valve Assembly 140
Figure 138: Natural Gas Compressor 141
Figure 139: Oil Cooling System Tank (bottom), Filter (middle) and Radiator (top right) 141
Figure 140: Cabinet Disassembly for EHPS Reconfiguration 142
Figure 141: Exposed Recuperator for Repositioning 143
Figure 142: HRU Removed from Elliott TA-100 143
Figure 143: Installed Steam-Injected Combustor on New Turbine Housing and Microturbine 144
Figure 144: Assembly of EHPS - Combustor and Microturbine Section 144
Figure 145: Assembly of EHPS - Heat Exchanger Section 145
Figure 146: Completed EHPS Cabinet Package 145
Figure 147: Replaced Encoder Card 146
Figure 148: Failed Inverter Board 146
Figure 149: Emission instrumentation bench 156
Figure 150: Variation in NOx versus SR 161
Figure 151: Variation of NOx with First Stage Gas Temperature 161
Figure 152: NOx versus Steam Flow Rate Relative to Engine Flow 163
Figure 153: CO versus Steam Flow Rate Relative to Engine Flow 163
Figure 154: NOx Emissions with and without Steam versus DReq 164

LIST OF TABLES

Table 1: CHP Estimates for Commercial Facilities 6
Table 2: Technical and Performance Objectives 6
Table 3: Elliott TA-100 Baseline Parameters 3
Table 4: EHPS System Performance Predictions Versus Baseline 9
Table 5: Energy and Mass Balance for EHPS 16
Table 6: Energy and Mass Balance Parameters 17
Table 7: ACA Input Parameters 33

Table 8: Baseline Microturbine Analysis Parameters 34
Table 9: Combustor Operating Conditions for 135 kW Generator Output 35
Table 10: Attained Emission Levels with 8% Steam Injection 37
Table 11: Key Operating Characteristics of Steam Injected Silo Combustor 40
Table 12: CARB 2007 EHPS Emission Targets 41
Table 13: Specifications of Emission Monitors 52
Table 14. EHPS Combustor Test Matrix 54
Table 15: EHPS Combustor Emissions Test Results 55
Table 16: EHPS Combustor Preliminary Emission Test Results 62
Table 17: Heat Exchanger Heat Duties 77
Table 18: Impact of Pressure Drop on Engine Performance 78
Table 19: Advantages of the HASF Design 85
Table 20: Non-Condensing and Condensing Heat Exchanger Test Conditions 93
Table 21: Boiling Water Heat Exchanger Test Condition 94
Table 22: Droplet Separation Methods 105
Table 23: HASF Parameters and Performance for EHPS Heat Exchangers 109
Table 24: EHPS Steam Generation and Heat Recovery Subsystem 116
Table 25: Elliott TA-100 Baseline Parameters 118
Table 26: EHPS Main Components 119
Table 27: Parameters and Performance for EHPS Heat Exchangers 133
Table 28: Elliott TA-100 Baseline Parameters (Source: CMC-Engineering) 148
Table 29: TA-100 Unit Baseline Tests 149
Table 30: 1-Atmphere Pressure Sub-scale Combustor Tests 150
Table 31: One-Atmosphere Full-scale Combustor Tests 151
Table 32: TA-100 Unit Baseline Tests 152
Table 33: Heat Recovery System Tests 153
Table 34: Integrated System Tests 154
Table 35: Data collection and accuracy levels 157
Table 36: Final Emissions Results 160
Table 37: Comparison of Heat Exchanger Performance as Built 165

EXECUTIVE SUMMARY

Introduction

The widespread application of small distributed generation (DG) systems in California depends on the availability of packaged combined heat and power (CHP) systems that are low-cost, have low emissions and are highly efficient. The Public Interest Energy Research (PIER) Program has supported demonstrations of low-cost, clean microturbine-based DG integrated with large industrial burners as a way to address the industrial market for small-scale process-integrated DG. An improved microturbine-based CHP technology is urgently needed to better match power to thermal ratio while also improving power conversion efficiency given the large number of potential DG applications in the commercial/institutional sectors. Importantly, this needs to be achieved at a reduced cost per kilowatt hour (kW) to improve return on investment (ROI) to attractive levels. Lastly, the system must also meet California Air Resource Board (CARB) 2007 emission standards.

Project Purpose

The overall goal of this project was to modify a 100 kilowatt electrical (kWe) Elliott microturbine CHP system to boost power and efficiency to create an Efficient Heat and Power (EHPS) system. The EHPS package relied on overlaying a steam cycle on top of a conventional Brayton cycle in a tightly integrated package to maximize the performance of the components. A key aspect of this modification was to have a recycled pressurized steam loop with a condensing heat exchanger and to replace some of the microturbine combustion air with this steam, reducing the power needed in the compressor while increasing turbine output power with steam injection. This would result in an increase in both power efficiency and specific power. CHP efficiency would be maximized by recovering sensible and latent heat losses.

With these goals in mind the research objectives were to demonstrate that the EHPS could:

- Increase power conversion efficiency of packaged microturbine CHP systems from 30 to 38 percent.
- Increase specific power by 38 percent to 138 kW. This performance objective was reduced from 165 kW to 138 kW due to limitations on steam raising.
- Increase the ratio of electricity to thermal heat delivery from 0.75 to 0.90 to improve the market for commercial and institutional sites.
- Boost overall CHP efficiency for integrated generation and co-production of hot water from current levels of about 70 to 87 percent, thus improving ROI to four or less years.
- Reduce greenhouse gas emissions by nearly 55 percent relative to state-of-the-art microturbine carbon dioxide (CO_2) emissions.

Project Results

This project engineered, designed, fabricated, assembled and tested an EHPS technology based on the conversion of a conventional Elliott TA-100 integrated CHP commercial unit to demonstrate the ability to increase power conversion efficiency and overall CHP efficiency of small-scale distributed generation combined heat and power, satisfying all project objectives. The EHPS was capable of boosting power output to 138 kWe from 100 kWe (a 38 percent power

gain) and achieved an overall combined heat and power efficiency of 87 percent. More importantly, the EHPS could boost the power/heat/loss ratio from the conventional 29/42/30 to 38/49/13, resulting in an overall combined heat and power efficiency of 87 percent.

The technologies developed and demonstrated in this project included a CARB 2007 compliant steam injected silo combustor fitted to a modified turbine housing and scroll assembly and the assembly of three advanced heat exchangers for the production of steam from condensed moisture in the exhaust using a closed loop water recycle system. Each of these components was developed form the laboratory and bench-scale tests, which coupled with detailed engineering and computational modeling provided the confidence to move to full-scale manufacturing. The assembly of these components into a complete EHPS was achieved at the Altex Laboratory together with all necessary support systems for the supply of fuel to the new combustor and the supply of water for the startup tests. The system operational status was checked out and a series of performance tests were undertaken to demonstrate the operational status and performance capability of the completed system.

The silo combustor was proven to achieve less than four parts per million (ppm) nitrogen oxides (NOx) and less than 100 ppm carbon monoxide (CO), corrected to 15 percent oxygen (O_2) with and without steam injection. Each heat exchanger was designed for maximum coefficient of performance resulting in maximum utilization of thermal energy available at the exit of the recuperator and with an acceptable increase in microturbine back pressure. Testing of the full capability of the EHPS was not possible in practice because of limitations of the available generator to 100 kW of power output. System performance analysis therefore relied on testing at a constant 100 kW power output with lower fuel use and added energy from the steam injection. Under these conditions the air compressor operated under less than ideal conditions because of the limitations on the size of the generator.

Future development should concentrate on resolving these development impediments so that the EHPS full capability can be demonstrated in a commercial setting under increased power output without constraints imposed by limitations in commercial generator capacity.

Project Benefits

This project demonstrated the viability of an Efficient Heat and Power System that could increase power conversion efficiency and overall CHP efficiency of small-scale DG CHP systems. Small-scale DG systems can produce electricity that is low-cost, has low emissions and are highly efficient. These systems can reduce electricity consumption, which will in turn reduce greenhouse gas emissions that contribute to climate change as well as other emissions that cause air pollution.

CHAPTER 1: Introduction

1.1 Background

The widespread application of small (<250 kWe), distributed generation (DG) systems in California depends on the availability of packaged combined heat and power (CHP) systems that are low in cost, have low emissions and are highly efficient. Microturbine-based DG CHP systems are attractive because of their good potential to comply with the California Air Resources Board (CARB) 2007 DG emission requirements. The market for these systems can be segmented into two high-potential areas: (1) small to medium-size industries that have high and constant thermal and power needs (i.e., process or district heating and cooling boilers and volatile organic compounds (VOC) thermal oxidizers), and (2) commercial installations (i.e., hospitals, schools, and commercial buildings) that have high power usage, with low and intermittent thermal needs.

The Public Interest Energy Research (PIER) Program has supported demonstrations of low-cost, clean microturbine-based DG integrated with large industrial burners, as a way to address the industrial market for small-scale process-integrated DG. By exhausting microturbines directly into industrial furnaces, the waste heat is recovered very efficiently and at low cost. For these applications, the current power conversion efficiencies of 28-30 percent recuperated, or about 15 percent unrecuperated, have no adverse impact on overall fuel utilization. For commercial and institutional sites, however, the thermal needs are low, intermittent, and of lower quality (i.e., hot water or warm air). Therefore, the 30 percent power conversion efficiency often leaves too much waste heat to be efficiently utilized by the site and results in unattractive Return on Investment (ROI).

Given the very large number of potential DG applications in the commercial/institutional sectors, an improved microturbine-based CHP technology is urgently needed to better match power to thermal ratio while also improving power conversion efficiency. Importantly, this needs to be achieved at reduced cost per kW, to improve ROI to attractive levels. Lastly, the system must also meet CARB 2007 emission standards. By combining recent successful experience in microturbines, ultra low emissions combustors and heat and water recovery heat exchangers, CMCE and Altex Technologies Corporation developed and demonstrated the Efficient Heat and Power System (EHPS) that can boost the net electrical power output and increase the electrical power to heat ratio thus improving the utilization of fuel in CHP systems for onsite power generation and diminish the dependence on waste heat recovery.

Small (<250kWe) integrated microturbine CHP systems from vendors, such as Capstone, Ingersoll-Rand (now Flex Energy), and Elliott Energy Systems (now Capstone), are limited in power conversion efficiency to about 30 percent, and overall CHP efficiencies on the order of 70 percent. This power conversion efficiency is low compared to that for modern central power plants (45-58 percent), or even a mix of older and modern plants (38-40 percent). In addition, cost per kW output is a high $2000 to $2500/kWe installed, relative to under $1000/kWe for large

gas-fired modern power plants. This makes DG relatively noncompetitive, and increases the dependence of DG success on the maximum utilization of waste heat in CHP configurations. For many commercial/institutional sites, this has resulted in four critical hurdles to potential users:

1. The capital investment cost is a relatively unattractive $2,000 to $2,500/kWe that, when combined with the lower power conversion efficiencies, results in a simple payback of 5 to 7 years at today's spark spreads, even with existing California PUC SGIP credits. Surveys show [7] that only 10 percent to 30 percent of users would accept 5 to 7 year paybacks, leaving most of the large commercial market untapped. By boosting power conversion efficiency and specific power output, as noted above, the proposed EHPS technology would reduce paybacks from 5-7 to 2.5-4.0 years, improving CHP acceptance to 40-60 percent.

2. Current DG systems must fully rely on CHP thermal heat recovery to minimize payback time. The low 30 percent/70 percent power to heat ratio limits application of conventional systems to the large commercial/institutional markets because the waste heat cannot be fully utilized or power generation is forced into an uneconomical size range. The DOE-compiled data, shown in Table 1 [7], indicate that electrical to thermal energy needs are typically higher than conventional CHP levels. CHP systems that have higher power to waste heat production, such as EHPS, are ideal.

3. When microturbine load is reduced to match the variable thermal or electrical needs of the site, power conversion efficiency rapidly falls off from the already modest 30 percent efficiency. The EHPS, besides having higher full load power conversion efficiency, also has even higher part load efficiency versus conventional systems. This is a significant advantage for EHPS.

4. High overall conventional CHP efficiencies are difficult to achieve, because these systems utilize high dilution, or excess air, which makes it costly to extract most of the sensible heat from the hot exhaust. Latent heat recovery is totally impractical. With the EHPS, excess air is reduced, because steam is used to displace air, making exhaust moisture condensation possible. CHP efficiencies are then 87 percent, versus 70-75 percent for conventional CHP.

1.2 Project Goals and Objectives

The overall goal of this project was to modify a 100 kWe Elliott microturbine CHP system to boost power and efficiency. To achieve this overall goal, the EHPS package relied on overlaying a steam cycle on top of a conventional Brayton cycle in a tightly integrated package that will maximize the performance of components. A key aspect of this modification was to have a recycled pressurized steam loop with condensing heat exchanger and to replace some of the microturbine combustion air with this steam, reducing the power needed in the compressor while increasing turbine output power with steam injection. This would result in an increase in both power efficiency and specific power. CHP efficiency would be maximized by recovering sensible and latent heat losses.

Table 2 summarizes the specific performance objectives of the EHPS.

Table 1: CHP Estimates for Commercial Facilities

Application	Total MW Potential	Number of Units	CHP Sales Estimates (Million $)	Power to Thermal Ratio	
				Total	Water heating only
Hotels/Motels	3269	2624	264	0.83	1.19
Nursing Homes	3851	1014	101	0.90	1.69
Hospitals	1551	647	65	0.90	1.69
Schools	13911	7130	713	0.67	1.94
Colleges/Universities	628	221	22	0.67	1.94
Commercial Laundries	462	183	18	0.90	1.69
Car Washes	281	253	25	0.90	1.69
Health Clubs/Spas	3504	665	67	0.82	1.19
Golf Clubs	1410	836	84	0.83	1.19
Museums	275	73	7	1.13	5.77
Correctional Facilities	778	261	26	0.89	1.94
Water Treatment/Sanitary	794	452	45	1.33	9.29
Restaurants	2975	2802	280	2.47	5.25
Supermarkets	1100	897	90	5.93	23.86
Refrigerated Warehouses	579	131	13	1.46	12.92
Office Buildings	12578	7523	752	1.13	5.77

Table 2: Technical and Performance Objectives

Parameter	Current CHP	EHPS
Electrical Efficiency at Full Load	30%	38%
Full Load Power, kWe	100	165[1]
Electrical Efficiency at 50% Load	24%	34%
NOx, lb/MWh (CARB 2007 CHP Limit)	0.07	0.07
CO, lb/MWh (CARB 2007 CHP Limit)	0.10	0.10

Parameter	Current CHP	EHPS
VOC, lb/MWh (CARB 2007 CHP Limit)	0.02	0.02
Electrical Power/Recoverable Heat Ratio	0.67-0.75	0.78
Fuel Utilization in CHP Mode	70-75%	87%
Return on Investment, years	5-7	2.5-4.0
CO2, lb/MWh	163	88

(1) This increase was reduced to 138% based on engineering analysis of maximum steam that can be raised with heat exchangers

Therefore, the project sought to demonstrate that the EHPS can:

- Increase power conversion efficiency of packaged microturbine CHP systems from 30 to 38 percent
- Increase specific power by 38 percent to 138 kW. This performance objective was reduced from 165kW to 138kW due to limitations on steam raising
- Increase the ratio of electricity to thermal heat delivery from 0.75 to 0.90 to improve market for commercial and institutional sites
- Boost overall CHP efficiency for integrated generation and co-production of hot water from current levels of about 70 percent to 87 percent
- Thus improving ROI to four or less years
- Reduce the greenhouse gas emissions by nearly 55 percent relative to state of the art microturbine CO_2 emissions.

1.3 Project Approach

To demonstrate this technology, the approach was to modify a conventional 100 kWe recuperated microturbine-generator (MTG) from Elliott Energy Systems (EESI) with a CARB 2007-compliant silo combustor with steam injection for emissions control and added mass throughput to boost power output. Waste heat recovery would then be achieved with a compact steam boiler and condensing heat exchanger that provide a self-contained closed water loop that achieves maximum overall efficiency without the need for makeup water. Coupled with heating of process water, the power to thermal ratio is boosted to 0.88.

Steam injection technologies have been employed in large utility gas turbines using air humidification and steam from heat recovery steam generators (HRSG) [8, 9] to boost power output. However, with steam injection overall turbine efficiency is reduced unless the latent heat of the moisture in the exhaust is somewhat recovered. This was attempted with a combination of compact non-condensing and condensing heat exchangers, to produce an 87 percent overall CHP efficiency. The steam injection in the combustor is also used to reduce NOx to CARB 2007 compatible levels, using a special design combustor.

CHAPTER 2:

Engineer and Model CHP System and Components

2.1 Goal and Objectives

The goal of this task was to perform detailed engineering analyses of the entire EHPS CHP system and each component, to arrive at design and operating specifications for the performance of the entire system. Specifically, the deliverables of this task are summarized below:

- Prepare a list of performance objectives and operational attributes of the CHP system
- Prepare an energy and mass (E&M) balance system diagram
- Conduct computational modeling of the entire process using process analysis and Computational Fluid Dynamics (CFD) software
- Prepare an engineering analysis of the silo combustor, with higher required firing rates and steam injection
- Analyze combustor prototype design NOx and CO performance using CFD and proprietary software
- Analyze needed air compressor, turbine, and generator modifications
- Analyze water-steam loop and performance specifications
- Evaluate startup and part load microturbine operation requirements
- Analyze alterations needed for recuperator with steam injected combustor and potential design alterations for turbine housing and scroll sections.

2.2 Approach to Engineering and Modeling

EHPS preliminary performance improvements are principally the result of the planned steam injection, along with associated upgrades that result in enhanced performance for the total package. Some of the upgrades were considered relatively easy to adapt to existing engine designs. However, some upgrades would require more modifications, and related development and testing, to prove. In the following sections, both relatively easy and more challenging upgrades are described, along with their impacts on EHPS performance. As noted in Table 2, meeting EHPS performance goals will result in substantial improvements in power efficiency, at full and part load, power output and overall (i.e. power plus heat recovery) efficiency. This results in fuel savings versus the conventional CHP (i.e. TA100) system, and importantly a reduction in simple payback of 2.5 to 4.0 years. This is a much more attractive payback than the 5 to 7 years for the conventional CHP system. In addition, the higher overall efficiency results in the net CO_2 conventional systems, as given in Table 2. Lastly, because of the better performance of EHPS, CARB 2007 emissions targets are easier to meet, as shown by the larger CARB 2007 targets in Table 2. However, because EHPS required a special ultralow NOx combustor,

emissions will be substantially lower than the limits, benefiting air quality where EHPS is deployed.

2.3 EHPS Process, Predicted Performance and E&M Balances

The project team relied on the proprietary computational models for turbine engine performance analyses. The model was modified to adapt to the EHPS configuration shown in Figure 1. The model uses a lumped parameter approach for all major components, including engine compressor, combustor, turbine, generator, recuperator, and heat recovery heat exchangers. By inputting performance factors for all of these components, overall system performance can be rapidly calculated. Many engineering tradeoff studies can then be accomplished to define the needed design and operating conditions to meet the performance goals as listed in Table 2. Also, the approach will identify the engine component performance factors that will have to be met to achieve the overall performance targets.

Figure 1: EHPS Process Diagram

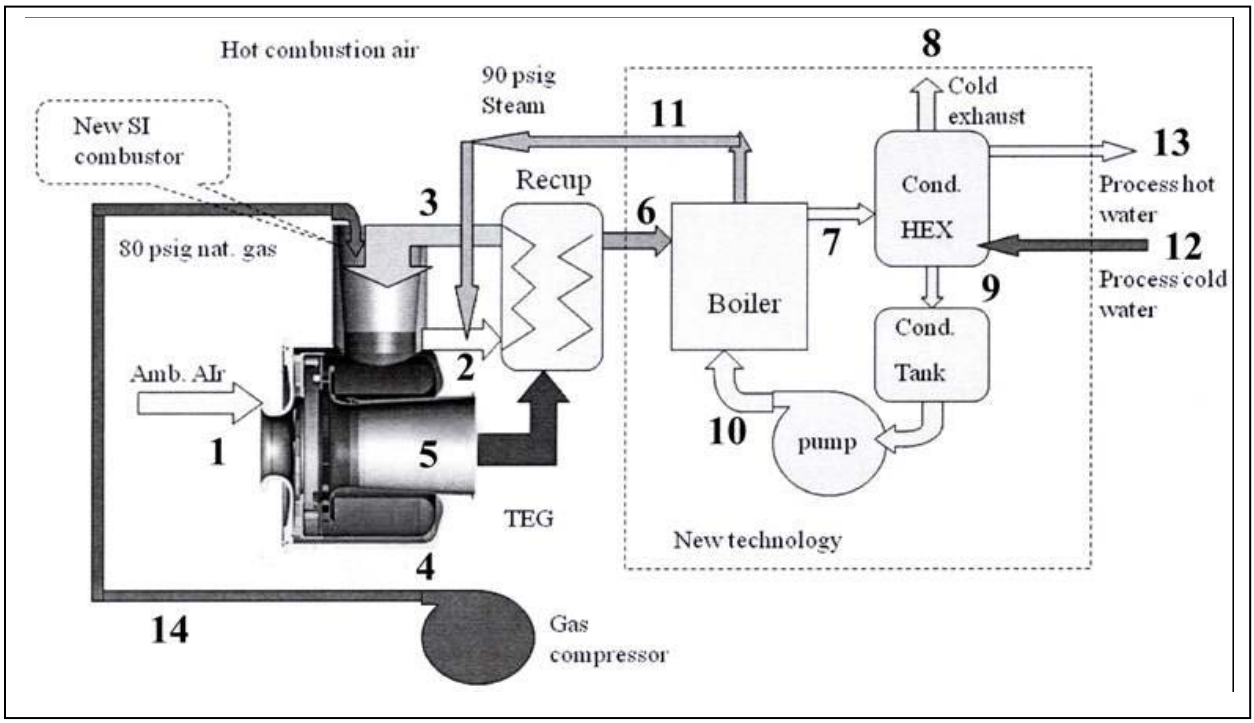

The computer model for turbine engine was modified to adapt to the EHPS configuration. Source: CMC-Engineering

The models were used and validated on conventional type microturbine designs prior to the EHPS effort. To adapt the model to predict EHPS performance, modules for boiler, condenser and steam injection were incorporated into the base model. Three sets of predictions were run. In the first set, the model was used to predict the performance of an Elliott TA100 recuperated engine, for reference purposes. Predicted performance compared well with tested performance, validating the ACA model. In the second set of calculations, EHPS specific components (i.e. boiler, condenser, steam injection) were activated in the model with a slightly modified Elliott

TA100 engine as the core of the EHPS system. The EHPS power, power efficiency and overall efficiency were significantly improved versus the baseline TA100 engine. In the third set of calculations, additional microturbine engine modifications were combined with advanced heat exchangers. Power, power efficiency, and overall efficiency for this advanced EHPS system met project goals.

As per the first set of predictions, the updated model was run with the Elliott TA100 design and operating condition parameters, as given in Table 3, and power and efficiency were calculated for Independent System Operator (ISO) and higher ambient temperature conditions.
Figure 2 presents these predicted results over a range of ambient conditions, including the ISO condition (i.e. 59 °F and sea level pressure). The ISO results matched the Elliott published performance numbers. Also, the falloff of power and efficiency with increasing ambient temperature matched the behavior for commercial engines. These results further validated the ACA model.

Table 3: Elliott TA-100 Baseline Parameters

Parameter	Value
Turbine Inlet Temperature	1600°F
Pressure Ratio	4
Stoichiometric Ratio	2.4
Stagnation Pressure Loss	10%
Recuperator Effectiveness	82%
Compressor Efficiency	80%
Turbine Efficiency	82%

Source: CMC-Engineering

In the second set of EHPS calculations, the effectiveness of steam injection rate, turbine inlet temperature, and heat exchanger (boiler and condenser) and pressure drops were varied, while the engine pressure ratio was held fixed at four. Figure 3 gives the predicted variation of power and power efficiency with steam injection rate, with other parameters fixed at modest TA100 levels, as given in Table 2. As shown in the figure, as steam injection rate increases, both power and power efficiency substantially increase, exceeding 37 percent efficiency at 20 percent steam injection. However, as shown in Figure 4, high engine recuperator exhaust temperatures are needed to meet the high steam rates, without supplemental firing. For the baseline engine, the exit temperature is in the range of 600F, which supports a steam injection rate of about 80 percent. For higher steam injection rates and performance, without supplemental firing, additional engine modifications are needed to raise exhaust energy.

Figure 2: TA 100 ISO and Non-standard Conditions Performance Predictions

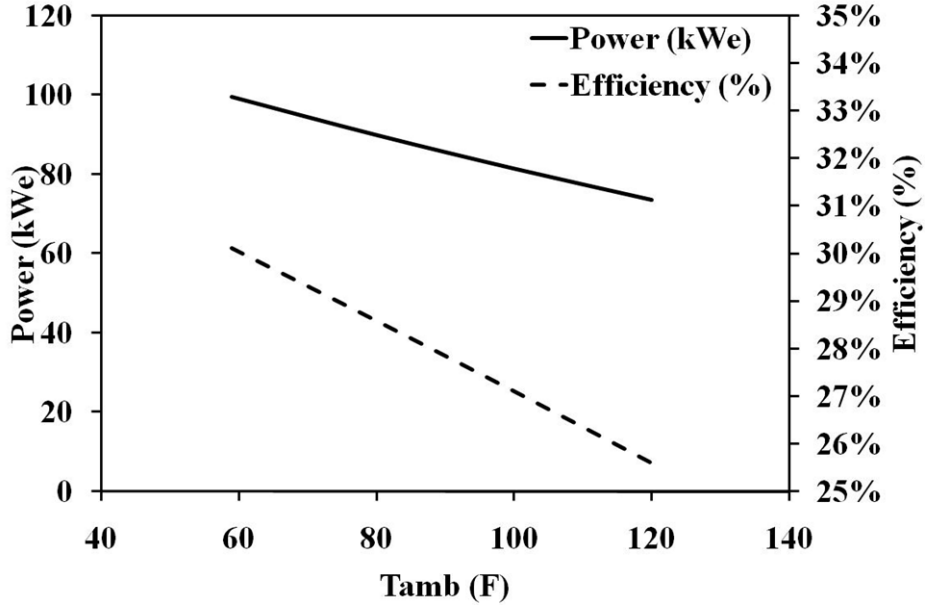

This figure presents predicted results over a range of ambient conditions, including the ISO condition (i.e. 59 °F and sea level pressure).
Source: Altex Technologies Corporation

Figure 3: Effect of Steam Injection on EHPS Power and Power Efficiency

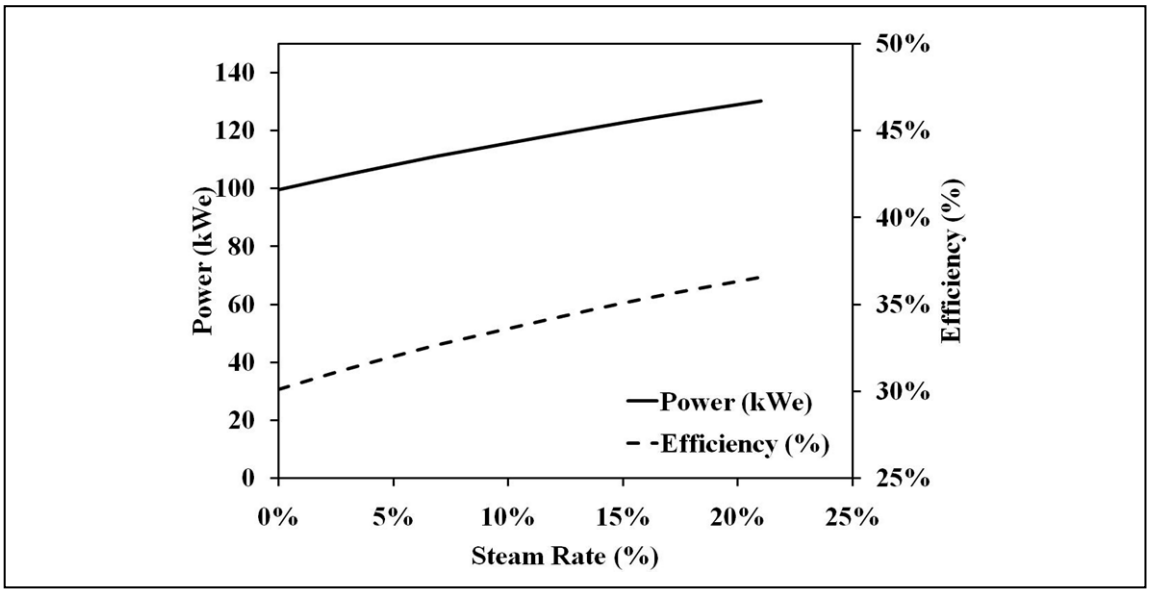

This figure shows the predicted variation of power and power efficiency with steam injection rate, with other parameters fixed at modest TA100 levels.
Source: Altex Technologies Corporation

Figure 4: Steam Injection Rate Potential

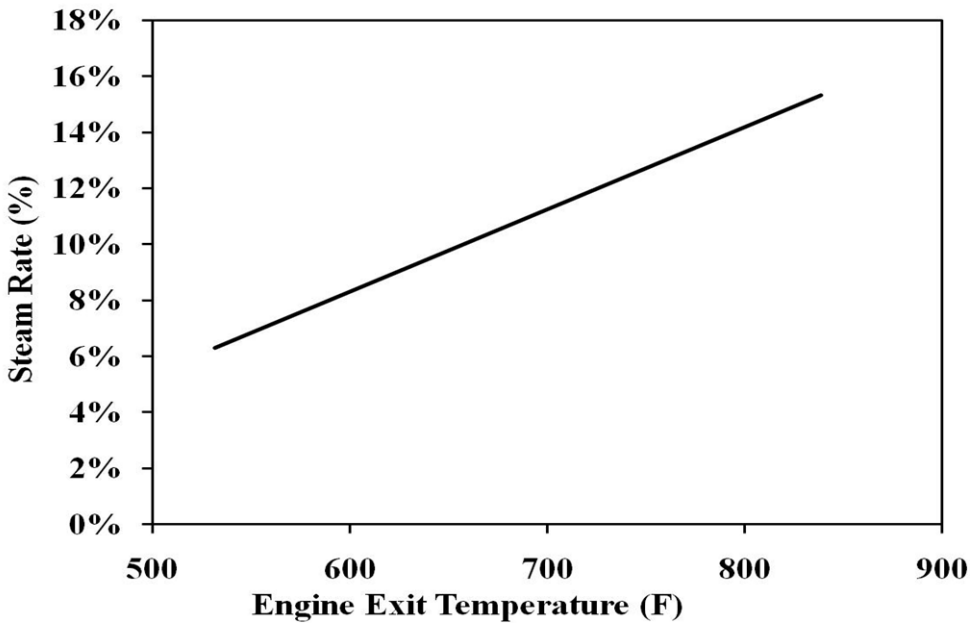

This figure shows that the high engine recuperator exhaust temperatures are needed to meet the high steam rates, without supplemental firing
Source: Altex Technologies Corporation

An important parameter to engine performance is Turbine Inlet Temperature (TIT). Increasing TIT substantially increases both power and power efficiency. Current TA100 engine TIT is limited to approximately 1600°F, as a result of combustor and recuperator design and durability constraints. However, with EHPS, both the combustor and recuperator designs will be upgraded to meet CARB 2007 limits as well as to ease the constraint on TIT. Therefore, these component updates, as described below, will provide an opportunity for increasing TIT and engine performance.

Figure 5 gives the power and power efficiency improvements as a function of TIT, for no steam injection. As shown, increasing TIT from the low baseline level to 1800°F substantially increases both power and power efficiency. By combining steam injection with TIT improvements, EHPS performance can be increased to near goal levels. It should be noted that increasing the TIT also increases recuperator inlet temperature, as shown in Figure 6. This would put additional stress on the standard TA100 recuperator. However, with EHPS, an improved recuperator "hot front end" will be incorporated into the engine to address the increased recuperator inlet temperature (see Section 8). Since the recuperator uses a counter-flow design, the hot front end section will only have a limited heat transfer duty, as shown in Figure 7, compared with the downstream recuperator section that uses less expensive materials. Therefore, the cost increment for this important performance enhancement feature will be limited.

Figure 5: Effect of Turbine Inlet Temperature without Steam Injection on Performance

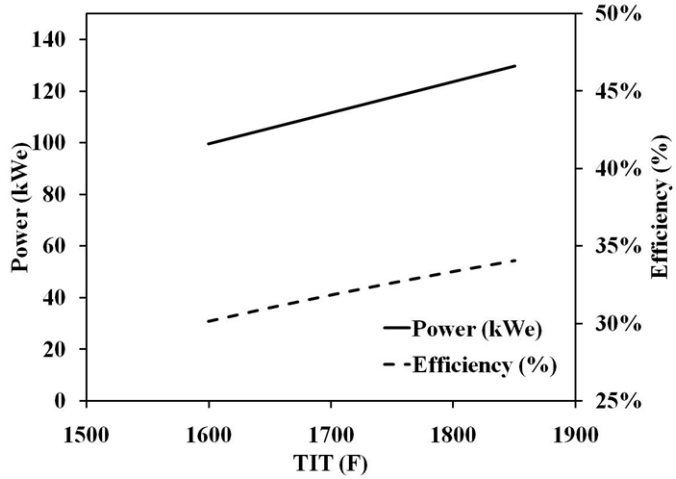

Source: Altex Technologies Corporation

While incorporating a recuperator hot front end promotes higher performance by accommodating higher TIT, increases in recuperator effectiveness has only a minor impact on performance for practical heat exchanger volume increases. **Figure 8** shows the variation of power and power efficiency as recuperator effectiveness varies over the range of interest. As shown, over a practical range of effectiveness levels, engine performance changes are modest. Given this behavior, the baseline recuperator effectiveness of 82 percent was maintained in the final design.

Figure 6: Higher TIT Gives Higher Recuperator Inlet Temperature

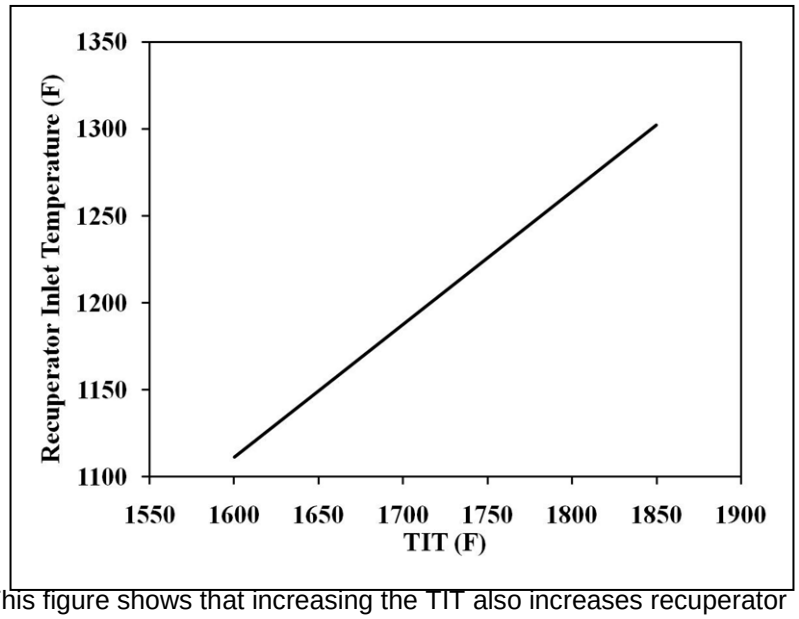

This figure shows that increasing the TIT also increases recuperator inlet temperature.
Source: CMC-Engineering

Figure 7: Recuperator Hot Front End Duty and Volume Estimates

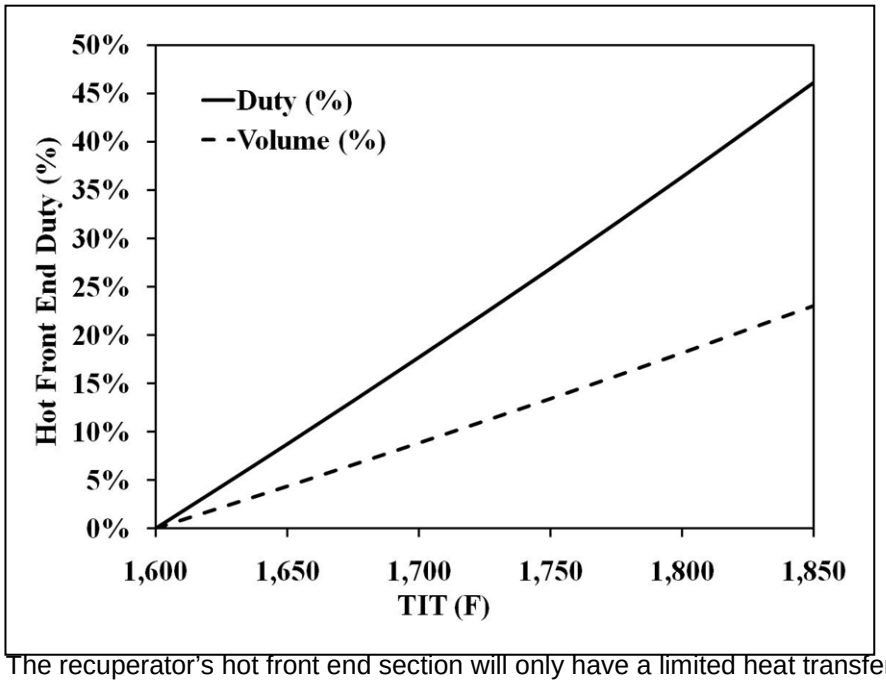

The recuperator's hot front end section will only have a limited heat transfer duty as shown in this figure.
Source: Altex Technologies Corporation

Combining steam injection at the achievable level, with TIT enhancement, the EHPS performance at a pressure ratio of four was calculated for a range of TITs. These results, given in Figure 9, show that power and power efficiency results are near the EHPS goals, even for a modestly modified TA100 type engine. With these limited parameter variations, power output and power efficiency and overall efficiency, reached the levels shown in Table 3. Even for these non-optimal conditions, EHPS performance is significantly better than the baseline TA100 results. However, to fully meet the EHPS goals, additional engine modifications would be needed.

Figure 8: Recuperator Thermal Efficiency Impact

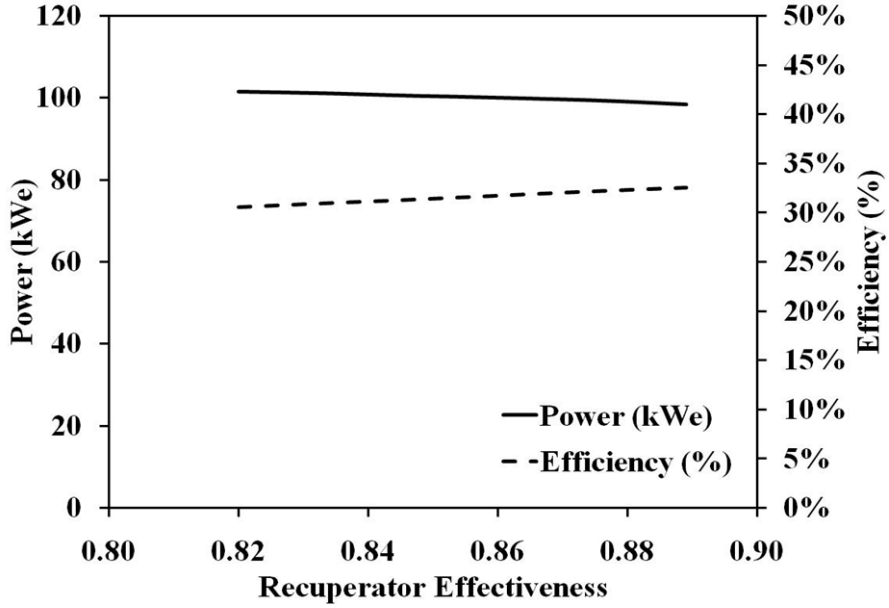

This figure shows the variation of power and power efficiency as recuperator effectiveness varies over the range of interest.
Source: Altex Technologies Corporation

Figure 9: EHPS Performance with Steam Injection

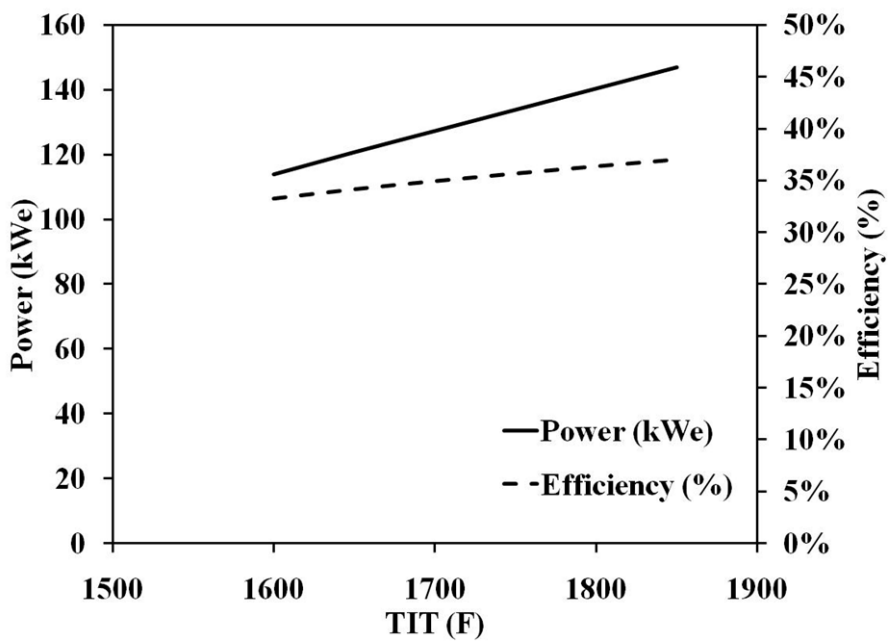

This figure shows that power and power efficiency results are near the EHPS goals, even for a modestly modified TA100 type engine.
Source: Altex Technologies Corporation

Table 4: EHPS System Performance Predictions Versus Baseline

System	Power Efficiency (%)	Power (kWe)	Overall Efficiency (%)
Baseline Elliott TA100	30%	100kWe	76%
EHPS Using TA100 Core	35.7%	134kWe	84%

This table shows that at a pressure ratio of six, a TIT of 1800F and compatible steam injection rate (i.e. no supplemental firing) the EHPS target goals are achieved.
Source: CMC-Engineering

In the third set of calculations, baseline turbomachinery efficiency parameters were maintained, but engine speed and pressure ratio, as well as steam rate, turbine inlet temperature and heat exchanger effectiveness and pressure drops, were varied. Figure 10 gives the best performance results for compatible (i.e. no supplemental firing) steam injection rates from 8.7 percent to 13 percent for three TIT levels (i.e. 1700°F, 1750°F, and 1800°F) and increasing pressure ratio. The left most point on each TIT curve is for the baseline pressure ratio of four. Moving along the curves to the right, each next point shown on the curve represents an increment of one in pressure ratio. As shown, power is substantially increased with pressure ratio for all TIT levels. However, beyond a limit, efficiency starts to decrease, even while power increases. A compromise has to be reached to meet both power and power efficiency targets. At a pressure ratio of six, a TIT of 1800F and compatible steam injection rate (i.e. no supplemental firing), the EHPS target goals are achieved, as shown in Table 3. While the pressure ratio of six is a modest level compared to larger gas turbine power systems, this pressure ratio is difficult to achieve in a single stage turbomachinery design. However, rather than a highly loaded and less efficient single stage turbomachinery design, such as in the TA100, a lightly loaded (i.e. stage pressure ratio of 2.5) and more efficient two-stage design could be utilized in EHPS.

Higher turbomachinery efficiency will further enhance both EHPS power and efficiency. As an alternative to turbomachinery multi-staging, a single stage approach at a pressure ratio of five could be selected, with the engine speed or compressor flow passage volume increased to enhance engine mass flow and power at a fixed efficiency. This approach is illustrated by results in Figure 11. Results in Figures 10 and 11 indicate that EHPS target levels can be reached via several design approaches. This flexibility can be beneficially used in design tradeoffs to identify the most reliable and low cost approach for meeting EHPS performance goals. Besides very good full load performance, EHPS also has very good part load performance. As load is reduced in the baseline TA100, and like engines, the fuel flow and TIT are reduced to match engine load to the external need. As shown in Figure 5, reductions in TIT cause a substantial reduction in both power efficiency and power. With a conventional engine, the falloff in efficiency with load is very substantial, as illustrated in Figure 12. However, with EHPS, steam injection can be reduced to match load at a fixed TIT. This will help to maintain a higher efficiency at reduced load. This is illustrated in Figure 12, where the EHPS efficiency remains nearly parallel to the conventional engine baseline efficiency as load is reduced. The fuel

savings increment over full load is 18 percent for EHPS versus the baseline. This is another advantage of the EHPS.

Figure 10: Best EHPS Performance Conditions

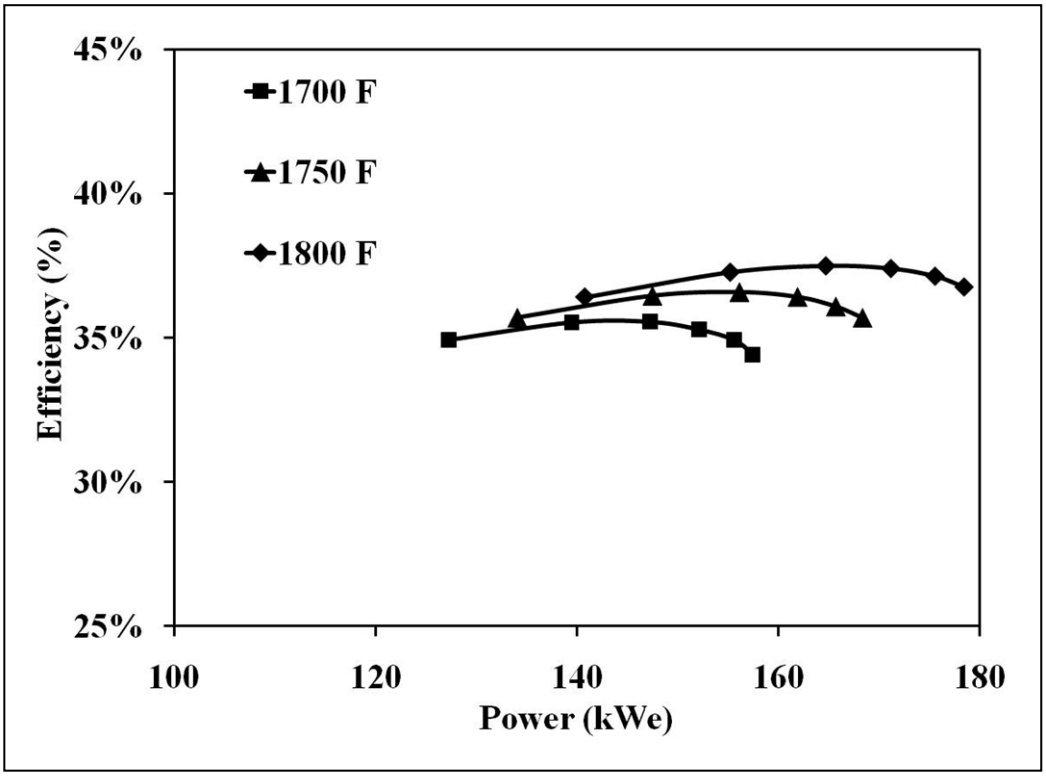

This figure shows the best performance results for compatible (i.e. no supplemental firing) steam injection rates from 8.7% to 13% for three TIT levels (i.e. 1700°F, 1750°F, and 1800°F) and increasing pressure ratio.
Source: Altex Technologies Corporation

Figure 11: Reduced Load Baseline and EHPS Power Efficiency Comparison

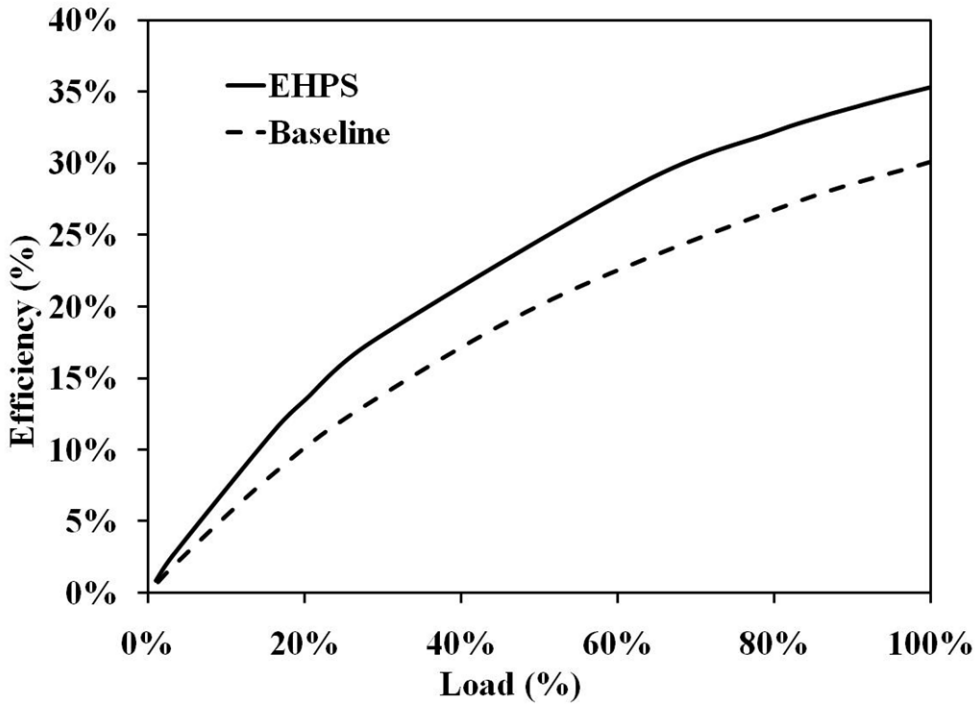

Source: CMC-Engineering

Figure 12: Better Performance Conditions with Enhanced Engine Mass Flow

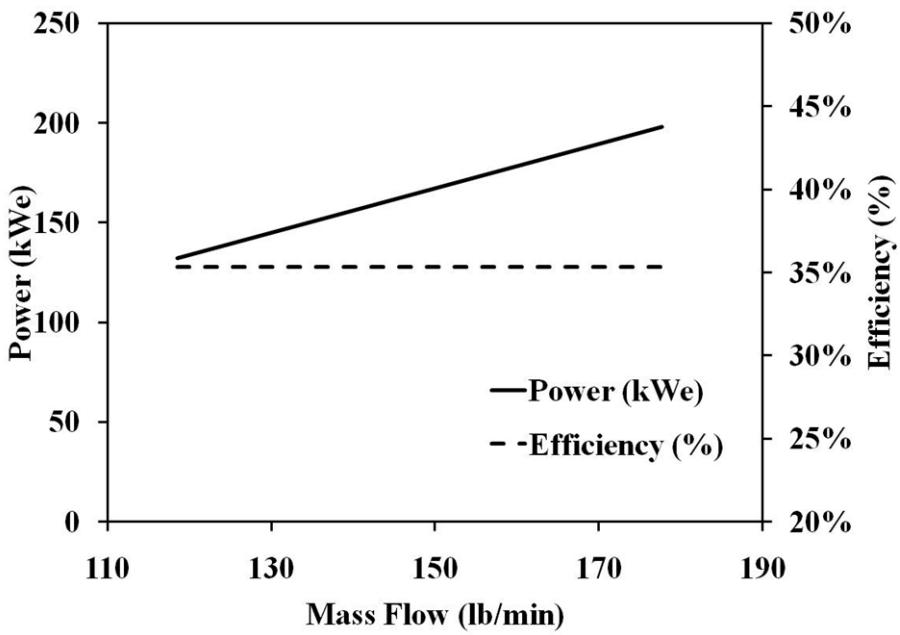

Source: Altex Technology Corporation

As part of the performance prediction efforts under Task 2, several EHPS mass and energy balances were calculated using process software customized for EHPS. Table 4 gives an example of the mass and energy balance for EHPS for the design and operating conditions listed in Table 5.

Using our conventional and advanced component engine and heat exchanger experience, a reasonable range of parameters was considered, as listed in Table 5, for this EHPS process analysis. As indicated in Figure 9, these conditions yield a power level of 133kWe and a power efficiency of 35 percent. These, and like results, will support component development efforts in Tasks 3 and 4. The EHPS requires compact and low-cost heat exchangers to condense exhaust water, heat the collected condensate and boil the recycled condensate ahead of steam injection into the TA-100 engine. In addition, a high temperature recuperative heat exchanger is required for maximizing power production efficiency. Process analysis has defined the duty requirements for each of these heat exchangers.

Table 5: Energy and Mass Balance for EHPS

	1	2	3	4	5	6	7’	7	8	9	10PRIME	10	11	12	13	14
TEMP(F)	59	387	1096	1747	1252	543	318	262	110	110	298	110	298	65	138	380
PRESS(PSIA)	15	59	55	53	17	16	15	15	15	15	67	66	65	50	49	85
TOTAL MDOT(LB/HR)	6460	6964	6964	7028	7028	7028	7028	7028	6525	504	504	504	504	10000	10000	65
AIR(LB/HR)	6460	6460	6460	6460	6460	6460	6460	6460	6460	0	0	0	0	0	0	0

Source: Altex Technologies, Corporation

The System locations listed in Table 4 are identified as follows:

1. Compressor air inlet
2. Compressed air to recuperator
3. Heated compressed air from recuperator
4. Turbine inlet
5. Hot exhaust from power turbine
6. Hot exhaust from recuperator
7. Hot exhaust from steam boiler
8. Exhaust from heat recovery (condensing) heat exchanger
9. Condensed water from heat recovery heat exchanger
10. Water inlet to boiler
11. Steam from boiler to recuperator inlet (mixed with compressed air
12. Condensing heat exchanger cold water inlet
13. Condensing heat exchanger hot water outlet
14. Compressed fuel gas to combustor

Table 6: Energy and Mass Balance Parameters

Parameter	Value
Turbine Inlet Temperature	1747°F
Pressure Ratio	4
Stoichiometric Ratio	2.4
Stagnation Pressure Loss	
Recuperator Effectiveness	82%
Compressor Efficiency	80%
Turbine Efficiency	82%

Source: Altex Technologies Corporation

The EHS requires compact and low-cost heat exchangers to condense exhaust water, heat the collected condensate and boil the recycled condensate ahead of steam injection into the TA-100 engine. In addition, a high temperature recuperative heat exchanger is required for maximizing power production efficiency. Process analyses, as illustrated by the results in Table 4, defined the duty requirements for each of these heat exchangers. Table 4 indicates that the amount of steam used by the engine is equal to the amount of condensate from the engine exhaust. This eliminates the need for make-up water, which is an important aspect of the self-contained CHP assembly package. The cold process water was given a 65°F inlet temperature, with an outlet temperature of 138°F for the flow rate of 10,000lb/hr, or a heat recovery of 730,000Btu/hr. The overall efficiency, given 133kWe of power, is then 91.3 percent, which is a very high efficiency level. This high efficiency is a result of the extraction of the latent heat of vaporization in the exhaust by condensing exhaust moisture. Other water based heat recovery conditions can be considered to extract heat and condense water for use in steam injection. Numerous commercial and institutional water heating uses are possible with EHPS, such as pool water, process water heating and space heating. The exhaust temperature of the gas leaving the EHPS will be reduced to 110°F, which is the condensation temperature for the steam injected engine considering combustion generated moisture and air relative humidity.

2.4 Microturbine Test Bed for EHPS

The prior section presented process analysis results for EHPS considering a modestly modified TA100 engine as a base or a more extensively modified engine for fully optimized performance. Given the high expense and risk of developing a completely new engine to demonstrate EHPS principles, the modestly modified TA100 engine EHPS test bed approach was selected for this effort. Based on good EHPS results achieved under this effort, more extensively modified engines can be tested in future efforts to demonstrate optimal performance. Figures 13, 14, and

15 illustrate the TA100 test bed engine purchased for this project with match funds from Southern California Gas Company (SCG). Figures 13 and 14 give external and inside-the-cabinet component arrangement pictures, respectively. Figure 15 gives the inside-the-cabinet layout of components. Figure 16 illustrates the dimensions of the power generation components consisting of the generator, compressor, and power turbine.

The major components of the TA100 that will require modification or additions to implement the EHPS are as follows:

- Microturbine air compressor
- Steam injected ultra-low emission silo combustor
- Recuperator
- Steam boiler
- Condensing heat exchanger

Figure 13: Elliott/Calnetix TA100 Microturbine

This photograph illustrates the TA100 test bed engine purchased for this project with match funds from Southern California Gas Company.
Photo Credit: Elliott Energy Systems

Figure 14: Inside View of the Engine Compartment

This photograph illustrates the inside view of the TA100 test bed engine purchased for this project with match funds from Southern California Gas Company.
Photo Credit: CMC-Engineering

Figure 15: TA 100 Component Arrangement of Purchased Engine

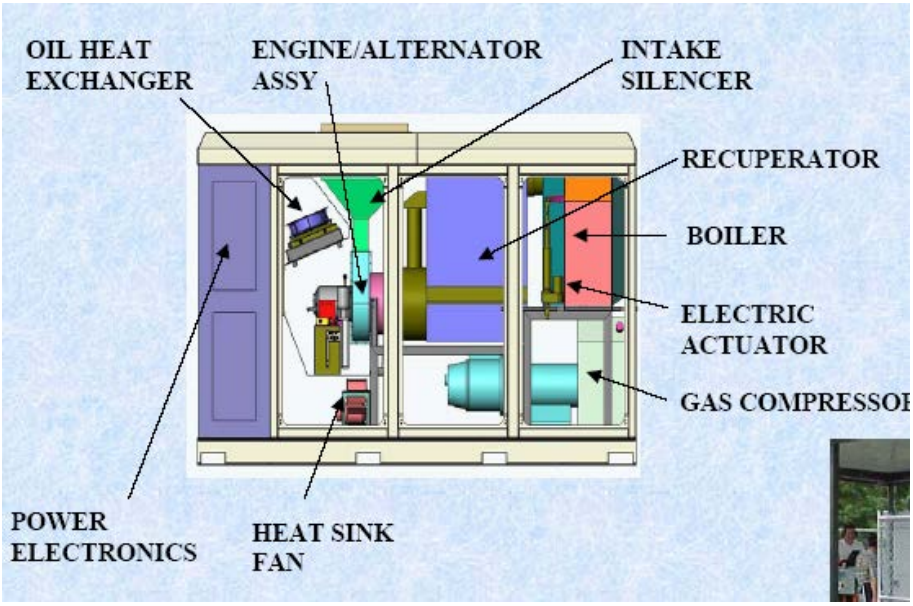

This photograph illustrates the inside-the-cabinet layout of components for the TA100 test bed engine purchased for this project with match funds from Southern California Gas Company.
Source: Calnetix Power Solutions

The component-specific performance, outlined in Table 6, was used to formulate the design specifications, such as dimensions, configuration and coefficient of performance for the CARB2007 compatible combustor and each of the three heat exchangers.

Figure 16: Microturbine with Planned New Housing for Silo Combustor Retrofit

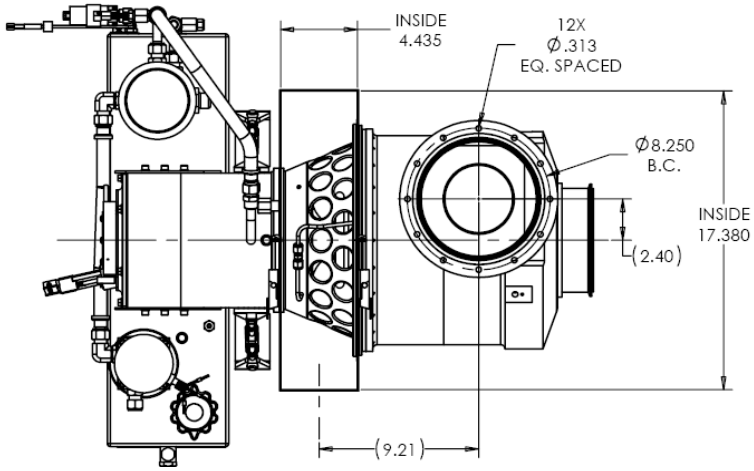

This figure illustrates the dimensions of the power generation components consisting of the generator, compressor, and power turbine.
Source: Calnetix Power Solutions

A series of tests were performed on the engine to evaluate its mechanical readiness. The engine was spun to full speed without power generation. A second series of tests was then performed to evaluate the Power Electronics readiness and to test the ability of the system to reach 135 kW of power. The engine fuel was delivered using a set of six compressed methane tanks in order to bypass the gas compressor and be able to deliver approximately 1.4 MMBtu/hr of fuel required by the engine at 100 kWe load. The bypass of the compressor was necessary because the current Altex facilities do not have the gas service necessary to provide this higher firing rate. The engine operation was proven satisfactory and the Power Electronics was determined to be able to handle the increased power output targeted with the EHPS.

The following sections highlight the performance specifications of each major component and resulting implications on design and testing requirements needed to validate EHPS performance.

2.5 TA-100 Microturbine Compressor

The EHPS modifications will increase the specific power (i.e. power per air mass flow) of the engine. At the planned power level, the microturbine test bed will operate with a reduced combustion air flow rate to avoid exceeding the power capability of the baseline generator. This will be accomplished by simply bleeding air from the compressor diffuser. In the production unit, the compressor will be trimmed to achieve the required reduced air flow versus the turbine flow at the planned power level. The steam from the boiler will replace some of the air

displaced. This will allow the combustor to fire at a higher firing rate and will result in greater specific power from the engine. Firing rate to the steam injected combustor will reach about 1.5 MMBtu/hr or about 17 percent increase from a conventional TA100 microturbine. The engine exhaust temperature was calculated to reach 1252°F at ISO conditions, which is higher than that of the standard TA100 version. This higher temperature into the recuperator will be addressed by the special EHPS recuperator to be implemented on the engine.

Higher power output from the generator will principally be the result of the lower energy demand for the air compressor, the increase in mass throughout the turbine with steam injection and an increase in turbine inlet temperature. The turbine exit temperature will be maintained below the design level to retain the integrity of the turbine and downstream components.

Figure 9 illustrates the anticipated increases in power conversion efficiency and total specific power for various levels of turbine inlet temperature and 7.7 percent steam injection. As presented in the last monthly report, the fuel firing rate for the combustor is set at 65 lb/hr, or 1.36 to 1.413 MMBtu/hr (HHV). The total air flow to the engine is set at 6,460 lb/hr. Steam injected levels are targeted for the new design at 504 lb/hr, or about 3,500 ft^3/hr of saturated steam at 55 psig. Therefore, the amount of steam injected relative to the total air and fuel flow to the engine corresponds to about 7.7 percent, which gives an increase in power to 133kWe relative to a conventional engine at 100kWe. Efficiency is 35 percent versus the conventional engine efficiency of 30 percent. This represents a fuel savings of 17 percent for power production.

As indicated above, the test bed engine will yield more power. At this time, we believe that the engine generator and power electronics can handle the anticipated 133 kWe power. However, additional generator and electronics heat dissipation loads may cause the components to run hotter than the design limits. The unit has safety trips to shut the engine down if this becomes a problem. If this is a limitation, we will add additional cooling to the generator oil cooling loop and electronics to expand power generation capacity to the required level.

2.6 Ultra Low NOx Combustor

The conventional TA100 microturbine uses a partial oxidation combustor illustrated in Figure 17. This combustor uses an annular fuel injection system consisting of 12 injectors introducing fuel gas with a tangential velocity. By only introducing a portion of the needed air, this part of the combustor can be reduced in volume. Also, temperatures are constrained because stoichiometric combustion conditions are initially avoided. The remaining air needed for clean combustion is then added downstream via cooling holes, slots and via an annulus around the combustor liner exit. Insufficient combustion air in this first zone produces lower peak temperatures and partial synthesis of the fuel gas. Although the partial oxidation combustion (POC) is a reliable method for engine ignition, this combustor design produces excessive NOx emissions or about four times that allowed under CARB 2007 standards. Furthermore, this

design has suffered numerous failures in the field due to high temperature metal fatigue at the cooling slots and eventual melting of the "fingers" causing catastrophic turbine failures after a relatively short operating life.

Given these significant limitations of the baseline combustor, the annular combustor was to be replaced with an advanced premixed silo design that is also capable of steam injection. A preliminary design for the combustor is illustrated in Figure 18. The combustor utilizes two fuel-lean stages that allow further minimization of peak flame temperature with higher stoichiometric ratio. Also, steam would be injected with the combustion air to control flame temperature and NOx. Use of the steam will prevent high local temperatures from being reached and thereby reduce NOx emissions as well as reduce degradation of combustion materials. Note that the combustor is scheduled to utilize about 500 lb/hr of steam (about 1 gpm of water). The compressed gas flow to the combustor accounts for 1.5 MMBtu/hr compared to a conventional fuel use of 1.36 MMBtu/hr (HHV). The extra fuel coupled with the steam will provide additional power conversion for a higher generating capacity. Air flow to the turbine will be reduced but the steam will add to the mass flow to generate the needed increase in power. The total mass throughput of the engine is set at 7,028 lb/hr for increased electrical power.

Preliminary engineering analyses and computational work preceded the actual design and fabrication of the EHPS steam-injected combustor. The engineering analysis was based on the design illustrated in Figure 19. In this design, a cyclonic type swirler was introduced in the primary zone, rather than the plate swirler illustrated in Figure 18. This gives a higher level of primary stability and turndown, compared to a plate swirler configuration. Furthermore, with steam injection, the heat load on the liner is reduced and any degradation mitigated. While the primary cyclone produces good stability, using a cyclonic action in the secondary zone results in excessive combustor volume to achieve the needed burnout. This was shown by CFDesign calculations. Figure 20 gives the combustor flow pattern with a cyclonic secondary combustor burnout zone. As shown, the active flow areas in the combustor are near the combustor periphery, with a slow moving recirculation zone occupying the central region. This slow moving recirculation zone is very important for stabilizing the primary zone. However, this is not needed for the high temperature burnout zone. In this downstream zone, jets can replace swirl as the primary and secondary gas mixing mechanism. Figure 21 presents this revised secondary mixing zone design flow pattern. As shown, the slow-moving central zones given in Figure 20 are replaced with more active jet mixing zones. This will better utilize the secondary combustion volume. Also, by going to a secondary jet configuration, the burnout zone has more of a plug flow character, which helps to avoid the carryover of pollutants from upstream zones and thereby fully minimize emissions for CARB 2007 compatibility.

Figure 17: Standard TA100 Combustor Showing Injectors (top view) and Cooling Slots (bottom view)

This photograph shows the conventional TA100 microturbine using a partial oxidation combustor.
Photo Credit: CMC-Engineering

Figure 18: Preliminary View of Steam Injector Combustor Configuration

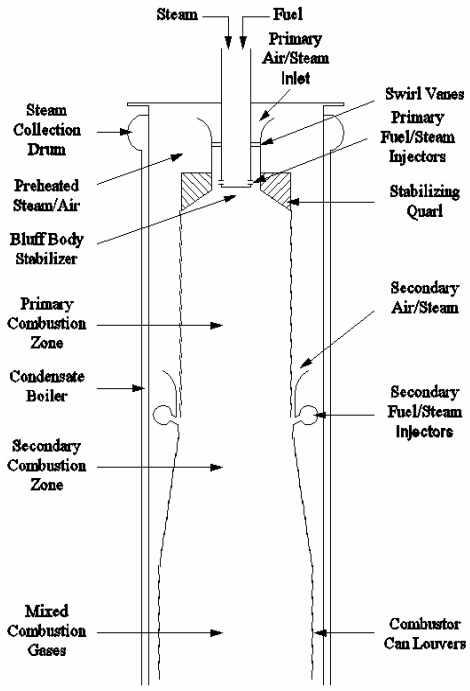

Source: Altex Technologies Corporation

Figure 19: Advanced Silo Combustor Design

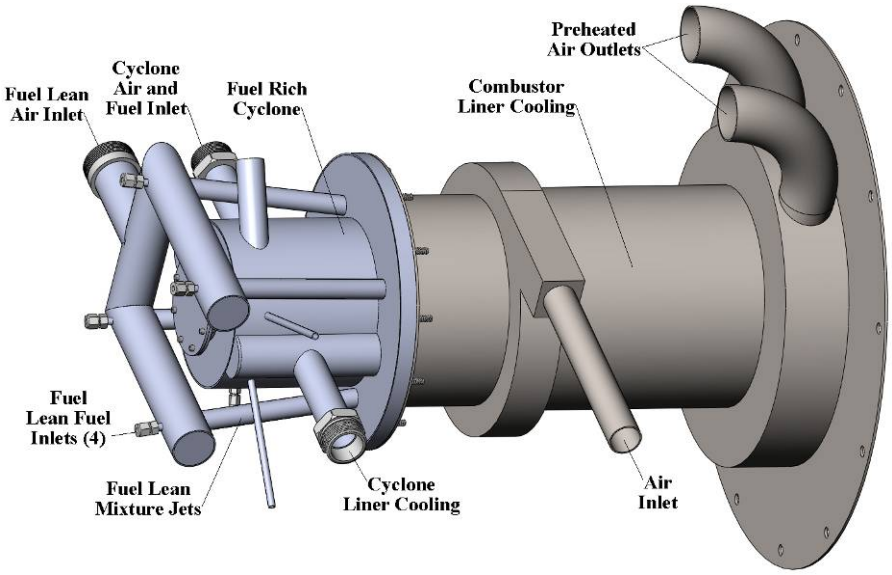

Preliminary engineering analyses and computational work is based on the design.
Source: Altex Technologies Corporation

Figure 20: Combustor Flow with Cyclone Secondary

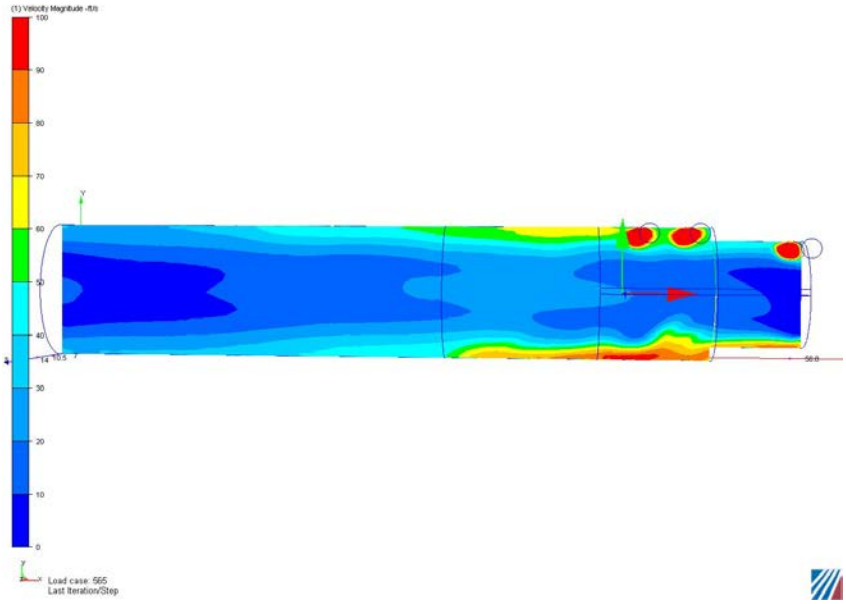

This figure gives the combustor flow pattern with a cyclonic secondary combustor burnout zone.
Source: Altex Technologies Corporation

Figure 21: Combustor Flow with Jet Secondary

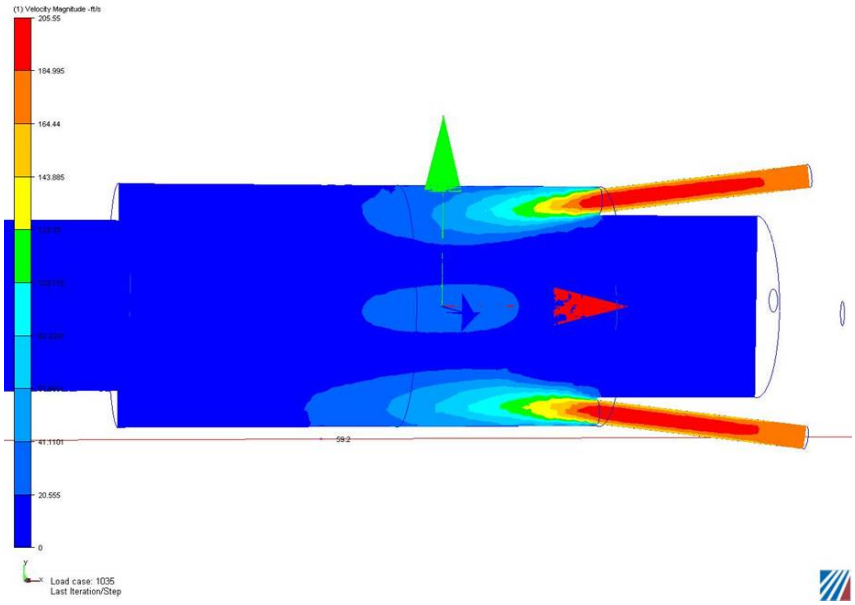

The slow-moving central zones shown in Figure 20 are replaced with more active jet mixing zones.
Source: Altex Technologies Corporation

Emissions performance that the new combustor would have to meet are dictated by the CARB 2007 emission levels of 0.07 lb/MWh and CO emissions of 0.7 lb/MWh, corresponding to

concentration levels of 4 and 10 ppm at 15 percent oxygen based on overall power conversion efficiency of 35 percent and overall CHP efficiency of 90 percent. Prior test results and proprietary emissions correlations were used to estimate the emissions profile for one set of steam injection conditions. These results are shown in Figure 22. This preliminary analysis shows that steam injection can assist in NOx reduction even at the higher firing rates necessary for EHPS goals of higher power. As shown by earlier data on the concept, CO emissions will be controlled with enhanced jet mixing and sufficient residence time, as guided by the computational analysis illustrated in Figure 20.

The fabrication design of the silo combustor would have to consider the use of an outer shell to allow the combustion air to enter the recuperator for preheating and returning preheated air to the combustor. A new turbine housing would also be necessary to adapt the silo combustor that would sit outside the engine enclosure. The approach for housing modification needed by the EHPS was based on the development and demonstration work supported by the Commission under project 500-03-037. The modified turbine housing used in the earlier project is illustrated in Figure 23. Figure24 shows a drawing of how the housing was integrated with the engine. The new housing for the EHPS would have to consider some of the features of the current Elliott design to maintain the functionality of the recuperated configuration to integrate with the heat recovery in the recuperator.

Figure 22: NOx Emissions Results with Steam Injection

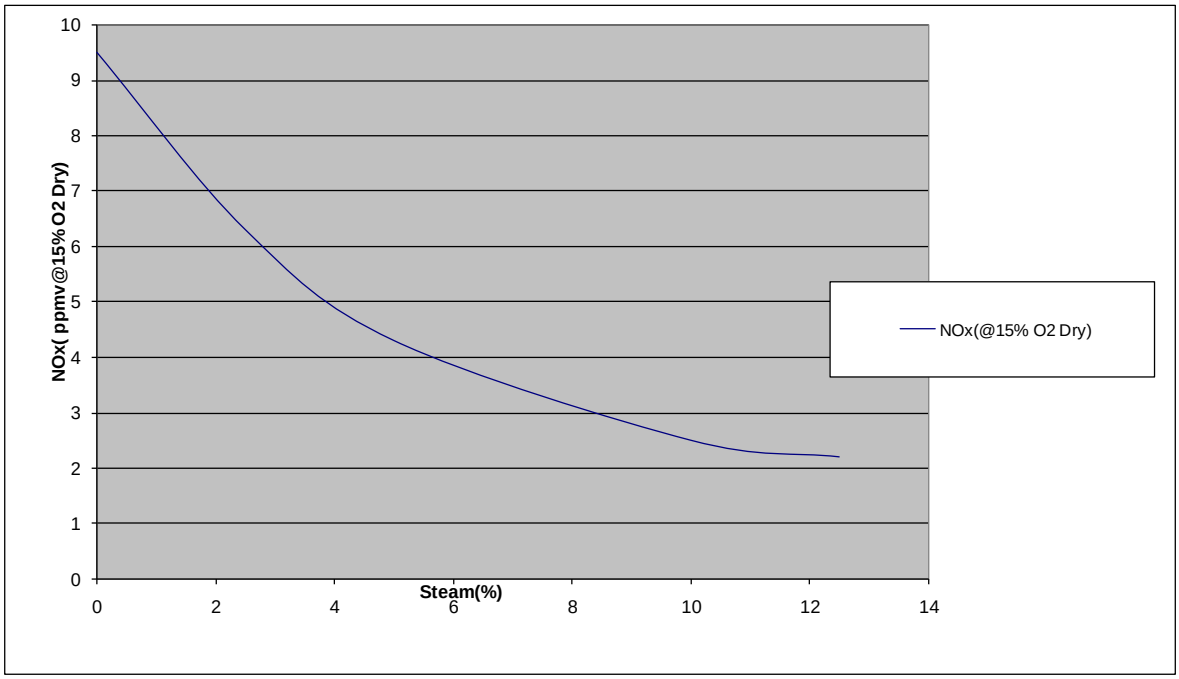

Source: CMC-Engineering

Figure 23: View of New Modified Turbine Housing for Silo Combustor Configuration

This figure shows the housing design used in a prior Energy Commission project that employed a modified TA100 engine test bed.
Photo Credit: CMC-Engineering

Figure 24: Modified Housing with Silo Combustor Developed under Project 500-03-037

Photo Credit: CMC-Engineering

2.7 Recuperator

Figure 25 shows the conventional TA100 recuperator available on a recuperated TA-100 engine. This original recuperator was used for the EHPS to retain this portion of the conventional TA-100. A new hot front was contemplated for the EHPS design as a way to enhance the durability and longevity of the recuperator. However, this may be needed in a commercial version of the EHPS to handle the higher turbine inlet temperatures and resolve the durability issues of the current recuperator. A modification to the air inlet connecting duct that sends compressed air to the recuperator inlet was also necessary to allow for the steam injection and recuperator modifications.

Figure 25: TA100 Recuperator, External View (top) and Internal Fins (bottom)

These photographs show the conventional TA100 recuperator available on a recuperated TA100 engine.
Photo Credit: Calnetix Power Solutions

2.8 Boiler and Condensing Heat Exchangers

Currently, the TA-00 CHP unit has a heat exchanger, identified in Figure 26 as heat recovery unit (HRU) that uses cold inlet water to extract heat from the exhaust and produce 140°F

process water, thus boosting overall CHP efficiency to 70 percent. However, this is a relatively large and inefficient unit that will be replaced with two more advanced heat exchangers to perform the two functions described above. In addition, the EHPS would require two additional heat exchangers. The first heat exchanger (boiler) is designed to be used to extract heat from the exit of the recuperator to produce steam for the steam-injected combustor. The second heat exchanger is used to extract the final heat from the exit of the steam generator using cold process water. The latter, or a separate demister, would function to condense the moisture in the exhaust to provide a self-generating reservoir of water for steam conversion and to increase the overall EHPS CHP efficiency to our target of 84 percent.

Figure 26: TA-100 Hot Water Boiler

The TA100 CHP unit has a heat recovery unit (HRU) used to produce 140°F process water.
Photo Credit: CMC-Engineering

The heat exchanger process analysis included EHPS heat exchanger component performance, weight, volume and cost assessments. Ahead of designing advanced compact and low-cost heat exchangers to meet these requirements, available conventional heat exchangers were reviewed to assess best practices and fit with the EHPS requirements. This assessment provided a contrast to the advanced heat exchangers proposed for use in the EHPS. Based on a survey of available equipment, a Clayton Industries heat recovery boiler and a Condex condensing heat exchanger were defined as conventional heat exchanger candidates that could be used in EHPS. While these components meet the heat duty requirement, it was concluded that these conventional heat exchangers were too large and costly for use in EHPS. A part of the high cost is associated with some custom manufacturing to adapt these heat exchangers to the application of interest. Nevertheless, the large scale and weight of these heat exchangers is a significant disadvantage

for EHPS. The proposed advanced heat exchangers will substantially shrink heat exchanger volume, as well as lower cost for comparable materials. Recent match funds work has shown this potential on sub-scale test articles. Figure 27 illustrates the Altex condenser design subjected to preliminary evaluation of performance for this application. Results showed that the advanced condenser had superior performance. Tests indicated that the flow power to drive the heat transfer for the special heat exchanger would be 50 percent lower than a conventional heat exchanger. This directly translates into improved engine performance. Special heat exchanger component assessments will be completed during the next reporting period.

The boiler is set to absorb about 680,000 Btu/hr dropping the temperature of the gas exiting the recuperator from 543°F to 252°F. This heat will be used to generate 504 lb/hr of steam for the condensed moisture in the flue gas. The process hot water exiting the microturbine is set at 138°F. This water can be used in installations directly for high temperature heating and sanitation activities. Further reductions in temperature from this level for applications such as pool heating will be possible for higher water flow rates.

Figure 27: Photograph of Steam Condenser and Boiler

Photo shows the Altex condenser heat exchanger design.
Photo Credit: Altex Technologies Corporation

In parallel with heat exchanger assessment and subscale tests, condensate water quality impacts on heat exchanger materials were identified. Starting with deionized water in the EHPS reservoir, it was determined that the nitric acid content in the condensate would be insignificant, with carbonic acid content leading to a pH of 4.85. If stainless steel and polymer surfaces are used in the system, then the carbonic acid level is acceptable, and no recycled condensate water treatment will be required. This reduces system complexity, maintenance and operating costs.

2.9 Auxiliary Equipment

Testing of the TA-100 in its original configuration and modified for EHPS operation was done at the laboratory and not at Elliott in Florida, as originally planned. To assist in loading the generator and monitor power output, the project team made use of the load bank illustrated in Figure 28. This piece of hardware was available from a prior Energy Commission project and purchased with SCG match funds and provided to the project by CMC-Engineering. An evaluation of the Power Electronics modules indicated that the generator could be loaded to a maximum of 108 kWe output and the electronics components are capable of handling a higher power output. However, because of generator limitations, the project team would be restricted to maintaining the current rating on the total generation for the EHPS.

Figure 28: Load Bank

To assist in loading the generator and monitor power output, the project team will make use of the load bank
Photo Credit: CMC-Engineering

CHAPTER 3:

Combustor Design Specifications

3.1 Goal and Objectives

Task 2 results, discussed in Chapter 2, defined the energy and mass (E/M) balance of the EHPS and the operating conditions for each key component of the EHPS. This effort was critical to validate that the efficiency and power output gains of the EHPS were thermodynamically achievable and what design and operating conditions would be necessary in the steam-injected combustor and in other key EHPS components in order to achieve these performance levels and limit emission for compliance with CARB 2007 levels. This section reviews these system analysis results and their impact on the design and operation of the steam-injected combustor. In addition this chapter addresses the following key technical objectives related to the design and fabrication of the steam-injected combustor:

- Specify the operating requirement of the steam-injected silo combustor
- Design a prototype combustor unit
- Fabricate a test unit
- Assemble a test rig to perform tests
- Perform laboratory tests to validate attainment of key performance goals and other key operating conditions
- Optimize combustor design and operating conditions

3.2 Approach to Combustor Design

The operating requirements of the steam-injected combustor are defined by the operating conditions of each component that are necessary to achieve the EHPS overall performance goals. For example, the amount of steam necessary to boost the power output from 100 kW to 138 kW must be equal to the amount of steam that can be efficiently condensed in the heat exchanger section of the EHPS so to achieve a closed loop water-steam cycle. Steam injection rate and turbine inlet temperature (TIT) define the additional power that can be extracted by the turbine. Compliance with CARB 2007 emission limits in the steam injected combustor must then be achieved with that amount of steam, flame equivalence ratio and TIT. These bulk combustor outlet conditions (i.e., turbine inlet location) define the localized flame condition in the combustor where NOx is formed and overall CO and HC emissions are controlled to meet the CARB 2007 emission limits.

In order to define the operating conditions of each system component in the EHPS, the project team employed computational thermodynamic analyses performed independently by Altex and CMC-Engineering. The mathematical model used by Altex relied on a lumped parameter

approach for all major components, including engine compressor, combustor, turbine, generator, recuperator, and heat recovery heat exchangers. By inputting performance factors for all of these components, overall system performance can be rapidly calculated. Many engineering tradeoff studies can then be accomplished to define the needed design and operating conditions to meet the performance goals as listed in **Table 7**. Also, this approach can identify the engine component performance factors that will have to be met to achieve the overall performance targets.

Table 7: ACA Input Parameters

- Air, steam and fuel flows
- Inlet stream pressures and temperatures
- Turbomachinery pressure ratios
- Turbomachinery efficiencies
- Heat losses
- Heat exchanger effectiveness
- Heat exchanger pressure loss coefficients

To adapt the model to predict EHPS performance, modules for boiler, condenser and steam injection were incorporated into the base model. Three sets of predictions were run. In the first set, the model was used to predict the performance of an Elliott TA100 recuperated engine, for reference purposes. Predicted performance compared well with tested performance, validating the model. In the second set of calculations, EHPS specific components (i.e. boiler, condenser, steam injection) were activated in the model with a slightly modified Elliott TA-100 engine as the core of the EHPS system. The EHPS power, power efficiency and overall efficiency were significantly improved versus the baseline TA100 engine. In the third set of calculations, additional microturbine engine modifications were combined with advanced heat exchangers. Power, power efficiency, and overall efficiency for this advanced EHPS system met project goals.

To predict the baseline TA100 system performance, the parameters listed in Table 8 were input into the Altex model. Pressure ratio, flow rate and fuel-to-air ratio were obtained from published results. From these, a turbine inlet temperature of 1600°F was estimated that was compatible with turbine exit temperatures. Compressor and turbine efficiencies were estimated based on typical small radial turbomachinery results. These were compatible with published recuperated engine exhaust temperature and turbine exhaust temperature for unrecuperated engines.

As per the first set of predictions, the updated model was run with the Elliott TA-100 design and operating condition parameters, as given in Table 7, and power and efficiency were calculated. As part of the performance prediction efforts under Task 2, several EHPS mass and energy balances were calculated using process software customized for EHPS over a range of ambient conditions, including the International Organization for Standardization (ISO) condition (i.e. 59 °F and sea level pressure). These conditions yielded a gross power level of 133 kWe and a power efficiency of 35 percent and an overall EHPS efficiency of 82 percent and a power conversion efficiency of 38 percent.

Table 8: Baseline Microturbine Analysis Parameters

Turbine Inlet Temperature, F	1747
Compressor efficiency	80%
Turbine efficiency	82%
Stagnation Pressure Loss	9%
Recuperator effectiveness	82%
Overall pressure loss	11%
Pressure ratio	4
Air/fuel stoichiometric ratio	2.4

In order to validate these results, CMCE performed a thermodynamic analysis focusing on the combustor and turbine performance with steam injection rates set by the Altex analysis. The results of this analysis are shown in Figure 29. The input parameters for the analysis were derived from the ACA model results and included the 504 lb/hr of steam injected, the turbine inlet temperature of 1,747 F, and compressor and turbine efficiencies of 80 and 82 percent respectively. As in the Altex model, the analysis was performed under ISO conditions. Under this scenario, the amount of fuel calculated to be about 79 lb/hr corresponding to a firing rate of 1.54 MMBtu/hr (LHV). The calculated generator gross power output was estimated at 130 kWe.

Table 9 compares the results of the two independent analyses and lists the key requirements for the silo combustor when operating in steady state conditions, namely with steam injection and rated power output conducive to the performance goals of the EHPS.

Table 9: Combustor Operating Conditions for 135 kW Generator Output

Combustor Operating Parameters	ACA Model	CMCE Model
Air Flow, lb/hr	6,460	6,460
Fuel Flow, lb/hr	65	79
Steam Flow, lb/hr	504	504
Combustor Exit Temperature, F[(1)]	1,747	1,740
Pressure, ATM	4.0	4.0
Steam Temperature, F	298	298
Turbine Exit Temperature, F	1,096	1,096

1. Combustor exit temperature is same as Turbine Inlet Temperature (TIT)

Figure 29: CMCE Calculated Energy-Mass Balance

Natural Gas (LHV)	Btu/lb	kJ/kg
	19,570	45,422
Isentropic Efficiency,	η	
* *Compressor*	0.80	
* *Turbine*	0.82	
* *Generator*	0.99	
Specific Heat Ratio		
* *Compressor*	1.37	
* *Turbine*	1.28	
Mass Flowrates, m	*lb/hr*	*kg/s*
* *Air*	6,460	0.8157
* *Steam,. Mst at loc 2*	504	0.0636
* *Fuel. mf into combustor*	79	0.0099
Steam P - psia, bar	80	5.44
Steam T - F, C	312	156
Compressor inlet (1)		
T - F, C	60	15.6
P, psia, bar,	14.7	1.0
H1 - Btu/lb, kJ/kg	-	0.0 Ref
Compressor Outlet (2)		
T - F, C	354.8	179
P, psia, bar,	58.80	4.0
H2 - Btu/lb, kJ/kg	72	167
Compressor W - MBtu/hr, kW	0.465	136
Compressor Air from Recup (2')		
T - F, C	1096	591
P, psia, bar,	58.80	4.0
H2' - Btu/lb, kJ/kg	249.7	580
Combustor Outlet (3)		
T - F, C	1740	949
P, psia, bar,	58.80	4.00
H3 - Btu/lb, kJ/kg	420	975
DH3 - Btu/lb, kJ/kg		117
cp(st) - Btu/lbF, kJ/kgK	0.542	2.27
Specific Fuel Consumption	0.012	0.012
Mfuel - lb/hr, kg/s	79	0.0099
Firing Rate - MMBtu/hr, MJ,hr	1.54	1,626
(Mst-Mfuel)/Mfuel	5.40	5.40
Turbine Exit (4)		
T - F, C	1,268	687
P, psia, bar,	14.7	1.0
H2 - Btu/lb, kJ/kg	290	673
Generator output, kWt		132
Generator output, kWe		130

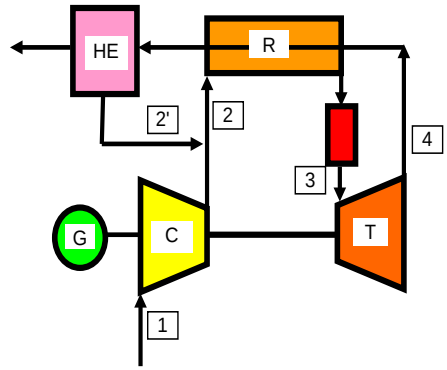

Temperature Increase in Compressor

$$T_2 - T_1 = \frac{T_1}{\eta_c}\left[\left(\frac{p_2}{p_1}\right)^{\frac{k-1}{k}} - 1\right]$$

Specific Fuel Consumption

$$\beta = \frac{H_3 - H_2 + \frac{\dot{m}_{st}}{\dot{m}_{air}} cp_{st}(T_3 - T_{st})}{LHV - H_3 - (1 + \frac{\dot{m}_{st} - \dot{m}_f}{\dot{m}_f} DH_3)}$$

Fuel Consumption

$$\dot{m}_f = \beta \bullet \dot{m}_{air}$$

Temperature of Turbine Exit

$$T_4 = T_3 - \left(T_3 - T_2)\eta_T \bullet \left(1 - \frac{1}{\left(\frac{p_4}{p_3}\right)^{\frac{k-1}{k}}}\right)\right)$$

CMCE performed a thermodynamic analysis focusing on the combustor and turbine performance with steam injection rates set by the ACA model; the results of this analysis are shown in this figure.
Source CMC-Engineering

Bench-scale experiments performed under a wide range of stoichiometries in the first and second stage and with a range of steam injection levels provided valuable input on the ability of the combustor to achieve target emission levels while maintaining stable combustion during

transients. During these tests, the combustion air was preheated to simulate recuperator outlet temperatures of approximately 1,100 F and with 300 F steam injection rates varying from 6 to 15 percent on a volumetric basis. EHPS performance targets were based on a steam injection rate of approximately 8 percent. Eight percent steam injection is equivalent to 504 lb/hr of steam or about 1 gpm

Table 10 summarizes the emission results of the parametric tests. The data illustrates that compliance with CARB 2007 emission limits was possible with this design in both the rich-lean and lean-lean conditions in the two zones of the silo combustor.

Table 10: Attained Emission Levels with 8% Steam Injection

Emissions	CARB 2007 Limits	Attained Emissions	
		Rich-Lean	Lean-Lean
NOx, ppm @ 15% O_2	4.33	2.5 to 4.0	2.5 to 3.5
CO, ppm @ 15% O_2	10.16	0.5 to 5.5	1.5 to 2.1
HC, ppm @ 15% O_2	3.55	ND to 0.22	ND

ND – Not detected.3.1Performance Targets of Steam-Injected Silo Combustor

3.3 Elliott TA-100 Combustor

The Elliott Power Systems[1] TA-100 microturbine uses a partial oxidation combustor. Figure 30 shows a rear and side view of the combustor. The combustor is housed in the turbine housing shown in Figure 31 and Figure 32. This combustor uses an annular fuel injection system consisting of 12 injectors introducing fuel gas with a tangential velocity. By only introducing a portion of the needed air, this part of the combustor can be reduced in volume. Also, temperatures in the fuel rich zone are constrained because stoichiometric combustion conditions are initially avoided since the fuel is only partially combusted. The remaining air needed to complete combustion of the fuel is then added downstream via annular cooling holes and axial cooling slots around the combustor liner exit. However, a key design flaw of this combustor design is the peak temperatures reached when this additional and final combustion air is added. Since the combustion takes place in near adiabatic conditions, the temperatures can reach excessive levels that exceed the metallurgical limits of the alloy steel used. This failure condition was accelerated when the power output of the engine was increased by Elliot from 80 kW to 100 kW without increasing the amount of air flow (i.e., the same size compressor wheel). As the fuel increased to achieve the higher power rating, the stoichiometry increased in both rich and lean combustion zones and resulted in excessive metal temperatures. After a relatively short operating life, numerous failures in the field occurred as evidenced by melting of cooling slots causing catastrophic turbine failures. An illustration of these failures is shown in Figure 33.

[1] Elliott Power Systems is now part of Capstone Microturbines

Figure 30: Standard TA-100 Combustor Showing Injectors (top view) and Cooling Slots (bottom view)

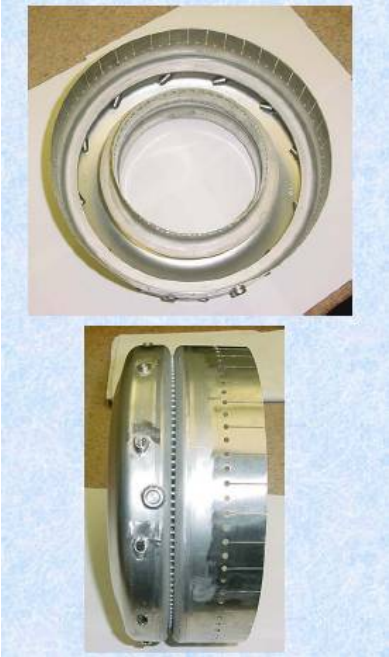

Photo Credit: Elliott Energy Systems

Given these design flaws and its inability to achieve CARB 2007 limits, the Elliott combustor design was not adequate for steam injection and a complete re-design of the original combustor was deemed necessary.

Table 11 lists the key operating requirements of a reliable and emission-compliant steam injected combustor. This combustor has to be able to light off on gas only and operate without steam injection until steam is available from the boiler. Once steam becomes available and starts being injected into the combustion air to the recuperator, the fuel control valve (FCV) has to respond in tandem to increased fuel demand. Careful control of the fuel and steam is necessary to maintain stable combustion conditions until full steady-state conditions at peak load are reached. The controls must also be capable of reducing fuel demand in cases when steam flow is reduced. These conditions can be controlled by monitoring the turbine exit temperature and generator power output, which signal the condition seen in the combustor and the amount of fuel required. Therefore, the combustor must be capable of operating over a wide range of conditions. Finally, when the power output reaches full rating, the localized flame conditions in the combustor must be such to be conducive to low NOx and CO emissions in compliance with CARB 2007 limits.

Figure 31: TA-100 Turbine Housing Showing Fuel Injector Holes

Photo Credit: CMC-Engineering

Emission limits are specified in lb/MWh and account for the waste heat recovery associated with CHP operation. Table 12 translates the NOx, CO, and HC emission limits dictated by CARB 2007 regulations using the EHPS improved power output and CHP efficiency. CARB 2007 compliance for the EHPS CHP configuration will require the combustor to operate with 0.07 lb/MWh (4.33 ppm @ 15 percent O_2) and 0.7 lb/MWh (10.16 ppm @ 15 percent O_2). The molar concentrations are calculated based on the increased power output of 134 kW, and overall CHP efficiency of 87 percent of the EHPS. HC emissions are generally below detection when these CO levels are met.

Figure 32: View of Combustor in Turbine Housing

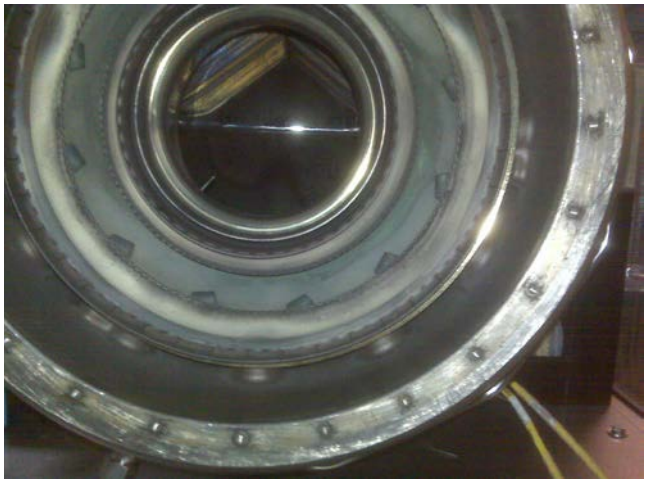

Photo Credit: CMC-Engineering

Figure 33: Combustor High Temperature Failure

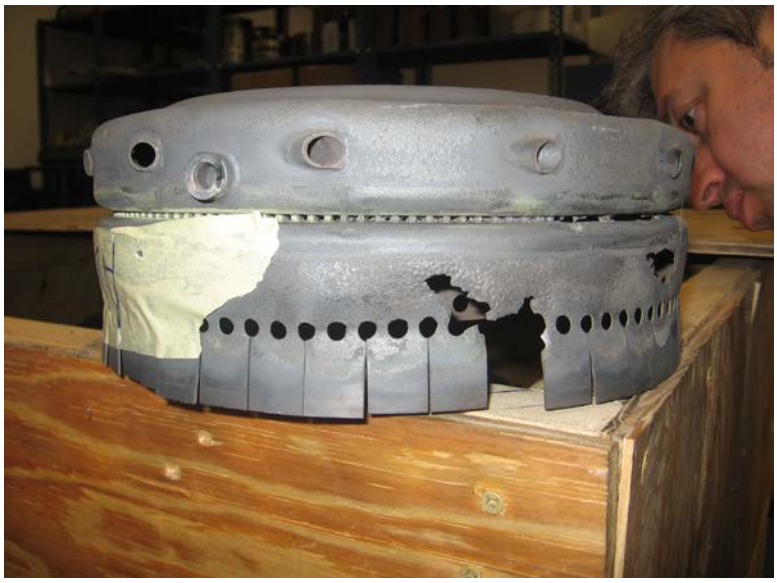

This photograph shows the melting of cooling slots causing catastrophic turbine failures.
Photo Credit: CMC-Engineering

Table 11: Key Operating Characteristics of Steam Injected Silo Combustor

Key Operating Requirements	Operating Conditions
Ease and reliable light-off without steam injection	Low noise and low vibration ignition
Overall fuel flow control	Required to maintain adequate monitoring and control of TIT, engine speed and power output
Transition from zero steam to maximum steam injection rate	Control of steam-fuel ratio to maintain combustion stability as maximum steam injection is reached
Metal temperature	Maintain combustor liner and other high-temperature components below metal temperature limits
Emission control	Compliance with CARB 2007 NOx, CO, and HC emission limits

Source: CMC-Engineering

These emissions levels are challenging to meet by conventional approaches. For example, in fully premixed approaches that can suppress NOx to needed levels usually have difficulty meeting CO emissions levels. However, when the excess air level is reduced to raise combustion temperature and reduce CO, the NOx emissions usually exceed the limit. Lastly, even if emissions targets when load is reduced are met at the design point, temperatures decrease and CO emissions can rise. These conditions are exacerbated when steam in injected in the combustion air.

Table 12: CARB 2007 EHPS Emission Targets

Emissions	Target Limit
NOx, ppm @ 15% O_2	4.33
CO, ppm @ 15% O_2	10.16
HC, ppm @ 15% O_2	3.55

Source: CMC-Engineering

3.4 Operating Conditions Conducive to Ultra Low NOx Combustor Emissions

NOx emissions in lean premixed flames are a known function of peak flame temperature, oxygen partial pressure and residence time. The equilibrium reaction of the fuel with air and steam is expressed as shown below:

$$C_nH_m + \lambda\left(\frac{n+m}{4}\right)[O_2 + 3.76N_2] + (s)H_2O \rightarrow (n)CO_2 + \left[(\lambda - 1)\left(n + \frac{m}{4}\right)\right]O_2 + \left[3.76\lambda\left(\frac{n+m}{4}\right)\right]N_2 + \left(\frac{m}{2} + 2\right)H_2O$$

For methane, "n" and "m" are 1 and 4 respectively; "s" is the mole of steam injected; and "λ" is the excess air coefficient and "1/λ" is the overall "bulk" equivalence ratio. Flame temperature in turn is a function of flame stoichiometry "λ" and steam injection "s". NOx formation in the combustor is expressed by the kinetics data from the Zeldovich mechanism[2], where the key reaction can be expressed as follows:

$$N_2 + O^- \xrightarrow{k} NO + N$$

and the reaction rate k is given by

$$k = 1.8 \bullet 10^8 e^{-38,370/T}$$

[2] Zeldovich, Y.B, Sadonvnikov, P.Y, and Frank-Kamenetskii, D.A. : Oxidation of Nitrogen in Combustion – Academy of Sciences if USSR, Institute of Chemical Physiscs, Moscow-Leningrad, 1947

where T is the peak flame temperature in a premixed fuel air combustion process. Because the local equivalence ratio and the amount of steam added to the flame, in a fully premixed combustor, determine the amount of NOx formed, the amount of NOx becomes principally a function of both equivalence ratio and steam injection rate. For example, at an equivalence ratio of 0.58 to 0.75 in a fully premixed silo combustor without steam injection the expected NOx emission profile is illustrated in **Figure 34**. These laboratory results show that the equivalence ratio has to be below 0.60 in order to meet NOx limits for the EHPS technology. The exponential increase in NOx as a function of equivalence ratio is similar to the NOx calculated based on peak flame temperature, as shown in **Figure 35**, indicating that equivalence ratio is a good surrogate for peak flame temperature in these premix combustors.

Figure 34: Laboratory Measured NOx versus Flame Equivalence Ratio

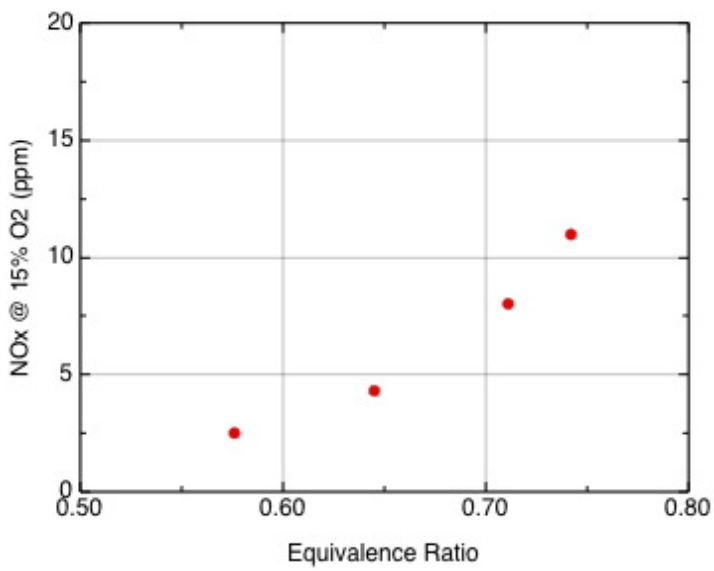

These laboratory results show that the equivalence ratio has to be below 0.60 in order to meet NOx limits for the EHPS technology. .
Source: CMC-Engineering

The turbine inlet temperature (TIT) at the exit of the premixed steam injected combustor before it enters the power turbine provides an indication of the overall bulk combustion temperature in the combustor. The TIT n the EHPS was calculated at about 1,740 °F. Because of the thermodynamic relationship between power output and temperature drop across the power turbine, the turbine exit temperature (TET) provides a good indication of the TIT and thus the bulk temperature in the combustor. However, the TIT is well below the localized peak flame temperature, where NOx is formed and CO is combusted, because of the additional air dilution that occurs before the combustor exhaust enters the turbine nozzle.

These conditions are further influenced by the amount of steam that is injected in the combustion air. The amount of steam "s" was calculated to be in the range of 8.7 to 13 percent of the value of the amount of combustion air, or $s = 0.087\lambda$ or $s = 0.13\lambda$. Because the EHPS

process injects steam in the compressor side of the engine, NOx formation then becomes strictly a function of the total amount of steam added to the air and how the air is mixed with the fuel. The latter is a function of the design of the combustor and its operating conditions. These conditions must be balanced with the need for reliable ignition and stable combustion under steady state and transient load variations. The following sections describe how the combustor was designed to meet these challenges.

Figure 35: Predicted NOx levels

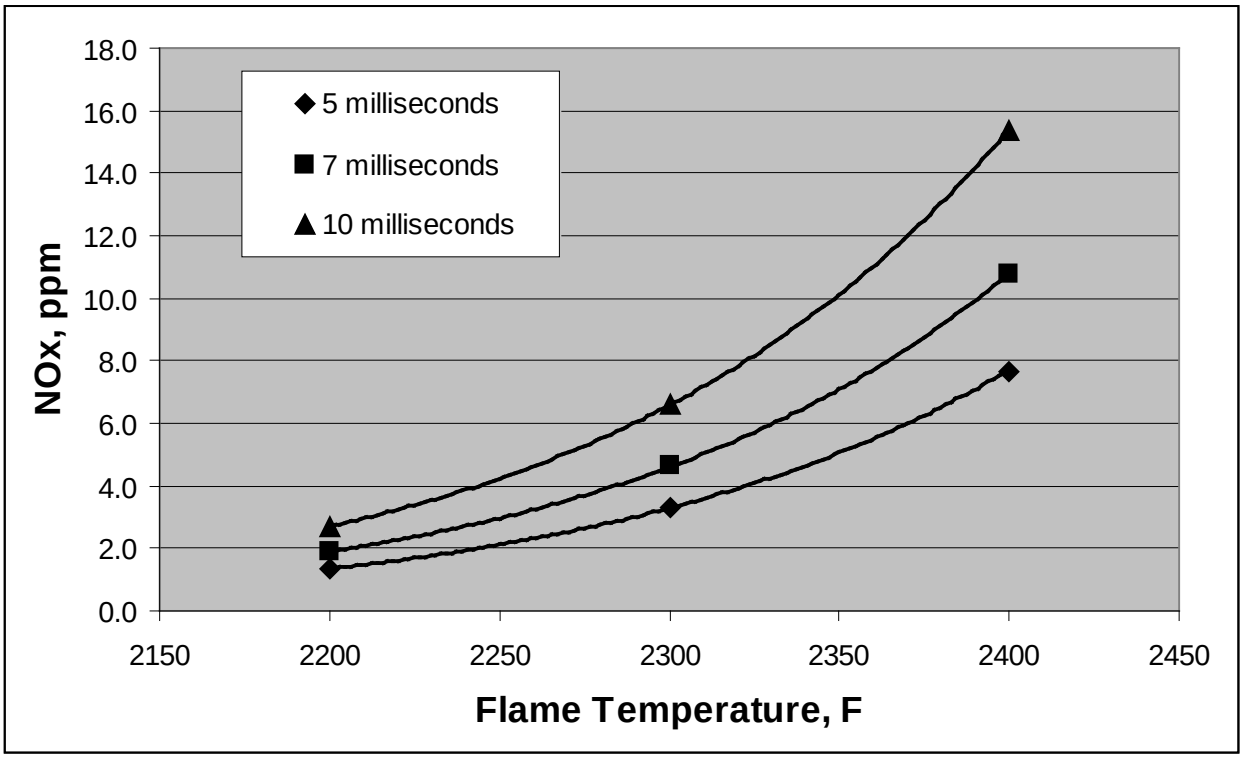

This figure indicates that the equivalence ratio is a good surrogate for peak flame temperature in these premix combustors.
Source: CMC-Engineering

3.5 Design, Fabrication and Modeling of Combustor Test Unit

The combustor design was based on Altex original combustor development efforts and experience that included preheated duct burners and steam-injected gas turbine combustors. A depiction of this preliminary combustor design was shown in Figure 36. In both developments, the steam is mixed with the combustion air to control flame temperature and NOx. The use of steam prevents locally high temperatures from being reached and thereby reduces NOx emissions as well as reducing degradation of combustor materials. Under steady-state conditions, the combustor is scheduled to utilize about 500 lb/hr of steam (about 1 gpm of water). The compressed gas flow to the combustor accounts for about 1.5-1.64 MMBtu/hr compared to a conventional fuel use of 1.36 MMBtu/hr (LHV). The extra fuel coupled with the

steam will provide additional power conversion for a higher generating capacity. Air flow to the turbine will be reduced but the steam will add to the mass flow to generate the needed increase in power. The total mass throughput of the engine is set at 7,028 lb/hr for increased electrical power output.

Figure 36: Preliminary View of Steam Injected Combustor Configuration

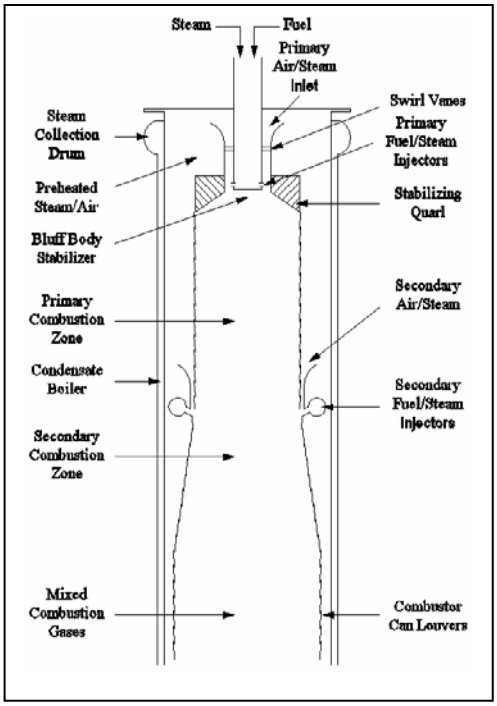

Source: Altex Technologies Corporation

3.5.1 Combustor Design and Fabrication

The preliminary combustor design was refined leading to a two stage combustor with a cyclone configuration to stabilize primary combustion and a multiple jet secondary combustion stage to add more heat while maintaining a consistent and low temperature zone to control all emissions.

Figure 37 shows a three-dimensional drawing of the EHPS combustor test article. The first-stage cyclone combustor is located on the left side of the illustration. To the right is the second combustor stage. First and second stage combustor diameters are 22.9cm (9.02 inches) and 26.7cm (10.5 inches), respectively, and lengths are 34.4cm (13.54 inches) and 94.6cm (37.24 inches). Cut-out depictions of the first stage and entire combustor are shown in Figures 38 and 39.

As shown, both first and second stages are air cooled, as in typical gas turbine combustors. However, because fuel-rich and fuel-lean flames are used, along with steam dilution to control NOx, peak gas temperatures are moderated and film cooling is not needed, as in conventional combustors. Shown in these illustrations is the single cyclone air and fuel inlet, which is

oriented tangential to the first stage cyclone chamber to drive the swirling flow needed for recirculation and stability. Also shown is the inlet for the fuel-lean flames for the second combustor stage. As indicated, the single inlet feeds four jets spaced around the cyclone combustor and set at an angle of 9 degrees to produce the proper penetration and mixing in the second stage. More specifically, in the cutout view of the first-stage cyclone combustor of **Figure 38**, the single tangential fuel/air entry is shown near the back of the combustor. While the outer shell of the second stage combustor is included, the inner liner has been removed in the illustration. Both this high temperature liner and the cyclone combustor liner are fabricated of Inconel 625, which has excellent heat and oxidation resistance. Similar alloys are utilized in commercial gas turbine combustors that face even higher temperatures because of operation near stoichiometric conditions in primary combustion zones. Therefore, the durability of the test article that uses lower temperature fuel rich and fuel lean zones should be good.

Figure 37: EHPS Test Combustor Illustration

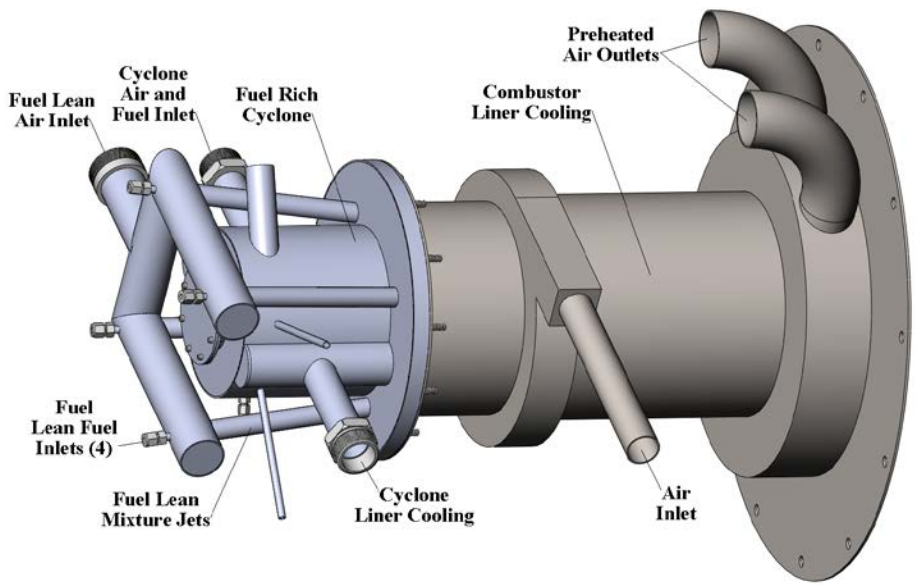

A three-dimensional drawing of the EHPS combustor test article
Source: Altex Technologies Corporation

Figure 38: EHPS Cyclone Combustor Cutaway Illustration

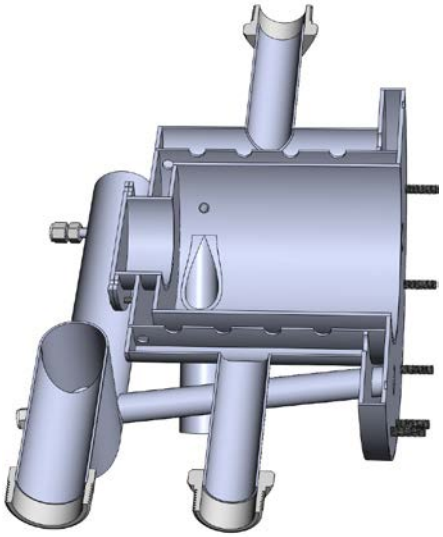

Cut-out depictions of the first stage of the combustor
Source: Altex Technologies Corporation

The small diameter hole in the path of the fuel/air port is the entry for the nichrome wire igniter. This igniter is supported by a high voltage transformer that produces a robust spark to positively ignite the fuel. Also, downstream of the test combustor igniter is a commercial flame rod detector that continuously monitors the presence of a flame, and is able to shut off the gas supply and sound an alarm, if the flame is extinguished for any reason. Hot gases from the cyclone exit along the combustor axis and flow into the second stage combustor. Lastly, the air cooling channel around the cyclone combustion chamber and manifold are included to maintain metal temperatures within material limits. This air cooling channel is consistent with gas turbine practice.

A picture of the back end of the first-stage cyclone burner is given in Figure 40, showing the tangential cyclone fuel/air entry port. Fuel and air mixing is facilitated by a 0.953 cm (3/8 inch) diameter fuel supply tube with 32 holes of 0.16 cm (1/16 inch) placed on the axis of the 3.175cm (1+1/4 inch) diameter air entry tube. For the four fuel lean jets, shown as the inwardly angled tubes surrounding the cyclone chamber in Figure 13, fuel/air mixing is facilitated by 0.635 cm (1/4 inch) diameter fuel supply tubes with eight holes of 0.16 cm(1/16 inch) placed on the axis of 3.17 cm (1+1/4 inch) diameter air entry tubes. Figure 41 gives a picture of the front of the cyclone combustor, showing the four fuel-lean jets that surround the exit from the cyclone. Lastly, Figure 42 gives a picture of the second-stage combustor liner, with the air cooling. The large flange was used to mount the combustor to the exhaust system.

Figure 39: EHPS Complete Combustor Cutaway Illustration

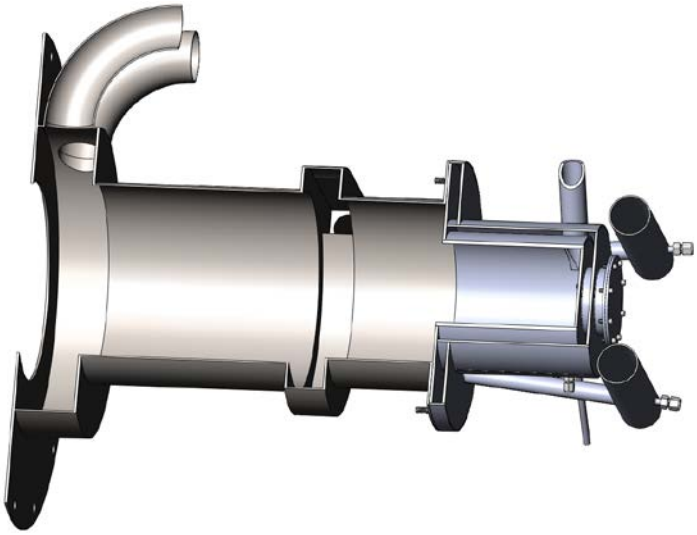

Cut-out depictions of the entire combustor
Source: CMC-Engineering

Figure 40: View of the Back of Cyclone Combustor

A picture of the back end of the first-stage cyclone burner showing the tangential cyclone fuel/air entry port.
Photo Credit: Altex Technologies Corporation

Figure 41: Front of Cyclone Combustor

Photograph of the front of the cyclone combustor, showing the four fuel-lean jets that surround the exit from the cyclone.
Photo Credit: Altex Technologies Corporation

Figure 42: Second-Stage Combustor with Heat Exchanger

Second-stage combustor liner with the air cooling
Photo Credit: Altex Technologies Corporation

3.5.2 Modeling of Combustor

Before testing, the combustor design was evaluated using computational modeling. Preliminary engineering analyses and computational work is based on the preliminary design illustrated in Figure 43. In this design, a swirler was introduced in the primary zone with linear jets used in the secondary combustion zone. However, analysis showed that a strong cyclonic configuration would provide a higher margin of stability in the primary zone. Given this important advantage, the primary zone was designed as a cyclone, with options of cyclonic or liner jets used in the secondary combustion zone. While the cyclonic configuration might yield increased

heat load on the liner under conventional conditions, with steam injection, the heat load on the liner is reduced and any degradation mitigated. While the primary cyclone produces good stability, CFD design calculations showed that using a cyclonic action in the secondary zone results in excessive combustor volume to achieve the needed burnout. Figure 44 gives the combustor flow pattern with a cyclonic secondary combustor burnout zone. As shown, the active flow areas in the combustor are near the combustor periphery, with a slow moving recirculation zone occupying the central region. This slow-moving recirculation zone is very important for stabilizing the primary zone. However, this is not needed for the high temperature burnout zone. In this downstream zone, jets can replace swirl as the primary and secondary gas mixing mechanism. Figure 45 presents this revised secondary mixing zone design flow pattern. As shown, the slow-moving central zones given in Figure 44 are replaced with more active jet mixing zones. This will better utilize the secondary combustion volume. Also, by going to a secondary jet configuration, the burnout zone has more of a plug flow character, which helps to avoid the carryover of pollutants from upstream zones and thereby fully minimize emissions for CARB 2007 compatibility.

Figure 43: Cutout of Steam-Injected Silo Combustor for Computational Modeling

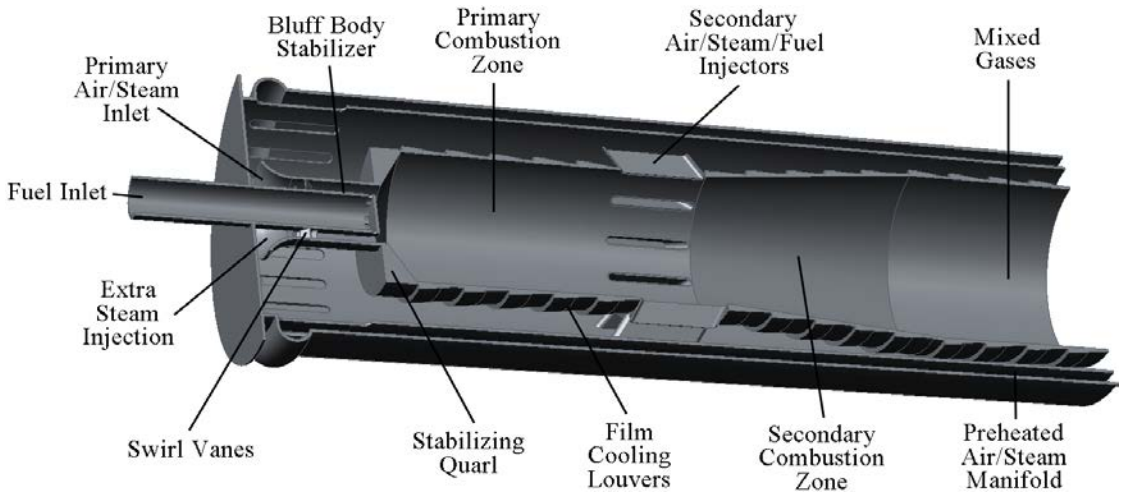

Preliminary engineering analyses and computational work is based on the design illustrated in this figure.
Source: Altex Technologies Corporation

Figure 44: Combustor Flow with Cyclone Secondary

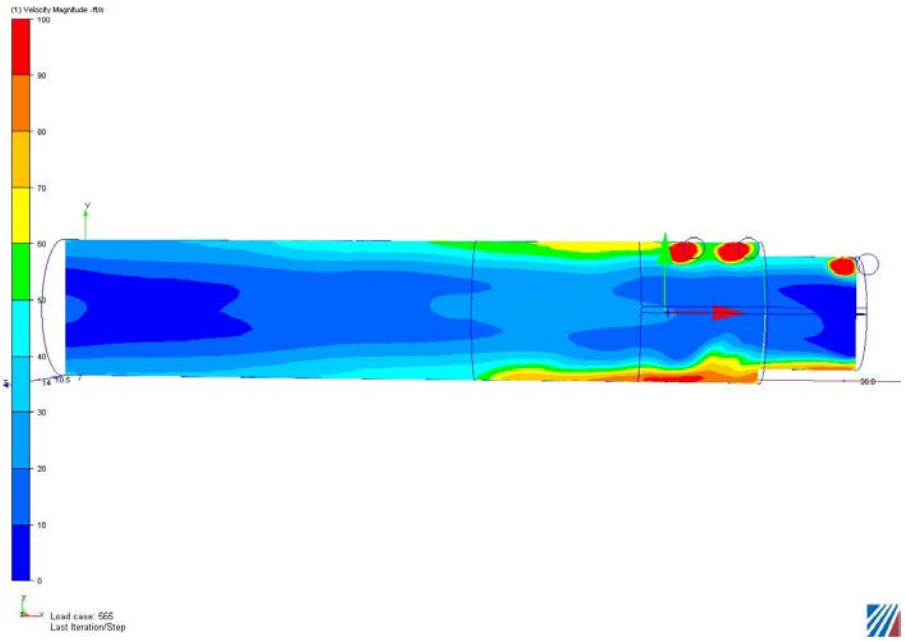

This figure gives the combustor flow pattern with a cyclonic secondary combustor burnout zone.
Source: Altex Technologies Corporation

Figure 45: Combustor Flow with Jet Secondary

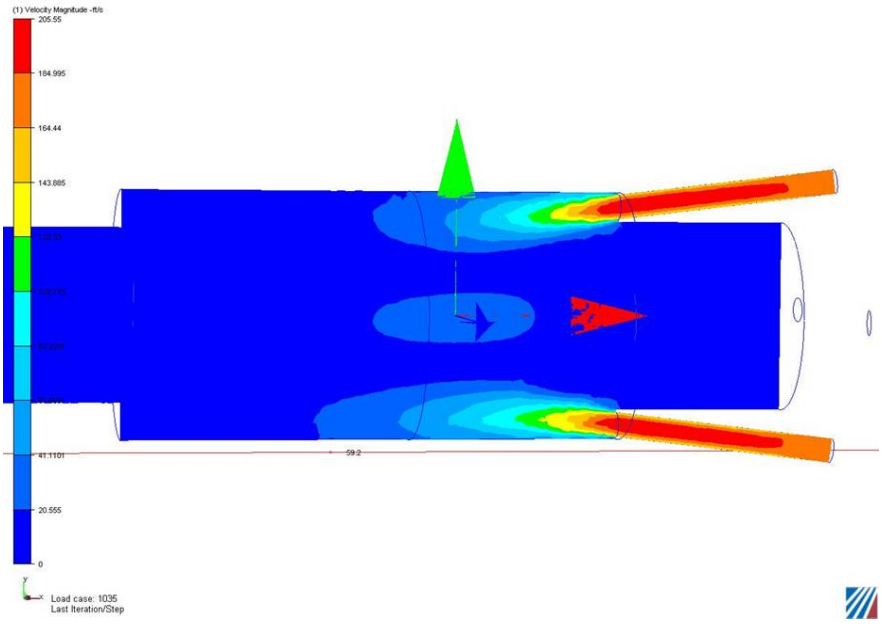

Slow-moving central zones given in figure 44 are replaced with more active jet mixing zones.
Source: Altex Technologies Corporation

3.6 Assemble A Combustor Rig

Laboratory testing of the silo combustor was performed at the Altex Combustion Test Facility. A picture of the test rig is shown in Figure 46. The back of the combustor is visible at the front of the test rig. The facility was retrofitted for steam injection. PVC piping carrying the water for steam generation are visible in the picture. The water was converted to steam in the combustor exhaust. The steam was then mixed with combustion air to simulate the EHPS operating conditions.

Figure 46: Combustor Test Rig at Altex Test Facility

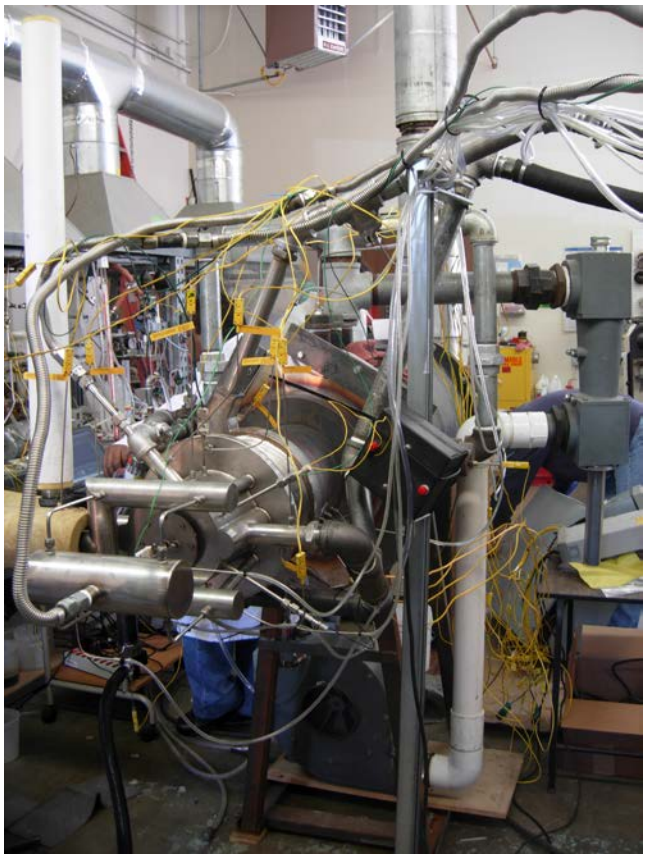

A Photograph of the test rig located at the Altex Test Facility in Sunnyvale, California.
Photo Credit: Altex Technologies Corporation

To monitor all important temperatures, both K and R thermocouples were utilized. In addition, flows were monitored by calibrated rotometers and orifice meters. Pressures at various locations were monitored by manometers. To monitor emissions, sample gases were extracted from the exhaust using a cooled stainless steel probe. The sample then flowed through a heated line, to avoid condensation, to a filter and desiccant trap to remove moisture ahead of the

emissions monitors. The calibrated emissions monitors used are shown in Figure 47 and listed in Table 13.

Figure 47: Continuous Emission Monitoring Instrumentation

The calibrated emissions monitors were used to sample gases, which were extracted from the exhaust using a cooled stainless steel probe.
Photo Credit: CMC-Engineering

Table 13: Specifications of Emission Monitors

Measurement Parameter	Analyzer Manufacturer	Measurement Principle	Ranges
NO/NOx	CN Instruments	Chemi-luminescence	0-2.5, 20, 25, 200, 580, 1000, 2500, 10000ppm
CO	CN Instruments	Gas filter correlation	0-1, 2, 5, 10, 20, 50, 100, 200, 500, 1000ppm
O_2	California Analytical Instruments	Galvanic Fuel Cell	0-5, 10, 25%
CO_2	California Analytical Instruments	Flame Ionization Detector (FID)	0-5, 15, 20%
Total Hydrocarbons	MSA/Baseline	Flame Ionization Detector (FID)	0-10, 20, 50, 100, 200, 500, 1000ppm

Source: CMC-Engineering

These are standard monitors typically used to certify that combustion equipment meets permitted standards. Before each test, these monitors were calibrated, using applicable gas

standards. It should be noted that, while the planned atmospheric pressure tests operate at a capacity of 75kWe, when pressurized to the level expected for actual microturbine operation, the test combustor could operate at 300kWe, consistent with the needs of the EHPS recuperated microturbine. Therefore, the atmospheric combustor would provide essentially full-scale data when operated at the expected pressure ratio of four for the actual engine.

It should be noted that primary parameters that drive emissions are fuel mixture ratio, temperature and residence time. Pressure is a secondary factor, particularly at a modest compression ratio of four, as utilized in the TA-100. Methane flame results suggest a NOx increase of around 20 percent in increasing pressure from 1 to 4 atmospheres [Miller,1977]. In addition, other work found no impact of pressure on NOx emissions from 5atm to 30atm. This is consistent with no change in volume with the global NOx production reaction. Also, CO and unburned hydrocarbon reduction reactions would be enhanced with increases in pressure. Therefore, results of the atmospheric pressure combustor tests should be within about 20 percent of those for a four-atmosphere pressure combustor when integrated into a TA-100 engine. While this emissions level is expected for the actual engine, if NOx emissions exceed this level, they can be reduced to the needed level by introducing more steam dilution. This flexibility of EHPS steam injection is an important advantage when addressing emissions limits.

3.7 Laboratory Testing

The EHPS combustor performance was determined over a range of operating conditions, including load. Also, flames were observed to define flame standoff, fluctuations and stability. Pressure drop across the EHPS combustor was also recorded. These results show that the EHPS combustor can meet CARB 2007 emissions limits with acceptable combustion stability and reliable ignition.

The primary objective of these tests was to characterize and then optimize the performance of the EHPS steam-injected combustor through testing, using the selected combustor design and the flexibility of the test rig available at the Altex facility. At the start of this effort, a test plan was prepared. Tests and parameters of interest evaluated in the test face of Task 3 are listed in Table 14.

As indicated in the previous chapter, the key parameters are the stoichiometry of the primary and secondary reactor zones and the amount of steam injected. Parametric variations around the design values established in the EHPS thermodynamic modeling were employed to evaluate the effect on emissions and confirm the applications of selected operating values.

The stoichiometry governs the species mix in the two zones of the combustor, and thereby the NOx reduction potential of the concept. In addition, the amount of steam impacts primary and secondary zone temperatures, which are important to emissions and burnout. Another key parameter is the amount of fuel that is injected in the main combustion zone. The third important parameter is the excess air level, or stoichiometry, of the burnout flame. Finally, the

last important parameter is the final burnout temperature, which is a function of steam injection. The mass ratio of steam to be injected with the air and fuel governs the temperature of the various zones.

Table 14. EHPS Combustor Test Matrix

Test Sequence	Parameter	Proposed Values
Design	Zone stoichiometries	
	Primary	0.4 - 0.7
	Secondary	1.2 – 3.0
	Zone residence times	
	Primary	.01 - .08 sec
	Secondary	.08 - .12 sec
	Primary Fuel Fraction	.3 - .7
	Steam Injection	
	Primary	0. - .1
	Secondary	.1 - .28
Performance	Best combination of above	TBD
Operating Conditions	Load	20% - 100%
	Excess air	20% - 200%
	Steam	0 – 29%

Source: CMC-Engineering

Preliminary tests showed that NOx, CO and HC (hydrocarbon emissions as CH_4) can be below target limits at all the combustor loads tested. This is summarized in Table 15. As shown, results meet the target CARB 2007 limits. However, these preliminary test results covered a limited range of conditions. To complete combustor testing, some facility improvements were defined and initiated. These included upgrading the natural gas supply and checking all equipment, including instrumentation and burner components for degradation and replacing components, as needed. Disassembly of key components showed that the combustor, flame detector and igniter had not degraded. The air dilution system for the condensing heat exchanger tests was

removed, and a high temperature stack was incorporated into the system for the planned higher capacity tests. These results are summarized below as compared to the CARB 2007 limits.

Table 15: EHPS Combustor Emissions Test Results

Parameter	Range of Values	CARB 2007 Limits
Loads (kW)	33.7 to 68.9	NA
Steam Injection (%)	7.5 to 15	NA
NOx, ppm @ 15% O_2	2.5 to 3.5	4.33
CO, ppm @ 15% O_2	0.5 to 4.7	10.16
HC, ppm @ 15% O_2	Not detected to 0.2	3.55

Source: CMC-Engineering

3.7.1 Test Results with Air Dilution Only

An initial set of tests were performed with only air dilution of the flame by increasing the stoichiometry of the first and second stages of the silo combustor. Test results with lean primary and lean secondary conditions were promising. Figures 48 and 49 give NOx and CO emissions as a function of primary zone stoichiometry, SRRL. These tests used a primary zone to total fuel fraction of 0.32. As shown in Figure 48, all conditions, except one (SRRL = 0.97) have SRRL greater than one, which is fuel lean operation. As SRRL increases, NOx decreases. These results were obtained for secondary zone fuel lean stoichiometries, SRLL, of approximately 1.4, 1.6, and 1.8. Of course, final stoichiometries, SRT, vary with these conditions, with all final conditions being fuel lean (i.e. SRT>1). As shown in Figure 48, NOx emissions can meet the CARB 2007 limit of 4.33ppm @ 15 percent O_2 at higher SRRL and SRLL conditions without steam injection. In addition, as shown in Figure 49, CO emissions can meet the CARB 2007 limit of 0.07 lb/MWh, for CHP with microturbine heat recovery, corresponding to 10.16 ppm @15 percent O_2 at all conditions tested, without steam injection. Hydrocarbon emissions were insignificant versus the limit at all conditions tested. This hydrocarbon emissions result was expected given the premixed nature of the combustor.

Figure 48: NOx Emissions versus Primary Zone Stoichiometry - Air Dilution Tests

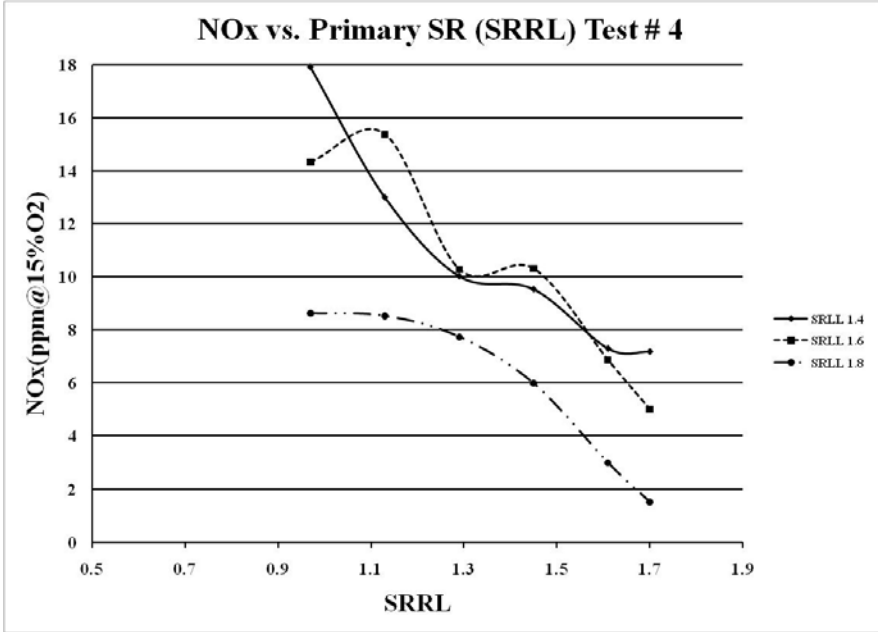

Source: CMC-Engineering

Figure 49: CO Emissions versus Primary Zone Stoichiometry - Air Dilution Tests

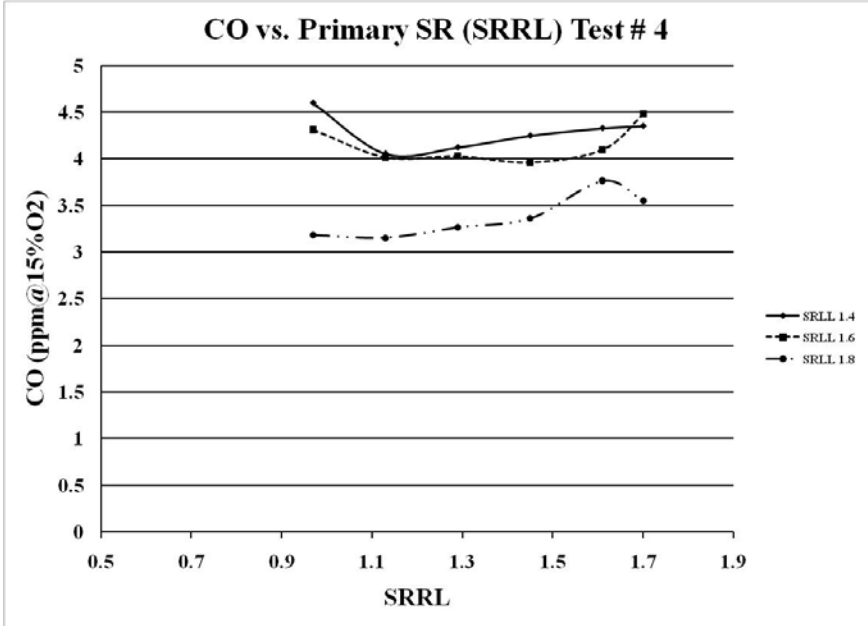

Source: CMC-Engineering

3.7.2 Effects of Steam Rate

This section summarizes the effects of variable steam injection rates on emissions for the two operating configurations of the silo combustor, namely (1) rich-lean and (2) lean-lean flame conditions in each of the two combustor zones.

Steam Injection Tests in Rich-Lean Combustor Configuration

Test results obtained prior to this project and proprietary emissions correlations were used to estimate the emissions profile for one set of steam injection conditions and set the operating parameters for the silo combustor. This preliminary analysis shows that steam injection can assist in NOx reduction even at the higher firing rates necessary for EHPS goals of higher power. As shown by earlier data on the concept, CO emissions will be controlled with enhanced jet mixing and sufficient residence time, as guided by the computational analysis illustrated in Figure 45.

Experimental tests performed with steam injection in the rich-lean combustor configuration are shown in Figures 50 and 51. These tests were performed at several load conditions to determine the impact on emissions as the engine load varies before reaching steady-state operation. Combustor test results indicated that the rich-lean combustor operation could meet the CARB 2007 emissions requirements of 4.33ppm NOx at 15 percent O_2 with 7 percent to 15 percent steam injection, as shown in Figure 52. CO and hydrocarbon results are given in Figures 53 and 54. These results meet the 10.16ppm @ 15 percent O_2 and 3.55ppm @ 15 percent O_2 emissions requirements for CO and hydrocarbons respectively, at all steam injection levels and combustor firing rates.

Figure 50: Combustor NOx Emissions versus Steam Injection - Rich-Lean Condition

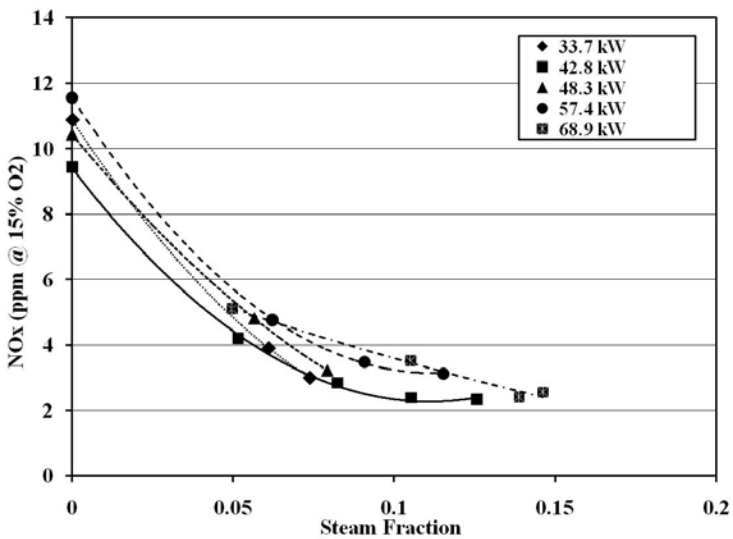

Source: Altex Technologies Corporation

Figure 51: Combustor CO Emissions versus Steam Injection - Rich-Lean

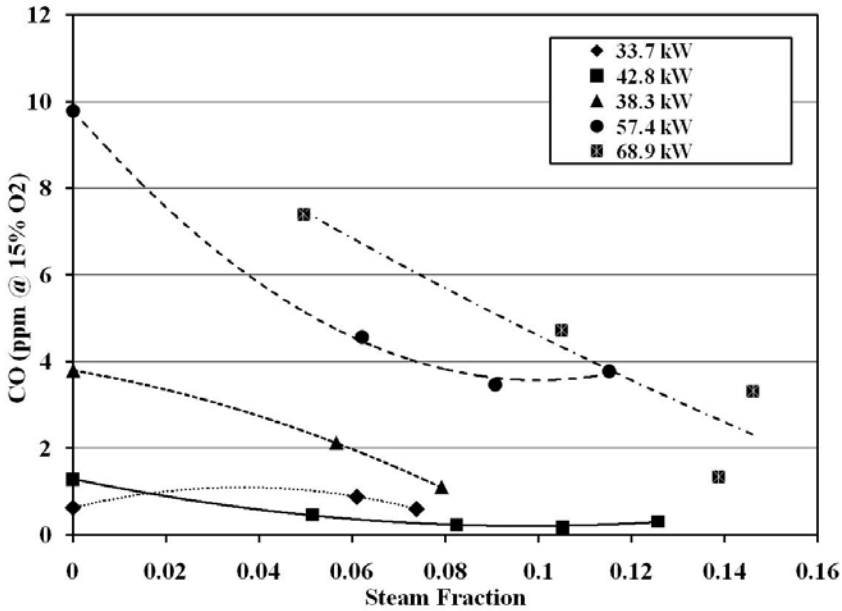

Source: Altex Technologies Corporation

Figure 52: Combustor Hydrocarbon Emissions versus Steam Injection

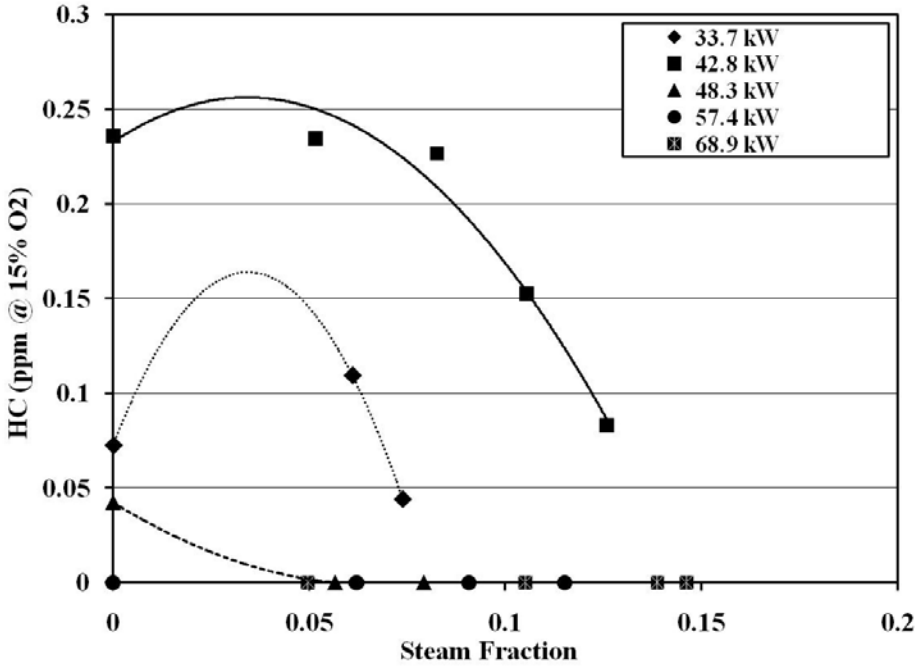

Source: Altex Technologies Corporation

Steam Injection Tests in Lean-Lean Combustor Configuration

The rich-lean tests show the flexibility and potential of the combustor design. By rescheduling fuel to the combustor, emissions can be brought to the needed level as steam injection levels change. Therefore, the combustor testing was again initiated exploring the effects of steam injection with the combustor operating in the lean-lean condition in both combustion zones. The emissions measured with steam addition when the combustor was operated in the lean-lean conditions are shown in Figures 53 and 54. In the range of steam fraction established for the EHPS, i.e., 0.08, both NOx and CO emission measured at the combustor exit are again in compliance with CARB 2007 limits.

While all emissions requirements can be met by use of steam injection, there will be periods during engine startup where steam injection will not be available. In addition, at low-load conditions, the quantity of steam might be limited as a result of reduced fuel flow and lower turbine exit gas temperature. In those cases, the NOx may rise above the CARB 2007 limits, as suggested by the NOx results at low steam fractions in Figure 53. To address this concern, combustor operating conditions can be changed to reduce or eliminate the requirement for combustor steam injection. With this approach, all or most of the steam would be introduced into the dilution air rather than the combustor. Currently, the base engine operates with twice as much dilution air as combustion air. Therefore, steam injection into only the dilution air would be easy to accomplish, with steam injection percent increasing from 7 percent to 15 percent to a still reasonable 10 percent to 22 percent versus dilution air.

Figure 53: NOx Results with Steam Injection in Lean-Lean Combustor Configuration

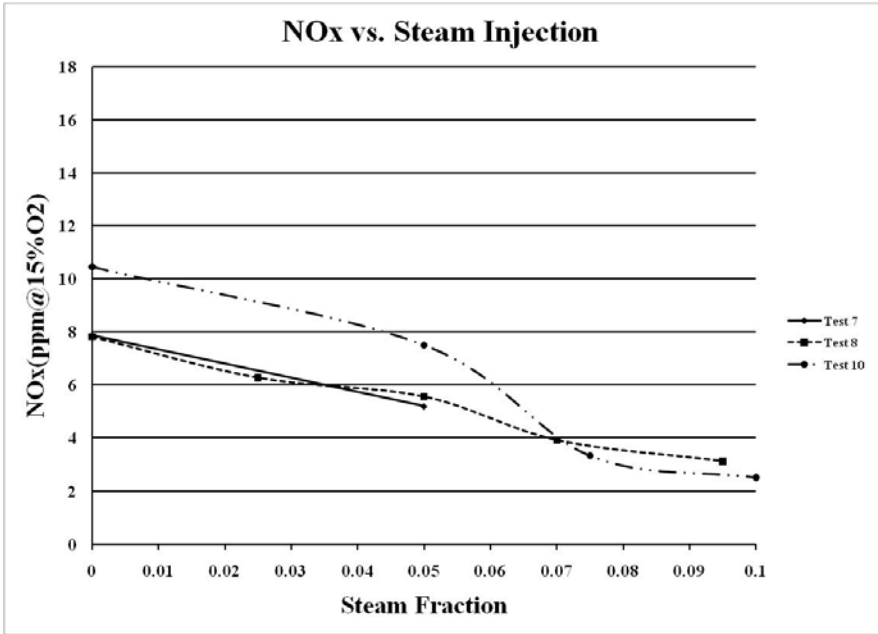

Source: Altex Technologies Corporation

Figure 54: CO Emission Results with Steam Injection in Lean-Lean Combustor Configuration

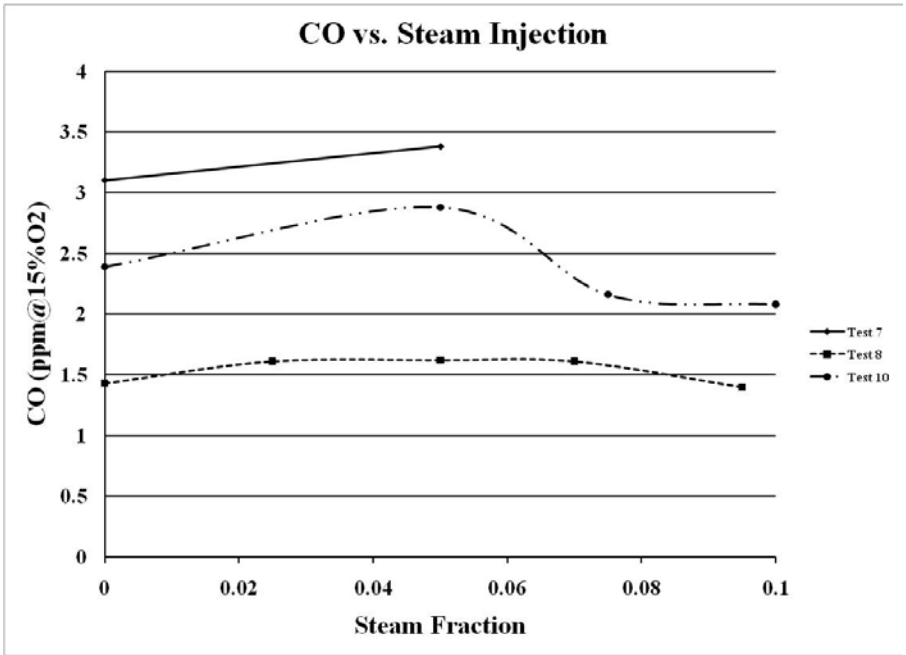

Source: Altex Technologies Corporation

3.8 Test Results Conclusions

Laboratory combustion tests results clearly show that the selected combustor design can achieve NOX, CO, and HC emissions that are in compliance with CARB 2007 limits with steam injection rate 0f 8 percent of the total air input and in either rich-lean and lean-lean operating conditions. These satisfactory NOx results can be attributed to flame temperature control as a result of steam injection which contributes to the control of peak flame temperature. This is shown in Figure 55, where steam injection fractions yield the needed low NOx levels. The importance of reduced temperature on NOx is also illustrated in a plot of NOx versus combustor gas temperature, given in Figure 56. Both results show that higher temperatures, and lower steam flows, have higher NOx emissions.

In summary, the NOx versus CO performance of the steam-injected combustor under the developed design and operation condition selected for the EHPS technology can be summarized as shown in Figure 57. These results confirm the ability of the combustor to meet the operating and emissions performance goals that were established for the EHPS project and therefore can be integrated into the EHPS design replacing the defective Elliott annular combustor.

Figure 55: EHPS Combustor NOx Emissions versus Steam Injection

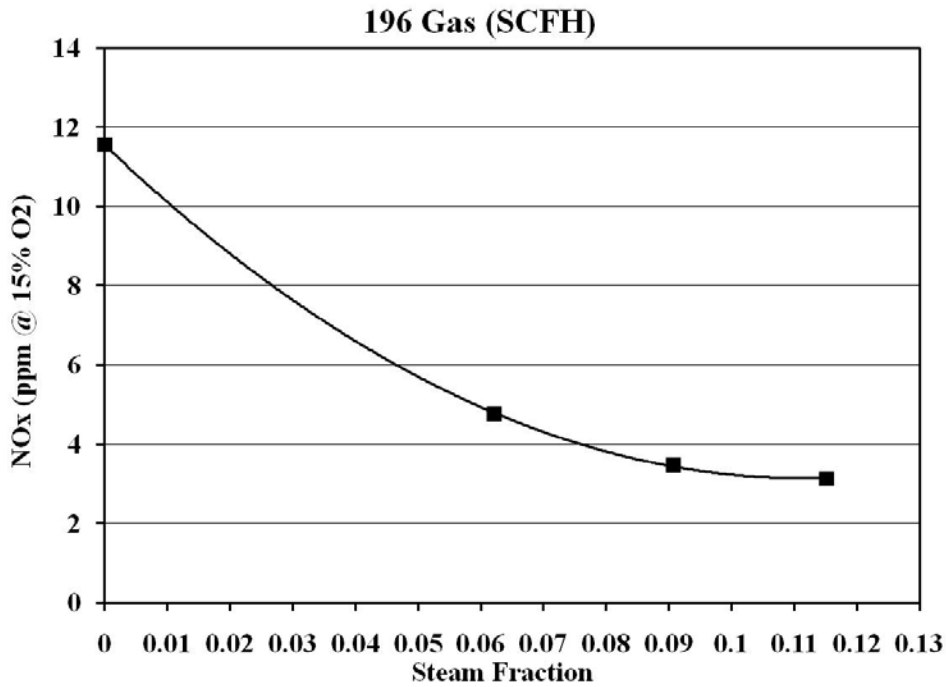

Source: Altex Technologies Corporation

Figure 56: EHPS Combustor NOx Emissions versus Combustor Temperature

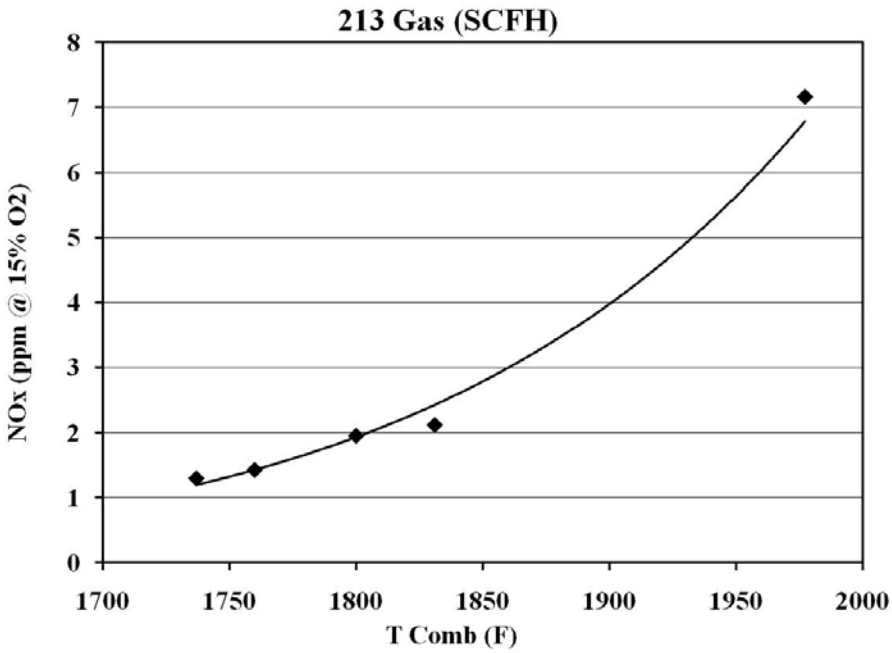

Source: Altex Technologies Corporation

Figure 57: EHPS Combustor NOx versus CO Emissions

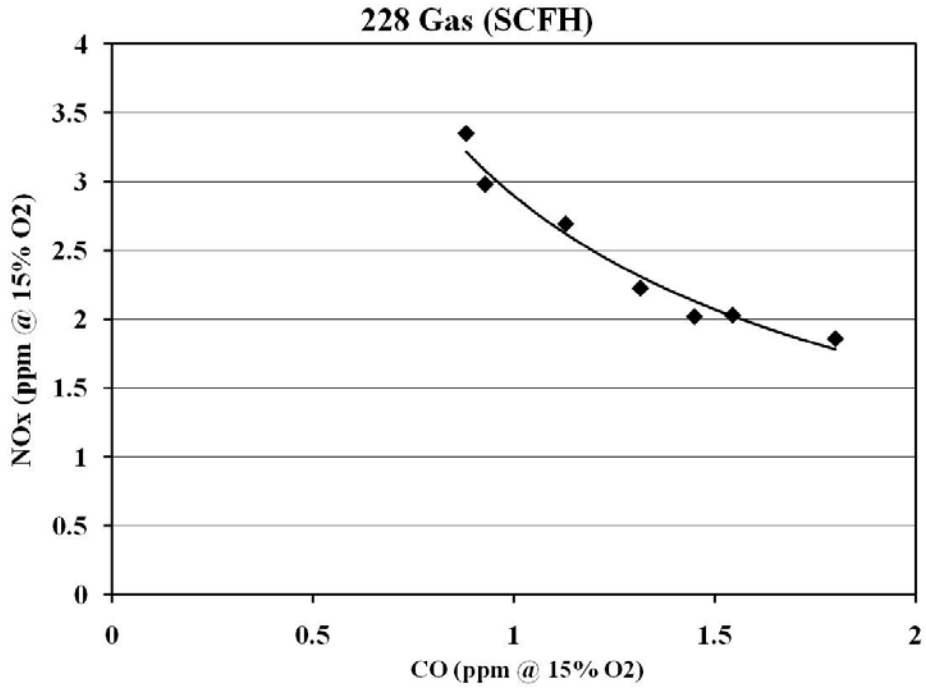

Source: Altex Technologies Corporation

Table 16 summarizes the overall achievable performance of the selected combustor configuration based on the results of the bench-scale tests. Overall, with a minimum steam injection rate of 7.5 percent, NOx and CO emissions can be maintained at 3.5 and 4.7 ppm respectively, which is well within the CARB 2007 emission limits for CHP systems and the increased efficiency of the EHPS CHP configuration. With these results in hand, the project team moved to the fabrication of a full-scale test prototype to be tested in a 1-atm test cell. Success in operating this full-scale test unit, including reliable light-off and stable combustion throughout the range in engine speed, led to the fabrication of the EHPS steam injected combustor. This development is discussed in the following section.

Table 16: EHPS Combustor Preliminary Emission Test Results

Parameter	Range of Values
Loads (kW)	33.7 to 68.9
Steam Injection (%)	7.5 to 15
NOx, ppm @ 15% O_2	2.5 to 3.5
CO, ppm @ 15% O_2	0.5 to 4.7
HC, ppm @ 15% O_2	Not detected to 0.2

Source: CMC-Engineering

3.9 Final Combustor Design and EHPS Interface

A new test combustor based on the design of the Altex bench-scale dual lean-burning zones was fabricated and tested in the Altex laboratory. A new 1-atm test cell apparatus was fabricated using project funds from other ongoing projects including the US DOE and Energy Commission projects (PIR-07-005, PIR-09-012). Following these test cell measurements, the EHPS combustor was fabricated specifically for the EHPS system. This included the adaptation to the Elliott TA-100 modified turbine housing and the steam injection capability with the improved recuperator design.

3.9.1 Full-Scale Test Rig Combustor

Figure 58 shows the fabricated test cell unit. The combustor is designed for the full-scale firing requirement of the EHPS unit without steam injection capability. This full-scale test cell unit provided the needed information on the operational reliability of the new combustor, including the critical specifications for material integrity, combustion stability and reliable light-off operation. The combustor liner was coated with thermal paint that allowed for a measurement of the peak metal temperatures to ensure material safety and integrity.

Figure 58: Full-scale 1-atm test combustor

The combustor is designed for the full-scale firing requirement of the EHPS unit without steam injection capability.
Photo Credit: CMC-Engineering

The completed combustor was installed in the one atmosphere test rig shown in Figure 59. The initial testing will be completed to prove out the correct airflow splits between the various zones and prove the combustor outlet temperature, which will become the turbine inlet temperature. The one atmosphere testing utilizes a scaled airflow and fuel flow rate. The combustor will run at four atmospheres when it is installed in the turbine, and the airflow and fuel will be increased by a factor of four. Air properties are able to be scaled reliably with temperature and pressure. This fact allows testing to be completed without risking damage to the turbine.

Figure 59: Fabricated Full-scale Test Unit for One Atmosphere Tests

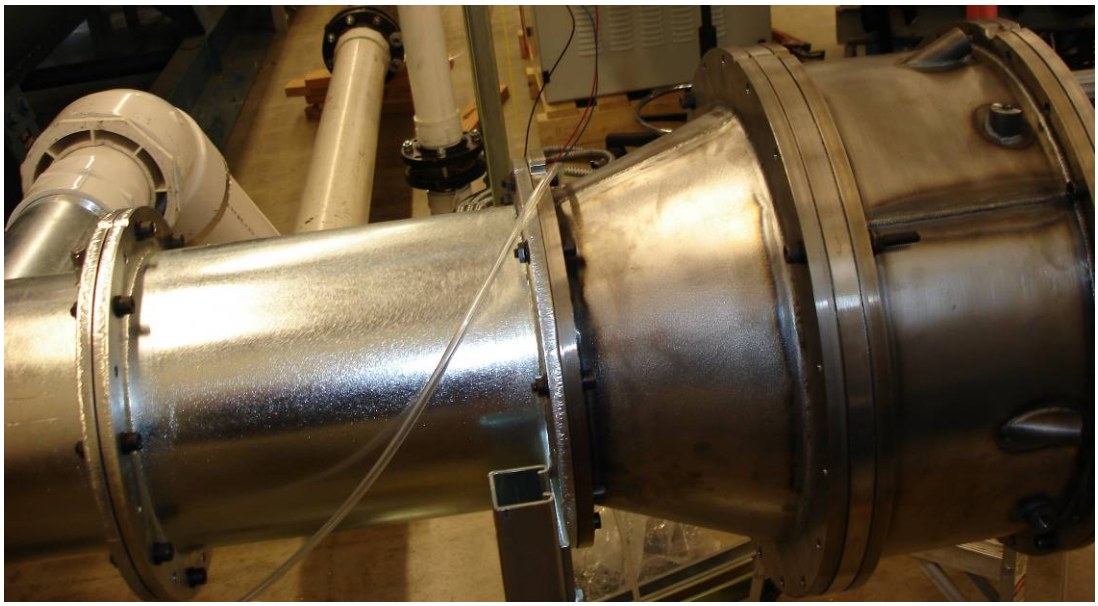

This photograph shows the completed combustor was installed in the one atmosphere test rig.
Photo Credit: CMC-Engineering

The fuel delivery system for the new silo combustor requires two proportional valves that control the fuel delivery to the primary and secondary zones. The control system is designed to use only a single valve, so this presents a challenge. To address this requirement, the team utilized a resistor network and a temperature controlled solenoid valve to control the flow to each of the two zones. The resistor network allowed the single signal sent from the controller to be split proportionally between the two fuel valves. The temperature controlled solenoid will allow the system to be started using the primary zone only to maintain the stability of the combustor and provide the lower heat input required by the turbine.

The novel EHPS combustor was tested at 1 atmosphere. As in the engine installation, there are four paths for air to flow into the combustor and exhaust duct to the turbine including (1) primary combustor, (2) secondary combustor, (3) dilution holes and (4) interface at combustor liner exhaust duct juncture. The first three paths would be the same as in the engine installation. Path 4 above, the juncture with the exhaust, is unique to the test installation; and for the 1 ATM

tests an initially flexible sealant was utilized. In the combustor installation, the juncture is based on a close and rigid alignment between the combustor liner and exhaust.
During the initial 1 ATM tests, the initial flow splits (1) through (4) were skewed significantly from the expected numbers. This was found to be a failure of the sealant at juncture (4) that allowed the incoming combustion air to bypass the combustor and flow into the exhaust. After inspection of the test setup, this leak was repaired by changing the sealant, and the flow splits were found to line up with the predicted numbers of 20 percent of the air flowing into the primary zone, 34 percent flowing into the secondary zone, and the balance into the dilution zone. The dilution flow is used to quench the combustion products to an acceptable temperature before they enter the turbine inlet. Further testing showed low emissions with good stability in the combustor. Unfortunately, the airflow had to be continually increased during test points in order to maintain primary zone temperature. This showed that the flow split was shifting during testing as a result of slow joint sealant failure. Multiple joint sealing attempts were made with different high temperature sealing materials. None of them would hold up for multiple tests, as the metal growth of the combustor and exhaust pipe caused them to fail. The final solution for the test setup was to add an additional test section, shown in Figure 60. This allowed access doors to the interfaces.

Figure 60: New Square Test Section

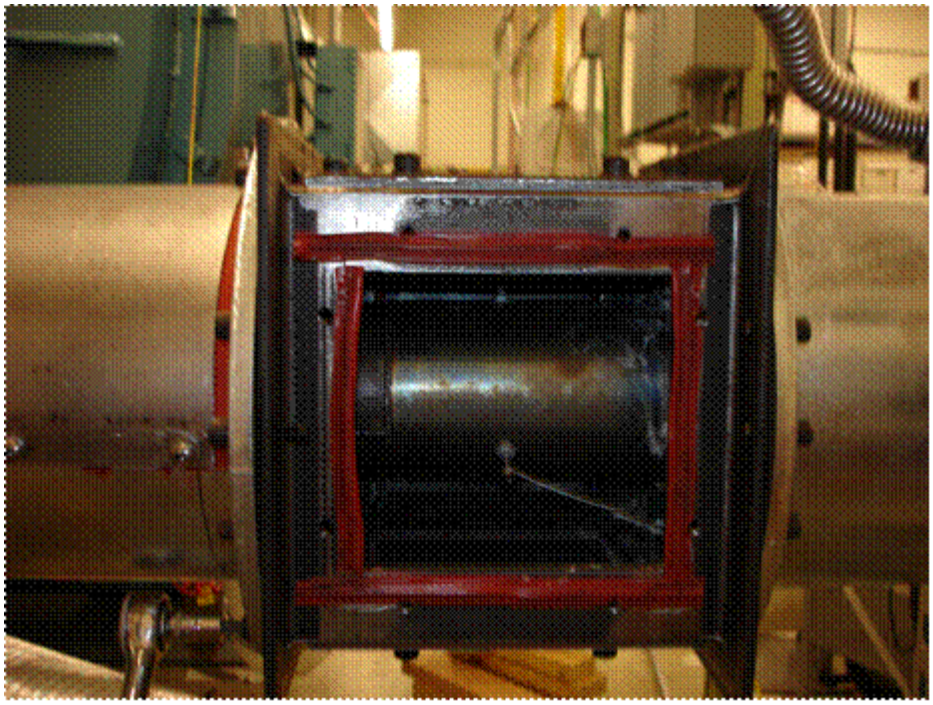

The new square test section added to the 1 atmosphere test setup allows for easier access to critical joints.
Photo Credit: Altex Technologies Corporation

The next step was to mount the exhaust tube with springs to the combustor to allow for a moving seal. The moving seal is necessary due to the thermal expansion of the metal. The

interface between the combustor and the exhaust tube is shown in Figure 61. The white material is a high temperature sealant that works well with a new support structure to hold it in place. The springs attached to the exhaust tube are mounted to the test housing to avoid drilling unnecessary holes in the combustor, for test purposes only. All of the air fed to the combustor flows through this region providing cooling to the springs before it splits into various ports. The cooled springs have less chance of relaxing under temperature and allowing the leak to reoccur. Atmosphere tests are almost complete, with only a few more tests required to validate emissions data we have collected thus far. These data will be aligned with prior test combustor data obtained in an earlier test version of the engine combustor.

Figure 61: View of Interface between the Combustor and the Exhaust Tube

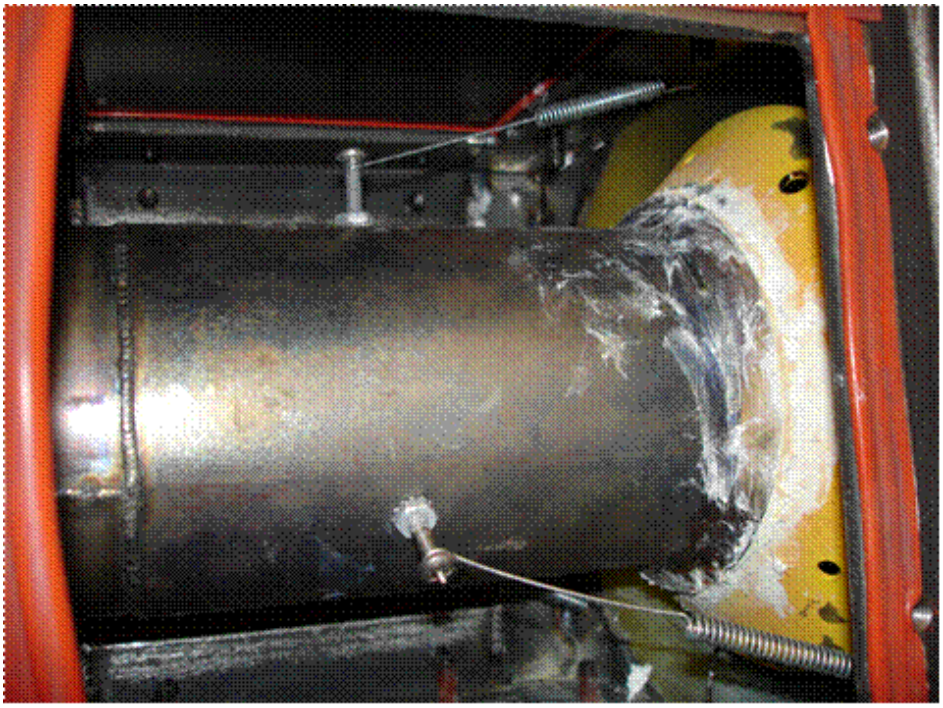

The exhaust tube is now spring held onto the end of the combustor to allow for thermal expansion.
Photo Credit: Altex Technologies Corporation

Prior combustor tests using the 1atm test article showed the potential to meet CARB 2007 emissions requirements. For the EHPS, these emissions limits are 4.4 ppmvd NOx and 10.2 ppmvd CO, corrected to 15 percent O_2. Based on the good results of the test article reported earlier, a full-scale combustor was built for the microturbine. Ahead of installation and testing in the microturbine, with and without steam injection, the combustor was tested at 1 atm in a special test system to prove stability and show potential to meet CARB 2007 required emissions. The test system was instrumented with thermocouples and natural gas flow meters. The test air blower used a VFD controller to modulate flow. Ahead of testing, the blower flow versus speed and pressure where measured using an orifice plate and manometer. The relationship of speed and pressure to flow were then used during combustor testing to define flow. A compliance

level emissions bench was used to measure NO, NOx, O_2 and CO. Tests covered cases with primary only and primary and secondary natural gas flows. Both load and primary and secondary stoichiometries were varied. Results showed the potential of the combustor design to meet CARB 2007 requirements, even without steam injection. These conditions required more fuel lean conditions than would be required with steam injection. With steam, the temperature ballasting requirements of excess air are reduced, and less fuel lean conditions can be utilized. By operating with reduced excess air, water can be more easily recovered from the exhaust and used for steam injection. This ability to operate with or without steam injection shows the flexibility of the design.

Combustor testing was completed at one atmosphere test conditions. The results defined the operating characteristics of the combustor including the relationship to outlet temperature and emissions. Figure 62 shows the NOx and CO corrected emission levels as a function of primary zone stoichiometry. In this series of tests, the primary zone was operated fuel lean. In these tests, the secondary zone stoichiometry was varied. As shown in Figure 62, at the highest SR of 1.5, the NOx and CO meet the CARB 2007 requirements. This initial testing shows promise that the combuistor will be able to meet CARB 2007 while installed in the microturbine and operating at 4.5 atm. Literature has shown the increases in operating pressure can change NOx from 0 percent to up to 20 percent. Therefore, the combustor should meet CARB 2007 requirements at 4.5 atm pressure. The emissions data shown below is also without steam injection. Altex has shown previously that injecting steam into the combustor suppresses the emissions further.

Figure 62: Combustor Emissions of Full-scale Test Cell Unit at One Atmosphere

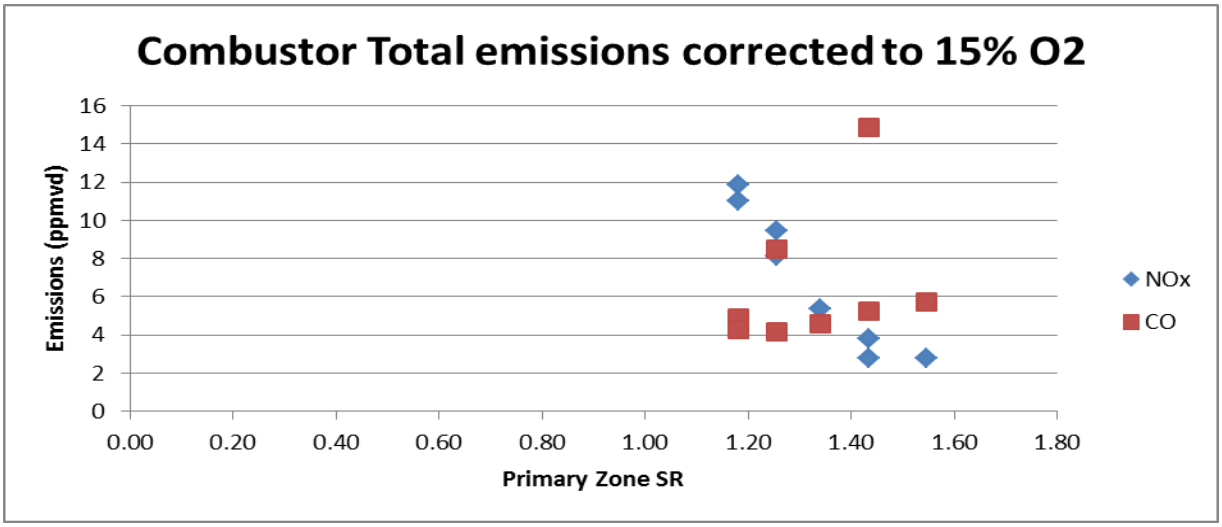

Source: Altex Technologies Corporation

3.9.2 Fabrication of EHPS Combustor and Turbine Housing

Figure 63 presents drawings of the EHPS special CARB 2007 compatible design combustor. This design has a generously sized primary combustor zone followed by a secondary combustion zone to balance stability, NOx emissions and hydrocarbon and CO burnout. Gas temperatures in all zones are suppressed to both control NOx and maximize durability and longevity. The baseline microturbine combustor that was replaced has a partial oxidation first stage that will pass through a stoichiometric condition when dilution air is mixed into the gases. In this case, the gas temperature can peak, resulting in NOx emissions that exceed the CARB 2007 requirement. Furthermore, the peak temperatures achieved at the air dilution point have resulted in degradation of the combustor, reducing Mean Time Between Failures (MTBF) to less than a year. With the special design combustor that operates at lower temperature, this problem should be mitigated.

Figure 63: Configuration of New Combustor and Modified Turbine Housing

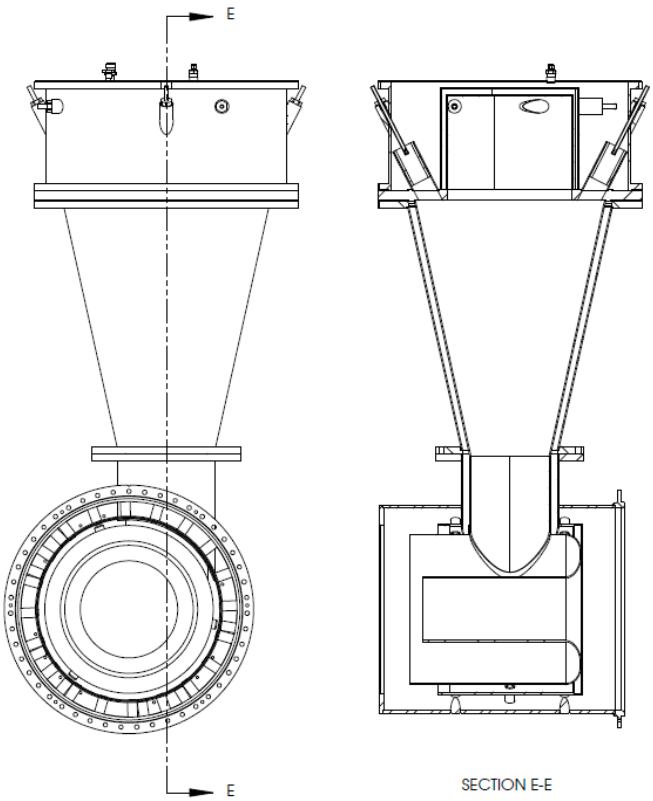

Source: Altex Technologies Corporation

As indicated in Figure 63, the special design requires a conical section to adapt the primary zone to the microturbine housing, which is shown in cross section at the bottom of the figure. As illustrated in the right side of Figure 63, the conical section consists of two conical shells, where the compressed air travels upward between shells and then is distributed to the air/fuel injection ports that feed both the primary and secondary combustion zones. This upward

flowing air serves to beneficially cool the inner combustor shell to control temperature and degradation. While this multiple cone configuration is needed for combustor adaptation to the housing, it is a difficult configuration to fabricate as a one-off component. With production tooling, this component could be more easily fabricated. However, for a one-off initial build and test, the high cost of tooling for the Haynes high temperature alloy would be prohibitive. Working with a local fabricator, fabrication has progressed on the combustor, combustor housing, and turbine housing.

As noted above, creating the shapes requires careful planning and forethought to ensure a quality outcome. The sheet metal fabricators have made multiple mock pieces to define a successful fabrication process before using the more expensive and longer lead time Haynes alloy material needed for the final product. Given the short timeline left for fabrication, the process is moving along quickly. The most difficult piece to make thus far has been the cones that form the bottom half of the combustor and the combustor housing. These pieces transition the larger diameter necessary for the upper part of the combustor down to the smaller diameter necessary for the turbine housing. The process of rolling a one-off cone is challenging due to how the rolling equipment is designed. The recommended formation process is to use a press break at set points along the curve to create the cone shape. The fabricators have moved to this process for the parts in question and are experiencing success. **Figure 64** presents an illustration of the combustor components prior to welding and assembly.

Figure 64: Fabricated Components Prior to Welding and Assembly

This photograph shows the combustor chamber, air ports and fuel injector components prior to welding and assembly at the Altex Laboratory located in Sunnyvale, California.
Photo Credit: CMC-Engineering

In order to integrate the new combustor with the formerly recuperated microturbine, a new housing for the turbine and interface for the combustor had to be designed. A simple-cycle turbine housing available from an existing Bowman engine purchased under ENERGY COMMISSION contract 500-03-037 was modified to adapt the silo combustor flange as illustrated in Figure 65. This modification required cutting out the access and welding the new flange assembly onto the housing.

The original turbine housing was a cast piece with post machining operations to create the locating and mounting features for the fuel injectors. Post machining operations also improved interfaces with the recuperator and the turbine. These features were recreated in the new housing design, but without a casting. Creating a cast piece would require far too long and far too much money for a single piece for the development project. Therefore, the housing was designed to be made from rolled sheet metal and machined pieces which are welded together. Design reviews with the welder and machinist were completed to ensure the design had a high likelihood of success. The original turbine housing being retrofitted with the new combustor utilized a cast piece, with post machining operations to create specific mounting features. One of these critical features is an interior annular wall that separates the compressed air from the heated recuperated air. This feature provides the sliding interfaces between the turbine and the recuperator. In order to adapt our novel CARB 2007 compliant silo combustor to the engine, the inner wall needs to be extended to give adequate space for combustor attachment. A final design effort has focused on recreating this housing and its critical features from machined and welded parts. Figure 65 gives a general layout of the planned housing and silo combustor configuration.

The annular liner is another piece that required a special design to avoid excessive tooling costs. Consultation with the welder and sheet metal shop indicated that a representative liner could be created without the need for large purpose built machinery. The liner has been designed to be made from parts that can be made with available equipment. Figures 66 and 67 illustrate the final design of the internal annular liner for the EHPS new turbine housing and steam injected combustor. The function of the liner has shifted slightly in that it no longer is responsible for holding the flame and diluting the flame gases before they enter the turbine. Now the liner will be used to direct the hot gases from the silo combustor to the turbine wheel. The plan is to begin introducing dilution air before the gases reach the liner to help prolong the life of the liner and decrease thermal induced stresses.

Figure 65: Fabrication Drawing of the New Turbine Housing

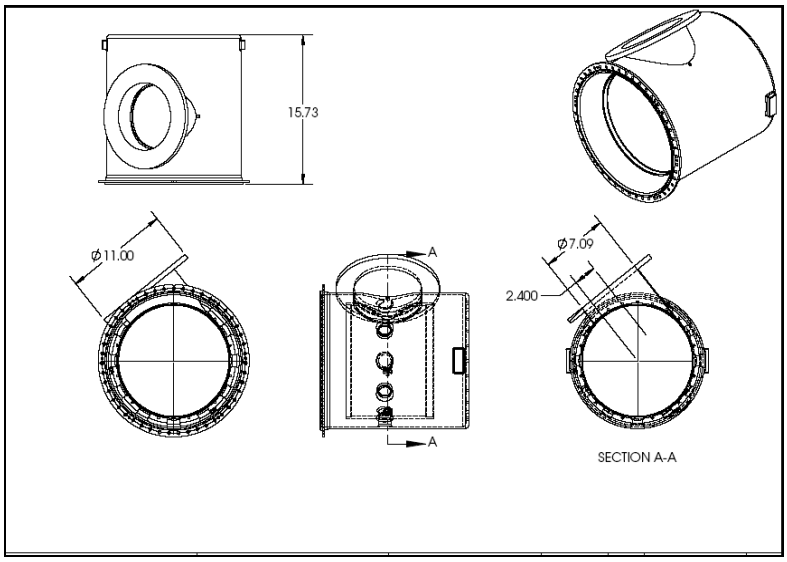

This diagram gives a general layout of the planned housing and silo combustor configuration.
Source: Altex Technologies Corporation

Figure 66: Mechanical Drawing of Updated Turbine Housing

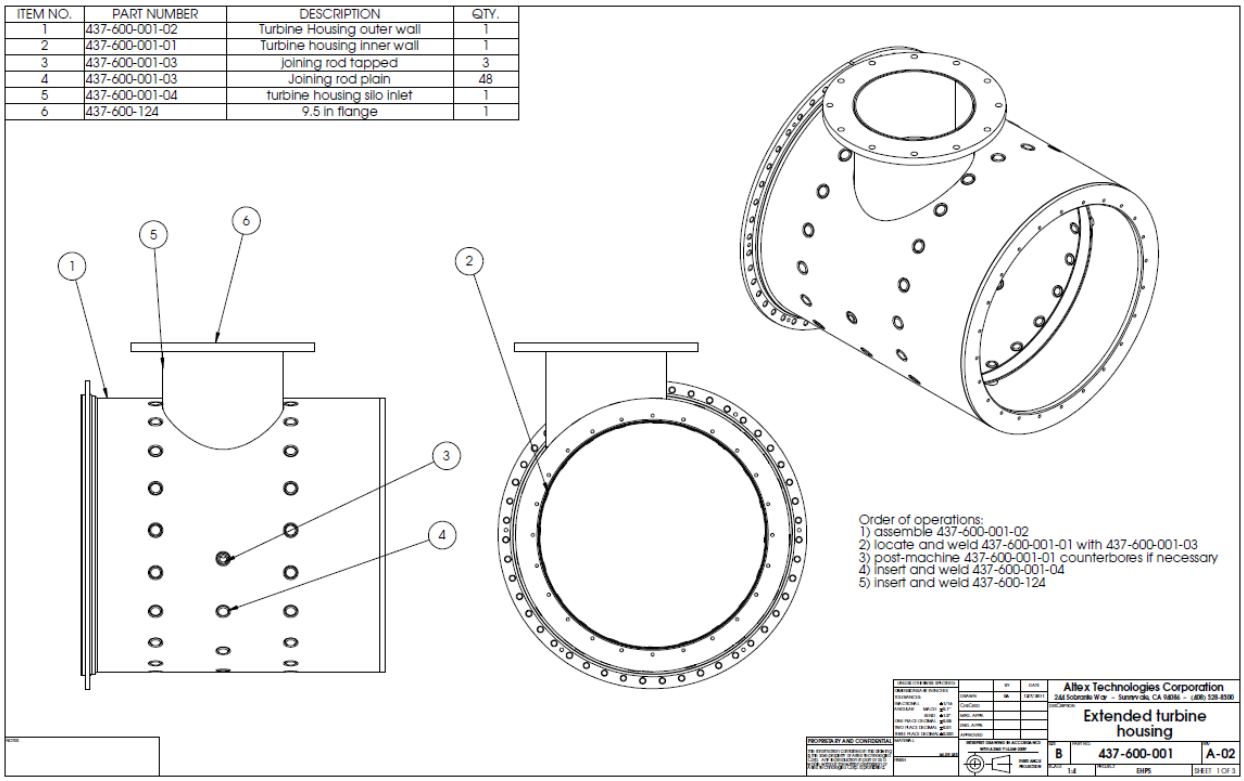

ITEM NO.	PART NUMBER	DESCRIPTION	QTY.
1	437-600-001-02	Turbine Housing outer wall	1
2	437-600-001-01	Turbine housing inner wall	1
3	437-600-001-03	joining rod tapped	3
4	437-600-001-03	Joining rod plain	48
5	437-600-001-04	turbine housing silo inlet	1
6	437-600-124	9.5 in flange	1

This figure shows a diagram of the updated turbine housing fabricated from sheet Metal and machine parts welded together. Source: Altex Technologies Corporation

Figure 67: Diagram of Annular Liner

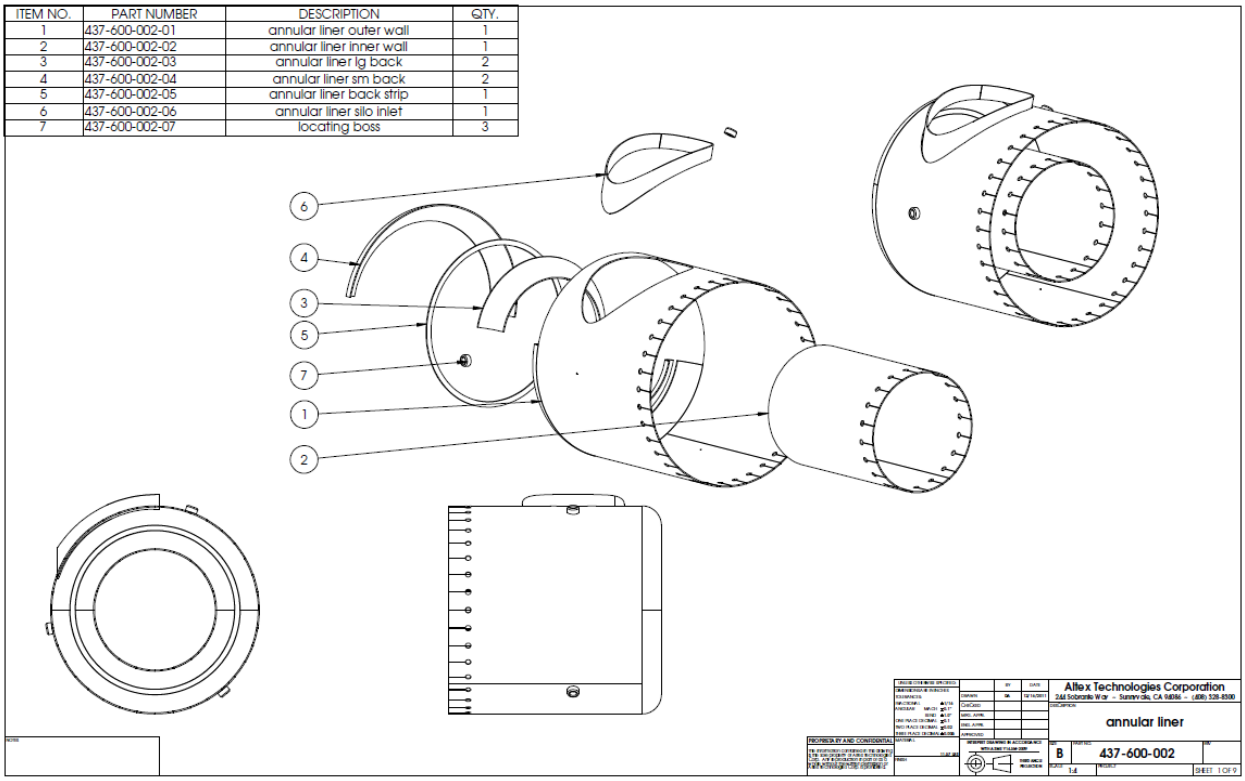

ITEM NO.	PART NUMBER	DESCRIPTION	QTY.
1	437-600-002-01	annular liner outer wall	1
2	437-600-002-02	annular liner inner wall	1
3	437-600-002-03	annular liner lg back	2
4	437-600-002-04	annular liner sm back	2
5	437-600-002-05	annular liner back strip	1
6	437-600-002-06	annular liner silo inlet	1
7	437-600-002-07	locating boss	3

This figure shows the diagram of the annular liner fabricated from formed sheet metal pieces welded together.
Source: Altex Technologies Corporation

3.10 Final Combustor Fabrication and Assembly

The silo combustor is mounted perpendicular to the housing, shown in Figure 68. A cast piece is not an option for the housing, as only one piece will be used for this research effort, and a special casting is not cost effective. As an alternative to casting, the housing will be formed from two main components, the outer wall and the inner wall. These components will be located and welded together to provide the finished product. Post-machining will likely be required to maintain the tolerances needed for the sliding interfaces with the turbine and the recuperator. The combustion liner used for the original annular combustor will need to be replaced by an annular duct that will direct the hot gases from the silo combustor into the turbine wheel. The design will allow for thermal expansion of the pieces without causing detrimental stresses. The silo combustor will grow along its vertical length, so the interface to the annular liner is a sliding fit to allow for this growth. The annular liner will tend to grow radially and along the central axis. To account for this the mounting features allow for radial growth along with the interface to the combustor. The growth along the central axis is accommodated via the sliding interfaces with the turbine and the recuperator.

Figure 68: Silo Combustor and Housing Configuration

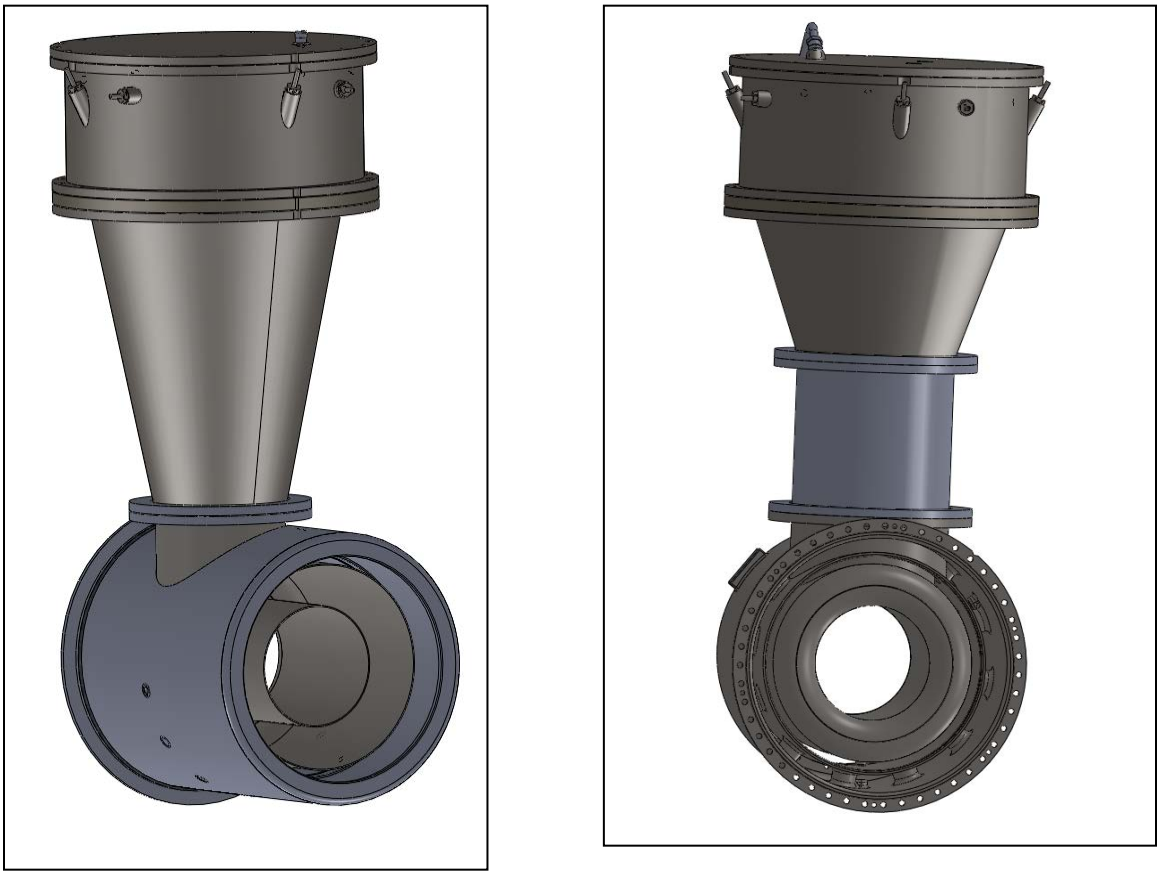

Source: Altex Technologies Corporation

During one atmosphere testing, it was found that the igniter was reaching excessive temperatures that degraded the power cable to the ignition probe. The original allowed the probe to be easily replaced by unscrewing the power cable and unthreading the probe from the combustor. A new design has relocated the igniter to a lower temperature location. Figure 69 shows the new igniter location outside of the primary combustion zone. The new location should protect the igniter from exposure to the radiation of the flame and direct impact of the flame. The combustion air will cool the back side, while the premixed flow cools the tip. The ignited flow will carry out into the combustion zone where it will stabilize and provide the stable primary zone required for successful combustor operation.

Figure 69: Combustor Igniter Location

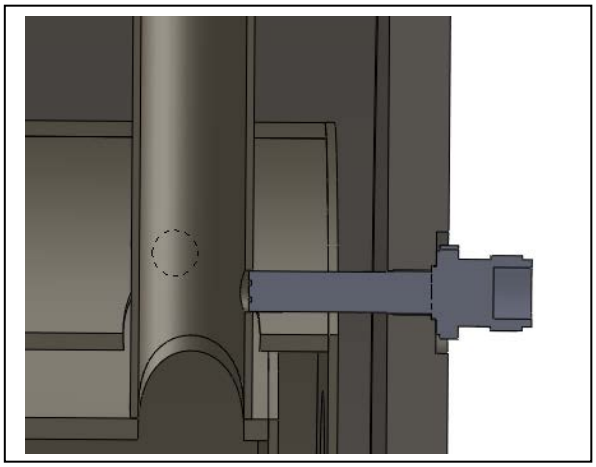

This figure shows the new igniter location outside of the primary combustion zone.
Source: Altex Technologies Corporation

The new EHPS steam-injected silo combustor was fabricated. Figure 70 shows the completed combustor. The silo combustor outer shell was modified to allow the combustion air to enter the recuperator for preheating and returning preheated air to the combustor.

Figure 70: Fabricated EHPS Steam Injected Combustor

Photo Credit: Altex Technologies Corporation

3.11 Combustor Operating Conditions

Figure 2 illustrates the anticipated engine startup sequence from initial engine spin (point 0) to full generator loading (point 8). Ignition with gas only occurs after the engine reaches 16,000 rpm (point 1) and is then reduced to about 12,000 rpm (point 3) in preparation for ignition. Ignition will occur with gas only as steam will not be available at that time. The following rise in turbine exit temperature (TET) indicates successful ignition. Following successful ignition, the engine speed ramps up to rated speed of 8,000 rpm (point 3) with a predetermined flow of fuel. The generator is then loaded and power starts to flow until TA-100 rated power output of 100 kW net is reached (point 4). The engine will continue at this rating until a minimum steam pressure of 90 psig) becomes available. Once steam injection to the air entering the recuperator (point 5) additional fuel is required to maintain combustor condition and prevent flame out. Steady state conditions (point 7) are reached when the power from the generator increases to the pre-established EHPS rating of 135 kW net. Loading of the generator from 100 to 135 kW during steam injection has to occur simultaneously with the amount of steam injected to ensure that the fuel valve responds to the amount of fuel needed in the combustor. During this period, the amount of steam will be increased incrementally in tandem with the increased in generator output and turbine exit temperature. The latter will be an indication of the safe combustion conditions in the combustor adequate to ensure flame stability and emissions control.

Figure 71: Engine Start Sequence

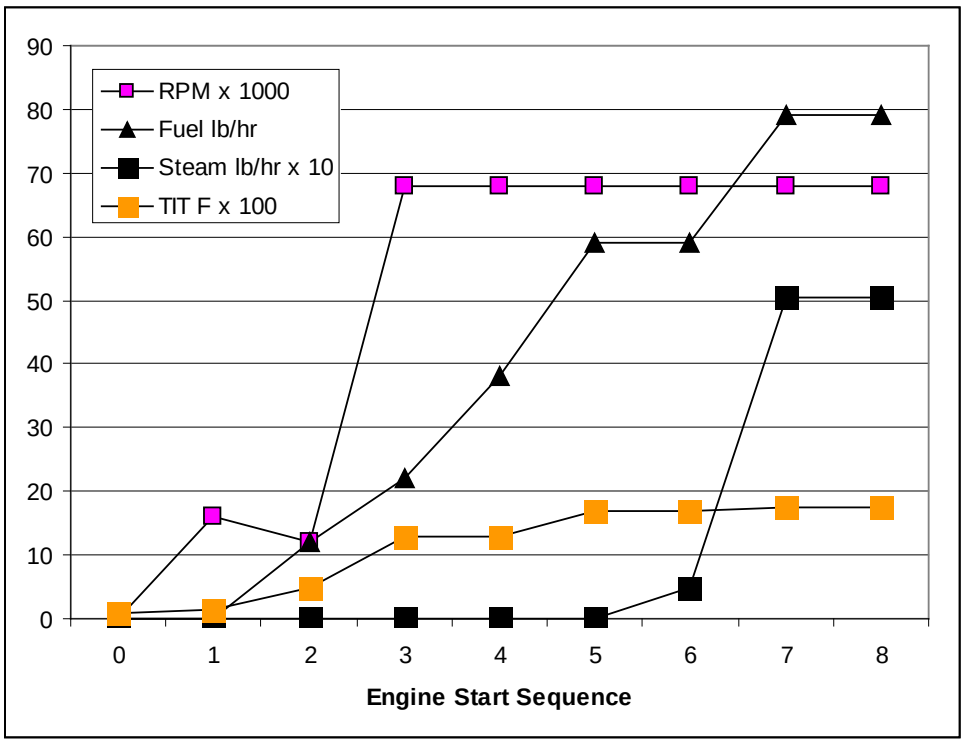

Source: CMC-Engineering

CHAPTER 4:

Develop, Fabricate and Test Water-Steam Heat Exchangers

4.1 Goal and Objectives

The goal of this task was to design, fabricate and test the water-steam closed loop that will supply steam to the silo combustor and recover exhaust waste heat and water. The components of this closed loop system will include the boiler heat exchanger, the condensate preheater, the condensing/heat recovery heat exchanger, the liquid water holding tank, the re-circulating water pump and water treatment components. Using component process design results from Task 2, the heat exchanger components were designed and fabricated. The heat exchangers will utilize an innovative high performance design that has been tested at Altex for other applications [1, 2].

The specific objectives of this work were to:

- Design the heat exchangers and holding tank
- Fabricate and procure heat exchangers and water pump
- Assemble a system and perform preliminary simulation tests

4.2 Approach to Developing and Testing Heat Exchangers

To reduce EHPS heat and water recovery thermal management system volume, weight and cost, the heat exchanger core approach was implemented for EHPS. This approach applies flattened tubes for a factor of three increases in water heat transfer capability. In addition, a special gas side fin configuration and material are utilized to enhance gas heat transfer by over 50 percent. This results in more compact and light weight heat exchangers. Lastly, because the fin material is less costly per square foot than conventional fins, and the special fins have more performance per square foot, then fin and heat exchanger costs are reduced.

Under this task, a sub-scale HASF based heat exchanger was tested to create a design database for EHPS boiler, water preheater and condenser/heat recovery heat exchanger design. An available test system was used to quantify the performance of the HASF test article under simulated EHPS conditions. Test results were converted to heat transfer coefficient and pressure drop correlations as a function of face velocity. Compared to conventional non-condensing and condensing heat exchanger results, the HASF results showed superior performance, with greater than a 50 percent improvement in heat transfer coefficient at the same face velocity. Importantly, because the HASF has a lower pressure drop for a given heat transfer, it can be operated at a higher face velocity, in the range of 1000fpm, where heat transfer is 100 percent higher than conventional heat exchangers. However, under condensing

conditions, the 1000fpm face velocity will strip water from the heat exchanger that will carry over as droplets into the exhaust. To address this carryover, a short blade demister was attached to the back of the condenser that recovered over 95 percent of the water droplets that would exit the heat exchanger when it is operated at a velocity of 1000fpm. This will allow operation at the higher face velocities where HASF heat exchangers are more compact, lightweight and lower in cost.

Using sub-scale unit test results and a proprietary design tool, the thermal management system for the EHPS was designed. Boiler, water preheater and condenser/heat recovery heat exchangers were designed and integrated. Together, these heat exchangers will recover condensate and create steam for injection into the EHPS engine for power enhancement and emissions control. In addition, the system recovers exhaust energy by making hot water for external use. Overall, efficiencies can reach the targeted 87 percent, using the HASF approach. Details on how this is accomplished are given below.

4.3 Review of EHPS Design and Operating Objectives of the Steam Generation and Heat Recovery System

To reach the needed engine and overall system efficiency goals, the steam generation and heat recovery components must meet specific metrics, as defined by process analysis. These metrics were defined in Task 2 and detailed in the task report. Results relevant to the Task 4 effort are summarized below.

Table 17 shows that the condenser/heat recovery heat exchanger has the largest heat duty need, with the water pre-heater duty almost an order of magnitude lower. As will be illustrated in Chapter 5, these differences result in substantially different volumes for these heat exchangers.

Table 17: Heat Exchanger Heat Duties

Heat Exchanger	Capacity (MMB/h)
Boiler	427,861
Condensate Preheater	94,559
Condenser/Heat Recovery	733,770

Source: Altex Technologies Corporation

To address the needed heat duties, the EHPS requires compact and low-cost heat exchangers to condense exhaust water, heat the collected condensate and boil the recycled condensate ahead of steam injection into the TA-100 engine. In addition, a high temperature recuperative heat exchanger is required for maximizing power production efficiency. Process analyses, as illustrated by the results in Table 18, defined the duty requirements for each of these heat exchangers. Table 18 indicates that the amount of steam used by the engine is equal to the

amount of condensate from the engine exhaust. This eliminates the need for make-up water, which is an important aspect of the self-contained CHP assembly package. The cold process water was given a 65F inlet temperature, with an outlet temperature of 138F for the flow rate of 10,000lb/hr, or a heat recovery of 733,770Btu/hr. The overall efficiency, given 133kWe of power and heat recovery, is then 91.3 percent, which is a very high efficiency level. Numerous commercial and institutional water heating uses are possible with EHPS, such as pool water, process water heating and space heating. For some examples, the exhaust temperature of the gas leaving the EHPS will be reduced to 110F, which is the condensation temperature for the steam injected engine considering combustion generated moisture and air relative humidity.

It should be noted that the total heat duty of the EHPS is considerably higher than a conventional CHP system, as a result of the need to condense water from the exhaust and then create steam for injection into the engine. This extra duty requires more heat exchanger surface area to accomplish and will generate more pressure drop. However, the EHPS payoff of higher power output and higher power and overall system efficiency more than offsets the negative impacts of increased pressure drop. Nevertheless, it will be important to limit pressure drop. This is illustrated in Table 18 by ACA calculations of the impact of pressure drop on engine efficiency and power. As shown, increasing pressure drop reduces engine efficiency and power. Fortunately the effect is small, but given the increased heat duty of the EHPS system, the heat recovery components should have low pressure drop per heat transferred. As described below, this is an important characteristic of the innovative heat exchangers to be implemented in EHPS [1, 2].

Table 18: Impact of Pressure Drop on Engine Performance

Pressure Drop (psi)	Efficiency (%)	Power (kWe)
5.31	34.5	131.8
5.9	34.1	129.7
6.49		127.6
7.08	33.3	125.4
7.67	32.9	123.3

This table shows increasing pressure drop reduces engine efficiency and power.
Source: Altex Technologies Corporation

4.4 Conventional Steam Generation and Heat Recovery Systems

At the start of this task, conventional system heat exchanger component performance, weight, volume and cost were assessed. Conventional designs were reviewed to get a more complete understanding of current best practice and limitations. Later in the task, these OTS components were then contrasted with EHPS advanced heat exchanger designs to determine the advantages of using advanced designs.

As noted above, the EHPS system retains the Elliott recuperator and adds a boiler and condenser (condensate and heat recovery) heat exchangers. By comparison, the baseline CHP system contains a recuperator and heat recovery heat exchanger, as shown in Figure 72. Therefore, overlap clearly exists in the recuperator, as well as with the heat recovery. However, as noted in Section 4.3, the heat recovery duty is higher with the EHPS. Figure 73 gives a picture of the conventional recuperator. It consists of a stainless steel shell that contains the hot gas that guides the flow through the air heat exchanger module shown in the lower part of the figure. Corrugated fins are placed between air channels to augment the transfer of heat from the hot gas to the air. While oxidation-resistant allows are used in the air heat transfer module, temperatures were hot enough to show some amount of oxidation at the hot end of the heat exchanger.

At the left end of the recuperator is the compressed air duct that is connected to the air heat transfer module. Modifications to this air inlet duct will be necessary to allow for the steam injection.

Figure 72: Conventional TA-100 CHP System Components

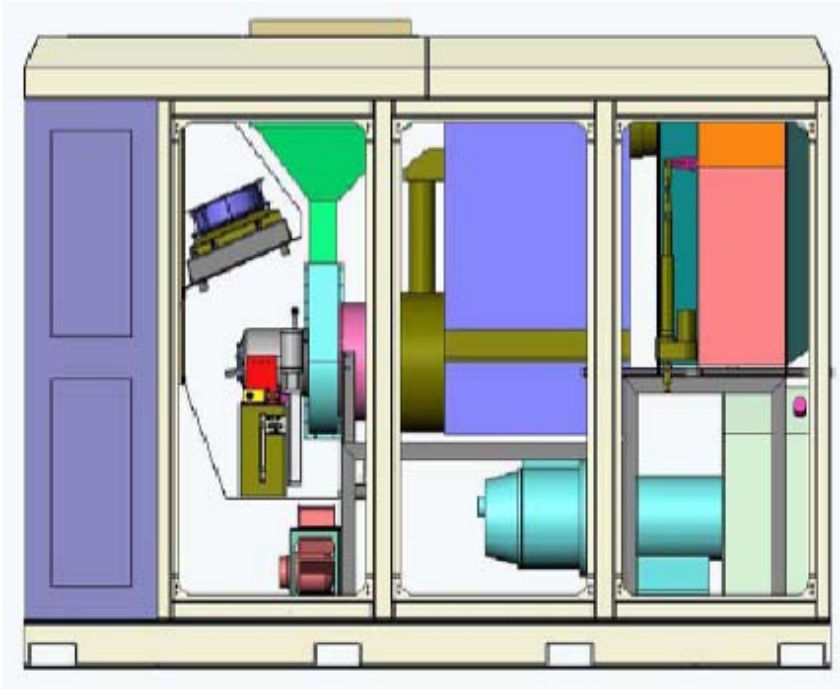

This baseline CHP system contains a recuperator and heat recovery heat exchanger.
Source: CMC-Engineering

Figure 73: External and Internal Photographs of the TA-100 Recuperator

Photographs of a conventional recuperator
Photo Credit: CMC-Engineering

For final exhaust gas heat recovery, the conventional TA100 system uses a finned cylindrical tube heat exchanger, as pictured in Figure 74. These are typical for water to gas heat transfer applications. As shown in Figure 75, the finned cylindrical tube core has 12 flat plate fins per inch. There are 14 tubes aligned horizontally across the core face that is 28.5-inches high by 19.5-inches wide. The cylindrical tubes are staggered, with the core 10-inches deep. The hot gas enters the heat recovery heat exchanger from the horizontal cylindrical duct shown at the back of the picture on the left side of Figure 74. The inlet manifold directs the gas through the finned tube bank, which then exits from the core shown at the front bottom of the picture. This cooled flow is then directed by a manifold chamber, shown in the right of the figure, into the open area above the core and then out the cylindrical exhaust duct on top of the heat exchanger.

As shown, these heat exchangers consist of a multiplicity of tubes in which the liquid flows (e.g. water). The liquid has over an order of magnitude better heat transfer coefficient than the gas. Therefore, the gas side heat transfer controls the heat flow resistance. As shown in Figure 75, the liquid side configuration is a simple cylindrical tube. To promote good gas side heat transfer, fins are placed perpendicular to the outside of the tubes. These flat plate fins channel heat in the gas to the cooler water flow. While advancements in fin technology have improved finned tube heat exchanger performance, new approaches are required to make these heat exchangers more compact and less costly.

Figure 74: Finned Cylindrical Tube Heat Exchanger

For final exhaust gas heat recovery, the conventional TA100 system uses a finned cylindrical tube heat exchanger.
Photo Credit: Altex Technologies Corporation

Figure 75: Finned Cylindrical Heat recovery Heat Exchanger Core

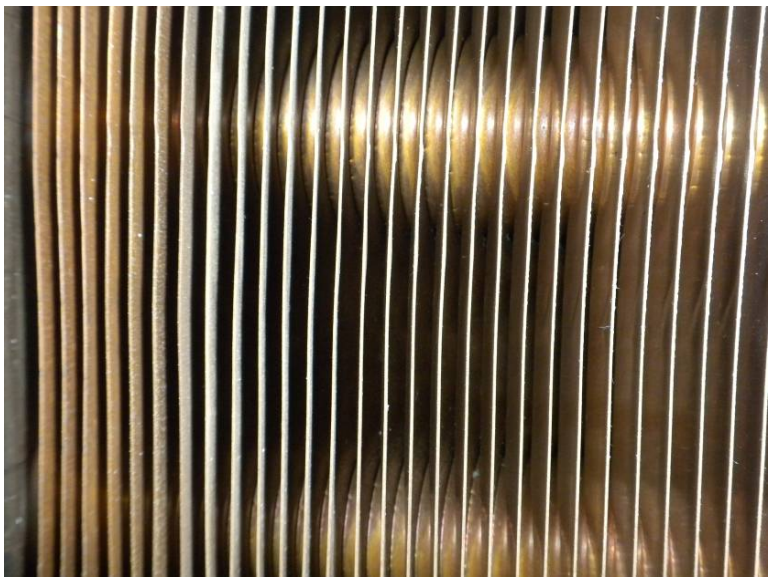

These flat plate fins channel heat in the gas to the cooler water flow.
Source: Altex Technologies Corporation

As noted above, gas side heat transfer is typically the limiting factor in heat recovery heat exchangers. To make heat exchangers more compact, fins are incorporated into the design to augment gas phase heat transfer [4, 5]. By including fins, the surface area in contact with the gas is substantially increased over that provided by fluid separation plates or tubes. In fact, in many compact heat exchangers, fin area can represent over 80 percent of the total heat transfer surface area [4]. Given the importance of surface area to HEX performance, fin characteristics can then dominate HEX performance. Over the years, many different fin configurations have been implemented to augment heat transfer and make HEXs more compact. While these fins beneficially increase heat transfer, they also tend to significantly increase pressure drop and drive up system cost [4]. This is undesirable. Through preliminary analysis and testing [1, 2], Altex has identified the HASF concept that can substantially increase heat transfer, but achieves this beneficial augmentation at lower pressure drop and lower cost. While the concept can be directly applied to the heat recovery need for the TA100 conventional design, it can also be utilized as a boiler and condensing heat exchanger for the EHPS concept, where compactness, low weight, and low pressure drop are required, and low cost is highly desired. Prior to describing this approach and test results, background is given on conventional boilers and condensers that might be applied to EHPS.

To meet the EHPS requirements as defined in Table 18, available conventional heat exchangers were reviewed to assess best practices and fit with the EHPS requirements. This assessment would provide a contrast to the advanced heat exchangers proposed for use in EHPS. Based on a survey of available equipment, a Clayton Industries heat recovery boiler [6] and a Condex [7] condensing heat exchanger were identified as conventional heat exchanger candidates that could be used for these purposes. Figure 77gives an illustration of the Clayton boiler. It consists of multiple "pancakes" of spirally wound tubes that contain the water. These bare tubes fill the cross section of the cylindrical shell. To achieve different capacities, the number of "pancakes" is changed. As shown in the figure, hot gas passes upward through the "pancake" stack, providing the heat needed to boil the water. The tubes do not have any fins, and gas side heat transfer is expected to be limited. Therefore, it is expected that this tube-and-shell design will result in a large volume and weight for the heat duty of interest. In fact, based on a vendor quote, the volume is 20cf, which substantially exceeds the target for the EHPS boiler. Also, the cost of this custom boiler would be $115,000, which is higher than desired.

Figure 78 illustrates the Condex condensing heat exchanger. It consists of multiple finned tubes, as shown in the left part of the figure, packaged in a separate standalone system as shown in the right side of the figure. As indicated in Figure 78, the unit has an induced draft fan that overcomes the higher pressure drop of the condensing unit when it is retrofitted to an existing heat process (e.g. boiler). Overall, this system has a high volume and weight, and a substantial cost of $43,570. While this unit is suitable for conventional boiler retrofit, the packaging and cost are not optimal for use in the EHPS.

Figure 76: Clayton Heat Recovery Boiler

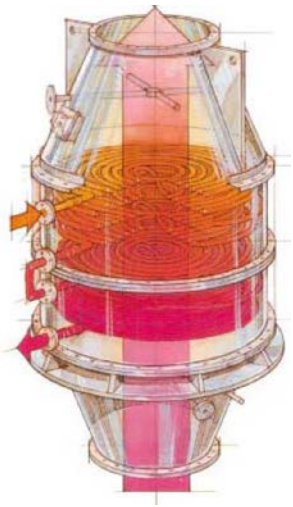

The Clayton Broiler consists of multiple "pancakes" of spirally wound tubes that contain the water.
Source: AHM Associates

Figure 77: Condex Condensing Heat Exchanger

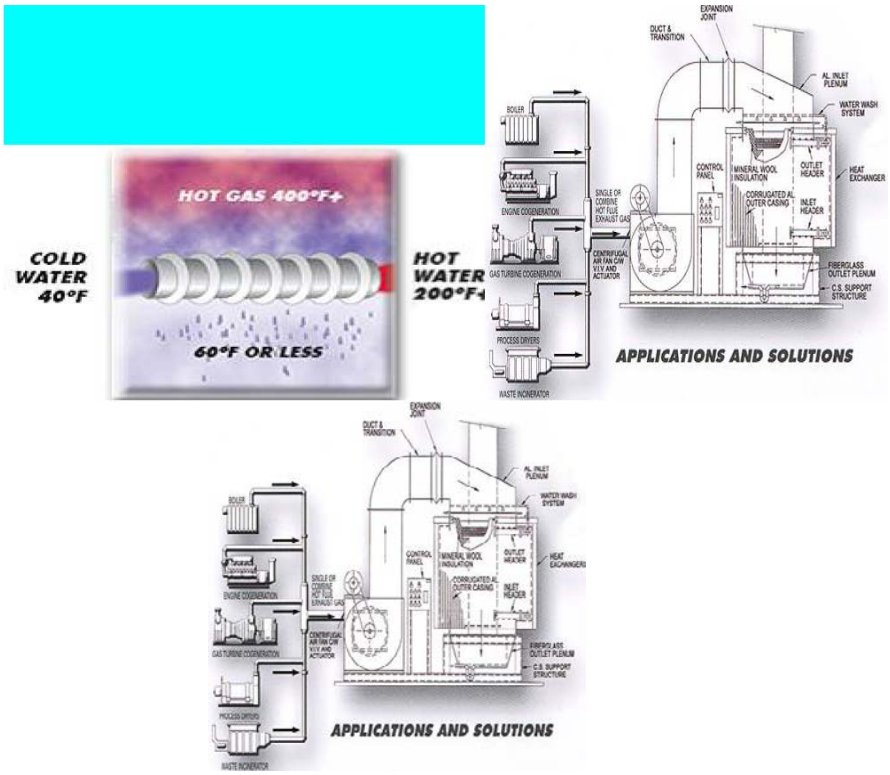

The Condex Condensing Heat Exchanger consists of multiple finned tubes, packaged in a separate standalone system. Source: AHM Associates

While these components of boiler and condenser meet the heat duty requirement, it was concluded that these conventional heat exchangers were too large and costly for use in EHPS. A part of the high cost is associated with some custom manufacturing to adapt these heat exchangers to the application of interest. Nevertheless, the large scale and weight of these heat exchangers is a significant disadvantage for EHPS. The proposed advanced heat exchangers will substantially shrink heat exchanger volume, as well as lower cost, for comparable materials of fabrication [1, 2].

4.5 Design and Fabrication of Test Units

4.5.1 Innovative Heat Exchanger Design

To better meet EHPS steam generation and heat recovery goals, the innovative Altex heat exchanger was considered for EHPS boiler and condensate and heat recovery duties. Figure 78 illustrates the Altex special heat exchanger core [1, 2] design for these applications. It should be noted that this figure illustrates the general concept, but the actual EHPS heat exchangers will use different number of tubes, tube size and material and fin height, number of fins and fin material to optimize performance for the application of interest. Nevertheless, the general design shown in Figure 78 illustrates the approach. For this innovative design there are three main departures from conventional designs shown in Figure 77. First, rather than use cylindrical tubes, flattened tubes are utilized to contain the flowing water. This results in the benefits as given in Table 19. Second, the flat plate fins illustrated for the conventional heat exchanger in Figure 77 are replaced by the special corrugated fins given in Figure 78. This results in the benefits shown in Table 19. Lastly, and most importantly, the fins are made of special material that augments heat transfer while reducing pressure drop. In summary, the special design has substantial advantages over the conventional approach that will result in lower volume, weight, pressure drop and cost for the innovative heat exchangers in EPS. As an example, Figure 79 gives a comparison of the innovative design Coefficient of Performance (COP) versus that for an advanced HMMWV radiator [1]. The COP is the ratio of the heat transfer to the power (i.e. flow rate times pressure drop) required to drive the heat transfer. A higher COP, for the same heat transfer, indicates a more efficient heat transfer approach, and in the case of the EHPS, higher overall engine performance. As shown in Figure 79, the innovative design has a 100 percent higher COP than the comparable advanced radiator design. This shows the potential of the HASF concept for the EHPS application.

Figure 78: Innovative HASF Heat Exchanger Core Design

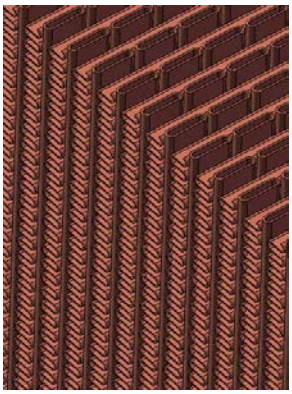

These fins are made of special material that augments heat transfer while reducing pressure drop.
Source: Altex Technologies Corporation

Figure 79: Comparison of HASF and Advanced HMMWV Radiator Performance

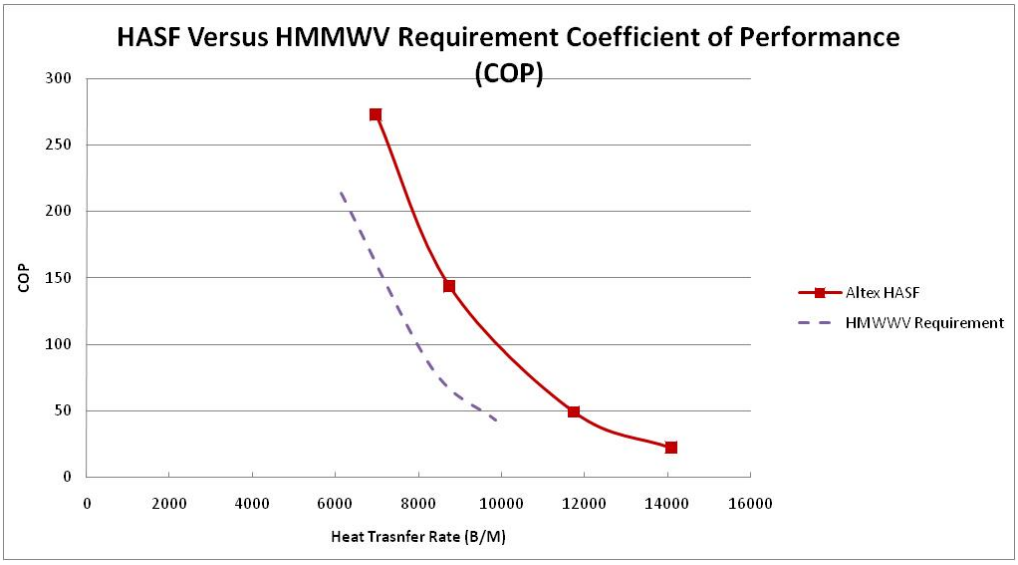

Source: Altex Technologies Corporation

Table 19: Advantages of the HASF Design

Parameter	Parameter	HASF Advantage
Conventional	HASF	
Round watertubes	Flattened watertubes	Increases water heat transfer by factor of three
Flat plate fins	Corrugated special material fins	Increases gas side heat transfer by 58%, Improves COP on gas side by 100%, reduces volume by 63%, reduces weight by 74%, reduces cost by 57%

This table illustrates the advantages of the HASF design over conventional heat recovery heat exchangers.
Source: Altex Technologies Corporation

4.5.2 Modeling of Heat Exchangers

Altex has available a heat exchanger design tool that can be used for preparing full-scale heat exchanger designs that utilize small scale test article data. Under this task, Altex updated a version of this heat exchanger design tool to develop and design EHPS heat exchangers for boiling of the recovered condensate, heating the condensate and recovering moisture and heat from the exhaust gas. While the subscale test results reported below show how selected operating conditions impact HASF heat exchanger subscale article performance, it is beneficial to model the full-scale heat exchanger to show how design and operating conditions impact the overall full-scale system performance. This reduces the time and expense required to optimize the heat exchanger parameters ahead of building the prototype full scale test article. In addition, the model can be used to determine the impact on performance of changes in EHPS operating conditions.

To model design parameter impacts, the model must be able to incorporate the influence of moisture condensation in the exhaust gas on performance. To address this need, an existing Altex heat transfer model that includes condensation was adapted to the analysis. The model includes a gas inlet that can have moisture levels from 0 to 100 percent Relative Humidity (RH). In the latter case, the gas is fully saturated with water vapor at the specified dry bulb temperature. At this condition, the dry and wet bulb temperatures are equal. After the gas enters the heat exchanger, the boundary layer develops on the cooled surfaces, and heat will flow from the hot gas to the water coolant within the tubes. Since the coolant inlet temperature will be less than 80F, the moisture in the entering gas can condense on the fin and tube surface, creating a liquid layer that is assumed to be in equilibrium with the gas at the interface. Figure 80 gives a schematic of this interface, including the bulk flow gas conditions, including gas temperature and vapor content, Ta and Wa. The heat exchanger wall and condensate temperature are assumed to be equal at Tw. Given Tw, the gas moisture content, Ww, can be calculated using equilibrium. The coolant bulk temperature is lower than the wall temperature and is given by Tc.

The above schematic applies at each location on the surface of the heat exchanger. As the gas flows from the front to the end of the heat exchanger, both heat and moisture are removed at the heat exchanger surface. The gas temperature, Ta, and moisture content, Wa, are then reduced with distance into the heat exchanger, achieving the needed level of condensation at the end of the heat exchanger. To calculate heat and mass transfer between the bulk gas state and the surface, and the bulk coolant state and surface, detailed finite difference or lumped parameter methods can be utilized.

Figure 80: Heat and Mass Transfer at Exchanger Surface Model Process at Each Location

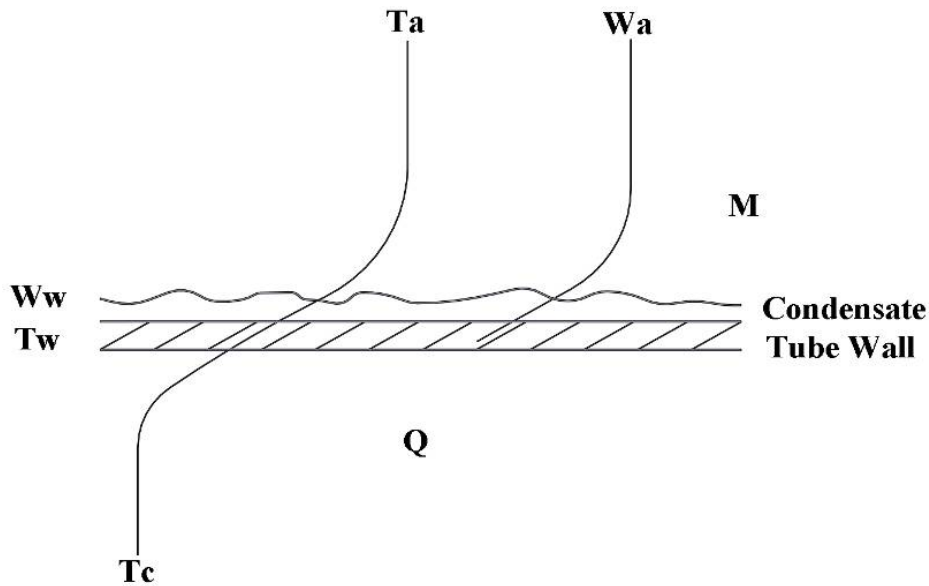

Source: Altex Technologies Corporation

While detailed analyses provides more accuracy, it is better suited to simple configurations (e.g. infinite flat plate separating fluids), rather than a complex three-dimensional configuration, such as the core of the heat exchanger. For ease in problem setup, much reduced runtime and calculation turnaround time, and ease of results interpretation, it is better to use a lumped parameter approach. In this case, the heat and mass transfer to the surface is modeled by single coefficients, with the transfer driven by the difference between the bulk gas and surface conditions. These fluxes on the gas side of the cooling coil are given by:

$$Q = Ah\,(Ta - Tw) \quad (1)$$

where Q is heat flux, A the surface area, h the transfer coefficient, and Ta and Tw are the bulk gas dry bulb and wall temperatures, respectively, at the location of interest, and

$$M = Ak\,(Wa - Ww) \quad (2)$$

where M is the mass flux of moisture, k the mass transfer coefficient and Wa and Ww the bulk gas and wall moisture fractions. To implement this approach, relevant heat and mass transfer coefficients must be defined. For the novel heat exchanger design, the data obtained in test efforts are used to define global heat transfer and pressure drop coefficients. Essentially, the model is run for the test article configuration and coefficients are defined by the matching of model results to tested performance. The derived lumped parameter can then be used to model different configurations (e.g. larger frontal areas and heat exchanger length) and operating conditions (e.g. dry and wet bulb temperatures, velocities and flow rates of gas and coolant).

Through the above validation procedure, the lumped heat transfer parameter can be determined. For the mass transfer parameter, it is assumed that the analogy between heat and mass transfer is applicable. This process is well supported by prior studies [5]. In this case, the non-dimensionalized mass transfer coefficient is equal to the heat transfer coefficient. Under typical turbulent flow conditions, this is a well-accepted result. Using the above to define applicable coefficients, the heat and mass transferred with EHPS heat exchangers can be calculated. To determine the variation in bulk gas temperature and moisture with distance from the front of the heat exchanger, the length of the heat exchanger is broken into many small distance steps. The heat and mass transfers occurring within each step, determined by expressions (1) and (2), are then used to change the initial to the final condition over the step, applying a simple energy and mass balance. Using this approach, the variation of gas and coolant conditions across the length of the heat exchangers can be determined. Preliminary calculations have shown that the model is operable. The model was then used to design the full scale EHPS heat exchangers for the conditions of interest.

4.6 Heat Exchanger Test Article Fabrication

Figure 81 gives the general special core design. For the test heat exchanger, a subscale version of this design is appropriate to define boiling, non-condensing and condensing heat transfer performance that can then be input into the model. While a fully optimized core design would yield best performance, to speed the development of EHPS heat exchangers, a straightforward core design that was successfully fabricated in the past was utilized [1, 2]. More optimized designs can be considered in future efforts, if higher performance is desired.

Ahead of fabrication of the test article, novel fin materials were acquired. This fin material was then shipped to Thermally Engineered Manufactured Products (TEMP) and formed into a corrugated fin configuration. The number of fins per inch was 13, with the height of the fin being 0.38-inch, consistent with the gap between the flattened tubes. This is a relatively standard spacing and fins per inch. To create the radiator core, each of these fins was attached to four in-line flattened copper tubes of 0.01-inch wall thickness. These tubes, shown in Figure 82, were 13.75-inches long and 0.67-inches wide.

By using flattened tubes aligned with the flow, as shown by the assembled test article in Figure 82, the heat path from the coolant to fins was shortened and the blockage of airflow through the core was minimized. It should be noted that the available OTS flattened tubes are not flat along their sides. Therefore, the contact of the corrugated fins will not be perfect along the side of the tubes. This will then reduce performance versus an optimally flattened tube. Nevertheless, these tubes served as a good starting point for this effort.

Figure 81: Flattened Copper Coolant Tubes

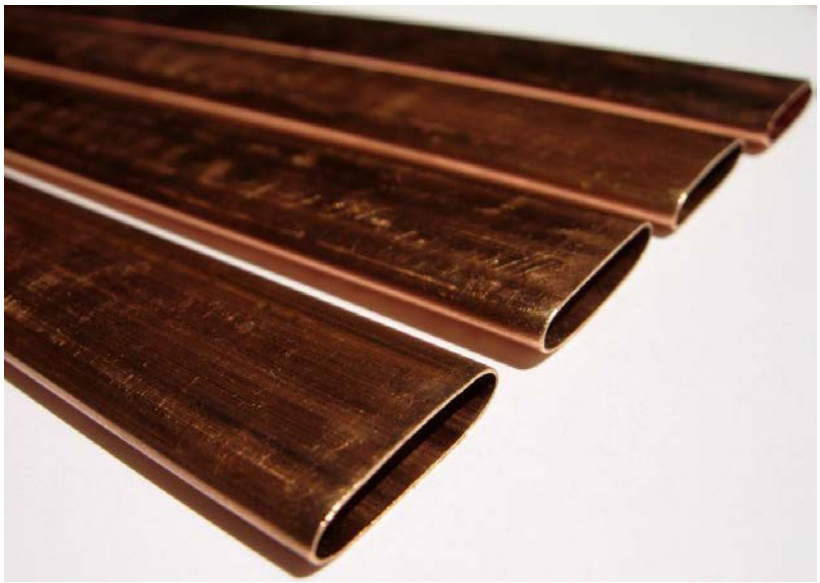

Photo Credit: CMC-Engineering

Figure 82: Photograph of Special EHPS HASF Test Article

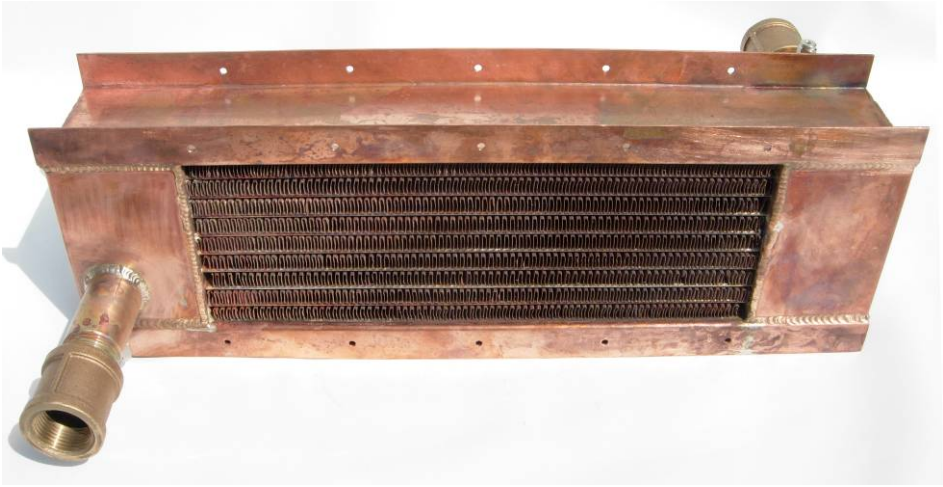

Photo Credit: CMC-Engineering

To create the heat exchanger core, nine rows of corrugated mesh fins were brazed to eight rows of flattened tubes (four tubes in flow direction) by Vacuum Process Engineering, Inc. (VPEI), using their available vacuum furnace. To align tubes and fins for brazing, and to form the base of coolant manifolds, the four tubes in each row were placed into the manifold end plates, as illustrated in the drawing of the test article given in Figure 83. As shown, the multiple row of tubes can be seen, along with their spacing over the width of the radiator. Besides holding the tubes in place, these tube plates formed the base for the water inlet and outlet manifolds. Figure

84 presents the actual end plates with some tubes installed, consistent with the drawing in Figure 83

Figure 83: Drawing of HASF Article Manifolds and Overall Structure

Source: CMC-Engineering

Figure 84: Manifold End Plates with Some Tubes Inserted

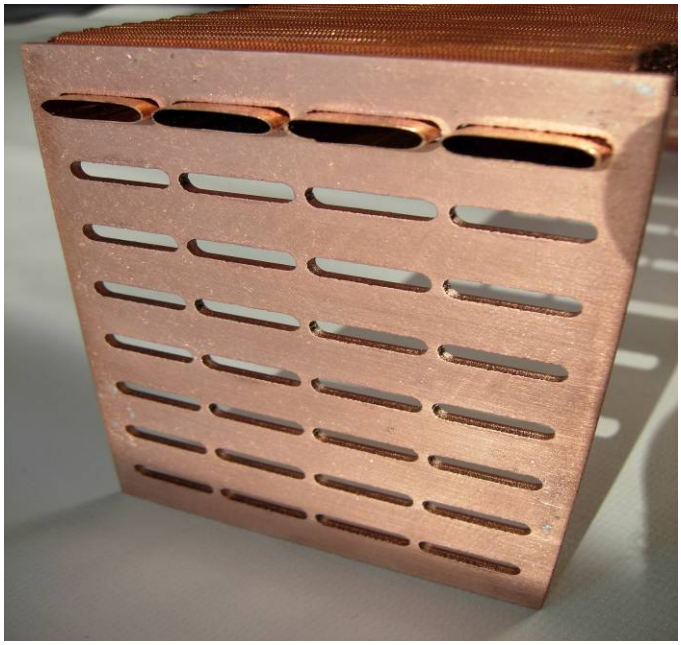

Photo Credit: Altex Technologies Corporation

To bond the heat exchanger structure, a 0.002-inch thick braze compound foil was placed between the tubes and fins at each tube juncture. Tube ends were then inserted through the

holes in the final tube sheet to provide some pressure to the tube/mesh joint. Once a row of tubes were installed, the process was repeated until all nine fin and eight tube rows were in place. At that point, the side plates on the core were installed ahead of placing the core in the furnace. For proper brazing, the furnace was heated to 800C under vacuum conditions. The assembly was manually loaded from the side to maintain good contact of tubes and fins during the brazing operation. However, as described earlier, the tubes were not flat and fin/tube contact was not optimal. With truly flat tubes, fin bonding will be more extensive and performance will be improved.

Once the radiator core was bonded, manifold pieces were then welded by VPEI to the end plates by to yield the complete test article. Figure 82 gives a picture of the completed test article. The multiple rows of tubes and fins can be seen in this picture. Also, the inlet and outlet manifolds with the water coolant supply and exit tubes attached can be seen in Figure 82. To mount the radiator in the test facility, and structurally stiffen the unit, the side pieces are attached to the core as shown in **Figure 82**.

4.7 Heat Exchanger Test Rig

The Altex heat exchanger test facility, illustrated in **Figure 85**, was used to test the special HASF heat exchanger under non-condensing and condensing conditions. As shown, the rectangular copper colored heat exchanger test article is in the middle of the similar shaped duct. The hot gas enters from the right, and is distributed evenly over the duct by a perforated plate insert in the duct. This provides the needed uniform flow ahead of the heat exchanger. Following the heat exchanger is an extension of the inlet duct that provides a uniform outlet flow for accurate flow, pressure drop and temperature measurements. To simulate EHPS steam injection conditions and resulting high moisture contents of the entering hot gas, water was injected into the EHPS combustor test component, shown in Figure 86. The water was converted to steam and the combustor exhaust plus steam was then diluted with air ahead of the duct entrance to yield the proper entering moisture and temperature for the heat exchanger tests. Using available instrumentation, all flows, dry bulb temperatures and wet bulb temperatures were measured. Table 20 presents the range of conditions tested for the non-condensing and condensing heat exchanger tests. In addition, the condensate was also collected to measure the heat balance across the heat exchanger. High, medium and low humidity gas conditions were tested for comparing results to conventional condensing heat exchangers. These results also provided the base data that were used to support the full scale EHPS heat exchanger designs.

Condensing and non-condensing test conditions are cases where heat is removed from the hot gas by the external water coolant, or by the cooler recovered condensate, respectively. These conditions are substantially different from the boiling water case, where the water is heated to boiling by hot gases. Therefore, in preparation for the boiling water heat transfer tests, the Altex heat exchanger test facility, shown in Figure 85, was modified. This modification included the special combustor, shown in Figure 86, which was used as a heat source. For the boiling tests, it was minimally modified. Specifically, the heat exchanger gas inlet temperatures

were increased to over 500F, consistent with recuperated engine exhaust temperatures, as given in Table 21. Prior heat exchanger test temperatures were limited to approximately 300F, by significant air dilution of the exhaust. For the boiling tests, air dilution was reduced to achieve the over 500F simulated exhaust temperatures. This then necessitated that the heat exchanger duct material and configuration, and also the exhaust system, be updated to handle increased temperature.

Figure 85: Heat Exchanger Test Facility - Heat Exchanger Test Duct Component

Photo Credit: Altex Technologies Corporation

Figure 87 gives a picture of the boiling water heat exchanger test configuration, with the special HASF boiling water heat exchanger shown in the middle. The heat exchanger is instrumented with multiple thermocouples and pressure gages to define both heat transfer and pressure drop performance. The heat exchanger is fed with preheated water generated by an electrically heated water reservoir tank. This is consistent with the operation of the full-scale EHPS system. A pump and meter is used to supply the HASF heat exchanger at the needed steam generation rate. Tests covered different gas flow rates and temperatures. With the constant face area heat exchanger, varying the flow rate will yield different face velocities. As illustrated by the prior heat transfer coefficient results [1, 2], the heat transfer coefficient varies significantly with face velocity. Table 21 gives the conditions tested. The gas temperatures correspond with that expected from the EHPS recuperator exit during normal operation.

Figure 86: Heat Exchanger Test Facility - Condensing Component

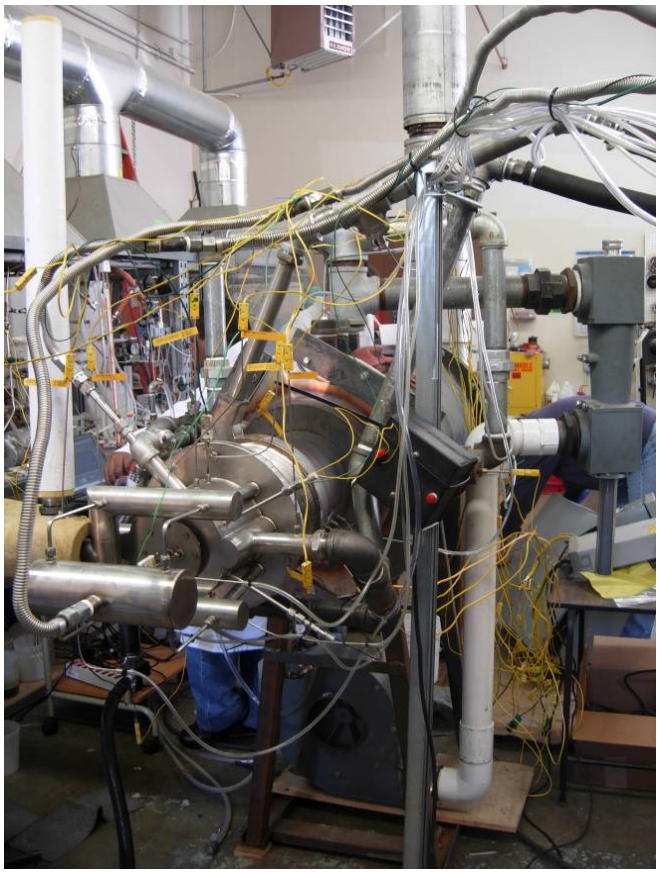

Photo Credit: Altex Technologies Corporation

Table 20: Non-Condensing and Condensing Heat Exchanger Test Conditions

Parameter	Range
Gas Inlet Temperature (F)	80-200
Gas Inlet Face Velocity (fpm)	500-2300
Water Inlet Temperature (F)	40-190

Table 21: Boiling Water Heat Exchanger Test Condition

Parameter	Range
Gas Inlet Temperature (F)	582-612
Gas Inlet Face Velocity (fpm)	469-576
Water Inlet Temperature (F)	100

Figure 87: Heat Exchanger Test Facility - Boiling Water Heat Exchanger Duct Component

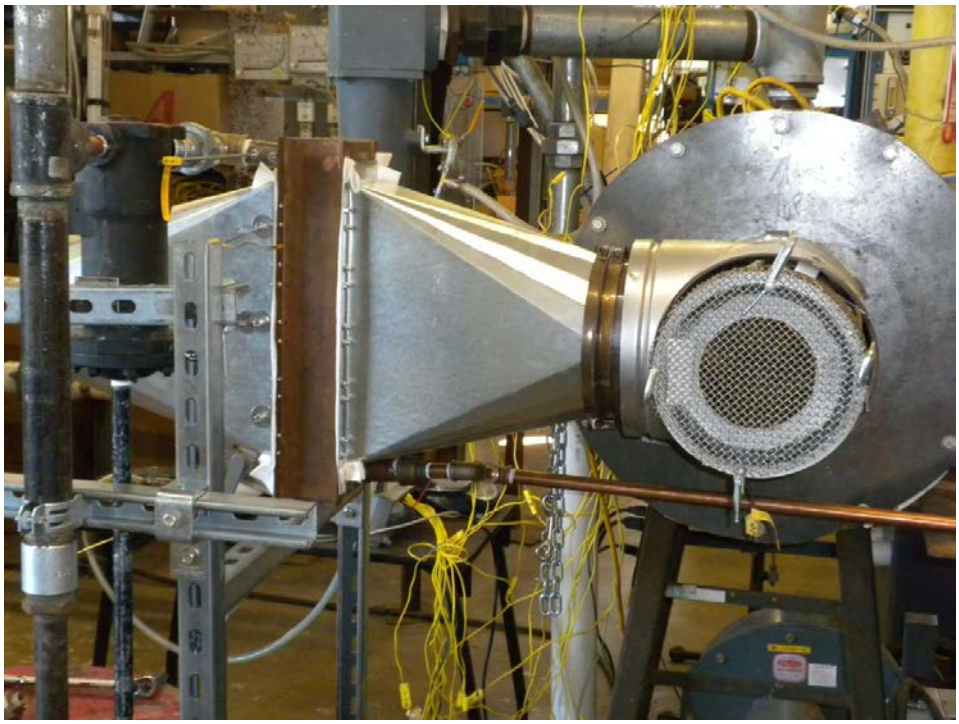

Photo Credit: Altex Technologies Corporation

4.8 Laboratory Testing

Using the test article, tests were run to develop the needed design data base for EHPS boiler, condensate heating and condensate and heat recovery heat exchangers. Test results are given below. In addition, for condensing test conditions, heat exchanger face velocities of greater than 500fpm will tend to strip condensate from the heat exchanger and droplets will be carried downstream into the exhaust duct. While the face velocity can be reduced to below 500fpm to avoid condensate carryover, prior test results showed that heat transfer increases with face velocity. This will reduce heat exchanger volume, which is an important advantage for the EHPS application. Furthermore, increasing face velocity will shrink the face area needed. Together, these impacts can help make the heat exchangers easier to package in the EHPS. Also, by reducing the volume and material required, costs can be reduced. To assess the potential of

higher face velocity, a special design demister was included at the back end of the condenser to collect condensate and prevent carryover of water into the EHPS exhaust. This demister design and successful test results are also presented below.

4.8.1 Non-Condensing Test Results

Figure 88 presents a comparison of the volume normalized heat transfer coefficient for the novel heat exchanger versus a conventional finned tube heat exchanger [2]. By comparing coefficients, derived by normalizing heat transfer data by temperature differences and volume, a more basic parameter is defined that allows a simple and direct comparison between heat exchangers. Also, by comparing results at the same face velocity, or approximately the same Reynolds number, heat exchangers will be compared at the same flow per face area. Again, this yields a more direct comparison for both heat transfer coefficient and pressure drop. For these tests, the Initial Temperature Differences (ITD defined as the entering hot gas dry bulb temperature minus the entering cooler water temperature) was 80 ^{o}F. As shown in Figure 88, the novel HASF heat exchanger (denoted ALHEX in the figure) has a significantly higher volume based heat transfer coefficient than a conventional finned tube heat exchanger, like that shown in Figure 78 [2]. The conventional heat exchanger results are given for a range of ITDs in Figure 88. Based on these results, the novel heat exchanger will be much smaller than a conventional heat exchanger as used in the TA100, while achieving the same heat transfer. In addition, the novel heat exchanger has a higher Coefficient of Performance (COP). This parameter determines the amount of heat transfer produced per flow power needed to drive the heat transfer.

As shown in Figure 89, the novel heat exchanger has a higher COP versus the conventional finned tube heat exchanger. Therefore, besides lower volume, the special heat exchanger will have lower pressure drop, which is an important consideration for a gas turbine based system, where higher pressure drop reduces power output, as indicated in Table 18. Note in Figures 88 and 89 that the conventional heat exchanger data is only obtained at lower face velocities. This is because pressure drop is excessive at higher velocities with these designs. In contrast, the novel HASF heat exchanger data is obtained at a higher velocity because the higher heat transfer coefficient can be achieved at a lower coefficient of performance, as indicated by the results in Figure 89.

Figure 88: Volumetric Based Heat Transfer Coefficient Comparison

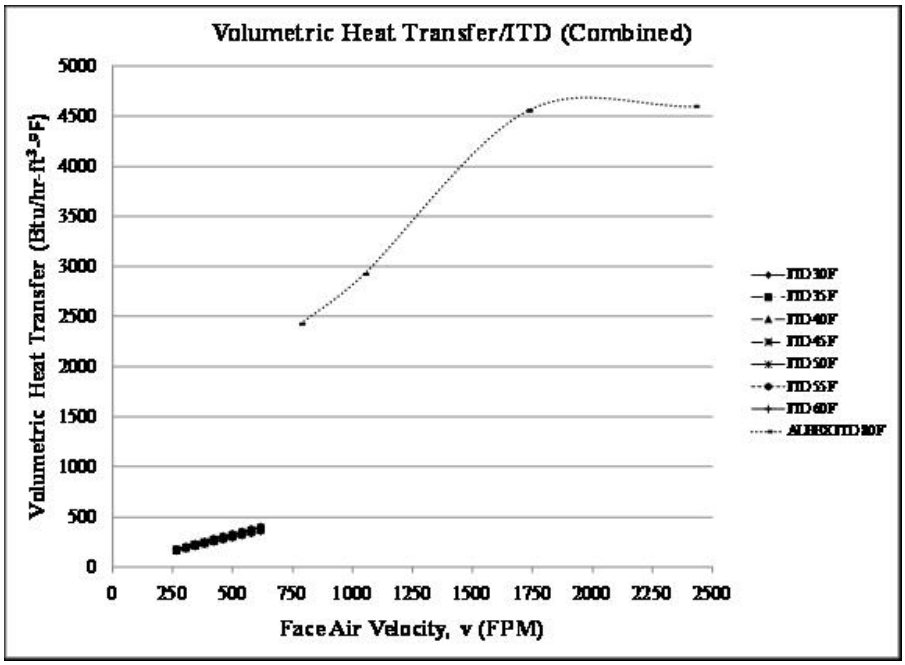

This figure presents a comparison of the volume normalized heat transfer coefficient for the novel heat exchanger versus a conventional finned tube heat exchanger.
Source: Altex Technologies Corporation

Figure 89: Heat Exchanger Coefficient of Performance Comparison

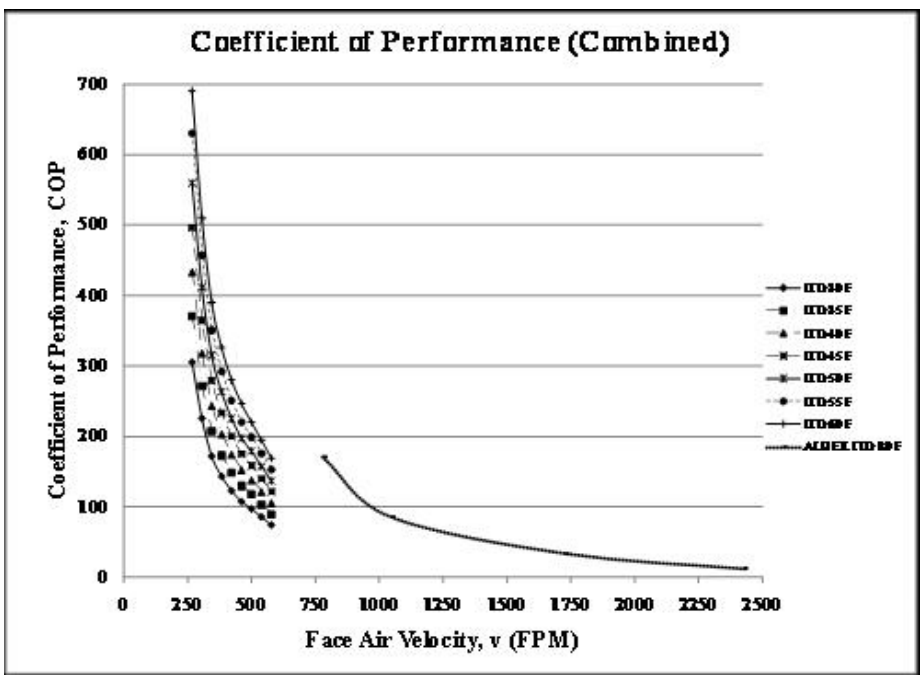

The novel HASF heat exchanger data is obtained at a higher velocity because the higher heat transfer coefficient can be achieved at a lower coefficient of performance.
Source: Altex Technologies Corporation

4.8.2 Condensing Test Results

Results presented in Section 4.81 above used a low relative humidity (RH) gas that avoided any possibility for condensation. For condensing condition tests, the entering gas was humidified, as described in above. His led to moderate and high levels of condensation that covered the levels of interest for the EHPS application.

Figure 90 presents a comparison of the volumetric heat transfer coefficient to a conventional condensing heat exchanger (i.e. DW62 [2]). The special and conventional low and high Relative Humidity (RH) heat exchanger conditions are directly comparable. Face velocities varied from 250 to 600fpm for the conventional heat exchanger to avoid condensate carryover. The special HASF heat exchanger was tested at 500fpm to over 1700fpm. These higher velocities for the HASF heat exchanger were of interest to demonstrate how heat exchanger volume could be minimized. The higher the face velocity, the smaller the frontal area is for a fixed gas flow rate. By using a face velocity of 1000fpm rather than 500fpm, face area is reduced by a factor of two. Even for the same length, the volume of the HASF heat exchanger would then be 50 percent lower than the conventional heat exchanger. Considering the greater heat transfer at higher face velocity, the volume reduction will even be greater than 50 percent.

Figure 90: Comparison of Special HASF and Conventional Heat Exchanger Heat Transfer Coefficients

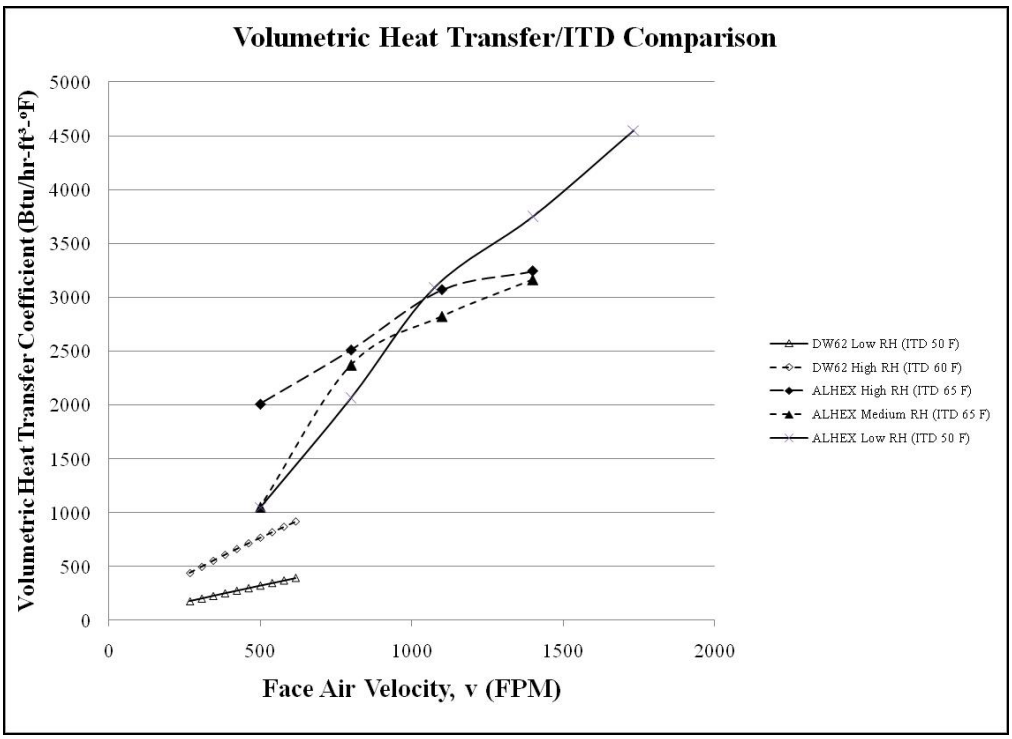

Source: Altex Technologies Corporation

Figure 90 shows that the HASF heat exchanger at low RH and high RH, where condensation is maximized, has 200 percent and 167 percent higher heat transfer coefficient than the conventional heat exchanger. This translates into a correspondingly smaller heat exchanger volume for a given temperature difference. Furthermore, if the special heat exchanger is operated at a face velocity of 1000fpm, then low RH and high RH heat transfer coefficients are 700 percent and 287 percent higher than those for a conventional heat exchanger at 500fpm. Importantly, it is possible to operate the special heat exchanger at 1000fpm and avoid condensate droplet carryover through the use of the special demister. In contrast, the conventional heat exchanger is limited to 500fpm face velocity before condensate droplet carryover becomes a problem. Therefore, the HASF heat exchanger with demister has the potential to yield very high heat transfer in compact configurations, by being able to operate at high face velocities. However, higher velocities will also have higher pressure drop. Figure 91 compares pressure drops for the special and conventional heat exchangers over a range of face velocities. As shown, at 500fpm face velocity, the special heat exchanger has 45 percent and 8 percent lower pressure drop than the conventional heat exchanger at low and high RH conditions. As can be seen, higher velocities produce more pressure drop in either case. The EHPS design must consider both volume and pressure drop requirements in defining the optimal velocity for this application.

Figure 91: Comparison of HASF and Conventional Heat Exchanger Pressure Drop

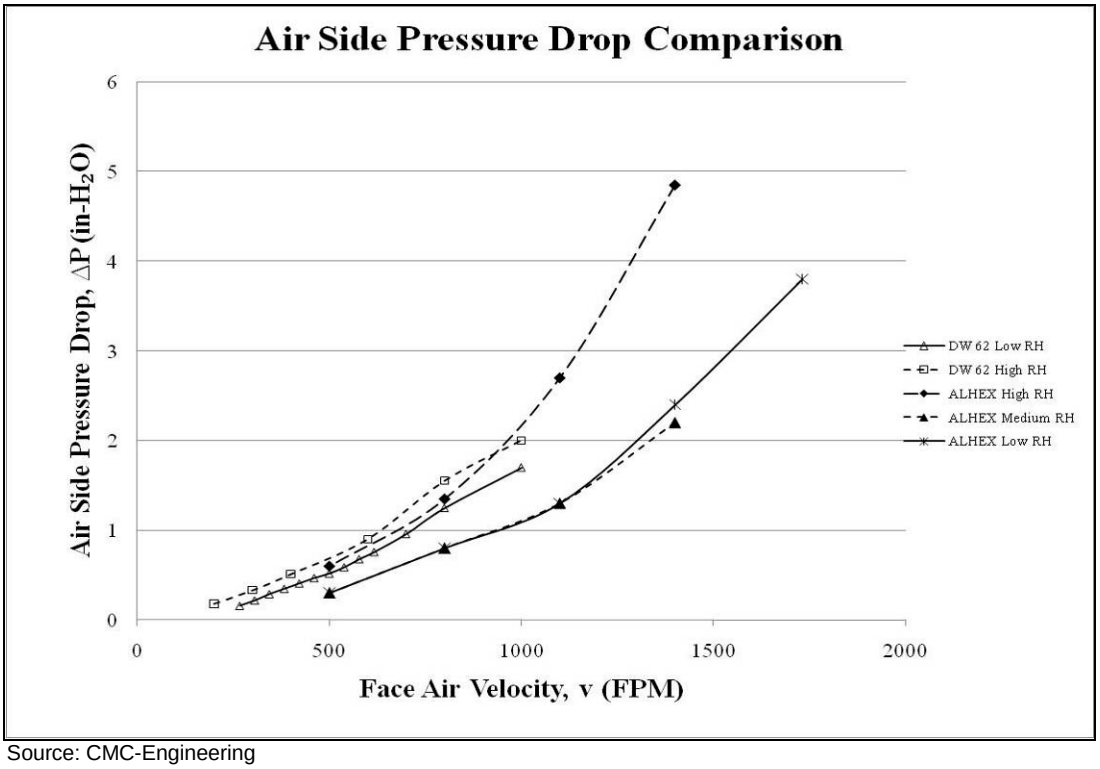

Source: CMC-Engineering

Coolant temperatures covered 60F and 80F conditions that are of high interest for EHPS water heating applications. These results augment earlier test results that covered coolant

temperatures down to 40F and up to 190F. While the high temperature coolant results are not condensing, they provide data for use in the boiler preheat portion of the EHPS system heat exchangers, as characterized above in Figures 88 and 89.

Figures 92 and 93 present the heat transfer and pressure drop for the 40F, 60F and 80F coolant temperatures as a function of face velocity. These results are consistent with prior condensing test results, as shown in Figures 90 and 91. In the figure, the coolant temperatures are given as well as the high (HM) or medium (MM) moisture conditions. In summary, the special heat exchanger condensing results are consistent, and provide higher heat transfer coefficients and lower pressure drop than conventional heat exchangers.

Figure 92: Comparison of HASF Heat Exchanger Heat Transfer Coefficients

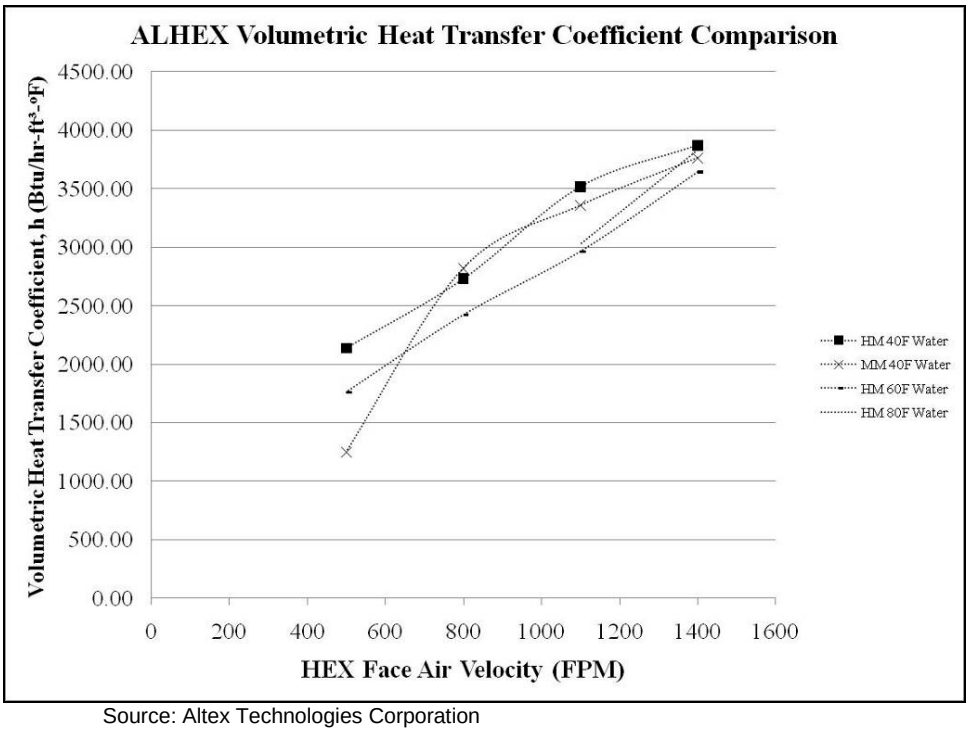

Source: Altex Technologies Corporation

Figure 93: Comparison of HASF Heat Exchanger Pressure Drop

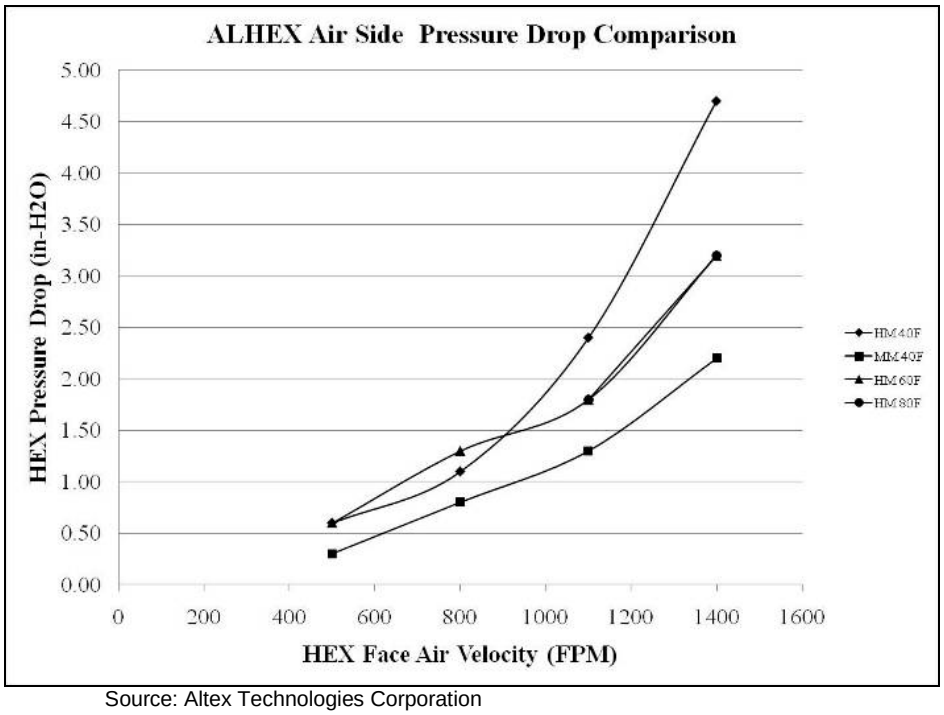

Source: Altex Technologies Corporation

As shown in Figures 90 and 91, the high condensation case has higher heat transfer at low face velocities and higher pressure drops as well. Figures 92 and 93 show the same behavior. This impact is somewhat expected since the presence of liquid condensate in the heat exchanger passages will alter surface heat transfer. In some locations, the condensate will form a resistance to heat transfer as a result of coating the surface. In other locations, the condensate will form drops that run off of the surface, thereby promoting boundary layer disturbances and augmenting heat transfer. Furthermore, these effects will vary with face velocity, where high velocities will tend to "strip" droplets from the surface. These complex condensate processes will alter heat transfer from non-condensing results, but as shown in Figure 90, differences between cases are not orders of magnitude larger. Furthermore, as indicated in Figure 91, pressure drop is increased by high levels of condensate. In this case, the condensate can build up inside the heat exchanger and lead to velocity changes that will increase pressure drop. This effect has been seen in conventional heavily condensing heat exchangers [2].

In parallel with heat exchanger assessment and subscale tests, condensate water quality impacts on heat exchanger materials were identified. Starting with deionized water in the EHPS reservoir, it was determined that the nitric acid content in the condensate would be insignificant, with carbonic acid content leading to a pH of 4.85. If stainless steel and polymer surfaces are used in the condensing part of the system, then the carbonic acid level is acceptable, and no recycled condensate water treatment will be required. This reduces system complexity, maintenance and operating costs.

4.8.3 Boiling Results

Given that heat exchanger performance is controlled by gas side heat transfer, it is expected that boiling water HASF heat transfer will also be excellent. However, the HASF design was only tested with liquid water within the tubes. With boiling heat transfer, a portion of water is converted to vapor, with a very large specific volume increase. Depending on the rate of boiling, a considerable fraction of the coolant tubes can fill with vapor and water, producing "slug" flow that can generate pulsations and vibrations [8]. While a preliminary analysis at the expected rate of boiling suggested that this type of flow should not develop, brief tests were needed to confirm that this was the case. By addressing this issue with the test heat exchanger, the design of the full-scale EHPS boiler can proceed with confidence. By measuring the boiling heat transfer coefficient and pressure drop over a range of face velocities, a data base can be created that can be used to perform the needed EHPS heat recovery design tradeoff study to yield the correct heat exchanger volume, weight and cost, at the needed heat transfer and acceptable pressure drop.

The face velocities for the boiling water tests were low because of the limited heat input and flow of the test system at the needed higher temperatures. However, these velocities were not unusual for typical heat exchanger practice. To simulate EHPS entering condensate conditions during boiling water testing, the water entering the heat exchanger was preheated to 100F. During testing, the water flow into the heat exchanger was varied to meet the steam conversion rate of the heat exchanger. This was determined by ensuring a constant water level in the heat exchanger manifold during steaming. Water droplets carried over in the exiting steam were separated by a commercial steam separator and returned to the heat exchanger. Figure 94 gives the volumetric heat transfer coefficient as a function of face velocity. As with other non-boiling heat transfer coefficient results the coefficient increases with face velocity. Of course, the higher face velocity also increases the pressure drop, as shown in Figure 95. These heat transfer coefficient and pressure drop results can be used as a data base in support of the EHPS heat recovery system design.

Figure 94: HASF Volumetric Heat Transfer Coefficient During Boiling

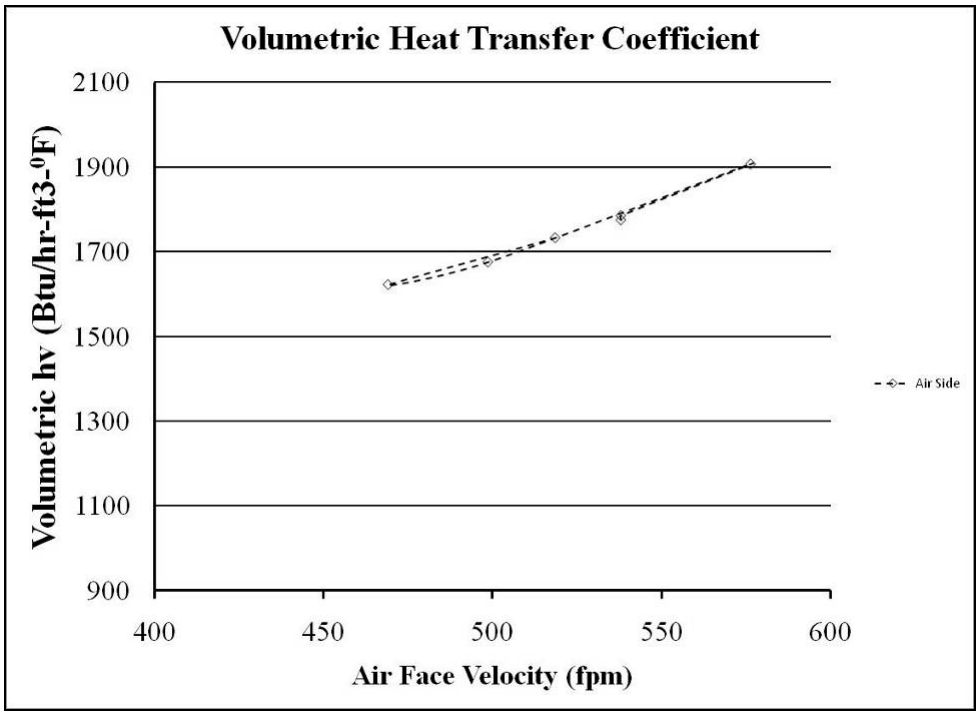

This figure gives the volumetric heat transfer coefficient as a function of face velocity.
Source: Altex Technologies Corporation

Figure 95: HASF Pressure Drop During Boiling

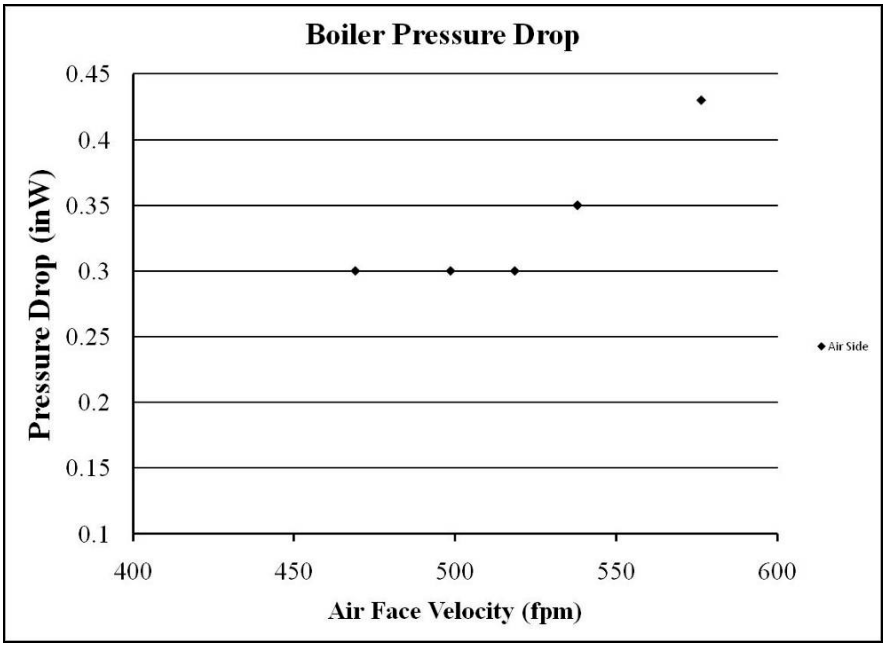

Source: Altex Technologies Corporation

As noted earlier, it was suggested that the novel heat exchanger heat transfer will be controlled by gas side heat transfer. In this case, the overall volumetric heat transfer coefficient should be similar between boiling and non-boiling conditions. Figure 96 compares boiling and non-boiling heat transfer coefficients over the face velocities measured. As shown, the boiling water results are consistent with the non-condensing results, confirming that results are controlled by the gas side heat transfer.

In addition to defining the heat transfer coefficient that will be used in the EHPS heat recovery system design, boiling water tests also showed that the boiling did not create any unusual flow regimes (e.g. slug flow), and that boiling did not produce any vibrations or noise.

In summary, the HASF boiling water heat transfer coefficient data were compared with heat transfer coefficient data obtained under gas condensing and non-condensing conditions. This comparison showed that the overall boiling water heat transfer coefficient aligned with the non-condensing, or modestly condensing, gas side results, which indicates that the heat transfer is controlled by the gas side heat transfer, rather than the water side (boiling or non-boiling) heat transfer. Given the very high heat transfer rates of boiling or non-boiling water, this result was anticipated, and test results confirm this behavior. The comparison also showed that the condensing gas heat transfer coefficient was higher than either boiling or non-boiling water results. It is speculated that heavy condensation on the gas side will produce a dynamic inventory of condensate on the gas side of the heat exchanger that participates in heat transfer and leads to augmentation at lower face velocities. This augmentation can be up to 29 percent for the configuration tested. As expected, results showed that both the heat transfer coefficient and pressure drop increase with face velocity, with the pressure drop rising more rapidly with face velocity than the heat transfer coefficient. Given the difference in behavior with face velocity, this parameter can be utilized in the EHPS boiling water heat exchanger design to reach a proper compromise between heat exchanger volume/weight and pressure loss.

4.8.4 Demister Design and Test Results

Within the condensing part of the EHPS system, temperature and moisture conditions are in a range where very substantial condensation of moisture is expected on cooled tube and fin surfaces. This can be readily shown by dew point calculations based on equilibrium conditions. Furthermore, bulk gas condensation, as well as cooled surface condensation, is also expected. For heat exchanger face velocities of less than 500fpm, the HEX condensate film Webber number is low, and droplet stripping from the surface back into the air flow will not be significant. However, as face velocity exceeds 1000fpm, the Weber number approaches one, and droplet stripping can become significant. These are the velocities targeted to reduce heat exchanger volume. Therefore, droplet stripping and condensate carryover from heat exchanger surfaces would be expected. To address this challenge, the EHPS HASF heat exchanger will employ a downstream section that collects droplets stripped from the surface and thereby prevents condensate carryover into the downstream duct. In addition, droplets condensed from the bulk gas will also be captured. By incorporating the droplet capture section downstream of the HASF condensing heat exchanger section, both sections can be independently optimized.

Figure 96: Comparison of HASF Boiling and Non-Boiling Volumetric Heat Transfer Coefficient

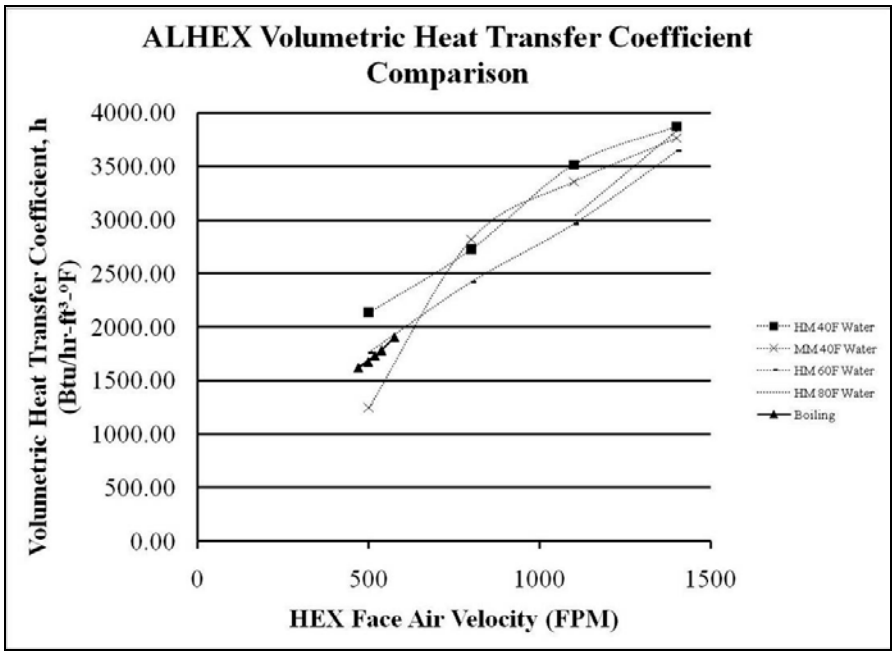

Source: Altex Technologies Corporation

Several methods are possible to capture water droplets. Table 22 lists a range of options that have been successfully applied to collect droplets. They are all based on the principle that the much higher density droplets tend to go in a straight line (i.e. high ballistic coefficient) while the low density gas will readily turn when presented with a flow obstruction. The droplets will then impinge on the surface and collect, while the gas flows around the surface. This dynamic decoupling effect is given by Stokes Law, or:

$$V = \frac{ad^2(\rho d - \rho g)}{18\mu}$$

where is the acceleration caused by changing flow direction, $a\rho a$ and ρg are droplet and gas densities, μ is viscosity, d is droplet diameter and V is the velocity difference between the droplet and gas. As indicated, the larger the value of the flow acceleration, the smaller the droplet can be and still impinge on the turning surface (i.e. higher V). For the cyclone or vortex cases in Table 22, can be high, and very small droplets can impinge on the cyclone wall and be captured. However, the high is driven by the flow being strongly turned in the cyclone or vortex chamber, which then creates high air pressure drops. Therefore, this is not a good method for capturing droplets. In addition, geometry and volume constraints are not compatible with the EHPS. Impinger trains also have geometry and volume constraints, and higher than desired pressure drop, particularly when multiple stages are utilized.

Table 22: Droplet Separation Methods

Method	Mechanism and Characteristics
Cyclone or Vortex	Spinning flow inside a cylinder drives droplets to wall via centrifugal force. Complex and high pressure drop volume system.
Impingers	High velocity jets directly impinge on perpendicular plates where droplets collect as a result of inertia. Larger drops stripped from initial collection are more readily captured by subsequent impingement. Complex and high pressure drop volume system.
Screens	Flow through staggered screens perpendicular to flow cause flow to stagnate on wires where droplets collect as result of inertia. Larger drops stripped from initial screen are more readily captured by subsequent screen. Simple and low volume, with lower efficiency than cyclone methods.
Packed Beds	Flow around packed particles leads to water droplet impact and collection. Good efficiency but low void volume gives high pressure drop.
Blade	Flow around blades leads to water drop collection that is channeled away by dams. Complex but higher efficiency per pressure drop than most methods.

Source: Altex Technologies Corporation

Screens are inexpensive, have straightforward geometries and can be used in multiple stages downstream of the HASF heat exchanger. They are typically placed perpendicular to the flow in multiple rows so that the flow is essentially presented with an array of staggered "tubes" (i.e. wires). Therefore, in some respects the multiple wire screens act like mini multiple and staggered impingers. Under low velocity conditions, small droplets that impinge on the screen wires collect and then run down the surface to the collection channel as larger drops. However, at the high face velocities, the droplets impinging on the screens create larger drops that could be readily stripped off before running down the screens into the condensate collection manifold. Also, multiple screen layers could produce excessive pressure drop. As noted in Table 22, packed beds have large surface areas where droplets can collect. However, small voids will give high pressure drop. Also, high void flow velocity could push water out and promote droplet carryover into the duct. Therefore, this approach has severe constraints as applied to ALHEX water droplet control. The last method in Table 22, blade mist collectors, use aerodynamically shaped surfaces to turn the flow at lower pressure drop than cyclone or impingers, and incorporate dams to channel water collected into the collection tank. These dams create slow moving flow recirculation zones where condensate can collect and run down without being stripped by the high velocity bulk flow.

Figure 97 presents a picture of a commercial blade-based mist eliminator [9]. In the second picture from the left, the middle and trailing edge dams that channel water to the collection tank can be observed. In the third picture from the left, three types of blades are shown. The single "wave" blades on the top are lower pressure drop devices that have less water collection

potential than the double "wave" blade at the bottom. This is shown in the pressure loss versus air speed plot for the three blade designs pictured. As shown, the two "wave" design has a high pressure drop, even for an air speed of 4m/s. The EHPS potential operating velocity of 1000fpm corresponds to approximately 5.1m/s, which is not compatible with the two "wave" design. Furthermore, of the single wave designs, only one is shown in Figure 97 to be operable beyond the 5m/s potential target. While not confirmed, it is likely that droplet carryover limits operation at the high velocities.

These results suggested that current blade designs must be refined to address the higher velocity requirement for EHPS. Key issues for these refined designs will be (1) the shape of the blade to promote droplet impact and collection, and (2) the shape of the dam to capture the collected water and channel the water to the tank below the droplet capture section, and (3) accomplish the collection at an acceptable pressure drop. These are somewhat conflicting needs that then require analyses and testing to reach the right compromise of design parameters to achieve the best solution. In support of this objective, CFDesign was used to calculate flow conditions on various mist eliminator blade designs to assess which blade shape and water collection dam configurations are optimal for EHPS [2]. This resulted in a special design [2] that had good condensate collection and a reasonable pressure drop.

Figure 97: Commercial Blade Mist Eliminator Configuration and Pressure Drop

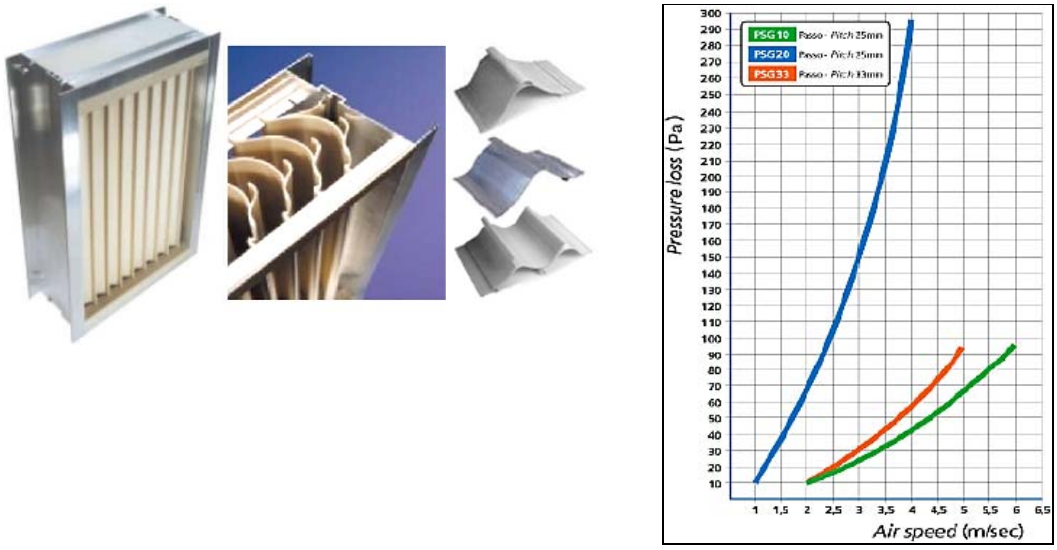

Source: Altex Technologies Corporation

Prior to testing the demister integrated with the condensing heat exchanger, it was separately tested using an ambient condition (100F and about 20 percent RH) air flow, into which a fine droplet spray was introduced. By measuring the water flow into the air and the amount of water collected by the demister, the efficiency of the demister could be obtained. Even though fine drops were produced by the spray nozzle, the cold air and water conditions were not expected to produce significant evaporation of the water through the demister. More specifically, assuming equilibrium conditions, and a water injection rate of 0.05lb water/lb air, the evaporation of the spray was estimated to be 5 percent of the water injected. The rest of the water drops would be collected by the demister, or carry over into the downstream duct.

Figure 85 above presented a picture of the heat exchanger test facility. For the demister test, the heat exchanger illustrated in the middle of the rectangular duct, was replaced by the demister section, which was two-inches long, with the same cross section as the test heat exchanger. To cover the 12.75-inches high by 4.25-inches wide cross section, a total of six vanes were included.

During testing, air flows of 90F air at demister face velocities of 500fpm to 1400fpm were produced by the test facility air blower. To produce the needed droplet stream a simple pressure atomization nozzle was used. The nozzle was mounted along the axis in the air supply duct approximately two-feet upstream of the demister. A clean water supply of 60F at 50psi pressure was utilized to drive the narrow angle spray. While the droplet size distribution was not characterized for these feasibility tests, a visual observation showed that the spray produced a fine droplet mist. Using simple spray nozzle correlations with pressure and orifice dimensions as key parameters, a mean droplet size for the spray was estimated to be 0.0015 inches [10].

During testing, the amount of water sprayed into the duct was measured with time. In addition, the water collected by the demister was also measured over the same period. Dividing the captured water by the sprayed water then yielded a demister capture efficiency. The difference was then the sum of the spray that went through the demister and that evaporated. As noted above, the evaporated water could be up to 5 percent. Any amount over this would then be droplet carryover into the downstream duct.

Figure 98 gives the demister efficiency as a function of air flow face velocity ahead of the demister. As shown, the demister droplet capture is about 95 percent at the conventional cooling coil face velocity of 500fpm. Considering evaporation loss, this indicates a very high level of droplet removal. For higher velocities, in the range of 1400fpm, the demister is outside the design point and droplet collection efficiency decreases to 60 percent. This low efficiency could be corrected by a more aggressive flow turning design, at the expense of increased pressure drop. This increase in pressure drop as velocity increases is illustrated by results from the current demister design tests.

Figure 98: Test Diameter Droplet Removal Efficiency Versus Face Velocity

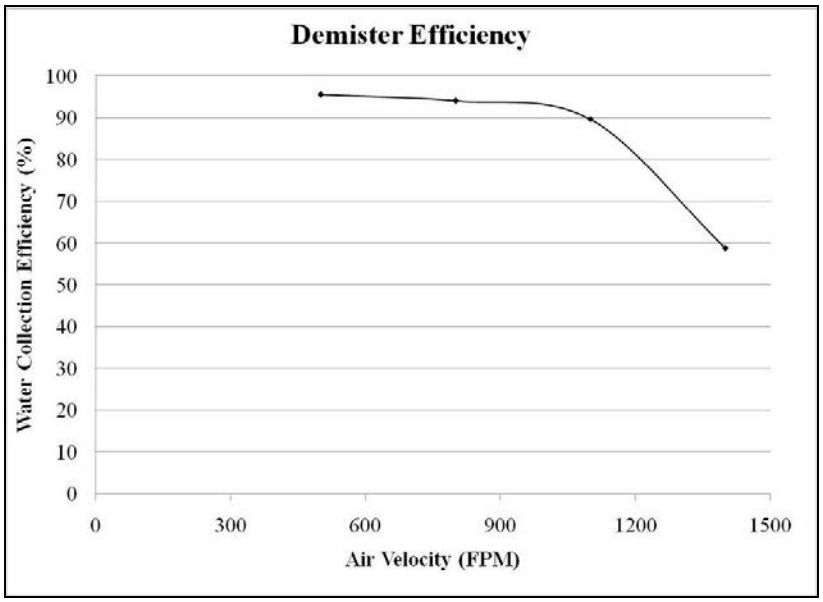

Source: Altex Technologies Corporation

As shown in Figure 99, pressure drop at 1400fpm exceeds 2-inches water column. This is over a factor of two higher than the approximately 0.9-inches water column pressure drop at the design point of 1000fpm face velocity. This is a reasonable pressure drop for the aggressive demister design that will handle large amounts of water in the air. This good result is supported by the comparison to the PSG20 commercial demister results given in Figure 97. As shown, the multiple turn geometry case has a pressure drop of over 1.2-inches water column, even at a face velocity of 800fpm, with an expected pressure drop of 1.9-nches at 1000fpm. This is double the current design demister pressure drop. While the single turn commercial vane demisters, illustrated in Figure 99, have lower pressure drops, these cannot handle large amounts of water, as required for the EHPS application at 1000fpm.

4.9 Final Heat Exchanger Design and EHPS Interface

Using the HASF flattened tube and corrugated special fin heat exchanger core design given in Figure 78, the boiler, water preheater and condenser/heat recovery heat exchanger design parameters were calculated for the conditions given in Tables 2 and 5. The model highlighted in Section 2.2 was utilized along with the volumetric heat transfer coefficient and pressure drop data presented in Figures 88 through 96. In addition, demister data in Figures 98 and 99 were utilized in the condensate recovery design for the condenser/heat recovery heat exchanger. Model results provided the overall heat exchanger core dimensions and pressure drop results for the three heat exchangers as given in Table 23. To determine overall dimensions, the manifold dimensions must be added to the core dimensions. These manifold dimensions will vary, depending on the type of heat exchanger. Also, the core dimensions given in Table 23 are

the minimum to meet the required heat duty at the design point. To cover limitations in model results, the cores will be oversized in the test system by 20 percent.

Figure 99: Demister Pressure Drop versus Face Velocity

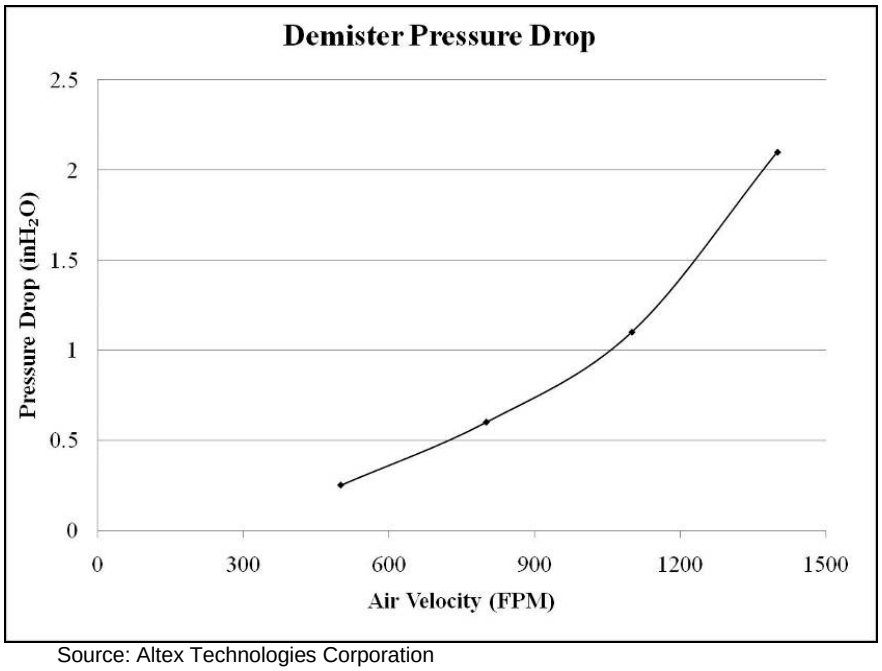

Source: Altex Technologies Corporation

Table 23: HASF Parameters and Performance for EHPS Heat Exchangers

Heat Exchanger	Capacity (B/h)	Core Height (in)	Core Width (in)	Core Length (in)	Pressure Drop (in H2O)
Boiler	427,861	18	13.5	4.25	5.67
Water Preheater	94,559	18	13.5	1.05	1.40
Condenser/Heat Recovery	733,700	18	13.5	7.95	7.95

Model results provided the overall heat exchanger core dimensions and pressure drop results for the three heat exchangers.
Source: CMC-Engineering

As examples of the calculated results, Figure 100 presents the predicted variation of gas temperature in the boiler with distance.

Figure 100: Decrease in Gas Temperature Along Boiler Length

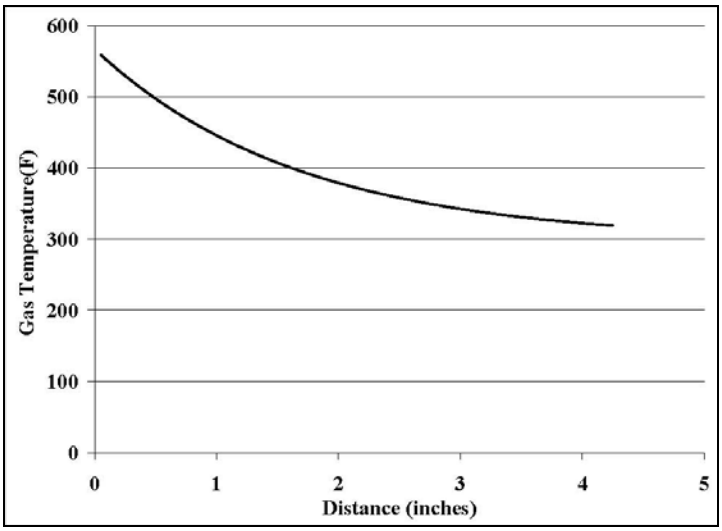

This figure presents the predicted variation of gas temperature in the boiler with distance.
Source: Altex Technologies Corporation

As shown, the temperature drops from the recuperator exit level of 559F to 318F in a distance of 4.25-inches even with a heat duty of 427,861Btu/h. This rapid reduction is both a function of the more effective fins, as well as the higher face velocity that promotes high heat transfer. With a lower heat duty of 94,559B/h, the water preheater only needs a length of 1.05-inches to reduce the gas temperature from 318F to 264F, as shown in Figure 101.

Figure 101: Decrease in Gas Temperature Along the Water Preheater Length

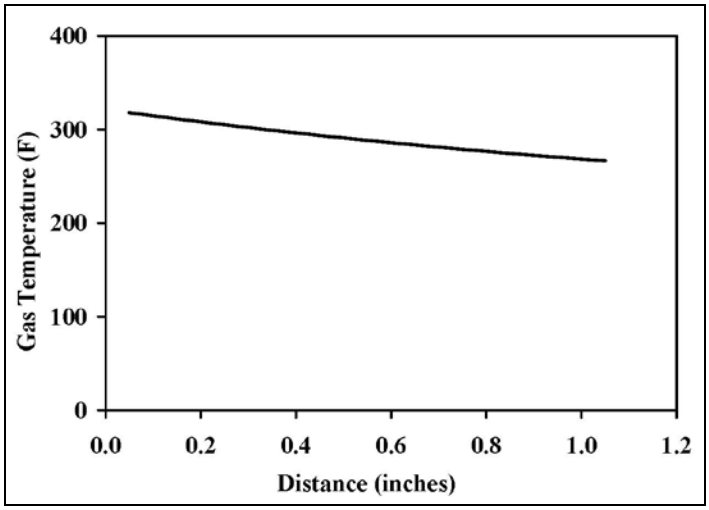

Source: Altex Technologies Corporation

The condenser/heat recovery unit has the highest heat duty of 733,770B/h, which includes both sensible heat removal and latent heat removal as a result of condensation of moisture in the

exhaust. As shown in Figure 102, gas temperature decreases from 264F to 110F in 7.95-inches along the special heat exchanger.

Taking the design parameters for the HASF heat exchangers, given in Table 23, mechanical designs were prepared and are given in Figures 103 through 105. The most complex component is the Condensing/Heat Recovery Heat Exchanger (CHRHE), which recovers heat from the exhaust by heating cold water. In this process, gas temperatures are reduced to 110F, where the moisture in the gas as a result of steam injection is condensed. Therefore, this heat exchanger must manage both heat and condensate on the gas side. As noted earlier, for lower volume, weight and cost, higher face velocities will be required, which will lead to condensate stripping and carry-over. However, by incorporating the custom demister, described in Section 4.4, condensate recovery is maximized and droplet carry over into the exhaust is minimized. As shown in Figure 103, the CHRHE prototype core consists of three separate sections bolted together. Gas flow enters from the right side and exits to the left. The two front sections contain heat exchanger core elements, while the last section on the left contains the demister elements.

Figure 102: Decrease in Gas Temperature Along the Condensed/Heat Recovery Heat Exchanger Length

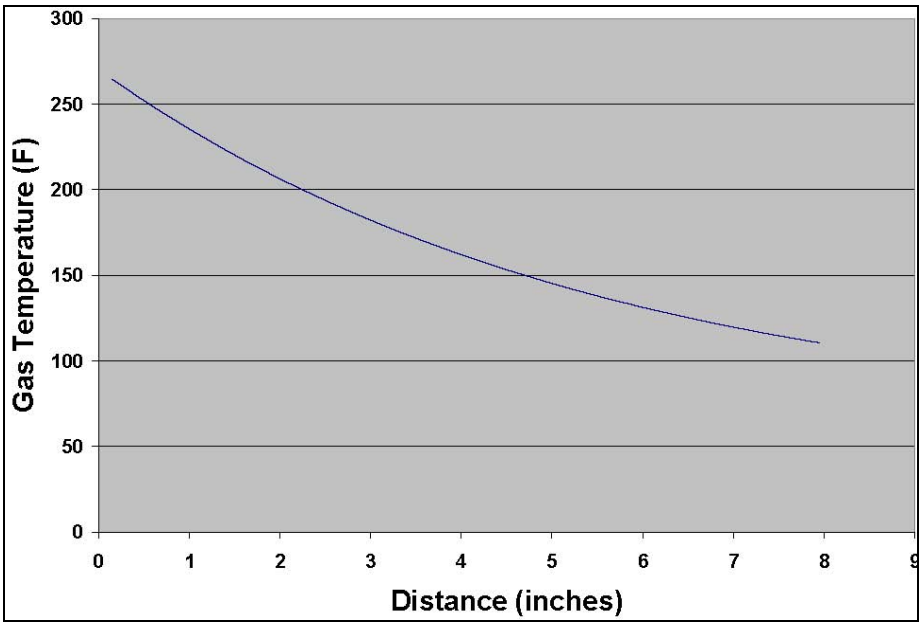

Source: CMC-Engineering

Figure 103: CHRHE Design Side View

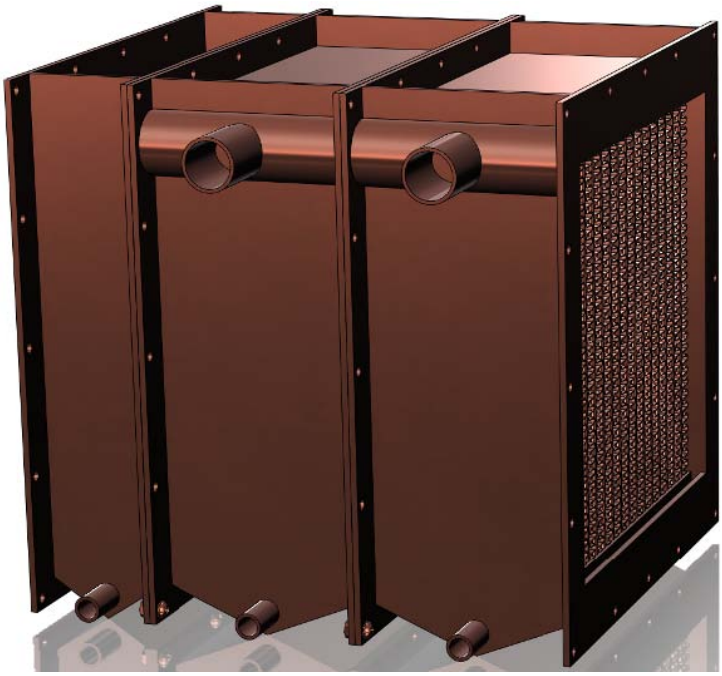

Source: Altex Technologies Corporation

Figure 104: CHRHE Design Separate Sections - Coolant Inlet and Outlet Side

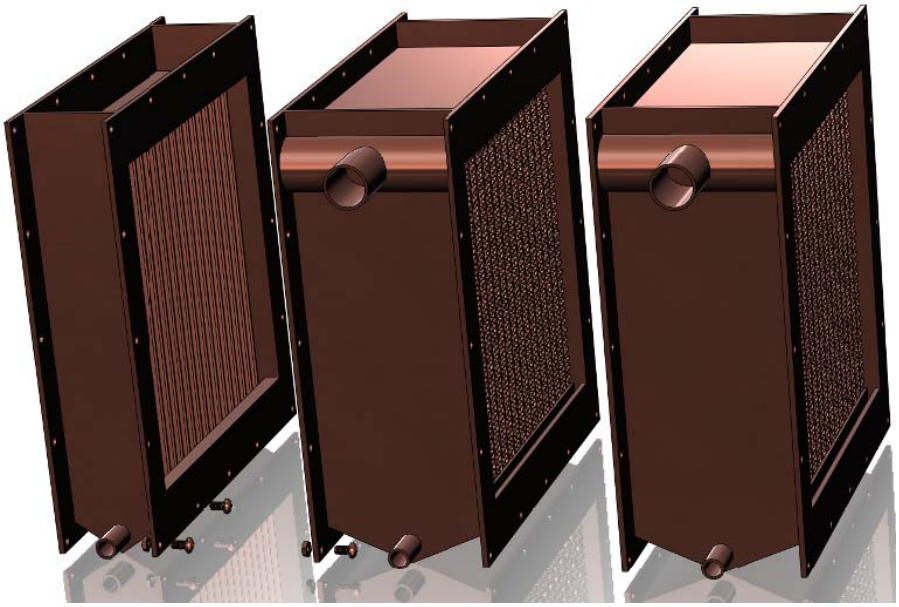

Source: Altex Technologies Corporation

Figure 105: CHRHE Design Separate Sections - Coolant Section Connection Side

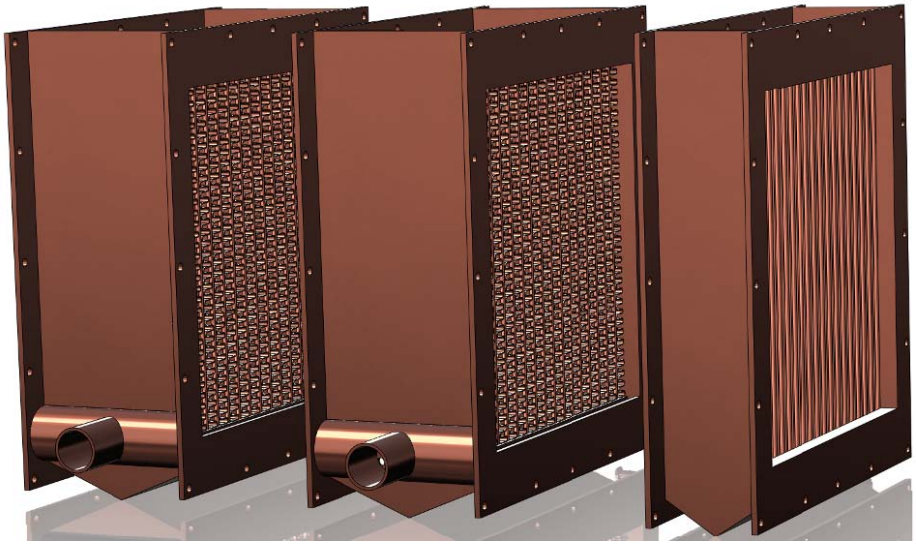

Source: Altex Technologies Corporation

The heat exchanger sections contain banks of seven flattened tubes each, with space between each bank for easy condensate drainage. Between the flattened tube rows are the special corrugated fins, as illustrated in Figure 80. By dividing the core into two heat exchanger sections in the prototype CHRHE, the option exists to replace a section with a longer or shorter section, depending on test results. Also, the sections could each be built with different fins and tubes to optimize performance or droplet capture. Figure 104 shows the sections separated, with the section on the left showing the front of the demister elements. As shown in Figure 104, the cold coolant water enters the second section at the tube near the top of the section. The coolant flows downward to the manifold on the bottom and then exits the second section through a tube at the bottom, as shown in Figure 105. This coolant is then routed forward to the first section, now on the left side of Figure 105. The coolant flows upward in the first section and then exits through a tube on the top of the section, as seen in Figure 104. Therefore, the CHRHE is a two pass counter-flow heat exchanger. As noted in Reference 4 and shown in Figure 106, the two pass design has an effectiveness that is within 6.25 percent of a true counter flow design at an Nusselt number (Ntu) of 4. Prototype manifolds are sized to yield uniform flow in the heat exchanger core. Figure 103 shows the water collection chambers below each section and the three condensate outlets. These are separate in the prototype to assess condensate collection for each section. In the production version, only one condensate collection chamber will be utilized. As with conventional heat recovery heat exchangers, the water inlet and outlet are placed on the same side, as shown in Figure 104. Typical flange configurations are utilized on the CHRHE, as typically used on conventional heat recovery heat exchangers, as illustrated in Figure 104.

Figure 106: Heat Exchanger Effectiveness for Multiple Pass and True Counter Flow Design

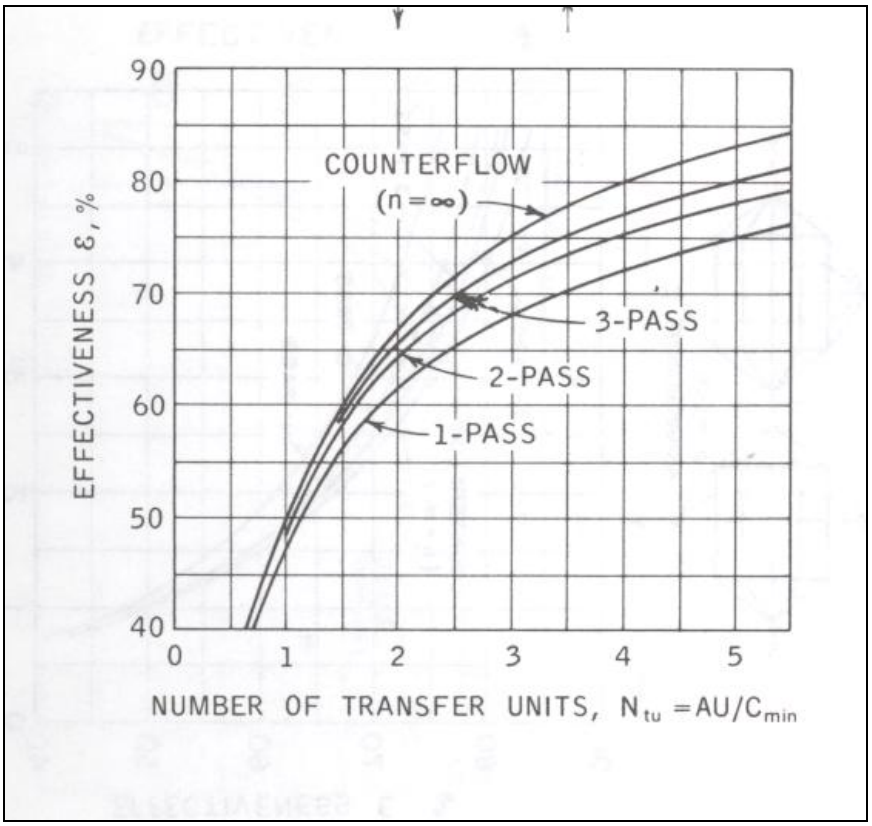

Source: Altex Technologies Corporation

The Boiling Water Heat Exchanger (BWHE) does not have the gas side condensate management challenge of the CHRHE, but it does require the management of a steam/water mix on the water side of the heat exchanger. As shown above in Section 4.8.3, the boiling of water in the BWHE tubes did not create any unusual flow regimes (i.e. slug flow) and associated pulses, noise or vibrations. In addition, to produce a "dry" steam, a conventional steam separator was successfully used in the tests. For the prototype BWHE, a simple steam separator is used at the top of the unit to produce the "dry" steam for injection into the recuperator. Figure 107 shows the core configuration for the BWHE. In contrast to the CHRHE, only a single segment is used to cover the total boiler heat transfer needs. The BWHE has water (i.e. preheated condensate) entering from the bottom, with demisted "dry" steam exiting at the top, ready for injection into the recuperator for final heating.

Figure 107: Boiling Water Heat Exchanger (BWHE) Configuration

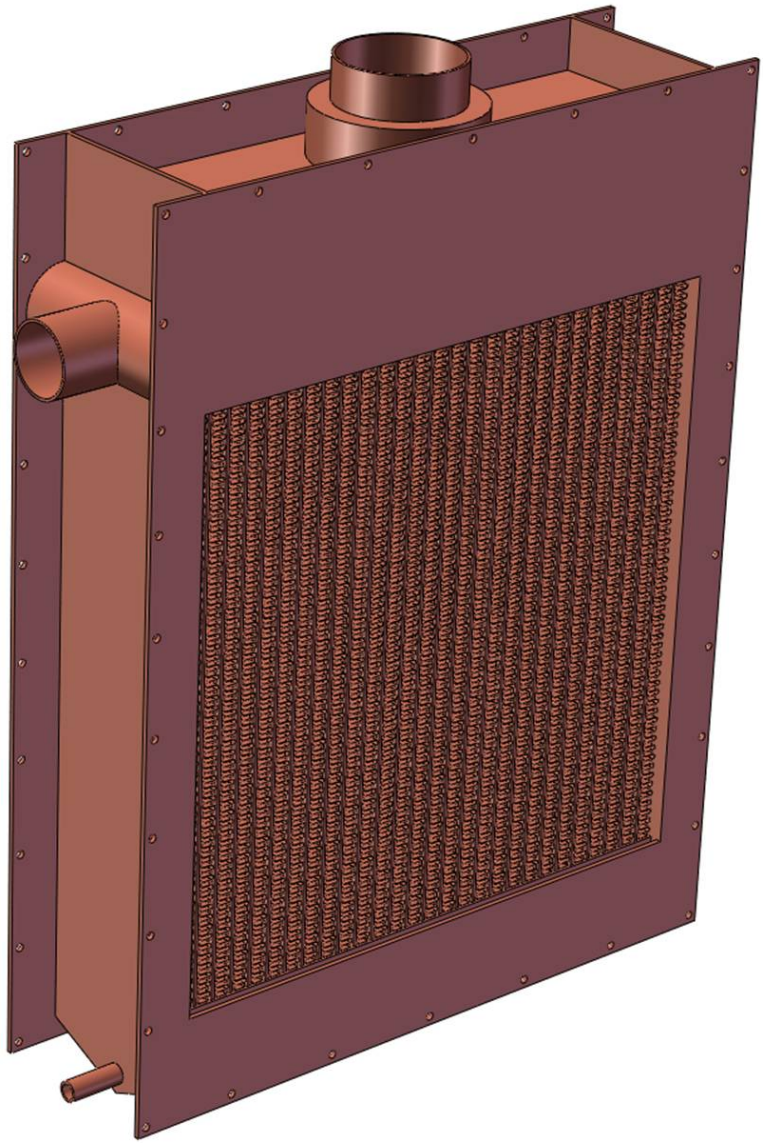

Source: Altex Technologies Corporation

The Water Preheater Heat Exchanger (WPHE) is the simplest heat exchanger incorporated in the EHPS heat and water recovery subsystem. In the WPHE, non-condensing hot gas flows through the core and heats up pressurized (i.e. 65psi) condensate from 110F to near the boiling point. Therefore, the water side fluid remains a liquid, and flow regimes and heat transfer are straightforward. Figure 108 presents the WPHE configuration. In this case, the pressurized water condensate is pumped in from the bottom and the preheated water exits from the top manifold.

Figure 108: Water Preheater (WPHE) Configuration

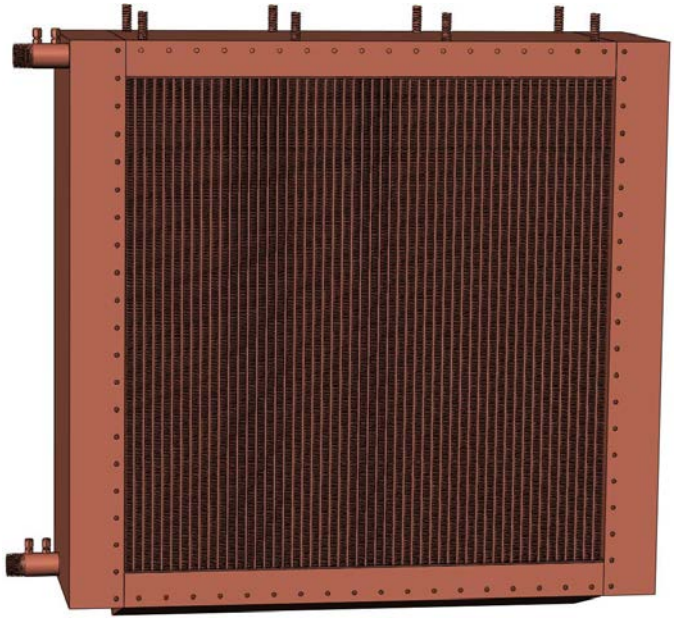

Source: Altex Technologies Corporation

Taking all heat exchangers, including manifolds and connecting flanges, the EHPS heat and water recovery system can be packaged into a single unit that has the overall dimensions, as given in Table 24.

Table 24: EHPS Steam Generation and Heat Recovery Subsystem

Height (in)	Width (in)	Length (in)	Pressure Drop (in H2O)
28	20	23	16.4

Source: CMC-Engineering

This unit will likely require additional cabinet space beyond that illustrated by the conventional configuration given in Figure 74. Extending the cabinet will also be needed to accommodate the placement of the external combustor as discussed in Task 3. Besides this equipment a small reservoir and water pump must be included within the cabinet. As shown in Table 24, total pressure drop for the system exceeds 16-inches H_2O. The microturbine operates at 59 psi and the heat exchanger pressure drop is less than 1 percent of this value. Given the pressure drop of the conventional heat recovery unit that will be replaced by the special EHPS system, power output impacts will be less than 2kWe. This is acceptable. During the next period, the heat exchanger drawings will be sent out for fabrication bids. Vacuum Process Engineering, a heat exchanger manufacturer that manufactured the test heat exchanger illustrated in Figure 84, was selected for fabrication of heat exchangers.

CHAPTER 5:

EHPS Component Assembly and Checkout Tests

5.1 Goal and Objectives

The goal of this task is to integrate all the new components, developed and proven in Tasks 3 and 4, with an Elliott CHP package, to create the EHPS CHP assembly and perform initial shake down tests. The initial assembly was performed at Altex laboratory where all the equipment, including the purchased Elliott TA-100 microturbine resided. To adapt a new steam-injected silo combustor to the engine, a new turbine housing design was necessary. This development was documented in Task 3. To adapt the steam boiler and condensing heat exchangers to the engine, a transition from the existing heat exchanger was fabricated to transport the hot exhaust gases from the microturbine into the boiler and condensing heat exchangers. Assembly of instrumentation to support the testing was also included. Following the initial assembly at Altex, the plan was to ship the system to Elliott in Florida for the final checkout tests and performance testing. However, this was not possible because Elliott was purchased by Capstone Microturbine Company and the Elliott facility was no longer available to the project

In addition to preparing this task report, the specific objectives of this task included the following:

- Purchase and fabricate all needed equipment, components and auxiliaries for the complete assembly
- Assemble the equipment into a fully-functional CHP package
- Develop a test plan for initial startup tests
- Perform initial startup tests and document operational readiness of all components

Figure 109 illustrates the EHPS configuration. The design uses as its basic component the Elliott TA-100 recuperated microtubine and heat exchangers. The microtubine operates with the strict design limits and specifications summarized in Table 25. These specifications were incorporated in the engineering and development of the EHPS system design with the assistance of computational modeling by Altex and thermodynamic analysis by CMC-Engineering Also, these analyses were used to identify the performance of new and modified system components that are necessary to achieve the overall performance targets of the EHPS system. These analyses are summarized in Task 2 report. Component design and fabrications are summarized in Tasks 3 and 4 reports.

As shown in Figure 109, the new technology consists of a new steam-injected combustor and new heat recovery assembly downstream of the existing TA-100 recuperator. Because the new combustor sits outside the turbine housing, in contrast with the inner annular combustor of the TA-100, the assembly of the new combustor requires new paths to connect the outlet of the recuperator and to provide steam injection. The new heat exchanger assembly requires the

removal of an existing heat exchanger and the placement of additional flow path for water condensation and steam generation. The entire system is then supported by new instrumentation and controls, including the monitoring of steam generation, pressure and injection rate into the silo combustor. The energy and mass flow balance of the EHPS system is describes in the task 2 report.

Figure 109: EHPS Process Diagram

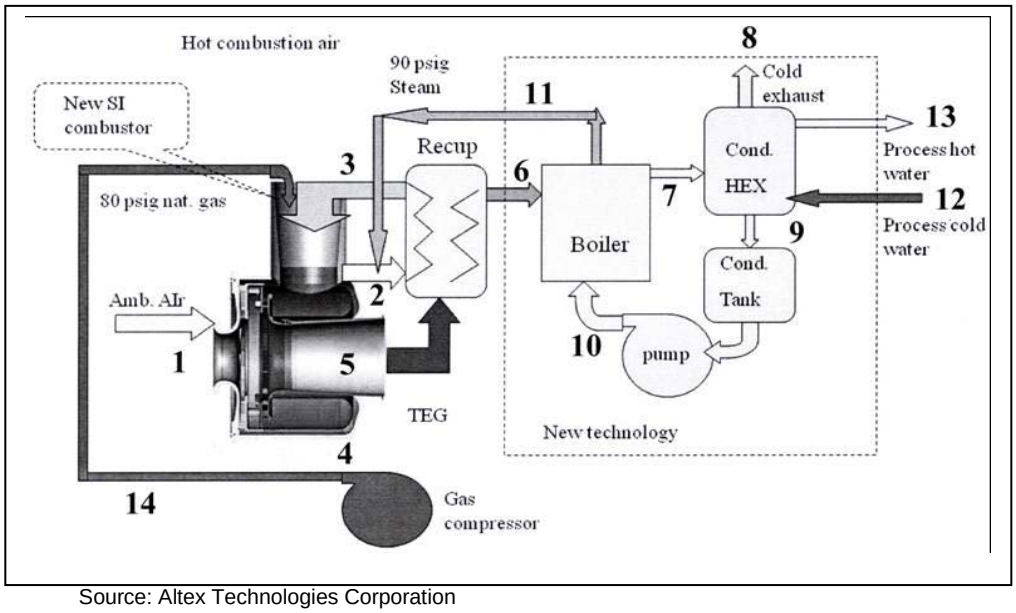

Source: Altex Technologies Corporation

Table 25: Elliott TA-100 Baseline Parameters

Parameter	Value
Turbine Inlet Temperature	1600°F
Pressure Ratio	4
Stoichiometric Ratio	2.4
Stagnation Pressure Loss	10%
Recuperator Effectiveness	82%
Compressor Efficiency	80%
Turbine Efficiency	82%

Source: CMC-Engineering

5.2 Approach to Component Assembly and Checkout Tests

The approach used in the assembly of the EHPS system included the dis-assembly of the TA-100 microtubine package to remove the cabinet frame, microturbine and housing, and the HRU unit. The removal of the cabinet frame allowed for easy access to sections of the cabinet to install new combustor and turbine housing and new heat exchanger sections. This also allowed for the upgrade of the fuel delivery and fuel control valves necessary to comply with the fuel requirements of the new combustor. Additional peripheral assembly of distilled water tank, recirculating pump, and load bank completed the system.

5.3 Description of Key Components

The main components of the EHPS system are listed in Table 26, along with the level of departure from existing components used in the Elliott microturbine based Combined Heat and Power (CHP) systems. As described in prior task reports, the combustor is totally new to meet CARB 2007 emissions requirements. Also, the boiler, water preheater and condensing heat recovery heat exchangers are totally new to enhance thermal efficiency to about 87 percent and produce steam for injection into the engine to increase both efficiency and specific power (i.e. power divided by entering enthalpy flow through engine).

Table 26: EHPS Main Components

Component	Level of Departure
Engine Core/Controls	Modest
Gas Compressor	Off the Shelf
Silo Combustor/Housing	New
Recuperator	Off the Shelf
Boiler/Condensate Preheater/Condenser	New
Steam Injector	New
Condensate Tank and Pumping System	Off the shelf
Exhaust System	Off the shelf

Source: CMC-Engineering

Other components are either unmodified or moderately modified off-the-shelf components.

5.3.1 Engine Core, Power Electronics and Control

The engine core is a 4-atmosphere pressure ratio Elliott commercial microturbine that is utilized in the T100 Combined heat and Power (CHP) system that generates 100kWe maximum power under ISO conditions. Figure 110 gives a picture of the TA-100 system purchased by CMC-Engineering with match funds from Southern California Gas Company. The microtubine was shipped and delivered to the Altex laboratory where it was subject to inspection testing and modifications described in the following section. Contained within the cabinet are the components as illustrated in Figure 111. Some of these components were utilized in the EHPS.

Figure 112 is a picture of the engine core (without the turbine housing, consisting of integrated permanent magnet generator (left in figure), compressor wheel and diffuser, bearings and turbine wheel and nozzle. The end of the compressor wheel can be seen in the right hand side of the figure, with the slots in the cylindrical section being the compressed air outlets. The generator, compressor, and turbine wheel rotate at 68,000 rpm under baseline conditions. These components are a precision assembly that requires many millions of dollars to develop, demonstrate and deploy as a product. Given the scope of the EHPS effort and the limited test need, the engine core remained unmodified, with primary engine modifications focusing on the unique CARB 2007 compliant combustor and housing that adapts the combustor to the engine. Consistent with the unmodified engine core, the EHPS test system also used the available T100 power electronics system that converts the high frequency generator output to the needed 60Hz 480 volts output needed for grid compatibility.

Figure 110: TA-100 CHP System

Photo Credit: CMC-Engineering

Figure 111: TA-100 Component Illustration

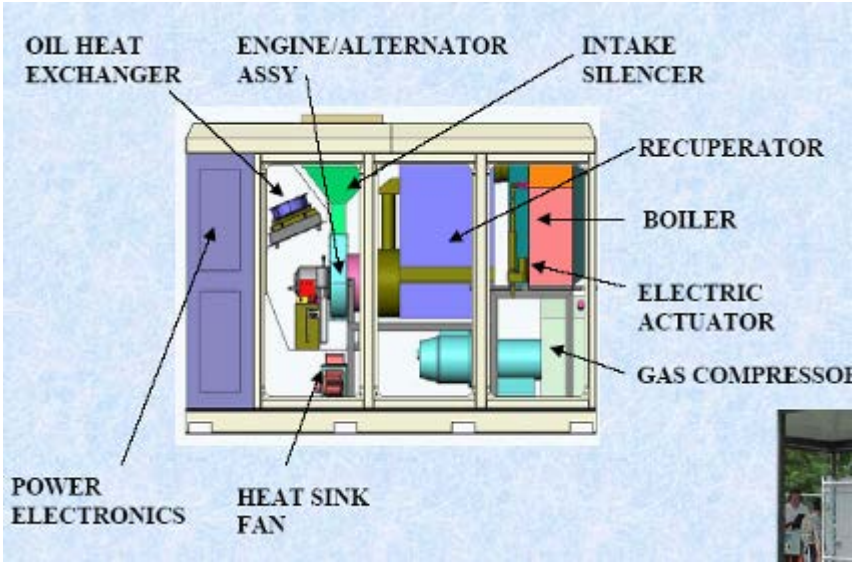

Source: Elliott Energy Systems

To accomplish the turbine housing modifications, the housing had to be removed at the completion of the operational tests. The engine had to be removed first which was accomplished with help from the engine removal tool illustrated in Figure 113. The engine removal tool was provided by CMC-Engineering at no cost to the project. Once the engine was removed the housing was unbolted from the recuperator and removed from the cabinet. The picture below shows the combustion liner reinstalled in the housing for examination and flow path mapping.

Figure 112: TA-100 Engine Core

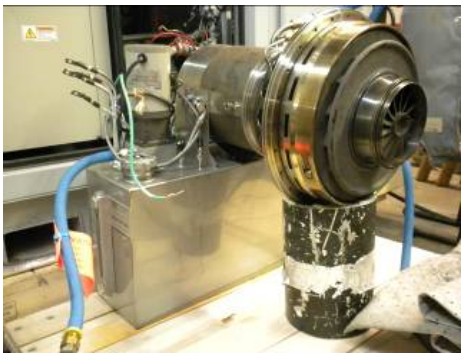

Photo Credit: CMC-Engineering

Figure 114 gives a picture of the power electronics used for the demonstration testing. As part of the power electronics package, a controls system is incorporated that manages the ignition and fuel control valve to start up and operate the engine according to pre-set operating specifications established by the manufacturer. For the EHPS operation, these pre-set operating specifications would need to be adjusted in order to allow the engine to operate with a new steam injected silo combustor and enhanced power output. Modifications to the controls were accomplished with the assistance of the Elliott field service engineer, contracted by CMC-Engineering.

Figure 113: Engine Removal Tool

Photo Credit: CMC-Engineering

Figure 114: TA-100 Power Electronics

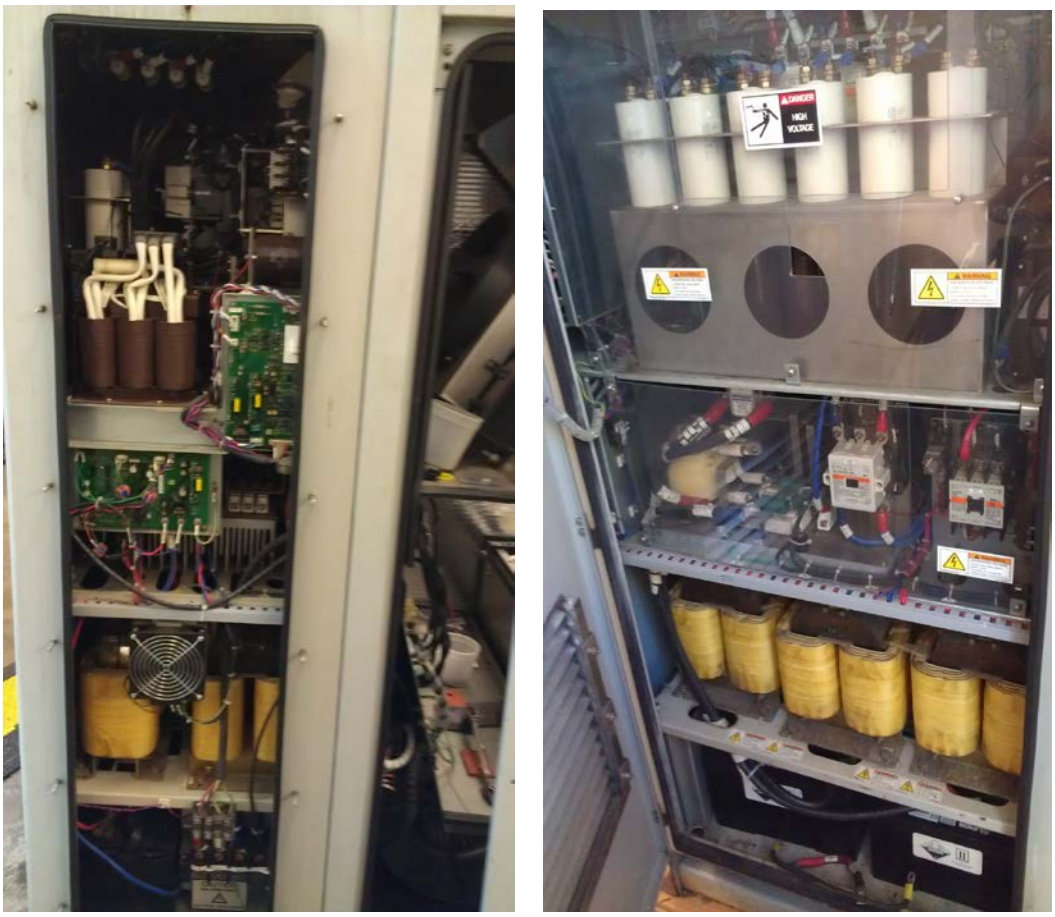

Photo Credit: CMC-Engineering

To maximize engine efficiency, the engine operates at a fixed speed design point, with load addressed by changes in fuel valve opening that drives turbine-inlet-temperature and thereby engine power output. As will be described in Section 5.3.1, the CARB 2007 combustor uses primary and secondary fuel injection zones. For demonstration test flexibility, two fuel control valves were utilized to modulate fuel into the primary and secondary combustion zones. This then necessitated that the original single fuel valve control output be split between the two valves to actuate both and meet the needed fuel profile for CARB 2007 emissions compliance.

5.3.2 Combustor and Housing

The Task 3 report fully described the CARB 2007 compatible silo combustor that was developed for the EHPS. Development included the building and testing of a sub-scale 100kW thermal two-stage combustor that was tested at 1-atmosphere pressure. As described in the Task 3 report, the NOx emissions performance at 1-atmosphere pressure was expected to be within 20 percent of that at the 4-atmospheres under microturbine test conditions. Given the success of the sub-scale combustor, the test article design was scaled up to the 333kW required for the

EHPS tests. In addition, the flexible test article design is repackaged to better integrate with the engine core and also produce a durable unit that would have a lifetime of at least five years. The design that can achieve this objective is presented in Figure 115. As reported previously, the combustor is expected to operate at lower temperatures than the unit it will replace. This will yield improved longevity. Nevertheless, a Haynes 230 oxidation resistant alloy was utilized in all hot section components. This included the primary and secondary combustor section liners and injection ports. Haynes 230 alloy is extensively used for high temperature gas turbine applications, such as the EHPS combustor. Lower temperature components, such as the cooling air duct and outer pressure containment housing were fabricated from 316-stainless steel.

Figure 115: EHPS CARB 2007 Compatible Steam Injected Silo Combustor and Turbine Housing

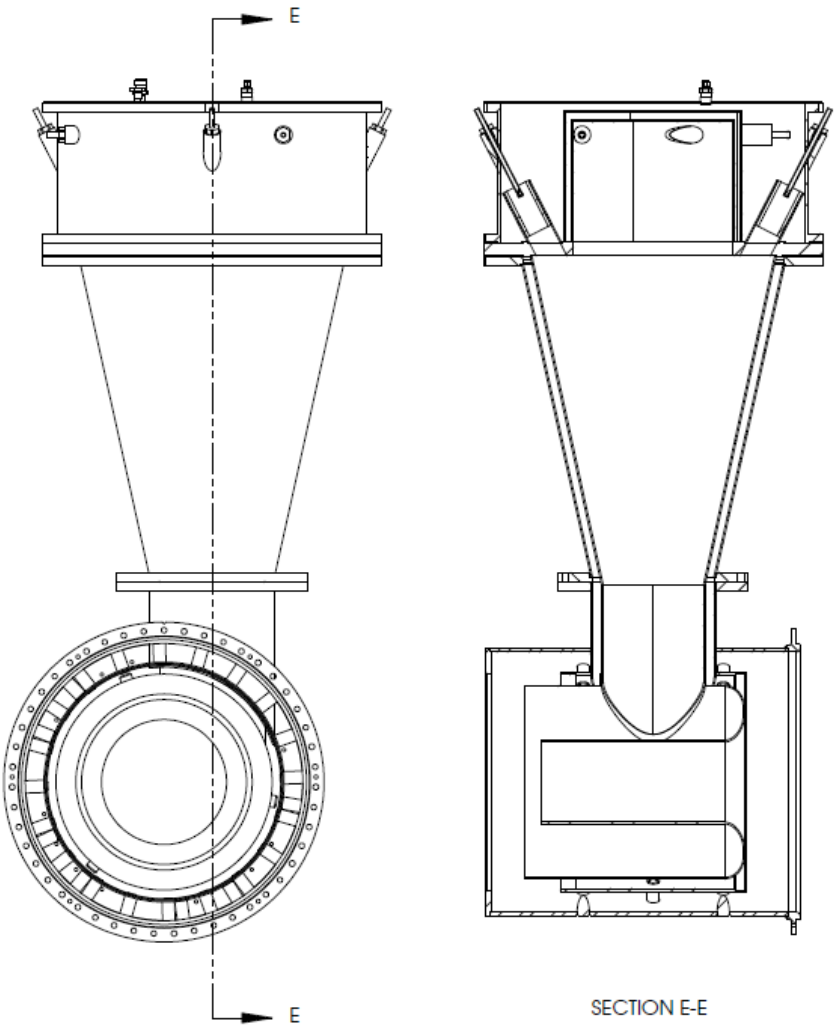

Source: Altex Technologies Corporation

Fabricated combustor components ahead of full assembly are shown in Figure 115, with the final assembled combustor shown in Figure 117. The combustor was modeled after the BBEST/Power Burner combustor used in the integrated microturbine-burner assembly developed under ENERGY COMMISSION Project PIR-07-005 and PIR-09-012 and under the UD DOE project EE-0004354. To integrate the combustor with the engine, a special housing was designed and fabricated.

Figure 116: Silo Combustor Components in Pre-Assembly

Photo Credit: Altex Technologies Corporation

Figure 117: Fully Assembled Steam-Injected Silo Combustor

Photo Credit: Altex Technologies Corporation

Figure 118 presents the design for the combustor housing. A new turbine housing was necessary for converting the TA-100 core from an annular combustor to the silo combustor. The new housing mates with and is supported by the recuperator on one end. On the opposite end, it is designed to mate with the engine core. This housing has to manage the flow of compressed air to the recuperator, where it is heated by the hot exhaust. The heated air then flows from the recuperator and upward around the combustor, thereby cooling the combustor liner to the needed temperature to prevent metal degradation.

Figure 118: Combustor Housing Design

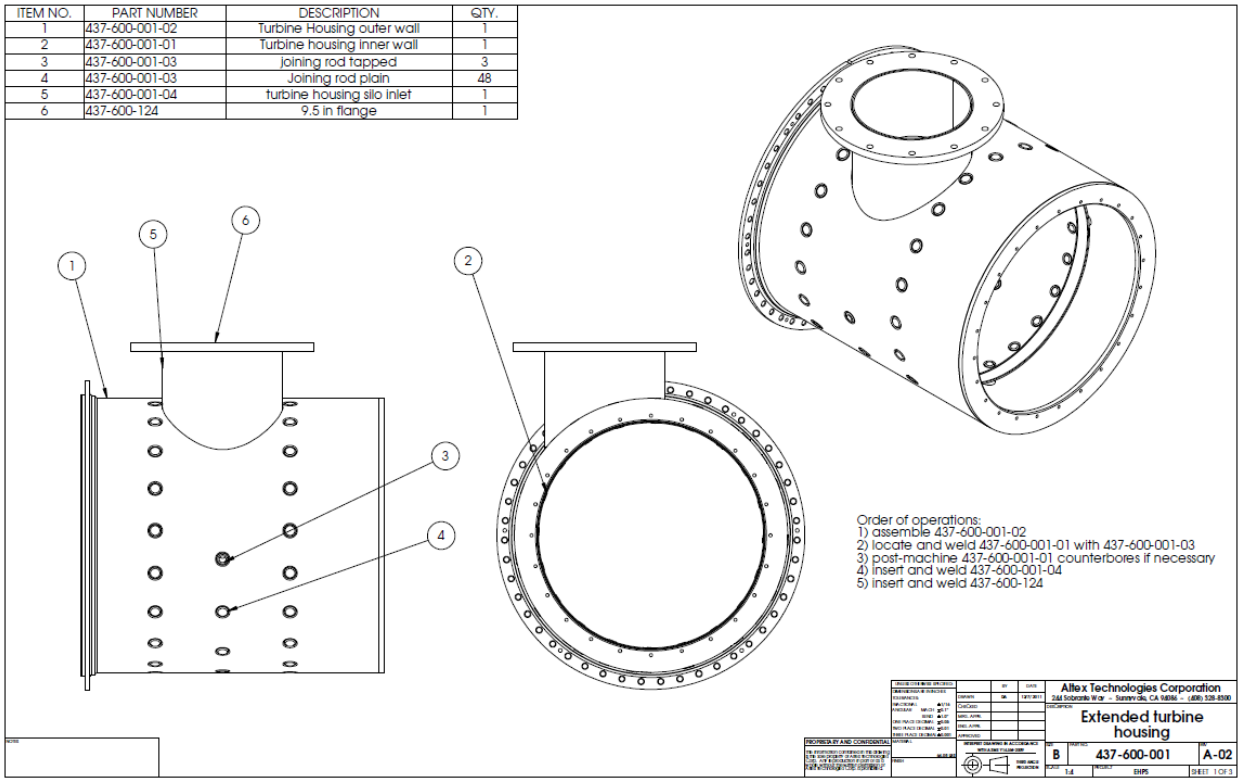

Source: Altex Technologies Corporation

The air then enters the combustor through primary and secondary ports and mixes with the fuel. The mixture is burned, and these hot gases are mixed with dilution air and are collected in an annular duct that interfaces with the turbine wheel nozzle. The hot gases then drive the turbine and exit into the recuperator. This brief description highlights the complex functions that the special housing design must provide.

The outer shell of the housing operates at lower temperature, but must withstand 4-atmospheres pressure. This section is constructed of 316 stainless steel. The inner annular liner must withstand higher temperatures, up to 1650F, but pressure differences across components are small. To handle the higher temperature, this section is constructed of Inconel 600. Figures 119 and 120 show photos of the completed housing prior to installation. This component is longer than the unit it replaces, which requires shifting the recuperator rearward in the EHPS cabinet. This was accomplished by modifying the recuperator mounts. Figures 121 and 122 show the fabricated scroll section. Tight tolerances made the installation difficult but with some minor modifications, the scroll was successfully inserted into the new housing.

Figure 119: EHPS New Turbine Housing

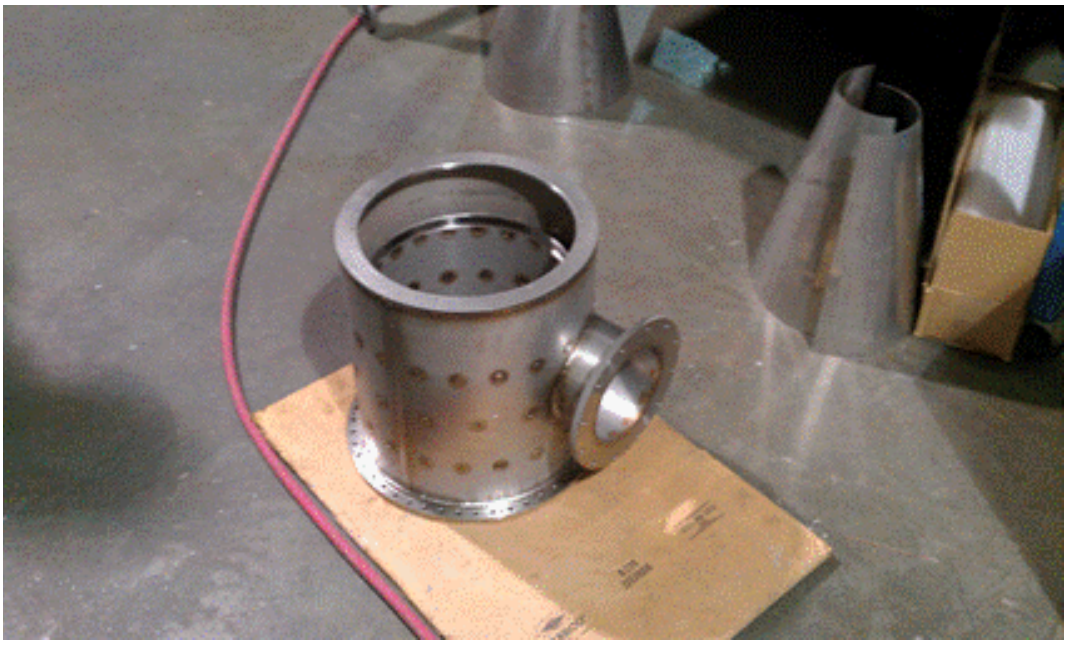

Photo Credit: CMC-Engineering:

Figure 120: Close-up of the New Microturbine Housing

Photo Credit: CMC-Engineering

Figure 121: Close-up of the New Scroll Section

Photo Credit: CMC-Engineering

Figure 122: Performing a Fit Check by Comparing New and Old Scroll Sections

Photo Credit: CMC-Engineering

As the design of the housing modification to accommodate the silo combustor progressed it was determined that a very small window was available in the housing. The secondary wall that separates the recuperated air from the freshly compressed air is only 2″ wide in the housing. Also, the recuperator and engine combustion liner interface with this wall decreasing the space to modify. With this difficult and critical interface, we investigated other options. In order to create more space the project team considered two options. The first was to move the engine back toward the electronics. This option was limited in space and already difficult to install the engine as is. The second option was to move the recuperator toward the back of the cabinet, as illustrated in Figure 123. In order to get the new heat exchangers integrated into the cabinet, the project team needed to extend the entire assembly in the back of the cabinet. Moving the recuperator required modifying only some support brackets, which was easily accomplished because there was ample space to do so.

Figure 123: Selected Option for Needed Space

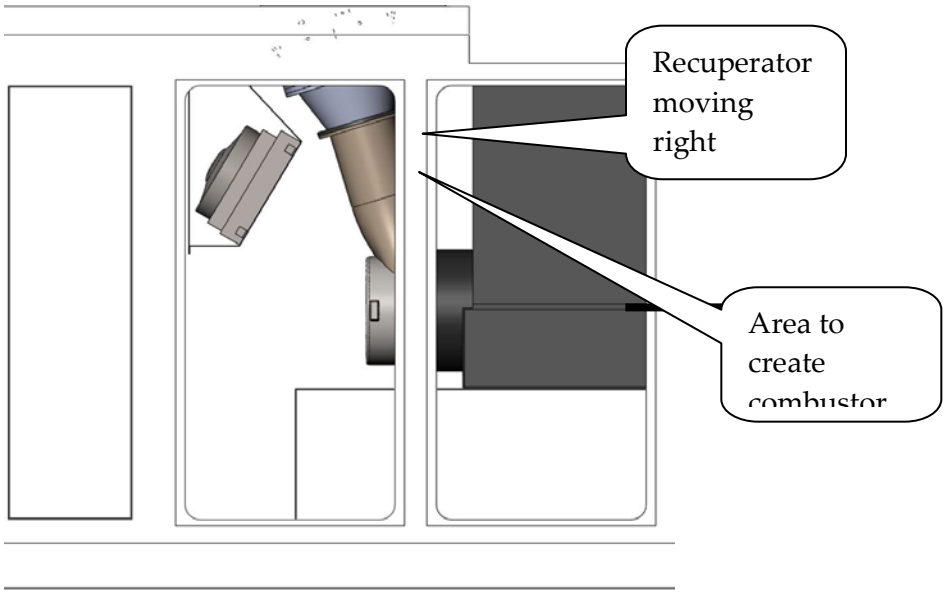

Selected option for creating needed space for external silo combustor
Source: Altex Technologies Corporation

The red box in **Figure 124** highlights the area in more detail that was used for the modification needed to place the silo combustor. The support structure is made from materials that are readily available and easily implemented. The system design for the integration of the heat exchangers created space that allowed for the recuperator to be moved backward. The cabinet could still be returned to its previous size with a new development cycle to better integrate the components and make better use of the space. **Figure 125** shows the rendering of the combustor position in the extended space.

Figure 124: Detail of Available Space for Extending the CHP Cabinet

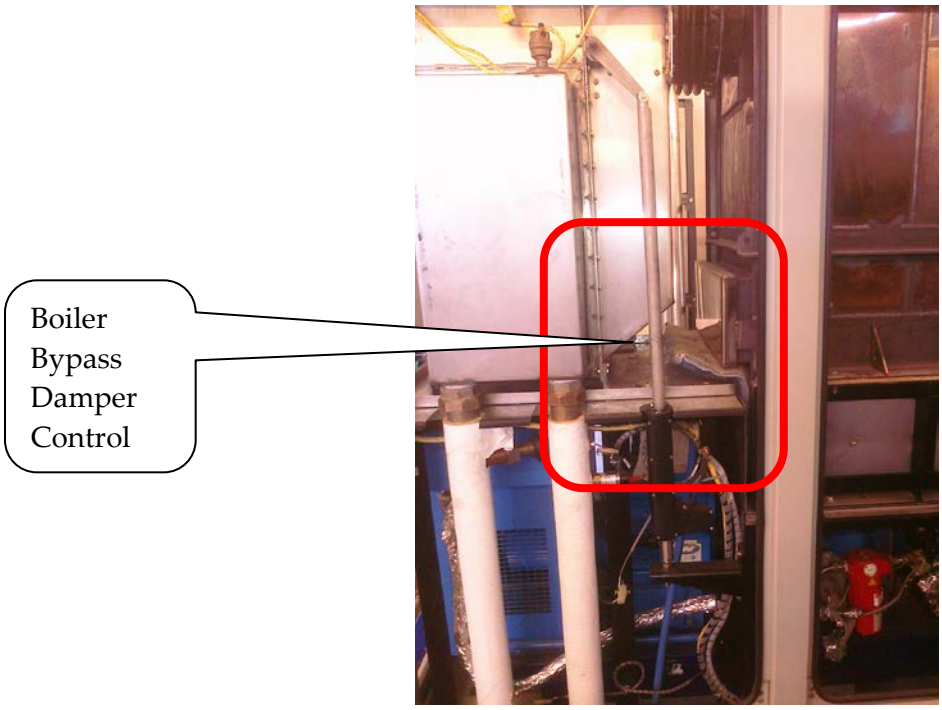

Photo Credit: CMC-Engineering

Figure 125: CHP Cabinet Rendering Showing Placement of Combustor

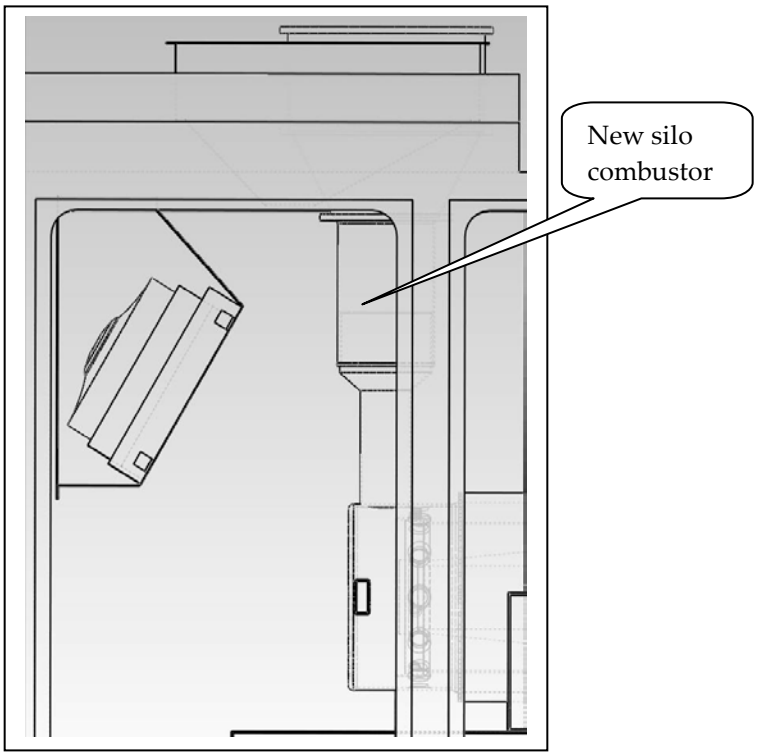

Source: Altex Technologies Corporation

5.3.4 Heat Exchangers

AS discussed in Chapter 4, there are three heat exchangers (HEX) that needed to be interfaced with the current recuperator and cabinet. The first HEX is the boiler, shown in orange below in Figure 126, and it receives the hot exhaust from the recuperator. The cabinet currently utilizes a bellows connection between the recuperator and the hot water HEX to allow for thermal expansion. The EHPS design adapts to that connection with a similar duct to what is currently used. This duct also seals to the boiler HEX to allow the hot gasses to pass through the air side of the HEX. Next in line is the water pre-heater, shown in green, which will take the water from the pump and heat it to the point of boiling. Next in line are the heat recovery heat exchanger, in condenser, and demister, shown in blue, which will have cold water flowing through it to cool the exhaust gases to the point at which the water vapor will condense out and be collected on the HEX fins and drip down into a tank. Finally the exhaust gasses will turn through the final duct and exit the cabinet. Figure 127 shows the general dimensions, with Table 27 providing individual component dimensions and pressure drops.

Figure 126: Section View of Three Heat Exchangers in Place

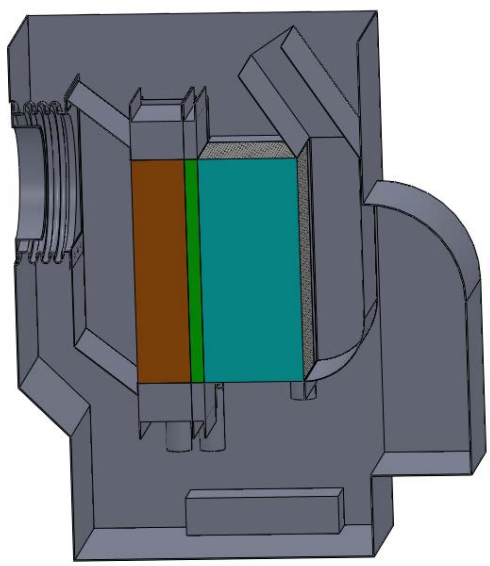

Source: Altex Technologies Corporation

The boiler, condensate preheater and condensing heat and demister heat exchangers are new and the photos of fabricated units are given in **Figures 128**, **129**, **130**, and **131** respectively. To address hot entering gas temperatures for the boiler and provide corrosion protection for the condensing heat recovery unit, all heat exchangers were constructed of 316 stainless steel.

Figure 127: Side (left) and Top (right) Views of Heat Exchanger with the Cabinet

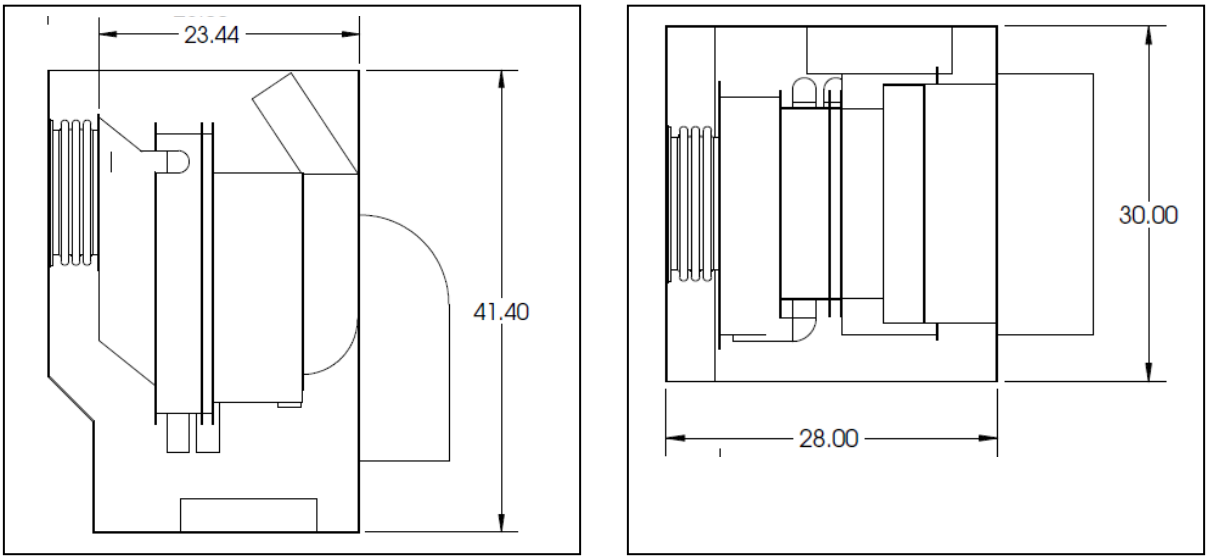

Source: Altex Technologies Corporation

Table 27: Parameters and Performance for EHPS Heat Exchangers

Heat Exchanger	Capacity (B/h)	Core Height (in)	Core Width (in)	Core Length (in)	Pressure Drop (in H2O)
Boiler	427,861	18	13.5	4.25	5.67
Water Preheater	94,559	18	13.5	1.05	1.40
Condenser/Heat Recovery	733,700	18	13.5	7.95	7.95

Source: Altex Technologies Corporation

Figure 128: Fabricated Boilers Ready for Installation Assembly

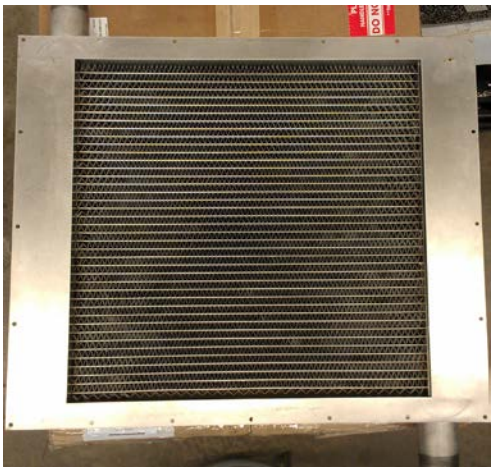

Photo Credit: Altex Technologies Corporation

Figure 129: Condensate Preheater Heat Exchanger

Photo Credit: Altex Technologies Corporation

Figure 130: Condensing Heat Recovery Heat Exchanger

Photo Credit: Altex Technologies Corporation

Given the relatively high velocity in the heat exchanger, some of the condensate will be stripped from the final heat exchanger and be carried downstream as a mist. The last step is to collect the remaining droplets from the air. The device used to accomplish this goal is the demister. The demister was mounted, along with the rest of the heat exchangers, downstream of the exhaust of the recuperator. A support structure, shown in Figure 132, holds it in place and an inlet and outlet duct will direct the exhaust flow.

Figure 131: Fabricated Demister Ready for Assembly

Photo Credit: Altex Technologies Corporation

Figure 132: Heat Exchanger Manifold Structure Picture

Photo Credit: Altex Technologies Corporation

5.3.5 Condensate Collection, Storage and Pumping System

In support of the condensate recovery and steam injection system, condensate reservoirs were incorporated in the design. Two units were utilized that are capable of storing 230 gallons of condensate. This volume allows a buffer for testing flexibility and covers start-up and shut-down transients related to water collection. Since the condensate is cool, these tanks are fabricated from polypropylene. Figure 133 shows the condensate collection and pumping station. After preheating and then boiling the condensate, the steam is separated from the water and injected directly into the recuperator. The injector is a simple nozzle that distributes the steam in the hot air to be further superheated by the hot exhaust gases. The amount of steam formed is controlled by the water flow that is pumped into the water preheater heat exchanger. For steam injection, the condensate must be pumped to a pressure of 90 psi. To accomplish this objective, a Berns pump shown in Figure 134. is utilized.

Figure 133: Condensate Collecting Station

Photo Credit: CMC-Engineering

5.3.5 Other System Components

Several ancillary components are needed to support operation of the CHP system. Some components are noted below.

Figure 134: Purchased Water Circulating Pump

Photo Credit: Altex Technologies Corporation

Exhaust System

The exhaust from the heat recovery heat exchanger was designed to mate with the 12-inch diameter test facility exhaust. With the heat exchanger bypass open, exhaust gases can reach over 500F. In this case, a high temperature duct is required. To meet this need, a double wall stainless steel exhaust by Selkirk was utilized. This was an off-the-shelf component.

Air Filter

The TA-100 package uses a combination air filter and silencer at the engine inlet to provide clean air to the engine, as well as suppress the compressor noise common to microturbines. This standard package is directly adaptable to EHPS, and was included in the EHPS test system.

Exhaust Transition and Bypass Stack

One of the major components required for the integration and performance testing of the upgraded unit is the transition from the recuperator to the heat exchangers. This transition was designed to allow direct the exhaust flow while maintaining low pressure drop and also to allow gas bypass of heat exchangers for initial testing. The transition also included an exhaust damper to control the amount of hot flow sent through the heat exchangers. Figure 135 shows an illustration of the transition duct. Figure 136 shows the completed assembly component for the housing of the heat exchanger section, bypass duct, and stack.

Figure 135: Recuperator to Heat Recovery Heat Exchanger Transition Duct

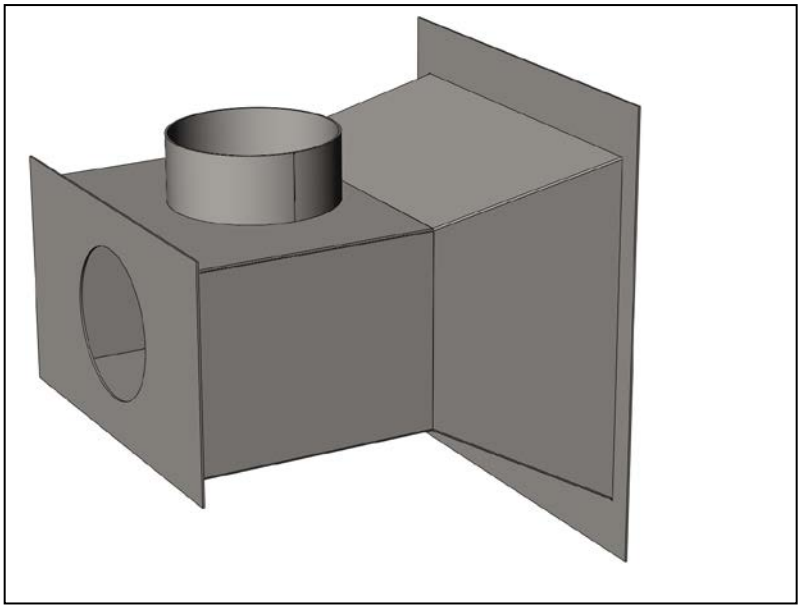

Source: Altex Technologies Corporation

Figure 136: Complete Assembly of Transition, HEX Section, Bypass, and Stack

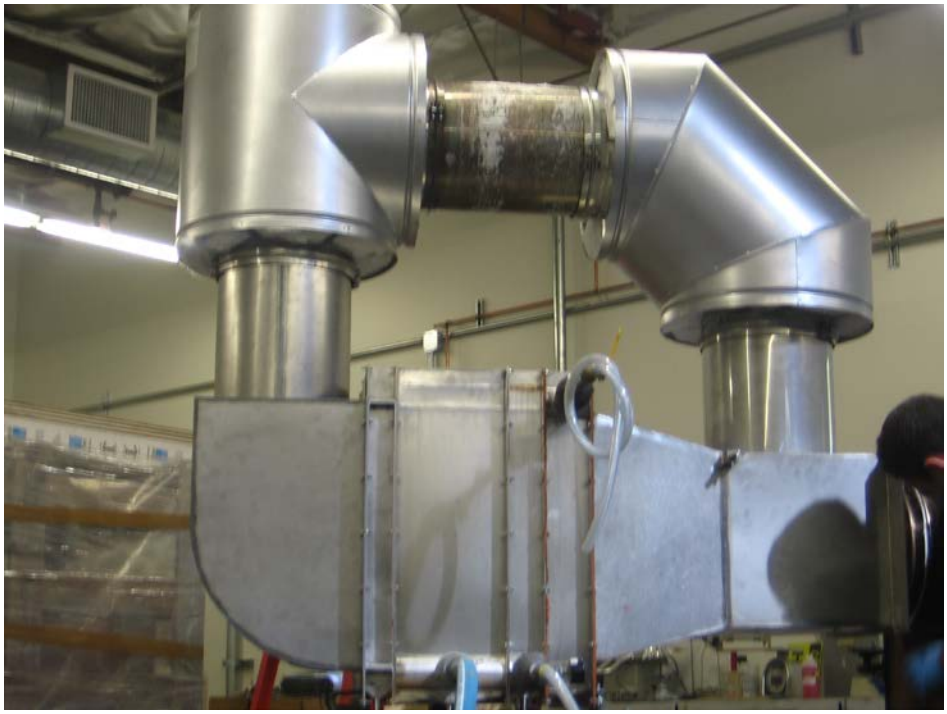

Photo Credit: Altex Technologies Corporation

Fuel Control Valve Assembly

A new fuel delivery system was necessary for the operation of the new combustor. This delivery system required the metered control of fuel flows to each of the two firing sections of the combustor, i.e., pilot and secondary. For this combustor this is more critical because the l[pilot fuel represents a significant amount of the total fuel to the combustor. Figure 137 shows the system which replaces the nominal single fuel control valve (FCV) of the original TA-100.

Figure 137: Redesigned Combustor Fuel Control Valve Assembly

Photo Credit: CMC-Engineering

Gas Compressor

The natural gas supply for the engine must be compressed to approximately 90 psi to feed the engine. A Hydrovane compressor is used for the TA-100 engine. This compressor is also fully compatible with the EHPS combustor as it is rated to deliver up to 30 scfm of natural gas. Therefore, this unit was directly adapted to the EHPS test system cabinet. Figure 138 gives a picture of the compressor.

Figure 138: Natural Gas Compressor

Photo Credit: CMC-Engineering

Generator and Bearing Oil Cooler

The engine core generator is cooled by oil. Also, the bearing oil must be cooled. The T100 applies an oil reservoir, pump, filter and radiator to accomplish this objective. This system meets the EHPS specifications and was used to support the EHPS. Figure 139 gives a picture of this oil cooling system.

Figure 139: Oil Cooling System Tank (bottom), Filter (middle) and Radiator (top right)

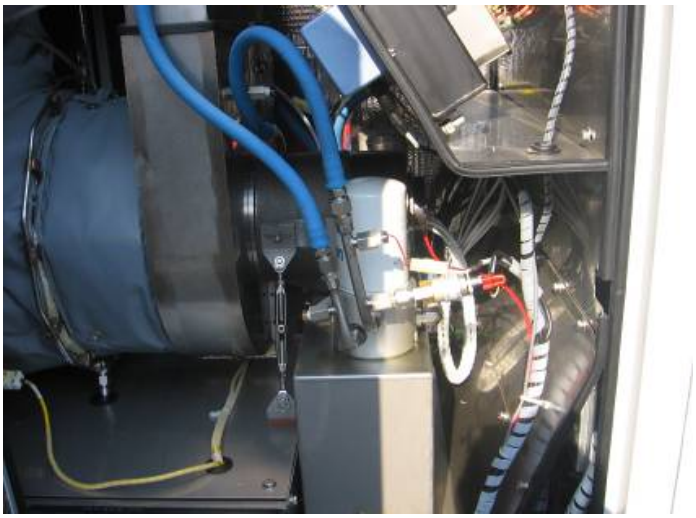

Photo Credit: CMC-Engineering

5.4 EHPS Assembly

The assembly of new and existing components of the EHPS required the complete disassembly of the original cabinet. This allowed the crew full access to each existing component for removal or relocation, and for installation of new components. The doors and entire framing of the cabinet were removed to permit ease access for the installation of new EHPS components. The heat recovery unit was replaced with the new heat exchangers, so that was removed. The recuperator, shown in Figures 140 and 141, will be moved further down in the cabinet to allow for placement of the combustor and the modified turbine housing. In order to move the recuperator, the surrounding cabinet structure was removed to facilitate the e-assembly of the various components.

Figure 140: Cabinet Disassembly for EHPS Reconfiguration

Photo Credit: CMC-Engineering

Figure 142 shows the heat recovery unit (HRU) that was removed from the TA-100 assembly. This unit will be replaced with the series of t exchangers described in Chapter 4 and Section 5.3 above. The components that were removed were stored safely in the event the cabinet is required to be reassembled. Figure 143 shows the assembly of the combustor and turbine housing section of the EHPS. As shown, the turbine housing was elongated for the sole purpose of allowing the wider silo combustor not to interfere with the air intake system for the engine. All of the above components were quality checked individually ahead of assembling into the EHPS. Figures 144 and 145 show the final stages of the assembly. Finally, Figure 146 presents a picture of the assembled system.

Figure 141: Exposed Recuperator for Repositioning

Photograph of exposed recuperator for respositioning furtheraway from the engine
Photo Credit: CMC-Engineering

Figure 142: HRU Removed from Elliott TA-100

Photo Credit: CMC-Engineering

Figure 143: Installed Steam-Injected Combustor on New Turbine Housing and Microturbine

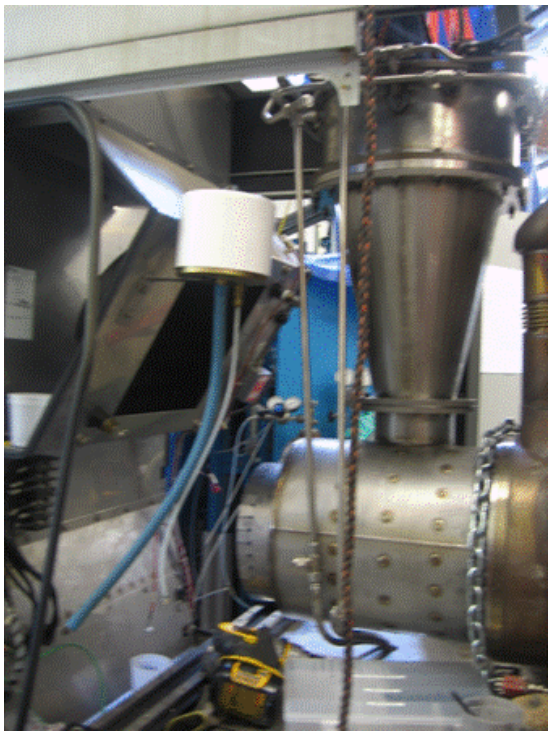

Photo Credit: CMC-Engineering

Figure 144: Assembly of EHPS - Combustor and Microturbine Section

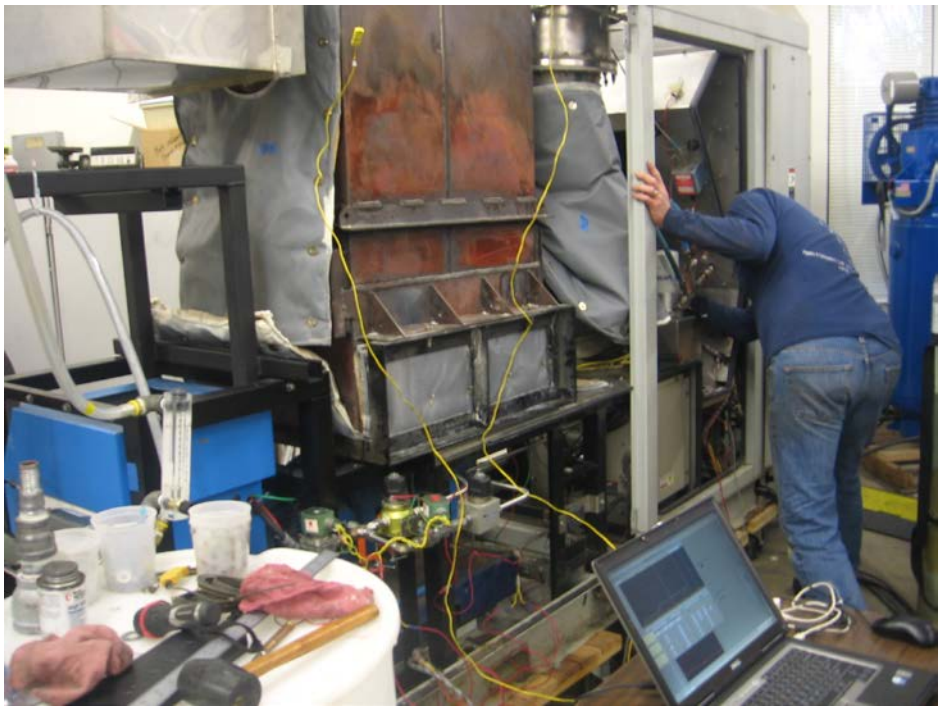

Photo Credit: CMC-Engineering

Figure 145: Assembly of EHPS - Heat Exchanger Section

Photo Credit: CMC-Engineering

Figure 146: Completed EHPS Cabinet Package

Photo Credit: Altex Technologies Corporation

5.5 System Checkout Tests

A series of system checkout tests were performed prior to final EHPS testing to evaluate the readiness of the assembled system to operation. During these checkout tests, the engine suffered some starting failures independent of the new EHPS components that were inserted for the EHPS. Failures were narrowed to two power electronics boards that had given us problems in the past: the encoder card shown in Figure 147 and the inverter board shown in Figure 148. Support from the ex Elliott field service engineer resolved these two problems and the system was commissioned ready for testing.

Figure 147: Replaced Encoder Card

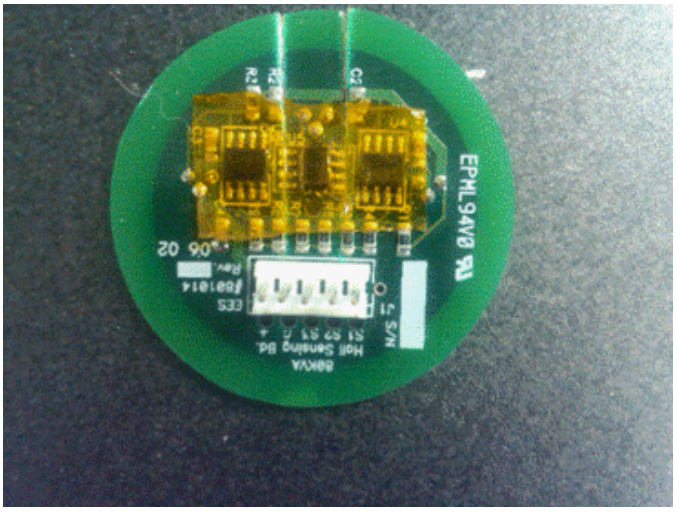

Photo Credit: CMC-Engineering

Figure 148: Failed Inverter Board

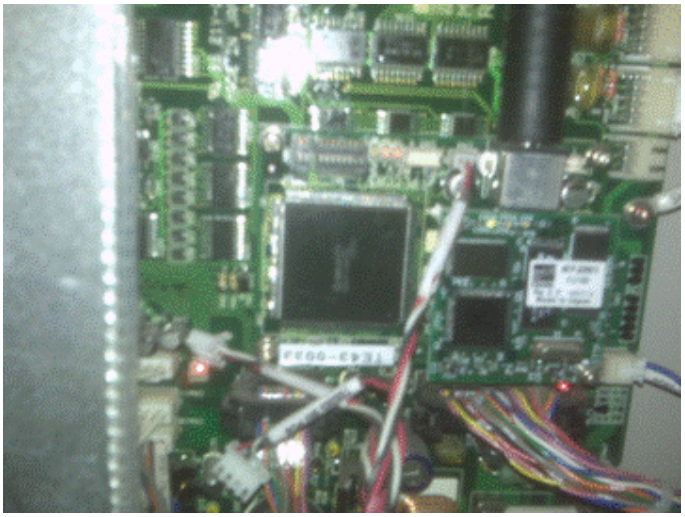

Photo Credit: CMC-Engineering

CHAPTER 6:

EHPS CHP Performance Testing

6.1 Goals and Objectives

The goal of this task is to take the functional CHP assembly through the operational tests to validate the performance goals and commercial readiness. The key objectives were identified to be as follows:

The initial assembly was performed at Altex laboratory where all the equipment, including the purchased Elliott TA-100 microturbine resided. To adapt a new steam-injected silo combustor to the engine, a new turbine housing design was necessary. This development was documented in Task 3. To adapt the steam boiler and condensing heat exchangers to the engine, a transition from the existing heat exchanger was fabricated to transport the hot exhaust gases from the microturbine into the boiler and condensing heat exchangers. Assembly of instrumentation to support the testing was also included. In addition to preparing this task report, the specific objectives of this task included the following:

- Ship all EHP equipment to Elliott
- Setup the prototype EHPS in one of Elliott test cell rooms
- Prepare a test plan
- Perform short-term testing according to test plan, protocols and procedures
- Monitor overall performance and system durability
- Perform material integrity checks

Table 28 lists the performance objectives for the EHPS and compares these to the conventional TA-100 integrated CHP unit subject to the same CARB 2007 emission limits. Because of the improved overall CHP efficiency of the EHPS, the emission compliance for the EHPS results in less stringent emission limits when measured on a concentration basis.

6.2 Approach

Following the initial assembly at Altex, the plan was to ship the system to Elliott in Florida for the final checkout tests and performance testing. Therefore, the tests were originally planned to take place at the Elliott test facility in Florida. However, this was not possible because Elliott was purchased by Capstone Microturbine Company and the Elliott facility was no longer available to the project. Therefore, the tests were performed at Altex laboratory in concert with other Commission activities for CHP development technologies.

Prior to the start of the performance tests, the project team developed a test plan. This is presented in Section 6.3. Test results are presented in Section 6.4.

Table 28: Elliott TA-100 Baseline Parameters (Source: CMC-Engineering)

Parameter	Conv. CHP	EHPS
Electrical Efficiency at Full Load	30%	38%
Full Load Power kWe	100	165
Electrical Efficiency at 50% Load	24%	34%
NO_x, ppm @ 15% O2 (CARB 2007 CHP limit)	2.5	3.9
CO, ppm @ 15% O2 (CARB 2007 CHP limit)	5.5	7.0
HC, ppm @ 15% O2 (CARB 2007 CHP limit)	2.0	2.7
[illegible]	[illegible]	[illegible]

6.3 Test Plan

The assembled EHPS system and each component will be taken through a shakedown test period to validate the operational status of the equipment. Following these shakedown tests, the EHPS will be tested at rated power output with and without steam injection. The latter will determine the increased power and efficiency of the system compared to the standard TA-100 performance specifications.

6.3.1 Baseline System Shakedown

The EHPS tests will cover baseline CHP system checks, component quality and integrity checks and modified system performance and durability tests. These will cover all of the needs to define EHPS performance potential and design strengths and weaknesses.

In support of testing, a Standard Operating Procedure (SOP) document has been prepared and approved by John Kelly and the Altex Laboratory Manager, George Miller. This document covers material safety, equipment manuals, process equipment description, supporting equipment and instrumentation description, process hazards, equipment hazards, safety equipment and operating steps.

To limit project costs, an existing TA100 Elliott CHP system is used as a base for upgrading to achieve needed features of the EHPS system. This will allow the potential of the concept to be tested at a cost-compatible with current ENERGY COMMISSION and DOE project activities. In subsequent efforts, the EHPS system will utilize more custom and expensive components to optimize the concept performance.

Ahead of modifying the TA100 system in support of the EHPS concept tests, some unmodified TA100 tests are needed to ensure that the baseline system is properly functioning in areas

needed to support EHPS system tests. Since the TA100 has been well characterized by the manufacturer, only limited tests and instrumentation are needed for the baseline unit testing. Specifically, the baseline test instrumentation and diagnostics were additional thermocouples, heat recovery heat exchange water flow monitor, with other instrumentation and diagnostics supported by the available standard machine integrated instrumentation. To provide specific generator loads, an available 100kWe load bank was utilized. Loads can be set in 20kWe increments up to a maximum of 100kWe. Table 2 summarizes the planned baseline tests with the unmodified TA100.

These brief baseline tests will show if the TA100 system components are reliably operating within specifications, as well as defining baseline performance for comparison to EHPS performance.

6.3.2 Rationale for EHPS Component and System Tests

Both component and system tests are planned to first prove components and then how they perform as integrated into the EHPS system. As fabricated components were delivered from the fabricators, they were checked for integrity and whether they meet design specifications.

Combustor Tests

The special EHPS combustor will meet CARB 2007 emissions requirements using a two-stage design, with steam injection in the combustion air introduced into the recuperator air inlet. Given the novel combustor design and stringent emissions requirements, several levels of testing were planned to maximize the probability of meeting performance targets, once the combustor is integrated into the EHPS system. Test sequences included sub-scale 1-atmosphere pressure tests, full-scale 1-atmosphere pressure tests and finally, full-scale 4.5-atmosphere pressure tests with the combustor integrated into the engine.

Table 29: TA-100 Unit Baseline Tests

Test	Purpose	Measurements Planned	Parameters Varied
Start-up	Prove fuel supply system, ignition system and control sequence	Tracking of engine speed, fuel valve position, fuel pressure and Turbine Outlet Temperature (TOT) with time. Note any out-of-spec conditions and faults in start-up sequence	Set fuel pressure within engine spec and let control sequence occur as per internal factory set program
Load Variation	Prove control strategy and generator/power electronics system capability to meet load requirements	Track all engine diagnostics, including load output as load bank is varied	Vary load bank in 20kWe increments from 0 up to 80kWe. Avoid 100kWe load to eliminate risk of over-temperature on baseline high temperature combustor

Heat Recovery	Characterize heat recovery opportunity under baseline condition	Hot water flow rate	Hot water flow rate and inlet and exit temperatures, engine load, TOT and heat exchanger gas entrance temperature

Sub-Scale One-Atmosphere Pressure Tests

Table 3 lists these planned sub-scale 1-atmosphere combustor tests. For the 88kWt sub-scale tests, the test article design allows the careful monitoring and control of all air and fuel flows to fully characterize performance (i.e. stability, noise, emissions), as a function of all important variables. Based on these results, the 333kWt full-scale combustor can be designed for turbine integration. This combustor will be more tightly packaged to be compatible with the CHP product needs. Furthermore, air flow flexible control features and monitoring, required for the development tests, will be removed from the full-scale prototype combustor. This is required to achieve the needed packaging, and at this stage of development, air flows should be set at near optimal levels. Ahead of integrating the full-scale combustor with the engine, the combustor will be tested at 1-atmosphere pressure to prove operation and performance without the complexities associated with an integrated engine test. With the 1-atmosphere tests, fuel and air flows will be scaled to achieve the same residence times at similar gas temperatures. This will provide a reasonable simulation of flame stability, hydrocarbon burn-up and CO burnout. As reported in the literature, NOx emissions results for 1-atmosphere pressure will be within 20 percent of those expected at the 4.5-atmospheres engine tests.

Table 30: 1-Atmphere Pressure Sub-scale Combustor Tests

Test	Purpose	Measurements	Parameters Varied
Sub-scale tests	Prove combustor concept at 1-atmosphere pressure and reduced scale under carefully controlled conditions	All air and fuel flows to the two stages, thermocouple temperature measurements of air preheat, first and second stage temperatures, diluted gas temperature, steam flow and NOx, CO, UHC, O2 and CO2 exhaust gas measurements with compliance-level monitors	Total fuel flow, first to second stage fuel fraction, first and second stage stoichiometries, air preheat temperature and steam flow

Full-Scale One-Atmosphere Pressure Tests

Table 4 presents the plans for the 1-atmosphere full-scale combustor tests. As noted above, the full-scale combustor has a fixed first and second-stage air flow design. Therefore, these are not

varied during testing. Also, for the higher flow capacity full-scale design, steam injection at the required levels will not be available for these brief tests. To simulate flame dilution by steam injection, extra premixed air will be utilized. Using the ratio of steam to air specific heats, the effect of different levels of steam injection on stability and emissions can be assessed using more excess air. Of course, full-load testing may not be achieved for the required higher excess air conditions. This steam simulation approach will be adequate to characterize performance in the brief 1-atmosphere tests ahead of integrating the combustor in the engine.

Once the full-scale combustor is proven in the 1-atmosphere tests, it will be installed in the engine and tested. In the first test sequence, the exhaust bypass will be used to divert hot gases from the heat recovery heat exchangers. This will allow the initial operation of the engine and combustor without the complexities of the heat recovery system. These initial integrated combustor tests will take place without steam injection. To simulate steam injection, the fuel flows will be reduced at the maximum engine speed point to provide more combustion dilution air per fuel flow. This higher first and second-stage stoichiometry will simulate various steam injection levels, as utilized in the 1-atmosphere tests described above. Once combustor operation and performance are proven without steam injection, heat recovery system tests will be initiated. After proving the boiler, water preheater and condensing heat recovery components, engine tests with recuperated air steam injection will be initiated. This will complete EHPS testing.

Table 31: One-Atmosphere Full-scale Combustor Tests

Test	Purpose	Measurements	Parameters Varied
Full-scale 1-atmosphere pressure tests	Prove full-scale combustor at 1-atmosphere pressure	Fuel flows to the two stages, thermocouple temperature measurements of air preheat, first and second stage temperatures, diluted gas temperature, and NOx, CO, UHC, O2 and CO2 exhaust gas measurements with compliance-level monitors	Total fuel flow, first to second stage fuel fraction and first and second stage stoichiometries

Full-Scale Integrated Combustor Tests

Table 5 presents engine integrated combustor test plans. These tests begin with the start-up sequence, similar to that of the baseline engine. However, in this case, the combustor will be instrumented with thermocouples to monitor temperatures. The control system will provide the proper purge and ignition cycle. As with the baseline engine, the generator will act like a motor and draw power to accelerate the shaft rotation to reach the self-sustaining engine speed, where driving power will be shut down. During this period, the control system will modulate the fuel flow to be compatible with the engine air flow. Given the large amount of power

needed to drive the compressor, the start-up sequence uses combustor fuel flow to raise the Turbine Inlet Temperature (TIT) that then provides turbine power to supplement electric power to the generator/motor at low speed.

It should be noted that the correct engine start depends solely on the TIT, and not on any details of combustor operation or dilution of the hot combustor gases. These will impact only whether the combustor can meet CARB 2007. If the combustor is able to burn the provided fuel and meet TIT for each engine speed, then the engine will start. Therefore, the start-up tests will use the baseline total fuel-flow profile during the initial baseline testing. Also, the first and second stage fuel schedule will be set at the optimal ratio for steady idle operation. If the start sequence experiences some problems in engine acceleration, stability, noise, etc., the first and second-stage fuel profiles will be varied to define acceptable conditions throughout the start-up sequence.

Once start-up has been proven, load variation will be tested using the load bank to impose load in 20kWe increments up to 100kWe. At these loads, emissions will be characterized, as well as any noise and stability issues. Again, first and second-stage fuel flows will be varied, as needed, to address emissions issues. If problems are not addressed by fuel flow variations, the combustor will be removed and the dilution air holes refined to shift combustor to dilution air ratio. Larger holes will reduce combustor air flow. Another strategy to refine performance will be to add different air sleeves to the secondary air ports to shift primary to secondary air flow split and secondary velocity. This is possible, but probably not needed. Once these non-steam injected tests are completed, the heat recovery system tests, as highlighted below, will be initiated.

Table 32: TA-100 Unit Baseline Tests

Test	Purpose	Measurements Planned	Parameters Varied
Start-up	Prove fuel supply system, ignition system and control sequence	Tracking of engine speed, first and second stage fuel valve positions, fuel pressure and Turbine Outlet Temperature (TOT) with time. Note any out-of-spec conditions and faults in start-up sequence NOx, CO, UHC, O2 and CO2 exhaust gas measurements with compliance-level monitors Thermocouples to monitor first and second stage combustor gas and shell temperatures	Set fuel pressure within engine spec and let control sequence occur as per internal factory set program. Depending on results, vary first to second stage fuel split to achieve desired emissions and stability results
Load Variation	Prove control strategy and generator/power electronics system	Track all engine diagnostics, including load output as load bank is varied and first and second stage fuel value positions, NOx, CO, UHC, O2	Vary load bank in 20kWe increments from 0 up to 100kWe. Avoid 100kWe load to eliminate risk of

	capability to meet load requirements	and CO2 exhaust gas measurements with compliance-level monitors	over-temperature on baseline high temperature combustor

Heat Recovery System Tests

The EHPS uses multiple heat exchangers to recover heat and condense water in the exhaust, and then preheat and boil the condensate, to create steam for injection. All of the heat exchanger components have the same high performance core design, as described in the Task 4 report. To assess component performance, sub-scale tests on a heat exchanger that uses a similar core design will provide needed design data that will support the design of all heat exchange components. These boiler, preheater condenser and heat recovery tests and results have been described in the Task 4 report. These test results provided a basis for the design and test of the engine integrated heat exchangers. These full-scale heat exchanger test plans are described below.

Table 6 presents the plans for the heat recovery system tests. The initial tests will confirm operation using the engine at the low temperature idle condition. These tests will minimally stress the heat exchangers during initial checkout of the heat recovery system. As required, the condensed water will be supplemented with de-ionized water in these initial tests. Steam generated will be vented rather than injected into the engine. Once these tests show that the heat exchangers are viable and working as planned, engine load will be incremented. All thermal and flow conditions will be recorded to obtain mass and energy balances for the heat recovery system components.

Table 33: Heat Recovery System Tests

Test	Purpose	Measurements Planned	Parameters Varied
Heat recovery system initial test	Prove heat recovery system operation at modest thermal conditions	Engine, speed, first and second-stage fuel valve positions, fuel pressure, TOT, combustor temperatures, NOx, CO, UHC, O2 and CO2, heat exchanger temperature and pressure measurements, cooling water flow and temperature, exit gas temperature	At engine idle, check heat exchanger integrity and operation
Heat recovery system condensing tests without steam injection	Show heat recovery system performance including condensing capability	Engine, speed, first and second-stage fuel valve positions, fuel pressure, TOT, combustor temperatures, NOx, CO, UHC, O2 and CO2, heat exchanger	Vary engine load and exhaust temperature without steam injection to vary

		temperature and pressure measurements, cooling water flow and temperature, exit temperature, condensed flow and temperature, steam flow	condensate flow and steam output

Results will be compared to projected performance, based on prior sub-scale heat exchanger tests and analyses. Given that operation meets expectations, the engine load and exhaust temperature will be increased. This will give thermal performance of the system over a range of engine loads, up to full load. Given that test results show adequate performance, the previously vented steam will be hooked up to the recuperator steam injector and the system tested with steam injection. These tests are listed in Table 7. As shown, the tests will start with the lowest steam injection rates at a part-load condition. This will be the condition where sufficient condensate is recovered for sustainable steam injection. At this level of steam injection, compressed air bypass will not be required. However, as the amount of steam injection increases, air bypass will ultimately be required to ensure that engine power does not exceed the generator limits. Besides monitoring steam flow into the engine, the air bypass, or bleed, will also be measured.

From these results, the EHPS specific output (i.e. power versus combustor air flow) will be determined. This will be a measure of power output. Also, this can be used to determine efficiency, which is power output divided by fuel input. During all of these tests, emissions will be measured to ensure the engine meets CARB 2007.

The above plan assumes that the heat recovery system performs as planned. If condensate and heat recovery falls short of planned levels, an additional heat exchanger section could be adapted to the end of the engine to augment heat recovery. This is straight forward, but will take additional time and effort. Ahead of this modification, the condensate flow could be supplemented with de-ionized water to demonstrate the engine performance enhancement expected for higher levels of steam injection.

Table 34: Integrated System Tests

Test	Purpose	Measurements Planned	Parameters Varied
Integrated system tests without steam injection	Show system performance including steam injection	Engine, speed, first and second-stage fuel valve positions, fuel pressure, TOT, combustor temperatures, NOx, CO, UHC, O2 and CO2, heat exchanger temperature and pressure measurements, cooling water flow and temperature, exit gas temperature, condensed flow	Vary engine load up to maximum with steam injection

		and temperature, steam flow and temperature	

6.3.3 Measurement Instrumentation

The emission bench as shown in the Figure 2 is equipped with the following flue gas emission analyzers. Please refer to the individual manuals of the analyzers for proper calibration setup and safe operation of these analyzers.

O2 Analyzer (Old)

Manufacturer: California Analytical Instruments (CAI), Model: 100F Serial No.: R10048. Detection Range: 0-5/10/25%, Sensor Type: Galvanic Fuel Cell

CO2 Analyzer

Manufacturer: Beckman, Model: 865, Serial No.: 0103222, Detection Range: 0-5/15/20%, Sensor Type: NDIR

HC Analyzer

Manufacturer: Mocon Inc., Model: 9000THA, Serial No.: 1208DN0042, Detection Range: 0-200 ppm, Sensor Type: FID

O2/CO Analyzer

Manufacture: California Analytical Instruments (CAI), Model: 600 Series with internal sample pump, Serial No.: W12028-MZ, Detection Range: CO 0-200/1,000 ppm, O2 0-25 percent, Sensor Type: CO–NDIR/O2- Paramagnetic

NO/NOx Analyzer

Manufacturer: California Analytical Instruments (CAI), MODEL: 600 Series HCLD with heated sample pump, Serial No.: W12018, Detection Range: 0-3/30/300/3,000 ppm, Sensor Type: CLD

An important feature of the test system is the extensive instrumentation to monitor all important temperature, pressure and flow parameters, as well as the use of multiple emissions monitors to characterize exhaust gas composition. This level of instrumentation is not readily available at field installations, and the more extensive instrumentation at the test facility is an important advantage of this test system. Table 1 presents a list of the various temperature, pressure and flow instrumentation installed in the test facility.

To accurately monitor emissions, a water-cooled probe was used in the stack to rapidly quench any reaction within the probe. Following the cooled probe section, the line connecting the probe to the monitors was heated to further reduction in temperature and any condensation in the line. Just ahead of the monitors, the sample passes through a desiccant dryer that removes

sample moisture. Therefore, all measurements are dry, which facilitates emissions measurement accuracy.

Figure 149: Emission instrumentation bench

6.3.4 Data Collection

Table 8 lists the process data that will be collected during the tests. The power electronics panel will provide data on microturbine (MTG) power output, gas turbine exit and recuperator exit temperatures. Because we are using two fuel control valves to operate the new combustor instead of the one valve of the standard engine, the normal data screen from the power electronics will not be useful in monitoring fuel gas use. Therefore, the project team will rely on the gas meter available from the local utility to monitor total gas flow. The gas meter is located at the inlet to the gas compressor. Also, because the heat recovery unit standard on the TA-100 was removed and replaced with a new set of heat exchangers, the associated instrumentation is not available. Therefore, the project team will rely on temporary set of thermocouples and pressure dials to measure the temperature and pressure associated with the water and steam flows.

Table 35: Data collection and accuracy levels

Parameter	Units	Maximum Uncertainty	Location of Instruments
MTG Power	kW	±0.45%	Customer electrical connection panel
Fuel Gas Compressor Power	kW	±1.0%	
MTG Intake Air Temp	ºC [°F]	±1.1ºC [±2ºF]	Steam injection line
Steam Temp	ºC [°F]	±1.1ºC [±2ºF]	
Barometric Pressure	" of Hg	±2.0%	Outdoor location at test site
Exhaust Temperature	ºC [°F]	±2.8ºC [±5ºF]	Exhaust stack
CHP Water Intake Temperature	ºC [°F]	±2.8ºC [±5ºF]	Heat Exchanger Inlet
CHP Water Flow	gpm	±1.5%	Heat Exchanger Inlet
CHP Water Discharge Temp	ºC [°F]	±2.8ºC [±5ºF]	Heat Exchanger Outlet
Gas Compressor Fuel Supply Press.	psia	±1.5%	Gas compressor fuel inlet
MTG Fuel Supply Mass Flow Rate	lb/hr	±1.0%	
Fuel Higher Heating Value	Btu/lb	±1.0%	Natural gas inlet supply line
Fuel Lower Heating Value	Btu/lb	±1.0%	
High-Temperature Coolant Flow	gpm	±1.5%	
Acoustic Measurements	dB	±3 dB	Per ISO Std 9614 2

Throughout the tests, the microturbine will operate at rated capacity. The power conversion efficiency of the microturbine generator is reported both as gross and net. Net power conversion efficiency accounts for parasitic losses due principally to the required compression of natural gas and energy losses in the power electronics. Therefore,

$$\varepsilon_{PC-gross} = \frac{H_{MTG}}{Q_{MTG}}$$

$$\varepsilon_{PC-net} = \frac{(kWe - kWc - kWpe) * 3412}{Q_{MTG}}$$

Where kWc is the compression power and kWpe is the energy losses in the power electronics to convert generator output to 480 volts 60Hz.

When full EHPS operation is reached, i.e., when steam is generated and injected in the combustor, the fuel input to the combustor will be slowly decreased to maintain maximum power output on the generator at its rated specification of 100 kW. The reduced fuel will be a measure of the increased power of the EHPS with the steam added. This process will be permitted as long as the combustor can operate with reduced fuel input and still maintain stable combustion.

Emissions are generated from the microturbine silo combustor. In order to demonstrate compliance with CARB 2007 limits, the measured emissions in ppm must be converted to lb/MMBtu and then to lb/MWh according to the following calculations. An indication of compliance for NOx will be evident if emissions in ppm are lower than 4.33 corrected to 15 percent O_2. Other pollutants such as CO and total hydrocarbons will be converted in a similar manner.

NOx Emissions from Microturbine in lb/MBtu

$$\frac{lb}{MBtu} = n_A \frac{M_A}{HV} x10^6 \text{ where,}$$

n_A=ppm $_{\text{as measured}}$ (NOx or CO) x n_{FG}x 10^{-6}, and

$$n_{FG} = \frac{4.762xn_C + 0.9405xn_H}{1 - 4.762x(\%O2)} = \text{moles of dry flue gas per lb of fuel}$$

Where n_C and n_H are the moles of carbon and hydrogen per pound of fuel gas, typically 0.0642 and 0.23

Conversion of Microturbine NOx to lb/MWh

$$\frac{lb}{MWh} = \frac{lb}{MBtu}(microturbine)x\frac{FF}{100 + WH/3412}x1000,$$

where

FF=fuel flow in MBtu/hr used by the microturbine, and

WH = the waste heat in the microturbine exhaust, Btu/hr

6.4 EHPS Performance Tests

The TA100 system initially had an electrical problem with the inverter board and would not operate. A new board was located and installed by an Elliott field service technician. The unit was started and transitioned to idle as planned. The engine was then loaded to 20kWe using the load bank, and the fuel supply automatically increased to meet the load demand. After steady state was achieved, the load was increased in 20kWe increments until 80kWe was achieved. As with the first 20kWe, the fuel supply was automatically increased by the control system to meet the increased load demand. While the engine is capable of reaching 100kWe, the conventional combustor degrades at the higher temperature 100kWe load. The combustor is based on a partial oxidation concept, where the dilution air zone experiences a brief peak temperature that can degrade the combustor over time. The EHPS combustor uses an ultralow NOx design that also has a low temperature. This then avoids the peak temperature problem experienced with the conventional combustor. Using this combustor, long term operation at 100kWe would be expected. These brief baseline tests showed that the TA100 system components are operating within specifications.

6.4.1 EHPS Component Tests

Both component and system tests were planned to first prove components and then how they perform as integrated into the EHPS system.

Combustor Tests

The special EHPS combustor will meet CARB 2007 emissions requirements using a two-stage design, with steam injection in the combustion air introduced into the recuperator air inlet. Given the novel combustor design and stringent emissions requirements, several levels of testing were planned to maximize the probability of meeting performance targets. Test sequences included sub-scale 1-atmosphere pressure tests, full-scale 1-atmosphere pressure tests and finally, full-scale 4-atmosphere pressure tests with the combustor integrated into the engine.

Sub-Scale One-Atmosphere Pressure Tests

The 88kWt sub-scale tests included monitoring and control of all air and fuel flows to fully characterize performance (i.e. stability, noise, emissions), as a function of all important variables. The Task 3 project report details the test results and they are not repeated here. The subscale test results showed that there were specific first and second stage air and fuel flows that could yield the needed CARB 2007 emissions at good stability. From literature test combustor results, it was expected that the NOx emissions at the 4 atm engine pressure were expected to be within 20 percent of the 1 atm test results. Therefore, the 1 atm results provide guidance on full scale performance. Given the success with these tests, the full scale combustor was designed, fabricated and tested. This 333kWt combustor was designed for turbine integration, and was more tightly packaged than the test combustor to be compatible with CHP product needs. To achieve the optimal packaging, air flow flexible control features and monitoring features were removed. Ahead of integrating the full-scale combustor with the

engine, the combustor was tested at 1-atmosphere pressure to prove operation and performance without the complexities associated with an integrated engine test.

Full-Scale One-Atmosphere Pressure Tests

During the 1 atm tests, the fuel flows to the first and second combustor stages was varied to control stage stoichiometric Ratios (SR) as well as fuel fraction. This variation allows the tuning of the combustor for stability, NOx, CO and unburned hydrocarbon emissions. A key parameter was expected to be the first stage SR, where higher levels have more excess air that cools the flame. This will reduce NOx to the desired level. Figure 150 shows this reduction of NOx with SR, where an SR of greater than 1.6 is needed to achieve the CARB 2007 NOx requirement of 4.43 for the EHPS CHP system. This reduction is primarily driven by temperature. This is illustrated in Figure 151, which shows that NOx begins to rapidly increase once the first stage gas temperature exceeds 700C. This temperature reduction to achieve the NOx target is also the basis of steam injection that would provide a similar effect.

Using the test data, a final condition was found where the emissions level met CARB 2007 requirements, as well as yielded a stable and low noise operation. Table 36 gives these final results.

Table 36: Final Emissions Results

NOx	**4.5 ppmvd@15% O2**
CO	**5.5 ppmvd@15% O2**

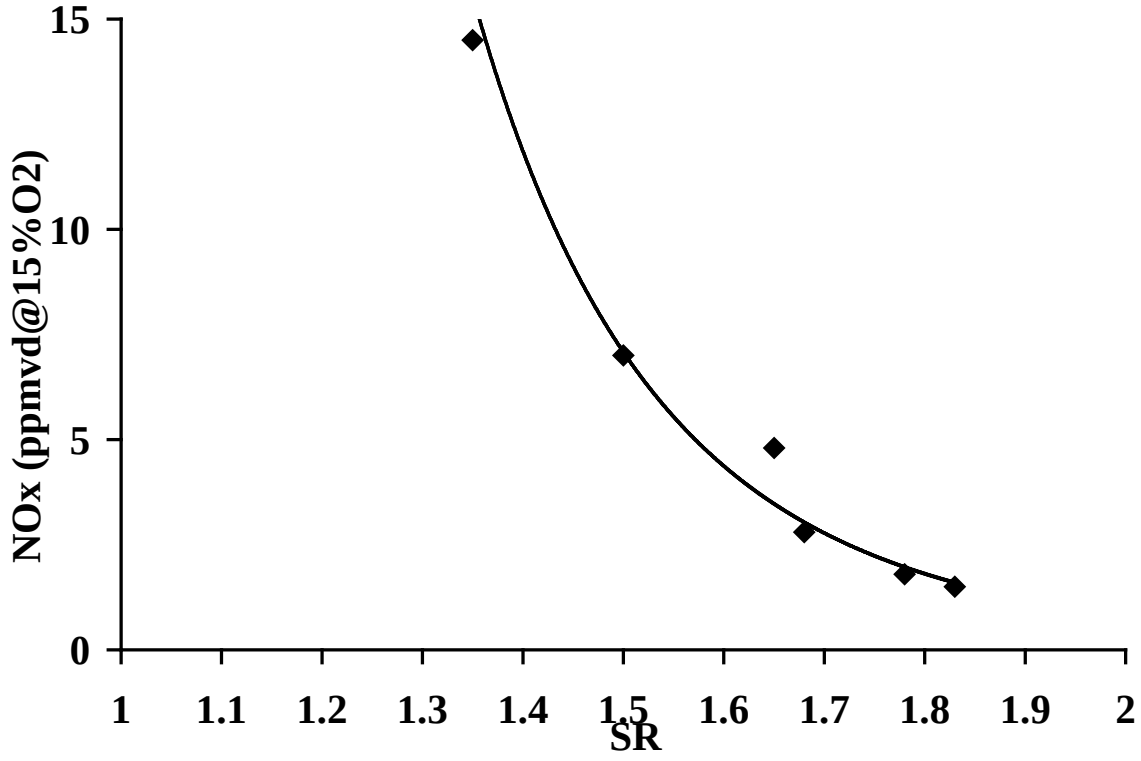

Figure 150: Variation in NOx versus SR

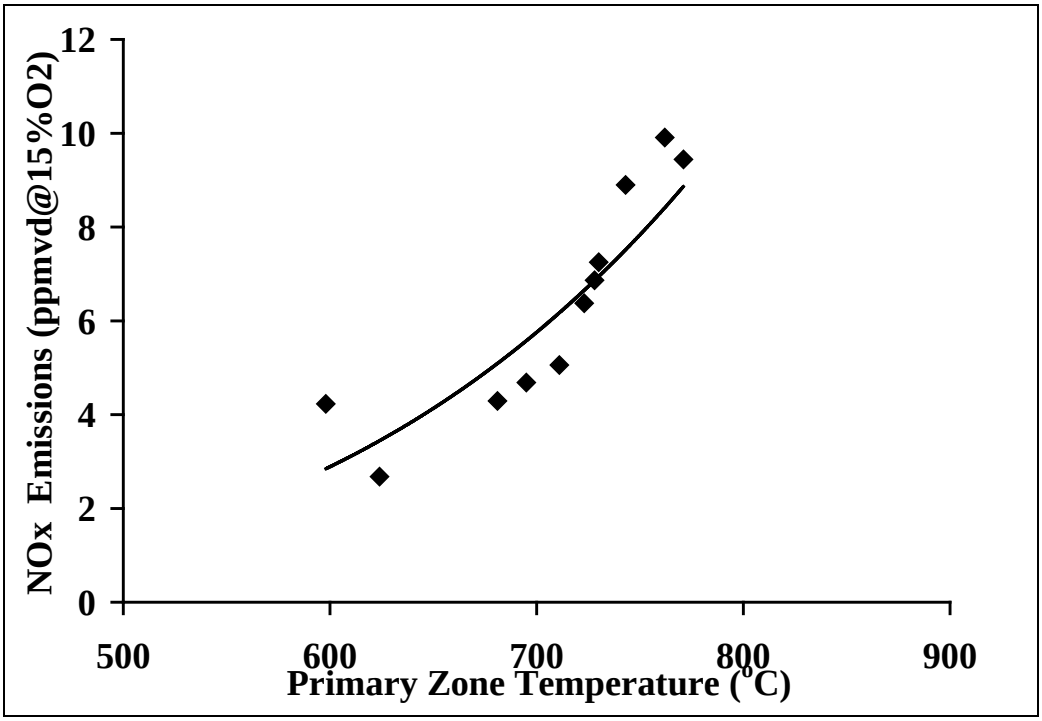

Figure 151: Variation of NOx with First Stage Gas Temperature

Full-Scale Four Atmosphere Pressure Integrated Combustor Tests

Once the full-scale combustor was proven in the 1-atmosphere tests, it was installed in the engine and tested. These initial integrated combustor tests took place without steam injection. To simulate steam injection, the fuel flows will be reduced at the maximum engine speed point to provide more combustion dilution air per fuel flow. This higher first and second-stage stoichiometry will simulate various steam injection levels, as utilized in the 1-atmosphere tests described above. Once combustor operation and performance were proven without steam injection, steam injection tests were initiated.

It should be noted that the correct engine start depends solely on the TIT, and not on any details of combustor operation or dilution of the hot combustor gases. These will impact only whether the combustor can meet CARB 2007. If the combustor is able to burn the provided fuel and meet TIT for each engine speed, then the engine will start. Therefore, the start-up tests will use the baseline total fuel-flow profile during the initial baseline testing. Also, the first and second stage fuel schedule will be set at the optimal ratio for steady idle operation. If the start sequence experiences some problems in engine acceleration, stability, noise, etc., the first and second-stage fuel profiles will be varied to define acceptable conditions throughout the start-up sequence.

A key issue with the integrated tests was the influence of steam on emissions. As described above, this steam impact was expected to follow that of the well-known higher excess air impact for premixed combustors. Figure 152 gives the NOx variation as steam flow to the combustor is increased. As shown, the NOx has almost a linear reduction with percent steam flow. This shows the effectiveness of steam in lowering NOx. While the impact is expected to taper off with very high levels of steam, for the conditions tested, a linear type decrease was observed. Figure 152 shows that the CARB 2007 NOx target can be reached at steam flows above 7 percent. As shown above in Figure 5, NOX reduction can be attributed to gas temperature reductions. This could have an impact on CO burnout. However, if the gas temperature in the second stage is high enough, then CO should be low over all of the conditions tested. Figure 153 shows that CO is lower than the CARB 2007 limit of 10.16 ppmvd @15 percent O2 over the range of testing. This supports that EHPS can achieve the needed emissions targets under stable operating conditions.

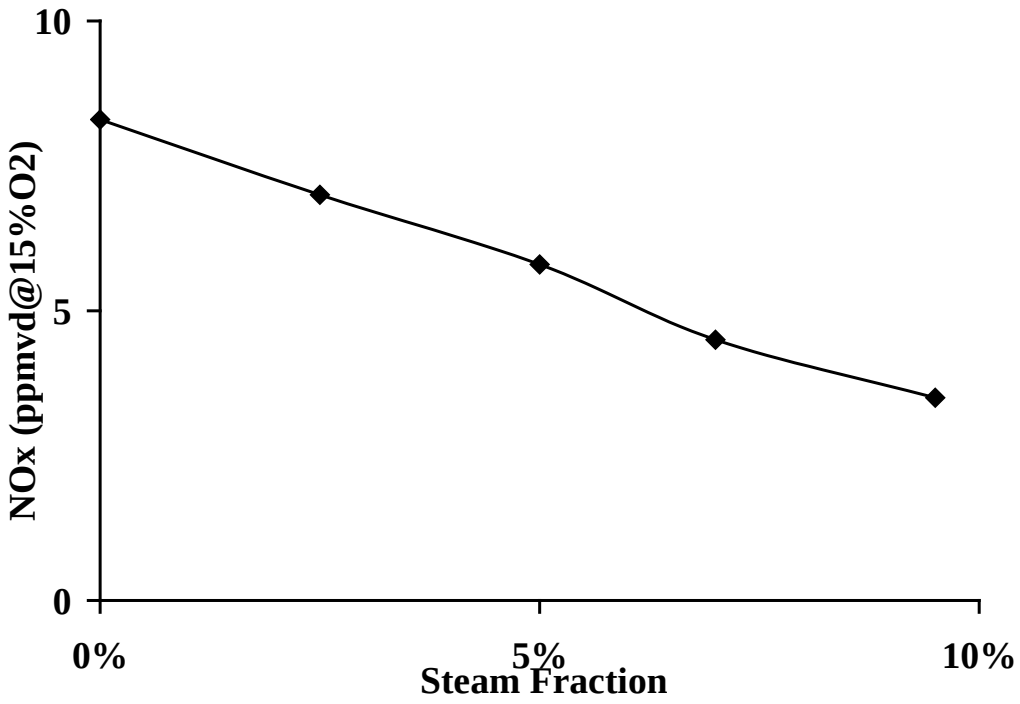

Figure 152: NOx versus Steam Flow Rate Relative to Engine Flow

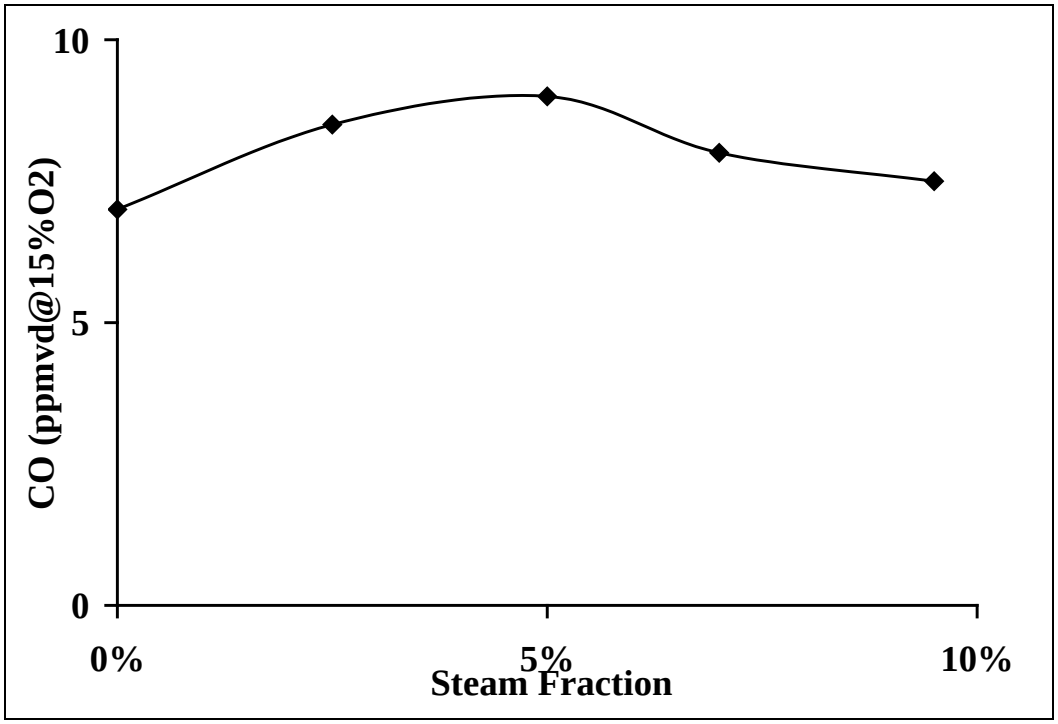

Figure 153: CO versus Steam Flow Rate Relative to Engine Flow

To evaluate the effect of steam versus excess air on NOX, the relative impact of steam on flame temperature can be estimated. Excess air dilutes the flame gases and thereby reduces gas temperature and NOx. If steam works in a similar way, then the thermal impact of steam rather than air can be estimated. Given that the specific heat of steam is 0.44 Btu/lbF and air is 0.2378 Btu/lb-F, then steam should have a factor of 2.2 higher impact on temperature versus excess air. A smaller amount of steam would then have a greater impact on NOx than excess air. To evaluate this effect, the steam rate was converted into the equivalent excess air impact, using the 2.2 factor, and results with and without steam were plotted using this equivalent SR (ie SReq). Figure 154 shows these results. As can be seen on this plot, there is a distinct overlap of the NOx results, supporting that the main effect of steam or air on NOx is the suppression of temperature. Furthermore, these results also show that steam is twice as effective as excess air.

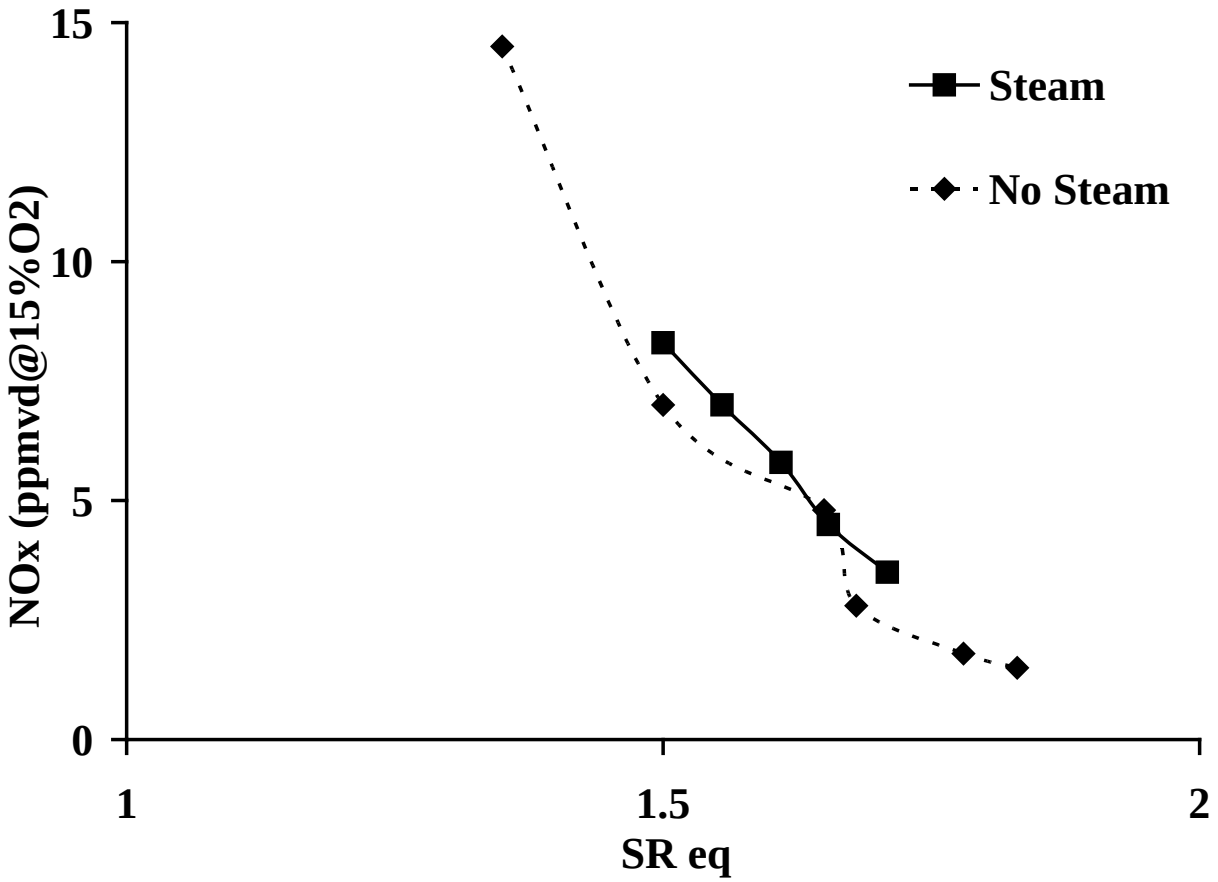

Figure 154: NOx Emissions with and without Steam versus DReq

6.4.2 Heat Recovery System Tests

Table 37 gives the final comparison of the projections based on subscale heat exchanger data compared to the as built results. As shown, the boiler has the heat transfer capacity to meet the steam flow. However, the water preheater and heat recovery heat exchangers fall short of the goal. Test results indicate that these units need to have a longer length to fully meet the recovery requirement. This can be accomplished by adding another segment to the assembly. The heat transfer and pressure drop for this augmented system is given in Table 9. It should be noted that the overall volume of the system is still one half of that for a conventional heat recovery system. In addition, the pressure drop is very low compared to conventional heat recovery systems. Even with the augmented length, the pressure drop is less than 50 percent of the conventional heat recovery heat exchanger. This advantage can be used to enhance the heat transfer by increasing the face velocity and thereby reduce the face area and volume for a given velocity. As an alternative, the lower pressure drop reduces parasitic power losses, which results in a greater net power output.

Table 37: Comparison of Heat Exchanger Performance as Built

Heat Exchanger	Base Heat (B/h)	Base DelP (in H2O)	As Built Heat (B/h)	As Built DelP (in. H2O)	Augmented Heat (B/h)	Augmented DelP (in. H2O)
Boiler	427,861	5.67	429,516	2.36	429,516	2.36
Water Preheater	94,559	1.4	47,251	0.44	94,502	0.88
Heat Recovery	733,770	7.95	357,735	2.80	715,471	5.6
Total		15		5.6		8.84

CHAPTER 7:

Conclusions and Recommendations

This project supported the concept of enhancing the power-to-heat ratio by boosting the power output of conventional 100 kW microtubine CHP systems to 138 kW while increasing the overall efficiency to a maximum of 87 percent using steam injection technology and advanced heat exchanger design. New technologies introduced in the EHPS systems included a new steam-injected ultra-low NOx silo combustor coupled with a new turbine housing and scroll section, and a series of three heat exchangers with a demister to condense and reheat the water to steam for injection in the combustor in a closed loop assembly. The silo combustor was shown to operate in CARB 2007 compliance with and without steam injection and the COP of new heat exchangers were demonstrate to complete system performance in a compact assembly with sufficiently low back pressure to conform with microtubine operating performance. Demonstration of the enhance power output could not be demonstrated in practice because the project was not able to secure a larger 138 kW generator from the original equipment manufacturer (OEM). This limited the performance testing to evaluating the improved performance with reduced gas input while achieving the same generator loading specified by the OEM.

The EHPS technology represent a potential energy and economic improvement on the small-scale (<250 kW) integrated CHP systems in use today. The implementation of this technology will require greater refinement of the new technology components and the commitment of OEMs to participate in future developments of a commercially ready system. The key areas of needed support include areas that were not explored in this project such as refinements in the compressor and power turbine to adapt to the greater mass flow through the system while minimizing system losses. Although conceptually more complex than current commercial systems, the EHPS can address markets where enhanced power-to-heat ratio are more in line with needs of the site. These installations are more frequently found in the commercial sector of the economy.

GLOSSARY

ACA – Altex Computational Model

BWHE -- Boiling Water Heat Exchanger

Btu/hr – British thermal units per hour

CARB – California Air Resources Board

CFD – Computational Fluid Dynamics

CHP – Combined Heat and Power

CHRHE – Condensing Heat Recovery Heat Exchanger

COP – Coefficient of Performance

DG - Distributed Generation

DOE – Department of Energy

EESI – Elliott Energy Systems Inc.

E&M = Energy and Mass Balance

E/M--Energy and Mass

EHPS – Efficient Heat and Power System

fpm – feet per minute

FVC - Fuel Control Valve

gpm – gallons per minute

HEX –Heat Exchangers

HHV – High Heating Value

HM – High Moisture

HMMWV –

HRSG – Heat Recovery Steam Generator

HRU – Heat Recovery Unit

ISO - Independent System Operator

IDT – Initial Temperature Difference

kWe – Kilowatt electrical

LHV – Low Heating Value

MFC – Mass Flow Controller

MM – Medium Moisture

MMBtu/hr - Million British Thermal Units per hour

MTBF - Mean Time Between Failures

MTG – Microtubine Generator

OEM- Original Equipment Manufacturer

PIER - Public Interest Energy Research

SCG – Southern California Gas Company

SR – Stoichiometric Ratio

SRLL – Stoichiometric Ratio for Lean Lean Combustion

SRT – Stoichiometric Ratio Total

TEMP – Thermally Engineered Manufactured Products

TET – Turbine Exit Temperature

TIT – Turbine Inlet Temperature

VFD – Variable Frequency Drive

VOC – Volatile Organic Compounds

VPEI – Vacuum Processing Engineering, Inc.

WPHE -- Water Preheater Heat Exchanger

REFERENCES

1. Kelly, J., "Advanced Low-Pressure Drop Radiator for the HMMWV", Final Report, Contract No. W56HZV-08-C-0073, June 2008
2. Kelly, J., "Compact and Efficient Cooling Coils for Naval Systems", Final Report, Office of Naval Research N000-14-09-M-0193, November 2009
3. Castaldini, C. and Kelly, J., "Efficient Heat and Power Systems for CHP Applications, Task 2 Report", California Energy Commission Grant PIR-07-003, August 2009
4. Kays, W.M. and London, A.L., "Compact Heat Exchangers", Krieger Publishing Company, Melbourne, Florida, 1994
5. Eckert, E.R.G. and Gross, J.F., Heat and Mass Transfer, McGraw Hill, New York, 1963
6. www.claytonindustries.com
7. www.condexenergy.com
8. Bonilla, C., Nuclear Engineering, McGraw Hill, New York, 1957
9. www.barclayend.com.au
10. Lefebvre, A., Gas Turbine Combustion, Hemisphere Publishing Corporation, New York, 1983